universität wien

DISSERTATION / DOCTORAL THESIS

Titel der Dissertation /Title of the Doctoral Thesis

„An interdisciplinary Approach:
On the Habitability of Enceladus' Potential Subsurface Water Reservoir“

verfasst von / submitted by

Ruth-Sophie Taubner, Bakk. MSc

angestrebter akademischer Grad / in partial fulfilment of the requirements for the degree of

Doktorin der Naturwissenschaften (Dr. rer. nat.)

Wien, 2018 / Vienna 2018

Studienkennzahl lt. Studienblatt / degree programme code as it appears on the student record sheet:	A 796 605 413
Dissertationsgebiet lt. Studienblatt / field of study as it appears on the student record sheet:	Astronomie
Betreut von / Supervisor:	ao. Univ.-Prof. i.R. tit. Univ.-Prof. Dr. Maria G. Firneis Univ.-Prof. Dipl.-Biol. Dr. Christa Schleper

Contents

Acknowledgement

I would like to take this opportunity to express my sincere gratitude to four remarkable people who heavily influenced my scientific life and became inspiring examples (in chronological order):

Dr. Margarete Obiditsch was my maths and physics teacher at school. She was the one who excited my passion and promoted my curiosity for physics and astronomy and who has been my first role model. I don't know if I ever would have written this thesis or even studied astronomy at all without her guidance in my school days and beyond.

Univ.-Prof. Dr. Maria G. Firneis (Institute for Astrophysics) was already my supervisor for my master thesis. She gave me the unique opportunity to be a member of the Research Platform: ExoLife and to write my PhD thesis under her supervision. She is an admirable person that guided me from the beginning through the different facets of the scientific life.

Univ.-Prof. Dipl.-Biol. Dr. Christa Schleper (Department Ecogenomics and Systems Biology) took the risk to allow an astronomer to use her microbiological lab facilities. She was an excellent supervisor and mentor and gave me the opportunity to delve into the fascinating world of microbiology.

I wish to say a big thank you to Dr. Simon Rittmann, who introduced me into the curious world of methanogens and who was the best advisor I could imagine during the laboratory work and during writing the papers. Simon, thank you so much for giving me the opportunity to be part of your group and for your endless work on our papers. I can think of no better supervisor, mentor, and inspiring example than you and hope we will continue to work together in future.

Further, I would like to thank the whole Archaea Physiology & Biotechnology Group for countless discussions on growth conditions, gassing and experimental settings. I like to thank the whole Division of Archaea Biology and Ecogenomics, who have welcomed me with warmth and hospitality, and who showed me how motivating and fruitful a positive group dynamic can be – in the lab and beyond. Special thanks to the people sitting with me in the "jungle"- guys, it's a pleasure to share an office with

you. Thanks to my wormies-buddies Nika, Philipp, and Tobi for your help creating nice figures. Many thanks to Jessica Kozlowski, who read my thesis and helped me finding my way through the jungle of English grammar. Furthermore, I would like to thank Johannes Leitner (Research Platform: ExoLife, University of Vienna) for countless discussions about my thesis, for his helpful comments, and for introducing me into the scientific world at the beginning of my studies. I would also like to thank Stefan Meingast for giving me some very good advises at the end of my PhD studies.

Special thanks to all the collaborators of our final, big paper: Patricia Pappenreiter, Jennifer Zwicker, Daniel Smrzka, Christian Pruckner, Philipp Kolar, Sébastien Bernacchi, Arne H. Seifert, Alexander Krajete, Wolfgang Bach, Jörn Peckmann, Christian Paulik and again Maria Firneis, Christa Schleper and Simon Rittmann. Without you this fantastic journey would not have been possible.

I would like to thank my team mates of the football team "Dornbach Sox" and of the tennis team "Terra Rossa": I'm honoured to be part of the world's best football and tennis teams. Thank you folks for unforgettable moments (like this year: two championship titles in one season, incredible!) and for giving me the strength to survive the sometimes very stressful and nerve-racking time during my doctoral studies.

Finally, I want to thank my family, who encouraged me in my studies during the last ten years and who supported all my interests. Without your never-ending support, your understanding, and especially your love, I would not have been able to get this far. This thesis is also your thesis!

List of Figures

List of Tables

1 Introduction

> *Two possibilities exist: either we are alone in the Universe or we are not. Both are equally terrifying.*
>
> **— Arthur C. Clarke**
> (British science fiction writer)

1.1 Context and Motivation

1.1.1 Prelude

When the German-born British astronomer Friedrich William Herschel discovered Saturn's moon Enceladus in 1789 [Herschel, 1790], nobody was able to predict that this small icy moon would change our thinking about habitable worlds in the Solar System. For life-as-we-know it, organic compounds, chemical energy, and water are the primary necessities. For water, the concept of circumstellar habitable zones was introduced by scientists like Strughold [1953] and Huang [1959] in the 1950s. Further development by Dole [1964] and Kasting et al. [1993] lead to the definition of the habitable zone as "the orbital region around a star in which an Earth-like planet can possess liquid water on its surface and possibly support life" [Lissauer, 2018]. The detection of the subsurface water reservoirs of Europa, Enceladus and other icy celestial bodies far beyond this so-called "Goldilocks zone" lead to a rethinking of this concept.

When the joint NASA/ESA/ASI spacecraft mission Cassini-Huygens was designed and built from the 1980s up to its launch in 1997, the idea that Enceladus may be an active moon and might be the source of the E-ring particles (see Fig. 1.1B) was already in the heads of the scientific community. Nevertheless, when Cassini arrived at the Saturn system in 2005, everybody was astonished by the discovery of the spectacular plume which so far makes this small icy moon unique[1] in the Solar System (see Fig. 1.1A). This plume gives us the unprecedented opportunity to get an

[1] At this point one should mention that by analysing data by the Hubble space telescope [Roth et al., 2014, Sparks et al., 2016] and the Galileo probe [Jia et al., 2018], there was some evidence found that also Jupiter's icy moon Europa might host some active plumes.

insight into the moon's subsurface water reservoir by sampling the particles emitting from its south polar region. Although the Cassini Saturn orbiter was not explicitly designed to sample Enceladus' plume, the mission helped to gain a deeper insight into the processes going on in this icy moon (see section 1.1.3). One example is provided by the detection of silicon-rich particles which can be seen as an indication for ongoing hydrothermal activity [Hsu et al., 2015]. This and the presence of many organic and inorganic molecules make Enceladus one of the hot spots in the search for extraterrestrial life in the Solar System.

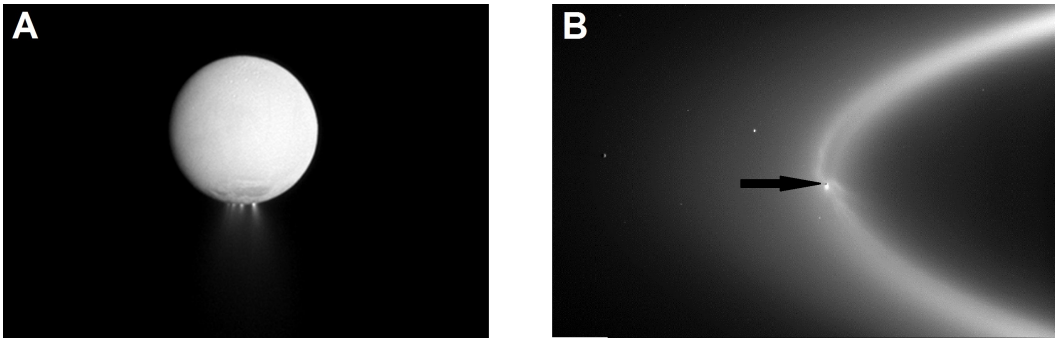

Fig. 1.1. A. Enceladus illuminated by reflected sunlight of Saturn (visible light, 25th Dec. 2009, PIA12733), Credit: NASA/JPL/Space Science Institute; B. Saturn's E-ring with Enceladus (dark spot, marked by an arrow) in its center (adapted, APOD, March 27, 2007), Credit: CICLOPS, JPL, ESA, NASA.

1.1.2 Enceladus in a Nutshell

The majority of the data on Enceladus were collected by the Cassini probe which was launched in 1997. Initially planned to have a mission duration of four years, it was extended two times and finally orbited Saturn between July 2004 and September 2017 for more than 13 years, *i.e.* almost half of a Saturn year. Cassini had 22 close encounters/flybys during its entire mission [NASA's Jet Propulsion Laboratory, 2015], the closest one on October 9^{th}, 2008, at an altitude of just about 25 km above Enceladus' surface [NASA's Jet Propulsion Laboratory, 2008]. Even if Cassini was not designed to sample such a dense plume, it revealed plenty of Enceladus' hidden secrets.

Tab. 1.1. Key Data of Enceladus.

Parameter	Value	Source
Mean Distance to Saturn	$2.38 \cdot 10^5$ km	NASA Planetary Science Division [2018]
Mean Distance to the Sun	9.54 AU	NASA Planetary Science Division [2018]
Mean radius	252.2 ± 0.2 km	Thomas et al. [2016]
Mean surface temperature	75 K	Spencer et al. [2006]
Mean bulk density	1609 ± 5 kg m^{-3}	Thomas et al. [2016]
Mass	$1.08 \cdot 10^{20}$ kg	NASA Planetary Science Division [2018]

Enceladus is Saturn's sixth largest moon with a mass of 0.15% of Earth's Moon (see Tab. 1.1 for detailed numbers). The relative high bulk density implies that Enceladus possesses a core with a high ratio of rocky material (see Fig. 2.1). This rocky core is surrounded by a (most likely) global ocean with varying depth, whereas the ocean's largest extension is located at the south pole of this icy moon. The ocean is covered with an icy shell between two and several dozens kilometres. The exact dimensions of the different layers are hard to determine and several studies (*e.g.* Rappaport et al. [2007], Olgin et al. [2011], Čadek et al. [2016], Iess et al. [2014], Thomas et al. [2016]), partly conflicting, were published on this issue, including the one presented in Chapter 2.

The most remarkable feature of Enceladus is its plume which is situated at the South Polar Terrain (SPT). This plume is composed of more than 100 small discrete jets [Porco et al., 2014] or, according to a more recent study, even broad, curtain-like eruptions [Spitale et al., 2015] along the four prominent, nearly parallel fractures called "tiger stripes" (see Fig. 1.2). These fractures "are linear depressions, typically about 500 m deep, 2 km wide, and 130 km in length, flanked on both sides by prominent 100-m-high ridges" [Porco et al., 2006, p. 1394]. They are called *Alexandria Sulcus*, *Baghdad Sulcus*, *Cairo Sulcus*, and *Damascus Sulcus*, whereby *sulcus* is a term used in astrogeology for long, parallel ridges. Besides being the source of the plume jets, this area is also interesting due to its high surface temperature (>190 K at *Damascus Sulcus* [Parkinson et al., 2008, Goguen et al., 2013]) compared to the calculated mean surface temperature of less than 90 K [Porco et al., 2006].

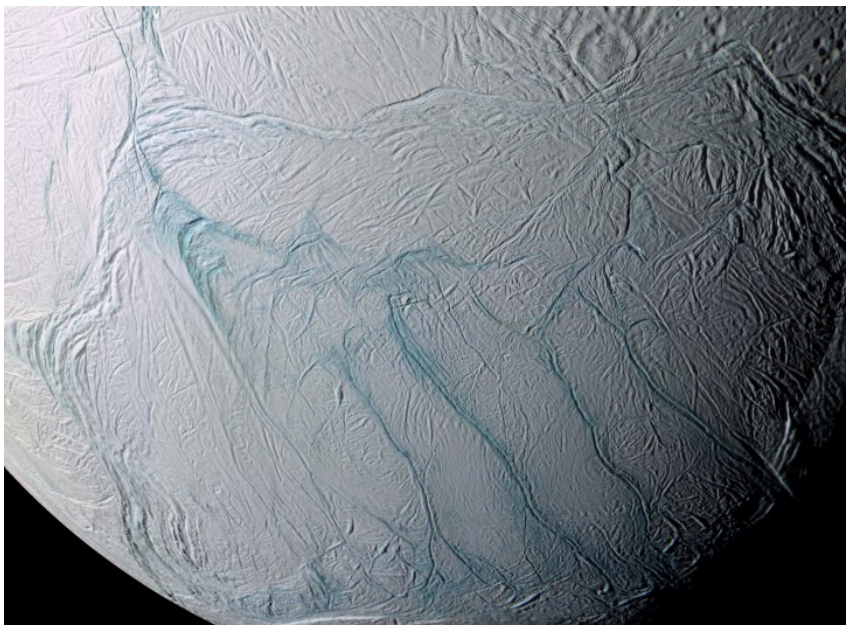

Fig. 1.2. Enceladus' tiger stripes at its south pole (10th March 2006, APOD 060310), Credit: Cassini Imaging Team, SSI, JPL, ESA, NASA.

The plume is feeding Saturn's extremely faint E-ring which extends from 3 to about 8.0-9.5 Saturn radii [Kempf et al., 2011] with a ratio of 51 $\pm$ 18 kg s^{-1} for the solid components [Ingersoll and Ewald, 2011]. However, the rate of water vapour injection can reach higher values of 200 $\pm$ 30 kg s^{-1} [Hansen et al., 2011] to up to 1000 kg s^{-1} [Teolis et al., 2017]. This rate is highly variable due to changes of the tidally driven expansion and compression of the surface fissures as a function of Enceladus' orbital position [Hedman et al., 2013, Teolis et al., 2017].

Besides H_2O, many other organic and inorganic molecules were detected via Cassini's *Ion and Neutral Mass Spectrometer* (INMS) with different abundances and ambiguities in Enceladus' plume (see Table 5.1). The five major species are water (H_2O), methane (CH_4), carbon dioxide (CO_2), ammonia (NH_3), and molecular hydrogen (H_2) with abundances higher than 0.1% relative to water [Waite et al., 2017, Magee and Waite, 2017].

The plume's water most likely originates in an ocean beneath a 2-40 km thick icy shell [Čadek et al., 2016, Iess et al., 2014, Thomas et al., 2016]. There has been a long debate about the extension of the subsurface water reservoir, either being a local aquifer underneath the SPT [Collins and Goodman, 2007, Iess et al., 2014] or being a global ocean [Patthoff and Kattenhorn, 2011, McKinnon, 2015]. In fact, the truth may lie in a combination of both models, *i.e.* a global ocean with a south polar depression [Čadek et al., 2016, Thomas et al., 2016, Le Gall et al., 2017].

The source of energy that keeps the subsurface ocean liquid and the plume and the hydrothermal vents active was highly debated over the last decade. To explain these events an extremely high heat power (more than 20 GW) is required [Choblet et al., 2017]. The contribution of radiogenic heating to the thermal budget of Enceladus is rather small (less than 0.25 GW [Choblet et al., 2017]). Other models based on *e.g.* secondary spin-orbit libration [Wisdom, 2004] or stored tidal energy that bursts out periodically [Howett et al., 2011] also don't receive such high values. However, a recent study showed that at least 10 GW could be generated by tidal friction by water transport through the potentially porous rocky core. Even higher input of up to 30 GW might be possible if the ice shell is thinner than predicted in the standard models [Choblet et al., 2017]. This represents the first study that can explain the observed internal heat-generated power.

1.1.3 Cassini's contribution to our knowledge about Enceladus

Several instruments on board of Cassini found indirect evidence for the subsurface ocean, examined the plume, or helped to understand the (geo-)chemical processes going on in Enceladus:

- *Ion and Neutral Mass Spectrometer* (INMS): This instrument measured the plume's neutral gas composition over ten flybys. Besides many other organic and inorganic molecules, the detection of NH_3, the probable detection of radiogenic argon (^{40}Ar), and the determination of the deuterium-to-hydrogen ratio in the detected water can be seen as strong sign for a subsurface water reservoir [Waite et al., 2009].

- *Cosmic Dust Analyzer* (CDA): By *in situ* analysis with this instrument, E-ring grains that are rich in sodium salts and even complex organics were detected. Particles of that kind can only originate in liquid water [Postberg et al., 2009].

- *Radar*: This instrument targeted a region north of the tiger stripes. Using microwave radiometry observations, thermal anomalies in consistence with large fractures imply a complex heat production and transport system below the SPT. This leads to the assumption, that the icy shell in this area might have a thickness of just a few kilometres [Le Gall et al., 2017].

- *Imaging Science System* (ISS) and *Composite Infra Red Spectrometer* (CIRS): co-discovered that the tiger stripes and the areas of the SPT, where the highest temperatures were observed, are correlating [Porco et al., 2006].

- *Visible and Infrared Mapping Spectrometer* (VIMS): With the aid of this instrument, the size and the temperature of the hot spots in the SPT were determined [Goguen et al., 2013].

- *Ultraviolet Imaging Spectrograph* (UVIS): helped to identify water as the primary composition of the plume. It was not able to detect any absorption features correlating with CO, H_2, and O_2 which leads to an estimation of the upper limits on the mixing ratio of these three gases [Hansen et al., 2011].

- *Magnetometer* (MAG): This instrument provided the first evidence of the Enceladian plume by analysing the bending of Saturn's magnetic field around the moon's south pole [Dougherty et al., 2006].

- *Magnetospheric Imaging Instrument* (MIMI), *Cassini Plasma Spectrometer* (CAPS), and *Radio Science Subsystem* (RSS): Analysed the plasma in Saturn's magnetosphere and identified Enceladus as the main source for the mainly water and water products (ions).

1.1.4 Enceladus' role in Astrobiology

With a high concentration of liquid H_2O and a range of organic and inorganic molecules including potential electron donors (see Tab. 5.1), Enceladus harbours many necessary elements for life (see Fig. 1.3). Phosphorus, one of the most essential elements for life, is missing in the data received by Cassini. However, due to assumed similarity of Enceladus' core and chondritic meteorites, which contain several different phosphorus-bearing minerals (*e.g.* schreibersite), phosphorus should be available in the liquid ocean due to weathering processes by water-rock contact.

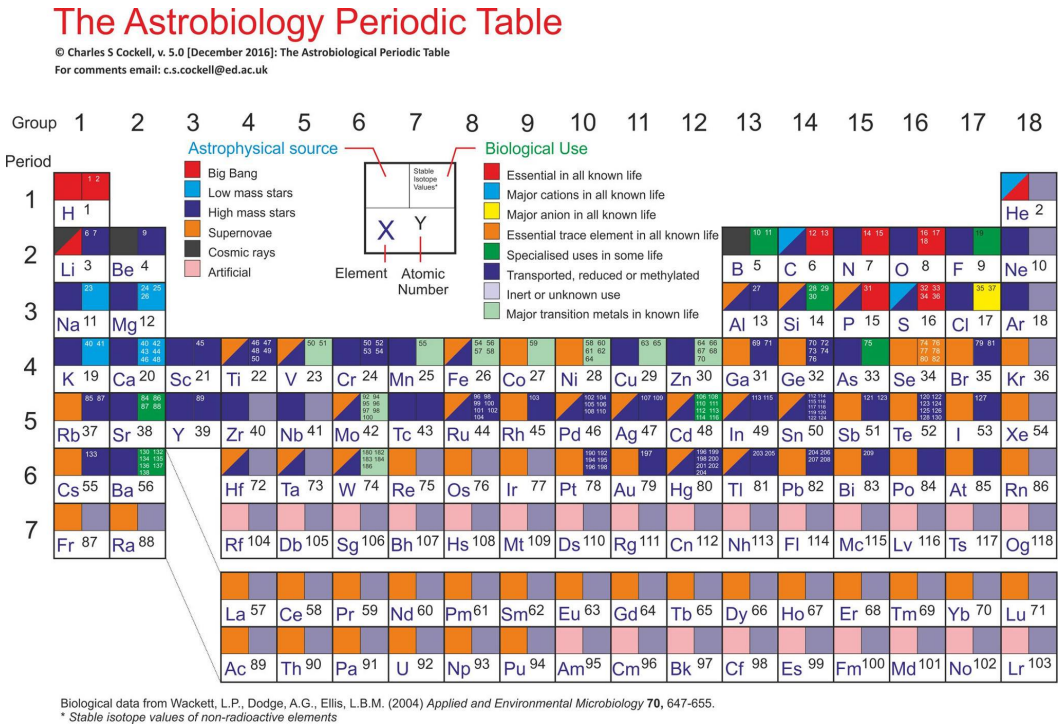

Fig. 1.3. The Astrobiology Periodic Table v. 5.0, Credit: Charles S. Cockell.

Possible metabolic capacities of life forms on Enceladus must be chemotrophic, *i.e.* independent of products of photosynthesis, and would need to be anaerobic, *i.e.* independent of oxygen. There are only three known microbial ecosystems on Earth which meet these requirements and could potentially exist on Enceladus [McKay et al., 2012]. Two of these systems deal with hydrogenotrophic methanogens (see section 1.1.7) that use H_2 derived from rock-water reactions and a third is based on sulfur-reducing bacteria that use redox couples produced by radioactive decay [McKay et al., 2008] (see Fig. 1.4). The latter process is mainly based on the conversion of H_2 and sulfate (SO_4^{-2}) into hydrogen sulfide (H_2S) and H_2O. However, the presence of SO_4^{-2} would require an oxic environment which is unlikely on Enceladus.

Nevertheless, a main requirement for life is that such a habitat is stable over a long period. Several studies showed that the ocean could have been liquid for over tens of

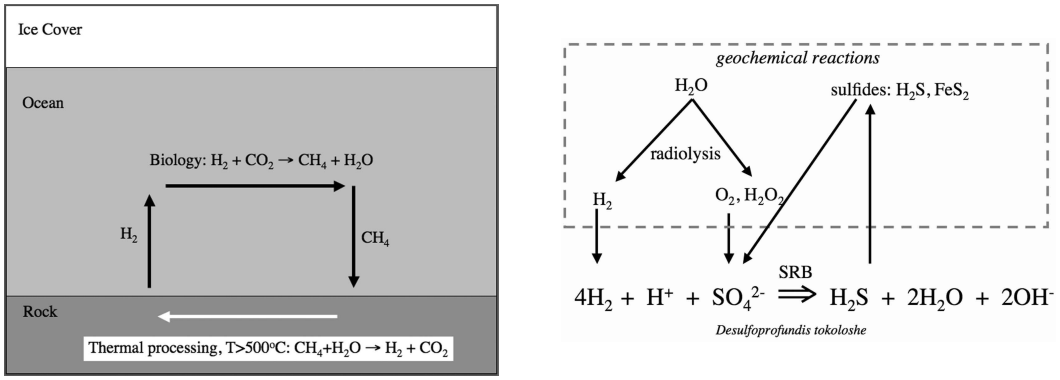

Fig. 1.4. Proposed biogeochemical cycles in the subsurface of Enceladus, McKay et al. [2008].

millions to billions of years [Travis and Schubert, 2015, Choblet et al., 2017] which could be a sufficient amount of time for life to arise.

1.1.5 What is life?

Before aiming to find extraterrestrial life on other celestial bodies, a universal definition of life is required. However, even if you can find hundreds of definitions of life in the literature [Leitner, 2014], none is generally accepted. According to Serhiy A. Tsokolov, the existing theories can be divided into three different groups:

- "Life is defined by using terms that are themselves undefined.
- A combination of descriptions of life is called a definition.
- A specific step in a continuous gradual transitional evolution from complex chemical systems to primitive living systems is arbitrarily defined as minimal life." [Tsokolov, 2009, p.402]

Edward N. Trifonov was analysing the vocabulary of 123 of these definitions and came to the conclusion, that it is possible to sum these up in a minimal set of just five words: "Life is self-reproduction with variations"[Trifonov, 2011, p.262]. However, this minimal version is vague and not suitable for scientific research. Very close is the "NASA definition of life" which says "life is a self-sustaining chemical system capable of Darwinian evolution"[Joyce, 1994, Foreward, p.xi–xii].

We just have one example of life, life on Earth, and it is hard to build up a definition by using just one sample. As Christopher McKay formulates it: "We don't know which features of Earth life are essential and which are just accidents of history" [McKay, 2004, p.1260]. Life is more like a process than a substance, which makes it so hard to find a universal definition. And even if we find a proper definition of

terrestrial life, we will not know if it would match extraterrestrial life. Further, many definitions include characteristics which we could not detect by the aid of common space missions, *e.g.* the feasibility of performing Darwinian evolution.

1.1.6 The origin of life

Since ancient times, mankind has been thinking and discussing the origin of life. Until today, the process of transition from non-living to living entities is still under debate and may never be fully understood. However, the discovery of microbes in extreme environments over the last decades has encouraged speculations about an extraterrestrial origin of terrestrial life. This hypothesis is called *Panspermia* and it states that life has been distributed all over the universe by small celestial bodies like meteoroids, asteroids, and comets. Nevertheless, this hypothesis doesn't explain how life first originated, but instead shifts it to another celestial body.

On Earth, the earliest detectable lifeforms arose more than 3.5-3.77 billion years ago [Schopf, 2006, Dodd et al., 2017]. However, life may have existed as early as 4.28 billion years ago [Dodd et al., 2017], just a few dozens million years after the formation of the terrestrial oceans (approx. 4.40 billion years ago [Wilde et al., 2001]) and just a few hundreds of millions of years after the formation of the Earth (approx. 4.54 billion years ago [Dalrymple, 2001]). Indications for these lifeforms were found in ferruginous sedimentary rocks from Nuvvuagittuq belt in Quebec, Canada, which are most likely seafloor-hydrothermal vent-related precipitates [Dodd et al., 2017]. In agreement with that finding, the most compelling ideas about the origin of life come from chemical and microbiological studies of hydrothermal vents, like black or white smokers. This environment supports chemolithotrophic life that uses the released compounds like H_2, ferrous iron, or sulfides for its metabolisms. Therefore, many theories have been postulated, that the origin of life was situated in the proximity of hydrothermal vents [Wächtershäuser, 1992, Martin and Russell, 2003, 2007, Weiss et al., 2016].

Whether the first life forms are of autotrophic [Wächtershäuser, 1992] or heterotrophic [Miller, 1953, Miller and Urey, 1959] origin is still widely discussed [Forterre and Gribaldo, 2007]. However, even if the origin of life was heterotrophic, the initial feedstock of organics would have been consumed after some time and life would have been forced to develop autotrophic pathways [Kral et al., 1998]. One of this first autotrophic pathways could have been methanogenesis, *i.e.* a form of anaerobic respiration accompanied by the formation of methane.

1.1.7 Methanogens

When Carl Woese and George E. Fox published their phylogenetic analysis in the late 1970s, the domain archaebacteria was born [Woese and Fox, 1977]. Later renamed to Archaea [Woese et al., 1990], this domain harbours some of the most intriguing lifeforms studied so far. These single-celled microorganisms are known to be widely distributed in nearly all habitats on Earth, even in very extreme environments like salt lakes or hot springs. The main difference between archaea and bacteria can be found in the cell membrane. Archaea lack the classical bacterial murein (peptidoglycan) in their cell walls and have a different kind of membrane lipids (ether-linked lipid membrane with isoprenoid side chains [Jain et al., 2014], see Fig. 1.5). The latter may be the reason why archaea can survive in extreme environments because ether linkages are more chemically stable than the ester linkages used by bacteria. Instead of the murein some Archaea have pseudomurein as major cell wall component. Although different in chemical structure, pseudomurein has a similar function and physical structure compared to the bacterial analogue. Another important component of the cell envelope is the paracrystalline protein surface layer (S-Layer), which is found in nearly all archaea described to date and in many types of bacteria [Rodrigues-Oliveira et al., 2017].

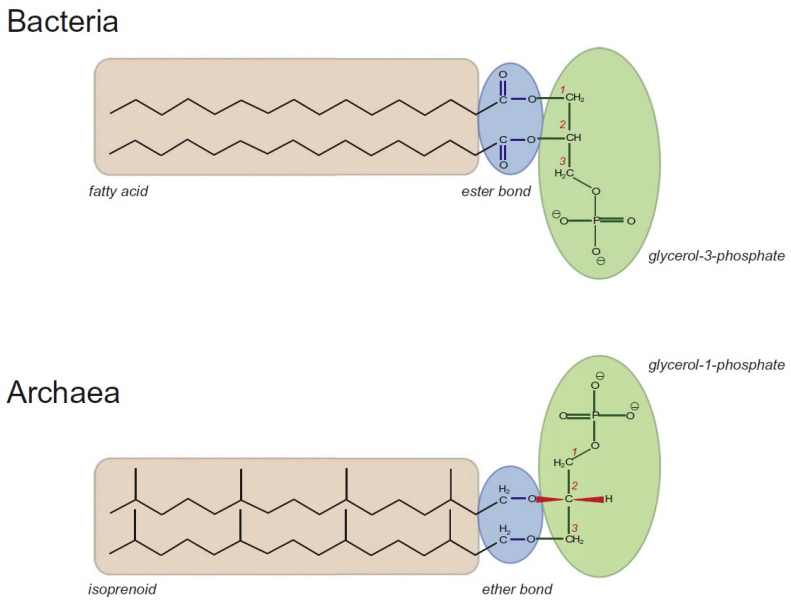

Fig. 1.5. Difference in bacterial and archaeal membrane lipid structure, Credit: Caforio and Driessen [2017], p. 1326.

Methanogens were the first organisms to be recognized as archaea [Woese and Fox, 1977]. Methanogens are obligate[2] anaerobic chemolithoautotrophs or chemolitho-heterotrophs who are known to be the only organisms capable of producing CH_4

[2]However, in 2017, Angle *et al.* reported the discovery of a methanogenic strain (*Candidatus* Methanothrix paradoxum) that performs methanogenesis in oxygenated soils [Angle et al., 2017].

as end product of their metabolism, *i.e.* end-product of their anaerobic respiration. About 95 percent of Earth's CH_4 is of biological origin [Maczulak, 2010].

From a phylogenetic perspective, methanogenesis is possibly among the oldest metabolisms of terrestrial life including the possibility that the last common ancestor of all archaea has already been a methanogen [Evans et al., 2015].

Even if methanogens are very diverse and can be found in various anaerobic environments, the necessary substrates are limited to just four major types [Liu and Whitman, 2008, Mayumi et al., 2016]:

- C_1 compounds (CO, CO_2, formate (HCO_2^-))
- methyl-group containing compounds (methanol (CH_3OH), methylamines (CH_3NH_2), or methylsulfides with or without H_2)
- acetate (CH_3CO_2)
- methoxylated aromatic compounds (MACs)

A large number of methanogens are hydrogenotrophs, *i.e.* microbes that use H_2 as primary electron donor for the reduction of CO_2 to CH_4.

1.1.8 Serpentinization

If life emerged at alkaline hydrothermal vents on the early Earth, a geochemical and water-dependent process called serpentinization could have played a central role. In this geological low to moderate temperature process low-silica, (ultra)mafic, primary ferromagnesian minerals such as olivine($(Mg,Fe)_2SiO_4$) and pyroxenes ($(Mg,Fe)SiO_3$) are transformed into serpentine ($Mg_3Si_2O_5(OH)_4$) accompanied by the production of H_2 [Holm et al., 2015]. The enrichment of early Earth's water with H_2, the circulation through ultramafic rocks and the accompanied mixing with organic substrates could have created some kind of "Darwinian soup" [Sleep et al., 2004] similar to the one simulated by Miller and Urey in the mid 1950s [Miller and Urey, 1959].

At a later stage, H_2 served as an electron donor for methanogens even down to partial pressures of H_2 of less than 4 Pa ($4 \cdot 10^{-5}$bar) [Kral et al., 1998, Chong et al., 2002]. These H_2-consuming autotrophs could consequently have been responsible for major effects on the atmosphere of the early Earth including being a dominant sink for H_2 [Kral et al., 1998]. Today, serpentinization occurs in many peridotite-hosted

terrestrial systems, like subduction zones, mid-ocean ridges, and ophiolites[3] [Schrenk et al., 2013]. Especially the hydrothermal vent site called Lost City discovered in 2000 is of great interest for studies about the origin of life [Russell et al., 2010]. This site is located approximately 15 km away from the Mid Atlantic Ridge.

In parallel to the early Earth, the most promising area on Enceladus where life may exist is at the seafloor of the subsurface water reservoir where this kind of interaction (or a similar one) between the liquid water and the rocky seabed could take place.

1.2 Research Questions and Goals of this Thesis

The habitability of icy moons has been discussed theoretically for already more than two decades. This study is the first attempt to show the habitability of Enceladus in extensive laboratory-based simulations. The goals of the thesis can be summarized in the following points:

- To determine the physical conditions at the bottom of the potential subsurface ocean of Enceladus.
- To find microorganisms (methanogens) that could theoretically thrive in Enceladus-like conditions ("screening").
- To estimate if the amount of H_2 produced by serpentinization would be sufficient to power methanogenic life on Enceladus.
- To show growth of at least one methanogenic strain under putative Enceladus-like conditions.

1.3 Thesis Structure

The thesis is mainly based on four first author publications which are all published in peer reviewed journals. Each publication represents one chapter of this thesis preceded by a short overview and publication details. Three publications are given in the original form as published by the respective journal. Chapter 6 summarizes the results.

Chapter 2

The chapter deals with the controversial interior structure of Enceladus. The final version of the manuscript presented in this chapter deals with the case of a suggested

[3] An ophiolite is a former part of the Earth's oceanic crust that was uplifted above sea level in course of plate tectonics.

local sea. However, the first submitted version of this paper worked with a global ocean but the model was changed due to the recommendation of the referees to include the new publication of Iess et al. [2014], where the authors presented a supposed proof for a local sea based on gravity measurements using Doppler data from three Cassini flybys. The main task of this study was to determine the physical conditions at the water-rock boundary, above all the pressure in this area.

Chapter 3

This review summarizes the potential of methanogens to act as model organisms for astrobiological studies. During the literature survey for the best candidate for microbial experiments, we realized that there does not exist a detailed review about the ecophysiology of methanogens from an astrobiological point of view. This paper shows the capabilities of these archaea to withstand extreme conditions which can also be found on other celestial bodies like Mars or the icy moons Europa or Enceladus. The article is divided into two main parts. The first part deals with the ecophysiology of methanogens in general, *i.e.* their ability to thrive under very harsh conditions like very high or low pH, temperature, or pressure. In the second part of the review, various celestial bodies are analysed in relation to their potential to host methanogens and an overview about past, current, and future astrobiological studies concerning methanogens is presented.

Chapter 4

There are several ways to quantify growth and/or CH_4 production of hydrogenotrophic methanogens, *e.g.* by determining optical density or CH_4 quantification by using gas chromatography, respectively. In general, these methods require expensive instruments and/or they are time-consuming. In this chapter a novel method for indirect quantification of methane evolution rate by measuring water evolution rate is presented. We show that this method is extremely accurate and precise. We used this method among others to rapidly screen various strains of methanogens regarding their CH_4 production potential.

Chapter 5

This paper represents the core of this thesis. It summarises the majority of the work done during the second half of my PhD studies. In this interdisciplinary paper, that combines studies of an international team in planetary sciences, chemistry, geochemistry, and microbiology, we analysed the potential of methanogens to thrive under putative Enceladus-like conditions. This study shows that there should be a sufficient amount of H_2, produced via serpentinization, to serve as electron donor for potential methanogenic activity on Enceladus. Further, it presents a very broad experimental setting for testing a methanogenic strain thriving under putative Enceladus-like conditions, *i.e.* in the presence of potential liquid and gaseous inhibitors detected in the plume, at high pressure, and at appropriate temperatures.

Chapter 6

This concluding chapter starts with summarizing the results of this thesis. Following, the idea of an origin of life on Enceladus and the impact of this thesis on future space missions are discussed. The chapter ends with a concluding statement together with an outlook on potential future studies related to this thesis.

2 Interior Structure of Enceladus

2.1 Overview

Enceladus' interior structure, *i.e.* a rocky core, a subsurface ocean and an icy shell, was heavily debated during the last decades. Pre-Cassini studies characterized Enceladus' interior as mostly water ice with a core that contains a small amount of rocks and/or metals by analysing the mean bulk density [Campbell and Anderson, 1989]. Even after the first Cassini data arrived, the possibility of a region of liquid water was not fully supported [Rappaport et al., 2007, Kieffer et al., 2006]. However, soon after acquiring more data, the first studies were presented of Enceladus having evolved from a satellite with a frozen, icy shell to combined liquid water-ice shell to a differentiated object, *i.e.* separated liquid and icy water shell, over the first 10 to 20 Myr after formation [Schubert et al., 2007]. During the duration of the Cassini mission the *status quo* was changing with each new dataset from a local sea embedded in the icy shell at the south pole [Collins and Goodman, 2007, Iess et al., 2014] to a global ocean [Nimmo and Pappalardo, 2006, Thomas et al., 2016, McKinnon, 2015] and *vice versa*. The current and most supported hypothesis is that Enceladus harbours a global subsurface ocean with a local depression at the south pole which leads to a thinning of the ice shell in this region (see Fig. 2.1).

This steady paradigm shift also affected the article presented in this chapter. It was first submitted in January 2014, when a global ocean was the current *status quo*. During the time the paper was under review, the study of Iess et al. [2014] was published which led the referees to ask us to include this new study and to revise the model towards one including a local sea. We made necessary changes to the paper and re-submitted it in December 2014. After some further delays the article was finally published in November 2015. At the time of publication, the paper was already outdated due to the findings by Thomas et al. [2016], who showed evidence for a global ocean and was able to explain the data presented by Iess et al. [2014].

However, I decided to include this paper into the present thesis due to the fact that it perfectly shows the dramatical changes on our point of view due to new findings by different instruments of the Cassini probe. In addition to the published version of the manuscript, I will also present the main results of the first version in the following section.

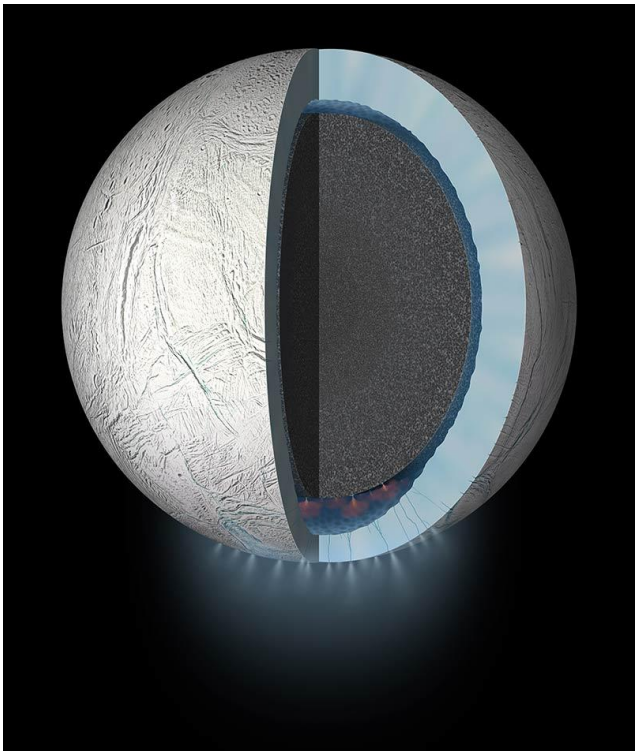

Fig. 2.1. Enceladus' interior structure: porous rocky core, global ocean with a local depression at the south pole and icy crust with a local thinning underneath the SPT (PIA20013), Credit: NASA/JPL-Caltech.

2.1.1 Global Ocean

In this model, three different cases concerning the mean density of Enceladus' core (ρ_C) were defined. As a function of ρ_C, the corresponding thickness of the water/ice shell was calculated. In the first case (C1) the assumption that the mean density of Titan's rocky core should be similar to Enceladus' core was used because both were formed in the same region in the Solar System. According to Titan's moment of inertia of about 0.34 [Iess et al., 2010], the secular Love number of Titan is about $k_s = 1$, which results in a core density of about $2\,550\,\mathrm{kg\,m^{-3}}$ [Sotin et al., 2010]. The next case (C2) was based on the study of Schubert et al. [2007] where the authors assumed Enceladus' core density to be similar to Io's bulk density ($\rho_C = 3\,530\,\mathrm{kg\,m^{-3}}$). According to Schubert et al. [2007] that is the highest possible value for a rock-metal core because Enceladus' core is likely to be less dense than Io's bulk density due to inclusions of, *e.g.* low-density hydrated silicates. The last case (C3) assumed a density similar to the grain density of typical hydrated carbonaceous CI chondrites ($\rho_C = 2\,500\,\mathrm{kg\,m^{-3}}$), which might be the building blocks of icy moons like Enceladus.

Furthermore, the composition and therefore the density of the overlying water/ice shell was varied between 917 kg m^{-3} (pure ice I) and 1 080 kg m^{-3} (water with some other constituents like NH_3 and tholins [Hendrix et al., 2010]).

2.1.2 Three Layer Model

For this model, Enceladus' interior is divided into a rocky core, a liquid water layer (ρ_{H_2O}=[960;1080] kg m^{-3}), and an ice shell (ρ_{H_2O}=[917;1 000] kg m^{-3}) and hydrostatic equilibrium is assumed. The core density varies between 2 500 kg m^{-3} (hydrated silicates) and 3 530 kg m^{-3} (bulk density of Io). Caused by the low mass of Enceladus and the resulting low radial pressure values, the density can be assumed to be constant within a certain layer.

In Table 2.1 the results for the three scenarios are presented and in Figure 2.2 the different ranges of the layers for the three scenarios are shown (for fixed ρ_{H_2O}=1 050 kg m^{-3} and ρ_{ice}=940 kg m^{-3}).

Tab. 2.1. 3-Layer Model for the three cases.

Case	$R_C^{(1)}$ [km]	$d_{H_2O}^{(2)}$ [km]	$d_{ice}^{(3)}$ [km]	$P_C^{(4)}$ [MPa]	$P_{MB}^{(5)}$ [MPa]	$MoI^{(6)}$
C1	184.55	41.79	25.76	35.12	4.17	0.328
C2	156.74	62.16	33.20	48.32	5.53	0.305
C3	186.58	40.38	25.14	34.47	4.06	0.330

(1) core radius, (2) thickness of the water shell, (3) thickness of the ice shell, (4) pressure at the centre of Enceladus, (5) pressure at the rock/water-layer boundary, (6) dimensionless moment of inertia

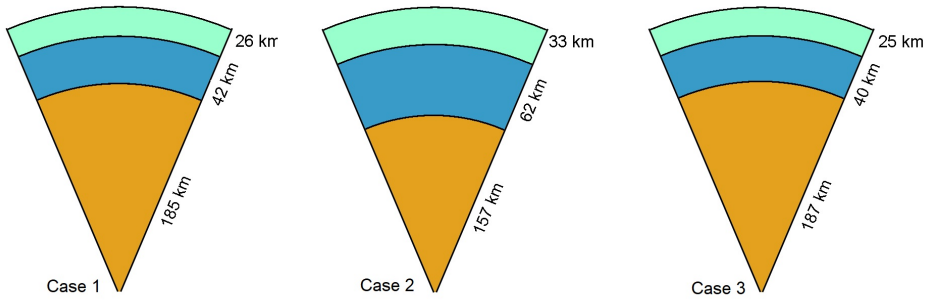

Fig. 2.2. Schematic diagram of Enceladus' interior for the three scenarios.

In this model, the thickness of the potential subsurface water ocean varies between approximately 40 and 60 km and is situated under an ice shell which is about 25 to 33 km thick. These results are in good agreement with previous studies (see, *e.g.* Barr and McKinnon [2007], Rappaport et al. [2007], or Schubert et al. [2007]).

2.1.3 Updated Calculations

In the methods part of the article shown in Chapter 5, a re-modelling concerning the hydrostatic pressure was made. In that updated version of the model shown in the present chapter, the core has an extension of 190 to 200 km, whereas the depth of the global ocean varies between 60 and 10 km with an ice shell thickness of 2.1 to 52.1 km. This leads to a pressure of approximately 44.3 to 25.2 bar or 80.1 to 56.2 bar (depending on the applied method, see Supplementary Methods in Appendix E) at the water-core-boundary. These numbers are in good agreement with the values presented in Hsu et al. [2015], where the upper pressure boundary for this region was also estimated to be approximately 80 bar. However, the presented model can only serve as a rough estimate as the ice shell has most likely a variable thickness with approximately 20 km on average and a local depression beneath the SPT, where the ice shell might be less than 5 km thick [Čadek et al., 2016].

2.2 Publication Details

Title: Modelling the Interior Structure of Enceladus Based on the 2014's Cassini Gravity Data
Authors: R.-S. Taubner, J. Leitner, M. G. Firneis, R. Hitzenberger
Status: Published online in *Origins of Life and Evolution of Biospheres*, November 12^{th}, 2015
Bibliographic reference: Orig Life Evol Biosph, Volume 46, Issue 2-3, pp 283-288
DOI: doi:10.1007/s11084-015-9475-9
Copyright Information: Due to copyright issues, the manuscript was added to this thesis in the "final accepted manuscript" version. The license for re-print of this version can be found in the Appendix A. Follow the doi to download the published version of the manuscript.
Own contributions: Literature research, method development, software implementation, testing and validation, preparation of figures and plots, drafting first manuscript version, coordinating correction state and finalization.

Noname manuscript No.
(will be inserted by the editor)

Modelling the Interior Structure of Enceladus Based on the 2014's Cassini Gravity Data

Taubner R.-S. · Leitner J.J. · Firneis M.G. · Hitzenberger R.

Received: date / Accepted: date

Abstract We present a model for the internal structure of Saturn's moon Enceladus. This model allows us to estimate the physical conditions at the bottom of the satellite's potential subsurface water reservoir and to determine the radial distribution of pressure and gravity. This leads to a better understanding of the physical and chemical conditions at the water/rock boundary. This boundary is the most promising area on icy moons for astrobiological studies as it could serve as a potential habitat for extraterrestrial life similar to terrestrial microbes that inhabit rocky mounds on Earth's sea floors.

Keywords Enceladus · icy moons · internal structure · subsurface water reservoir

1 Introduction

From the astrobiological point of view, icy moons are among the most interesting objects in the Solar System. Some of these moons could have subsurface oceans which may host extraterrestrial life. In this study we present a model for the interior structure of the icy moon Enceladus and discuss its potential habitability. Enceladus provides a unique insight into its interior through its active plumes which may originate in a potential subsurface sea [14]. The small mean radius of only 252.1 km [21] (for further parameters, see Table 1) indicates that the uncompressed density (see, e.g., [4]) of the satellite is almost equal to its bulk density, so a simplified model of Enceladus' interior is reasonable.

Taubner Ruth-Sophie
Research Platform: ExoLife, University of Vienna
A-1180 Vienna, Türkenschanzstraße 17
Tel.: +43-1-4227-23401
Fax: +43-1-4277-9234
E-mail: ruth-sophie.taubner@univie.ac.at

Previous studies of Enceladus' interior (e.g., [1,5,12,19]) assumed a two-layer structure with a rocky core (core density ρ_c between 2500 and 3527.5 $\mathrm{kg\,m^{-3}}$) and an icy outer shell (shell density $\rho_s \approx 1000\ \mathrm{kg\,m^{-3}}$). These estimations led to an ice shell thickness of approximately 100 km and a moment of inertia factor (MoI) of around 0.31. On the other hand, Rappaport et al. assumed a hydrated silicate core with $\rho_c \approx 2500\ \mathrm{kg\,m^{-3}}$ which results in an ice shell thickness of just 60 km [15]. According to the latest gravity measurements performed by the NASA spacecraft Cassini, Enceladus has a high MoI of 0.335 [7], which leads to the conclusion that this satellite is not in a fully relaxed shape, but is differentiated with a low-density core.

Table 1 Enceladus' main parameters.

$R^{(1)} = 252.1 \pm 0.2\,\mathrm{km}$, [21]	$\bar{\rho}^{(2)} = 1\,609.79 \pm 2.99\ \mathrm{kg\,m^{-3}}$, [20]
$M^{(3)} = 1.079888 \pm 0.001653 \cdot 10^{20}\,\mathrm{kg}$, [20]	$C_{22}^{(4)} = 1.5498 \pm 0.0156 \cdot 10^{-3}$, [7]
$T^{(5)} = 1.37$ days, [8]	$\omega^{(6)} = \frac{2\pi}{T} = 5.30818 \cdot 10^{-5}\ \mathrm{s^{-1}}$

(1) mean radius, (2) mean density, (3) mass, (4) degree-2 gravity coefficient, (5) mean sidereal period, (6) rotation rate

2 Model

2.1 2-Layer-Model

The MoI of Enceladus can be estimated using the Radau-Darwin approximation (see, e.g.,[18]):

$$MoI = \frac{C}{MR^2} = \frac{2}{3} \cdot \left\{ 1 - \frac{2}{5} \sqrt{\frac{4 - k_2}{1 + k_2}} \right\}, \tag{1}$$

where $k_2 = \frac{4C_{22}GM}{\omega^2 R^3} = 0.9896 \pm 0.0103$ is the fluid potential Love number. Therefore, Enceladus has a MoI of 0.3386 ± 0.0826. This is in agreement with the study by Iess et al. where the moment of inertia factor was estimated to be around 0.335 [7]. Because this value is less than 0.4, it also falls under the maximum MoI for a differentiated body [2].

Enceladus' mean radius R, its mean density $\bar{\rho}$, and the calculated MoI serve as the starting points for our model. Because of the low mass of Enceladus and the resulting low radial pressure values, the density can be assumed to be constant within a certain layer. To calculate the core mean density ρ_c and core radius R_c, we use a 2-layer-model (see, e.g., [5]):

$$\rho_c = \left(\frac{(\bar{\rho} - \rho_s)^{5/3})}{\frac{5}{2}\bar{\rho} \cdot MoI - \rho_s} \right)^{3/2} + \rho_s \ , \tag{2}$$

$$R_c = R \cdot \sqrt[3]{\frac{\bar{\rho} - \rho_s}{\rho_c - \rho_s}} \ . \tag{3}$$

We varied the composition, and therefore the density ρ_s of the overlying water/ice shell between 917 kg m^{-3} (pure ice I) and 1 080 kg m^{-3} (water with some other constituents such as NH_3 and tholins [6]). To illustrate our results we selected three different cases (C_{min}, C_{mean}, and C_{max}; see Table 2).

Table 2 Different cases for Enceladus' interior structure (2-Layer-Model).

case	$\rho_s^{(1)}$ [kg m^{-3}]	$R_c^{(2)}$ [km]	$d_{ice}^{(3)}$ [km]	$\rho_c^{(4)}$ [kg m^{-3}]
C_{min}	917	198.8	53.3	2327.1
C_{mean}	1000	190.4	61.7	2412.7
C_{max}	1080	179.3	76.3	2550.8

(1) mean shell density, (2) core radius, (3) thickness of the ice shell, (4) mean core density

2.2 Local Southern Subsurface Sea

According to previous studies, either a local subsurface water reservoir beneath the South Polar Terrain (SPT) of Enceladus (e.g., [7]) or a global ocean with a thinned out ice shell at the southern region [22] seems likely. Therefore, the second aim of our model is to estimate the pressure at the water/rock-boundary of this potential aquifer beneath Encealdus' southern region. We assume the sea or the depletion, respectively, to have the shape of a rotational paraboloid. For each of the cases C_{min}, C_{mean}, and C_{max} (Table 2) we calculated the pressure at the water/rock boundary depending on the longitude and the maximum depth of the subsurface aquifer. As seen in Figure 1 for C_{mean} and in Table 3 for all three cases, the pressure value at the sea floor of the potential subsurface water reservoir lies between 28 and 45 bar.

2.3 Radial Pressure Gradient

We also calculated the radial distributions of pressure ($dp = \rho \cdot g(r)dr$) and gravitational acceleration ($g(r) = \frac{GM(r)}{r^2}$) for case C_{mean} with a subsurface water aquifer 10 km thick (see Figure 2). Under these assumptions we obtained a pressure at the core/water-boundary of $32.9 \cdot 10^5$Pa and a gravitational acceleration of 0.128 ms^{-2}.

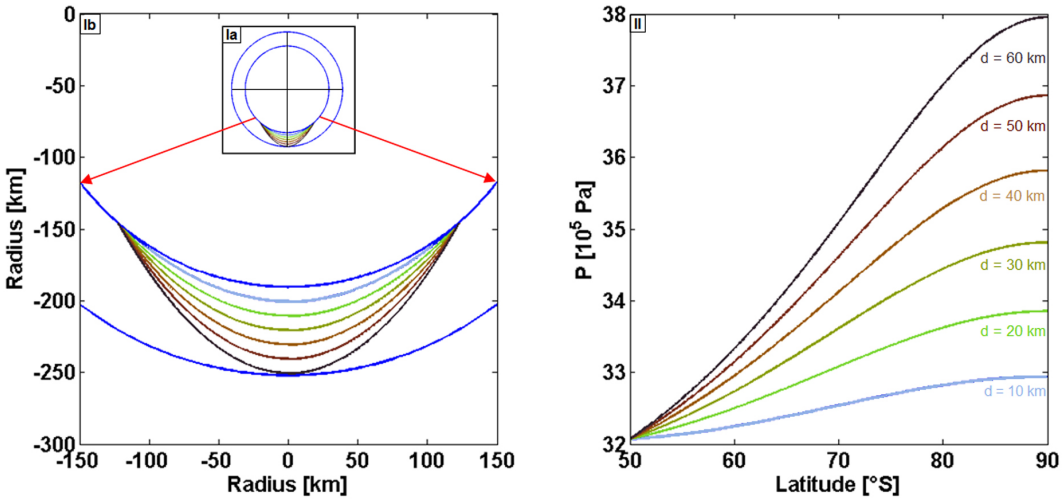

Fig. 1 Ia: Position of the local southern subsurface sea; Ib: magnified representation of the relevant area in Ia; the coloured lines give different potential depths of the local sea; II: pressure at the core/mantle-boundary for case C_{mean} for various water depths between 10 and 60 km.

Table 3 Pressure at the water-rock boundary for different water depths for the three cases C_{min}, C_{mean}, and C_{max}.

case	$p^{(1)}_{min}$ [10^5Pa]	$p^{(2)}_{max}$ [10^5Pa]
C_{min}	28	33
C_{mean}	32	38
C_{max}	38	45

(1) minimum pressure, (2) maximum pressure

To validate this model we applied it to the different layers of Earth. Gravitational acceleration as well as the pressure gradient in the outer layers obtained by our model agree well with the Preliminary Reference Earth Model (PREM, [3]), but the pressure values for Earth's inner core are too small. This deviation is due to the exclusion of compression or phase transition effects from our model, as these effects are negligible for small bodies like Enceladus where the uncompressed density is equal to the bulk density.

3 Conclusion

The most promising area on Enceladus where life may exist is at the sea floor of the potential subsurface water reservoir. Geochemical low-temperature interactions between these layers seem reasonable (see, e.g., [23]). One of these processes may be serpentinization of ultramafic rocks which is accompanied by the production of H_2 [17]. Furthermore, in such an environment dissolution of minerals could provide nutrients for possible lifeforms.

The organisms would have to be able to live without photosynthesis or its by-products such as oxygen. According to McKay et al., there are three

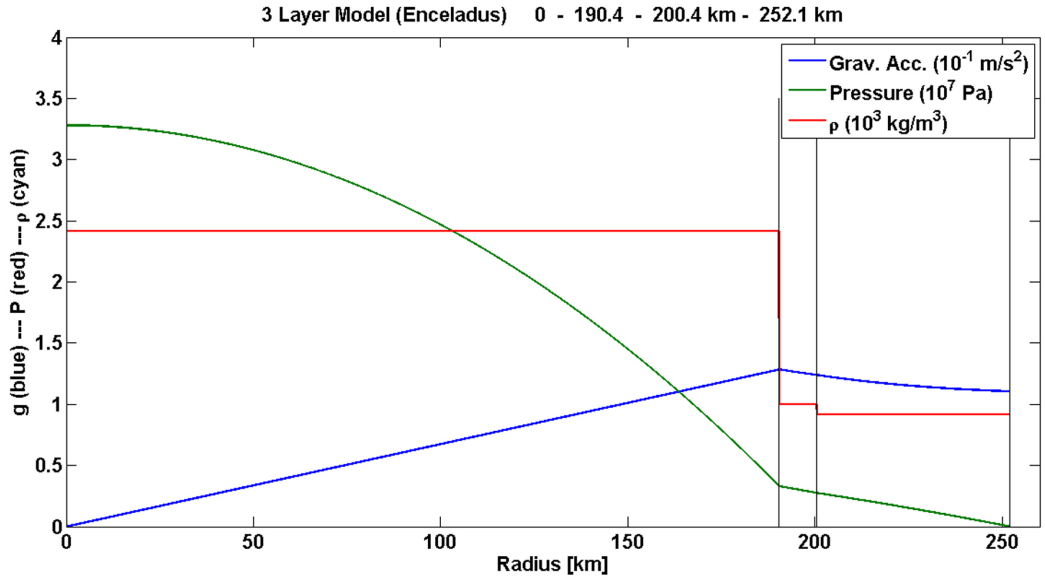

Fig. 2 Physical parameters for case C_{mean} and a 10 km thick water layer. Estimations were made for the radial gradient from the moon's core to its south pole.

known terrestrial microbial ecosystems that would fit into such a habitat [11]: two are based on methanogens and the third is built on sulphur-reducing bacteria. However, the existence of sulphur-reducing bacteria is questionable because oxidized sulphur may not exist on Enceladus, which limits/excludes the process of sulphur (sulphate) reduction.

In further experimental studies, we will investigate the habitability of the subsurface water aquifer. In accordance with our model, microorganisms would have to resist a pressure of approximately 28 to 45 bar (equivalent to 2.8 to 4.5 MPa, see Table 3), which is roughly equivalent to the pressure at a depth of 290 to 460 m below sea level on Earth. Microorganisms tolerant to such pressures (and higher) are well known on Earth, e.g., the barotolerant bacteria *S. hanedai* IAM12641 (optimal growth at 0.1 MPa, [10]) or even obligate barophilic microbes such as *M. yayanosii* DB21MT-5 which was isolated from the Mariana Trench and for which no growth was detected at pressures of less than 50 MPa [9]. Even multicellular organisms like deep-sea fish and worms can easily resist the pressure at this depth in the terrestrial seas, e.g., the hadal snailfish *Pseudoliparis amblystomopsis* which was even found at a depth of 8 145 m in the Mariana Trench [13].

To conclude, pressure should not be a limiting parameter for life in Enceladus' subsurface sea.

Acknowledgements We acknowledge financial support of this study by the University of Vienna in the framework of Research Platform ExoLife (FPF-234).

References

1. Barr A. C. & McKinnon W. B., Convection in Enceladus' ice shell: Conditions for initiation, Geophys Res Lett, 34, Issue 9 (2007)
2. de Pater I. & Lissauer J. J., Planetary Sciences, 33. Cambridge University Press, Cambridge, UK (2010)
3. Dziewonski A. M. & Anderson D. L., Preliminary reference Earth model, Phys Earth Planet In, 25, 297-356 (1981)
4. Faure G. & Mensing T.M., Introduction to Planetary Science: The Geological Perspective, 28-32. Springer Netherlands (2007)
5. Hussmann H. & Sohl F. & Spohn T., Subsurface oceans and deep interiors of medium-sized outer planet satellites and large trans-neptunian objects, Icarus, 185, 258-273 (2006)
6. Hendrix A. et al., The ultraviolet reflectance of Enceladus: Implications for surface composition, Icarus, 206, 608-617 (2010)
7. Iess L. et al., The Gravity Field and Interior Structure of Enceladus, Science, 344, 78-80 (2014)
8. Jacobson R.A., SAT339 - JPL satellite ephemeris (2010)
9. Kato C. et al., Extremely Barophilic Bacteria Isolated from the Mariana Trench, Challenger Deep, at a Depth of 11 000 Meters, Appl Environ Microbiol, 64, 1510-1513 (1998)
10. MacDonell M.T., Colwell R.R., Phylogeny of the Vibrionaceae and recommendation for two new genera *Listonella* and *Shewanella*, Syst Appl Microbiol, 6, 171-182 (1985)
11. McKay C. P. et al., The Possible Origin and Persistence of Life on Enceladus and Detection of Biomarkers in the Plume, Astrobiology, 8, 909-919 (2008)
12. Roberts J.H., The fluffy core of Enceladus, Icarus, 258, 54-66 (2015)
13. Morelle, R., New record for deepest fish, BBC News, 19/12/2014, `http://www.bbc.com/news/science-environment-30541065` (2014)
14. Postberg F. et al., Sodium salts in E-ring ice grains from an ocean below the surface of Enceladus, Nature, 459, 1098-1101 (2009)
15. Rappaport N. J. et al., Mass and interior of Enceladus from Cassini data analysis, Icarus, 190, 175-178 (2007)
16. McKinnon, W.B., Effect of Enceladus's rapid synchronous spin on interpretation of Cassini gravity, Geophys. Res. Lett., 42, 2137-2143 (2015)
17. Schrenk M. O. et al., Serpentinization, Carbon, and Deep Life, Reviews in Mineralogy & Geochemistry, 75, 575-606 (2013)
18. Schubert G. et al, Jupiter: The Planet, Satellites and Magnetosphere, 281-306. Cambridge planetary science, Vol. 1, Cambridge, UK: Cambridge University Press (2004)
19. Schubert G. et al., Enceladus: Present internal structure and differentiation by early and long-term radiogenic heating, Icarus, 188, 345-355 (2007)
20. Taubner R.-S., The possibility of the existence of a nitrogen cycle within Enceladus, Master Thesis, University of Vienna (2012)
21. Thomas P. C., Sizes, shapes, and derived properties of the saturnian satellites after the Cassini nominal mission, Icarus, 208, 395-401 (2010)
22. Thomas P. C. et al., Enceladus's measured physical libration requires a global subsurface ocean, Icarus, 264, 37-47 (2015)
23. Zolotov M. Y., An oceanic composition on early and today's Enceladus, Geophys Res Lett, 34, L23203 (2007)

Methanogens in the Solar System 3

3.1 Overview

On Earth, methanogens are known to be the only organisms to be capable of producing methane (CH_4) as a product of their metabolism. Therefore, the detection of CH_4 in relation to other carbon containing isotopes or certain hydrocarbons on other celestial bodies could be an indirect sign for biological activity (for more details, see the section "Discussion" in the paper presented in Chapter 5). Due to the fact that CH_4 was already detected on several bodies in the Solar System (in the atmosphere of all planets, on the icy moons Enceladus and Titan, and the dwarf planets Pluto, Eris, and Makemake), compiling a comprehensive review about the ecophysiology of methanogens in the context of astrobiological and planetological studies was long overdue.

In this review, an overview about the main ecophysiological characteristics of methanogens is given, *i.e.* growth under a wide range of temperatures, different amounts of radiation, osmolarities, pH values, and levels of desiccation. Further, these characteristics are compared to the environmental conditions of potential extraterrestrial habitats in the Solar System, in particular to Mars and icy moons. The potential capability to be able to inhabit these extraterrestrial biospheres is shown. The following chapter deals with an overview about studies of methanogens with an astrobiological relevance. At the end, there is a discussion about the role of methanogens in the search for extraterrestrial life in the Solar System and an outlook on the feasibility and the necessity of future astrobiological studies with methanogens. The expanse of this review can be seen in the amount of 270 cited references.

3.2 Publication Details

Title: Assessing the Ecophysiology of Methanogens in the Context of Recent Astrobiological and Planetological Studies
Authors: R.-S. Taubner, C. Schleper, M. G. Firneis, S. K.-M. R. Rittmann
Status: Published online in *Life*, December 3rd, 2015
Bibliographic reference: Life, Volume 5, Issue 4, pp 1652-1686
DOI: doi:10.3390/life5041652

Own contributions: Literature research, preparation of figures and plots, writing parts of the first manuscript version (focus on chapter 1, 3, 4, and 5), editing and approving manuscript.

life

MDPI

Review

Assessing the Ecophysiology of Methanogens in the Context of Recent Astrobiological and Planetological Studies

Ruth-Sophie Taubner [1,2,*], Christa Schleper [3], Maria G. Firneis [1,2] and Simon K.-M. R. Rittmann [3,*]

Received: 8 May 2015; Accepted: 10 November 2015; Published: 3 December 2015
Academic Editors: Hans-Peter Klenk , Michael W. W. Adams and Roger A. Garrett

1 Research Platform: ExoLife, University of Vienna, Türkenschanzstraße 17, 1180 Vienna, Austria
2 Institute of Astrophysics, University of Vienna, Türkenschanzstraße 17, 1180 Vienna, Austria
3 Archaea Biology and Ecogenomics Division, Department of Ecogenomics and Systems Biology, University of Vienna, Althanstraße 14, 1090 Vienna, Austria
* Correspondence: ruth-sophie.taubner@univie.ac.at (R.-S.T.); simon.rittmann@univie.ac.at (S.K.-M.R.R.); Tel.: +43-1-4277-51111 (R.-S.T.); +43-1-4277-76515 (S.K.-M.R.R.); Fax: +43-1-4277-51186 (R.-S.T.); +43-1-4277-876515 (S.K.-M.R.R.)

Abstract: Among all known microbes capable of thriving under extreme and, therefore, potentially extraterrestrial environmental conditions, methanogens from the domain Archaea are intriguing organisms. This is due to their broad metabolic versatility, enormous diversity, and ability to grow under extreme environmental conditions. Several studies revealed that growth conditions of methanogens are compatible with environmental conditions on extraterrestrial bodies throughout the Solar System. Hence, life in the Solar System might not be limited to the classical habitable zone. In this contribution we assess the main ecophysiological characteristics of methanogens and compare these to the environmental conditions of putative habitats in the Solar System, in particular Mars and icy moons. Eventually, we give an outlook on the feasibility and the necessity of future astrobiological studies concerning methanogens.

Keywords: Archaea; extremophiles; metabolism; Solar System; methanogenesis; space; microorganism; Mars; Earth; icy moons

1. Introduction

Methane (CH_4), the smallest hydrocarbon molecule, is frequently detected in different anoxic environments as well as in the atmosphere of Earth, and its presence has also been verified on other Solar System bodies, e.g., on Saturn's icy moons Titan [1] and Enceladus [2] or on Mars [3–5]. On Earth, CH_4 is currently contributing to global warming, because it is a potent greenhouse gas, but nowadays it is also one of the most important fossil fuels for human society. Most of the CH_4 present on Earth is of biogenic origin [6] and there is still the elusive possibility that also CH_4 detected on other Solar System bodies could be of biological origin. To date, the only organisms known to be capable of producing CH_4 as a side product of their energy conserving metabolism are methanogenic microorganisms (methanogens) [7].

Methanogens are an intriguing group of prokaryotes from the domain Archaea. Initially, Archaea were often considered being extremophilic microorganisms with adaptations to high temperature or high salt. However, the importance of archaea contributing to biogeochemical cycles in extremophilic, but also in non-extremophilic habitats, on Earth is tremendous [8]. Within the domain archaea methanogens so far only belong exclusively to the phylum Euryarchaeota, one of

the currently five established archaeal phyla [8], but metagenomic sequencing revealed a putative methanogenic micoroganism in the phylum Bathyarchaeota [9].

Methanogens are divided into five classes (Methanobacteria, Methanococci, Methanomicrobia, Methanopyri, and Thermoplasmata) and seven orders (Methanobaceriales, Methanococcales, Methanomicrobiales, Methanosarcinales, Methanocellales, Methanopyrales, and Methanomassiliicoccales) [6,8,10]. The seventh order of methanogens (Methanomassiliicoccales) has only recently been discovered and belongs to the class Thermoplasmata [11,12]. All yet characterized methanogens are known to be obligate anaerobic chemolithoautotrophs or chemolithoheterotrophs capable of producing CH_4 in order to acquire energy in a process referred to as methanogenesis [6,10,11,13–16], from the following substrates:

(1) from hydrogen (H_2) and carbon dioxide (CO_2) or from carbon monoxide (CO) or from formate (HCO_2^-)
(2) from methanol, methylamines, methanethiol or methylsulfide
(3) from acetate
(4) or from methanol (CH_3OH), methylamines and methylsulfide as methyl group donor and H_2 as electron source.

From a phylogenetic perspective, methanogens putatively resemble one of the oldest life forms having emerged on Earth. Furthermore, membrane lipids of putative methanogenic origin were detected in fossils dating 2.7 billions years back in Earth's history [17]. Moreover, also CH_4 of putative biological origin, and therefore of possibly methanogenic origin, was detected in samples dating 3.7 billion years back in time [18]. Regarding the ability of methanogens for fixing CO_2 into cellular carbon biological methanogenensis could have emerged as first metabolic reactions next to hydrothermal vent systems [19]. However, this view is still under investigation and discussion [20,21].

Methanogens can be found in almost every anoxic environment, like in swamps, deep soil sediments, peat bogs, sediments, permafrost soils, anaerobic digester, sediments of aquatic environments, and in the intestine of half of the human population as well as in animals [6,10,22–37]. Methanogens play an important role in Earth's global carbon cycle where they are involved in the last step of biomass breakdown [6,10]. Moreover, methanogens are of relevance to agriculture in general and to livestock production in particular, because CH_4 emissions from industrialized animal production farms and from wetland crop production (e.g., rice fields) are substantially contributing to an increase in global warming. Furthermore, methanogens are interesting study objects because they can withstand extreme environmental conditions [38,39].

Methanogens are utilized biotechnologically for biogas production in anaerobic digesters or for anaerobic wastewater treatment. In the former process methanogens perform the final step in anaerobic digestion of organic waste or biomass by producing CH_4 [6,37]. Currently methanogens are being explored to be applied in biological CH_4 production processes, referred to as biological methanation or biomethanation. Therein hydrogenotrophic methanogens are examined to be used for high rate volumetric CH_4 production from CO_2 and H_2 and/or microbiological (bio)gas upgrading [13,40–44].

Astonishing morphological features of methanogens include, e.g., the methanochondroitin sheath of certain methanosarcia species [45], but typical morphologies of methanogens are shown in Figure 1.

Hitherto more than 150 pure cultures of methanogens are described [46,47] exhibiting extraordinary biochemical, morphological, physiological, metabolic and biotechnological features [6,10,11,13,14,40,42–44,48–51]. Due to their ubiquitous presence, their metabolic versatility and their ability to endure multiple extreme environmental conditions methanogens are being considered in astrobiological research.

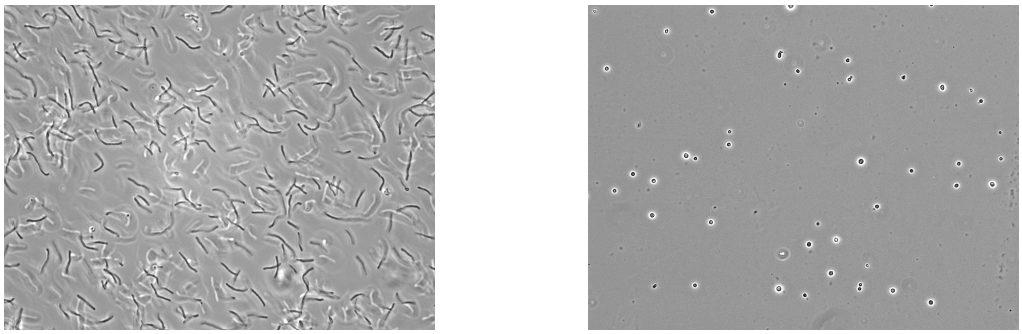

(a) **(b)**

Figure 1. Phase contrast images of *Methanothermobacter marburgensis* and *Methanosarcina soligelidi*. (**a**) Phase contrast image (magnification 1000×) of *M. marburgensis* DSM 2133. Specimen was obtained in late exponential phase from a fed-batch fermentation. The cells are rod shaped and elongated; (**b**) Phase contrast image (magnification 1000×) of *M. soligelidi* DSM 26065. Specimen was obtained from a closed batch cultivation. The cells are coccoid.

In the last decade, new findings about extrasolar planetary systems, icy moons in the Solar System, but also the newly explored capabilities of extremophiles led to a rethinking of the extent of the classical habitable zone [52,53]. Various attempts have been made to define new potential niches of life in the Solar System, e.g., in the concept of the "life supporting zone" [54]. This is a generalization of Kasting's concept of a habitable zone, where alternative solvents—*i.e.*, other than water or solvents of water/ammonia—determine their own habitable zones around a star. Nevertheless, the detection of liquid water in the outer Solar System opens up entirely new areas far beyond the water snow line [55] where life-as-we-know-it could be situated.

Of astrobiological interest are those Solar System bodies on which we assume at least local areas that could fulfil the physical and chemical requirements that methanogens could propagate in an extraterrestrial environment. This includes the residues of near-surface melt water on Mars and subsurface oceans or local seas on various icy moons like Europa or Enceladus.

Mars, the fourth planet in the Solar System, seems to have possessed a huge amount of liquid water on its surface in the Noachian period [56] and therefore could have been a habitable planet in its "early" years. Due to its low atmospheric pressure, there cannot be liquid water on its surface currently. Nevertheless, there are indications for subsurface aquifers [57]. Methanogens would perfectly fit into this subsurface environment especially due to their ecophysiological capabilities to tolerate and endure extreme conditions. Several studies focus on the potential of methanogens to grow under Martian-like environmental conditions [58–71]. The detection of subsurface water aquifers on the icy moons in the outer Solar System extended the group of potential habitats by far. However, at the moment, methanogens and sulfur-reducing bacteria seem to be the only terrestrial microbes that could propagate in such an environment (see Section 3).

In this contribution we outline the main ecophysiological characteristics of methanogens. We compare these characteristics of methanogens to the environmental conditions of their putative habitats in the Solar System, in particular to Mars and icy moons. We will point out their potential capability to be able to inhabit extraterrestrial biospheres in the planetary system. We present an overview concerning studies of methanogens with an astrobiological relevance and we present our conclusions about the role of methanogens for the search for extraterrestrial life in the Solar System. Eventually, we give an outlook on the feasibility and the necessity of future astrobiological studies with these microbes.

2. Ecophysiological Characteristics of Methanogens

Methanogens are well known for a variety of astonishing morphological and ecophysiological features. One of these ecophysiological features is their ability to grow hydrogenotrophically while varying their growth-to-product-yield $Y_{(x/CH4)}$—a mechanism also referred to as uncoupling [6,10,40,44,72–78]. Uncoupling in methanogens occurs when environmental factors (*i.e.*, pH, temperature, reducing compounds, H_2 concentrations) become sub- or superoptimal or if they change. As a consequence of changing environmental factors methanogens react rapidly by altering their metabolism redirecting the carbon flux to either biomass formation or to maintaining cellular homoeostasis. As an example it has been found that *Methanobacterium thermoautotrophicum* responds to variations in H_2 concentration by differentially expressing methenyl-tetrahydromethanopterin dehydrogenase and methyl coenzyme M reductase isoenzymes [77]. Other examples include the varying $Y_{(x/CH4)}$ in *Methanothermobacter marburgensis* upon exposure to different ammonia concentration or dilution rates [40,44]. Also phosphate limitation [72] and iron- or H_2-limited cultures [73] as well as temperature [78] were shown to uncouple $Y_{(x/CH4)}$. In their natural environment methanogens are occasionally confined to a shallow reaction zone where they might achieve only little net growth in order to be able to propagate or gain energy for metabolic reactions [79].

We will review studies on methanogens in relation to their ecophysiological adaptations to different temperature zones. Furthermore, we will highlight the main ecophysiological and metabolic features of methanogens that allow them to grow under different amounts of radiation, osmolarities, pH values, and desiccation.

2.1. Temperature

Methanogens span a huge temperature range with organisms that are psychrophilic, mesophilic, thermophilic, and even hyperthermophilic [22–35,80] (see Figure 2). Recently a novel hydrogenotrophic methanogen, "*Candidatus* Methanoflorens stordalenmirensis" was identified to be frequently present in permafrost wetland and members of *Candidatus* familiy "Methanoflorentaceae" are widespread in permafrost and appear to be key mediators of CH_4 emissions in cold but seasonally thawing environments [36]. Another psychrophilic strain, *Methanosarcina* sp. SMA-21 (now referred to as *M. solegelidi* SMA-21) was shown to tolerate freezing and survival of 98.5% in comparison to, e.g., *Methanobacterium* sp. MC-20 exhibiting only 1% survival [81]. Furthermore, the temperature-dependent starvation tolerance compared among different *Methanosarcina* species and *M. solegelidi* SMA-21 was shown to comprise a high survival potential at 4 °C and at 28 °C compared to the two other methanogens tested [81].

Although individual strains of methanogens comprise a temperature window for growth of approximately 45 °C, the main biochemical methanogenesis pathways are not restricted to a certain temperature. However, pathways of methanogenesis are functional under conditions spanning a temperature range from below 0 °C [38] up to the hottest ever determined metabolic reactions of any organism described, as high as 122 °C [80]. The methanogen exhibiting the highest ever measured growth temperature is *Methanopyrus kandleri* strain 116. This organism is able to grow at 122 °C [80].

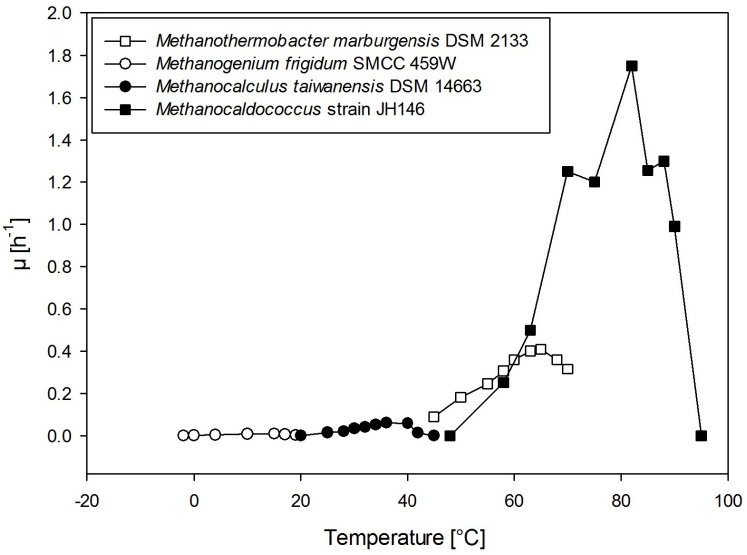

Figure 2. A plot of specific growth rates (μ) of four methanogenic strains. The four strains were arbitrarily selected independent of the specific metabolism as well as independent of growth conditions, but to span the entire temperature range from psychrophilic to hyperthermophilic growth conditions. Each single data point has been carefully retrieved from literature; for *M. marburgensis* DSM 2133 [82], for *M. frigidum* SMCC 459W [33], for *M. taiwanensis* DSM 14663 [83], for *Methanocaldococcus* strain JH146 [78]. Interestingly, with increasing growth temperature maximum μ values were found to increase.

Outer Solar System bodies, which could putatively support methanogenic life, are situated in the temperature range of psychrophiles [84] (especially in the subsurface water reservoirs) or even colder (see Section 3, Table 3). Therefore, especially psychrophilic methanogens should be of great interest to astrobiological research. However, the temperature can be locally higher, especially near potential hydrothermal vents.

In order to distinguish different levels of psychrophily, psychrophilic methanogens are classified according to their temperature niche, which is narrow or wide [38,85]. For this reason the terms "stenopsychrophile" and "eurypsychrophile" have been introduced [38,86,87]. Stenopsychrophiles are considered true psychrophiles, which can only thrive in a narrow temperature range and cannot be cultivated when exposed to elevated temperatures. In contrast, eurypsychrophiles can tolerate higher temperatures and comprise a higher mean optimum growth temperature compared to stenopsychrophiles. Psychrophilic methanogens have already been the topic of many research endeavours, because they play an important role in 75% of Earth's habitats [38,85]. A summary of psychrophilic methanogenic strains can be found in Table 1.

Mechanisms for temperature adaptation in methanogens were identified on different cellular and structural levels. At the protein level cold adaptation mechanisms were examined in *Methanococcoides burtonii*. Elongation factor 2 (EF2) has been found to be active at low but to be unstable at high growth temperatures [88–90]. Furthermore, EF2 interacting proteins of *M. burtonii* but also compatible solutes are involved in activating as well as stabilizing the protein machinery under low growth temperatures [90]. In a study by Lim *et al.* a putative DEAD-box RNA helicase gene (deaD) was identified in *Methanococcoides burtonii* that was abundantly expressed at 4 °C [91].

Table 1. Summary of currently known psychrophilic strains and their main temperature and pH features.

Strain	Temp. [°C]			pH			Ref.
	min.	opt	max	min.	opt.	max.	
Methanospirillum psychrodurum	4	25	32	6.5	7	8	[92]
Methanosarcina baltica	3	21	28	6.3	7.2	7.5	[32]
Methanosarcina lacustris	1	25	35	4.5	7	8.5	[93]
Methanolobus psychrophilus	0	18	25	6	7–7.2	8	[94]
Methanogenium marinum	5	25	25	5.5	6–6.6	7.7	[95]
Methanogenium frigidum	0	15	17	6.3	7.5–7.9	8	[33]
Methanohalobium evestigatum	50	n.a. [1]	n.a.	n.a.	7.4	n.a.	[96]
Methanogenium cariaci	15	20–25	35	6	6.8–7.2	7.5	[97]
Methanogenium boonei	5	19.4	25.6	6.4	n.a.	7.8	[98]
Methanoculleus marisnigri	15	20–25	48	6	6.2–6.6	7.6	[99]
Methanoculleus chikugoensis	15	25	40	6.7	6.7–7.2	8	[100]
Methanococcoides alaskense	2.3	23.6	28.4	6.3	n.a.	7.5	[101]
Methanococcoides burtonii	1.7	23.4	29.5	6.8	n.a.	8.2	[102]
Methanospirillum stamsii	5	20–30	37	6.0	7.0–7.5	10	[31]
Methanosarcina soligelidi	0	28	54	4.8	7.8	9.9	[34]
Candidatus "Methanoflorens stordalenmirensis"	n.a.	n.a.	n.a.	n.a.	n.a.	n.a.	[36]

[1] not available.

A similar observation was made in the hyperthermophilic archaeon *Thermococcus kodakarensis* where a homologous DEAD-box helicase gene TK0306 (Tk-DeaD) was induced under suboptimal growth temperatures [103] suggesting that this DEAD-box helicase is generally expressed as a result of cold stress. Different from cold shifts of thermophiles the methanogen *M. burtonii* did not show decreased modifications of its tRNAs. Like in bacteria the organism generally exhibited few modifications, in particular dihydrouridine incorporation into tRNA.

Furthermore, a genome comparison of two cold-adapted archaea, *Methanogenium frigidum* and *M. burtonii*, was done in order to identify genomic characteristics distinguishing these two-species from other organisms. Predicted and modelled proteins from *M. frigidum* and *M. burtonii* comprise a higher quantity of non-charged polar amino acids in the solvent-accessible protein area. Hence, glutamin and threonin were detected in higher abundance in the proteins. Also a lower content of hydrophobic amino acids, particularly leucin, could be revealed [104]. Furthermore, Saunders *et al*. identified a cold shock domain (CSD) protein (CspA homolog) in *M. frigidum* as well as two hypothetical proteins with CSD-folds and a unique winged helix DNA-binding domain protein in *M. burtonii* [104]. In another study, a proteomics approach was employed to analyze the functional characteristics of *Methanosarcina barkeri* in a low-temperature shock response (from 37 °C to 15 °C) or for its low-temperature adaptation strategies at 15 °C. By applying a combined approach of proteomics and growth studies insights into the low-temperature adaptation capacity of *M. barkeri* could be revealed [105]. Above mentioned findings indicate that mechanisms on the genome level (e.g., expression of deaD at suboptimal growth temperature) as well as on the proteome level (e.g., activity of EF2) distinguish stenopsychrophilic, eurypsychrophilic as well as (hyper-)thermophilic methanogens regarding their ecophysiologcal adaptations forced to grow at suboptimal temperatures.

Another adaptation mechanism of methanogens to growth temperature variation is their ability to modify membrane lipids in order to maintain membrane fluidity, *i.e.*, the lipid membrane of organisms has to be kept in the liquid crystalline phase in order to stay functional. Generally, the archaeal lipid membrane was found to stay in the liquid crystalline phase between 0 to 100 °C [106]. In

order to maintain membrane fluidity psychrophilic methanogens have adapted growth temperature mediated lipid unsaturation by selective saturation through the action of geranylgeranyl reductase instead of applying unsaturation mechanisms occurring in bacteria [107]. On the other hand, a recent survey indicated that the ether lipid membrane composition in general, or its unsaturation properties of methanogens in particular, are not a clear indicator whether the organism is adapted to a life in cold or hot environments [106]. For example the lipid membrane of *M. thermoautotrophicus*, growing at 65 °C, contains both archaeol and the membrane spanning caldarchaeol as do some methanogens growing at 37 °C. Moreover, the core membrane lipids of *M. kandleri*, growing at 90 °C, is archaeol [106]. However upon increasing growth temperature of *Methanocaldococcus jannaschii* from 45 °C to 65 °C the lipid membrane composition changes from initially, mainly archaeol containing lipid membranes, to cyclic archaeol as well as caldarchaeol [106,108]. Interestingly, the presence of double bonds in isoprenoid chains also does not indicate an adaptation to lower growth temperatures [106].

2.2. Pressure

Methanogens are also fascinating organisms due to their ability to tolerate and to grow at low-pressure as well as under overpressure conditions. In some of their natural environments (e.g., sea floor) methanogens have to tolerate >20 MPa overpressure [28,29,79]. Cultivation of methanogens under moderate overpressure conditions (up to 300 kPa) can be performed in closed batch fermentation in serum bottles [109] as well as in bioreactors [43,110]. Cultivation of methanogens under low pressure conditions and at pressures beyond 300 kPa requires special equipment for cultivation [58,59,111–113]. Low-pressure experiments are relevant for astrobiological research, because on some Solar System bodies (e.g., Mars, see Section 4.1), compared to Earth, lower above ground pressure occurs, which is due to special planetary and atmospheric characteristics.

Two different methanogenic strains were examined under moderate overpressure conditions, up to 300 kPa, regarding their growth and CH_4 production kinetics using bioreactors in continuous culture and under fed-batch conditions [42,43,110]. Cultivation of the thermophilic methanogen KN-15 was examined under pressurized fed-batch as well as under continuous culture conditions. In fed-batch culture, both, the point at which biomass growth kinetics changed from exponential growth to linear growth as well as μ increased with an increase of overpressure [110]. Results for the cultivation of *M. marburgensis* showed that CH_4 production is substrate limited in relation to gas availability [43]. Although applying overpressure the maximum physiological capacity could not be reached. However, unfortunately, no experiments were conducted yet aiming to elucidate the intracellular response to substrate limitation in *M. marburgensis*.

M. jannaschii was cultivated under overpressure as well as under gas limited conditions. Growth only occurred if gas availability was sufficient and it was found that *M. jannaschii* exhibited a stress response under both, overpressure and low-pressure cultivation conditions. Moreover, pressure induced a response on the transcriptional level in addition to a substrate limitation stress [113].

Overpressure and decompression experiments were performed using *M. jannaschii* in a specially equipped high-pressure bioreactor [111]. Upon rapid decompression from approximately 26 MPa to atmospheric pressure, *M. jannaschii* cell envelopes ruptured. However, when the decompression time was increased from 1 s to 5 min the rupture of *M. jannaschii* cell envelopes significantly decreased [111]. Additional overpressure and high-temperature investigations using *Methanococcus thermolithotrophicus* were accomplished in 10 mL nickel tubes and applying a set of autoclaves connected in series. This set-up enabled fast (10 min) temperature and overpressure changes of 400 °C and 400 MPa, respectively [114]. While overpressure of 50 MPa was found to be optimal for the growth of *M. thermolithotrophicus* applying overpressure of >75 MPa resulted in increased cell lysis as well as in changes of morphology and propagation characteristics [114]. Furthermore, *M. jannaschii* was studied under overpressure conditions by applying helium or argon and H_2/CO_2 at different temperatures. At both 86 °C and 90 °C growth and CH_4 production of *M. jannaschii*

became accelerated at up to 75 MPa overpressure, and $Y_{(x/CH4)}$ was uncoupled above 90 °C. The high-temperature limit for CH_4 production of *M. jannaschii* was found to be increased by increasing pressure, but not if H_2/CO_2 (4:1 ratio) was applied [112].

The response to an increase in CO_2 pressure on methanogens has been inconsistently examined in microcosms experiments mimicking a biocoenosis found in deep subsurface oil reservoir formations (55 °C, 5 MPa). Methanogenesis was found to occur under both, overpressure as well as low-pressure CO_2 conditions. By increasing CO_2 pressure the rate of methanogenesis was accelerated and, depending on the pressure of CO_2, different methanogenic pathways were found to be activated [115].

These adaptations towards low- and also high-pressure reveal that methanogens can survive and may be cultivated under a variety of growth conditions including multi-factorial stress conditions (e.g., substrate limitation, pressure) [10,44,58] and they respond to environmental changes in plentiful metabolic adaptations such as the utilization of different methanogenic pathways as well as the activation of overflow metabolism due to variations of CO_2 and CO partial pressure [15,16,115]. Due to their potential to adapt to changing and sometimes extreme environmental conditions, methanogens seem to be ideal candidates for astrobiological studies (see Section 4).

2.3. pH

Organisms adapted to extremely acidic conditions are found among bacteria, archaea and fungi. Many hyperthermophilic archaea of the family *Sulfolobaceae* may thrive at pH values between 1 and 4.5 [116–118] and strains from the euryarchaeotal order Thermoplasmatales are capable of growing even below pH = 0 [8]. However, the record holder regarding growth at acidic pH is *Picrophilus oshimae* [119].

To date most of the characterized methanogens, which were obtained in pure culture, preferentially grow at neutral pH values. Astonishingly, some methanogens, *i.e.*, *Methanocaldococcus* sp. and *M. marburgensis* exhibit a broader pH range niche ranging into the acidic pH conditions [44,78]. Moreover, there are other methanogens known to be able to grow at acidic pH [98,120]. However, only recently, a natronophilic methanogen has been isolated exhibiting growth at pH values between 8.0 to 10.2 with a pH optimum between 9.0–9.5 [121]. A summary of methanogens cultivable in either acidic or alkaline conditions is presented in Table 2.

Table 2. Summary of currently known methanogens cultivable in either acidic or alkaline conditions.

Strain	Temp. [°C]			pH			Ref.
	min.	opt.	max	min.	opt.	max.	
Methanospirillum stamsii	5	20–30	37	6	7–7.5	10	[31]
Methanocalculus natronophilus	14	30–37	45	8	9–9.5	10.2	[121]
Methanospirillum hungatei	20	37–45	50	6.5	7–9	10	[12]
Methanobrevibacter millerae	33	36–42	43	5.5	7–8	10	[122]
Methanobrevibacter olleyae	28	28–42	42	6	7.5	10	[122]
Methanotorris igneus	45	88	91	5	5.7	7.5	[123]
Methanosphaerula palustris	14	30	35	4.8	5.5	6.4	[120]
Methanoregula boonei	10	35–37	40	4.5	5.1	5.5	[98]

2.4. Osmolarity

Methanogens accumulate compatible solutes in order to reduce the difference between osmotic potentials between the cytoplasm and the environment. Compatible solutes are small osmoprotective molecules which do not alter cellular processes, even if they are intracellularly concentrated up to

high molarities. All methanogens are dependent on low salt concentrations in order to maintain cellular integrity and homoeostasis [26,124].

The main compatible solute of methanogens was found to be trimethylglycine (glycine betaine) [125], herein referred to as betaine. Betaine can be accumulated intracellularly in high quantities in, e.g., *Methanosarcina thermophila* TM-1 [126]. *M. thermophila* TM-1 was furthermore shown to be adaptable to different osmolarities either by synthesis of α-glutamate and N-ε-acetyl-β-lysine, by accumulation of betaine or by accumulating potassium ions. Betaine can be accumulated through an uptake system consisting of a single, high-affinity H^+ and/or Na^+ driven transporter [126].

By applying different NaCl concentrations (from 0.05 to 1.0 mol·L^{-1}) the effect of osmolarity on growth kinetics as well as on changes of morphology of different *Methanosarcina* species was investigated [127]. Between 0.4 to 1.0 mol·L^{-1} NaCl the outer surface methanochondroitin layer, which is a characteristic feature of the multicellular aggregated stage of *Methanosarcina* spp., disaggregated and *Methanosarcina* spp. were found growing as single cells. All *Methanosarcina* spp. strains tested, comprised of a methanochondroitin layer, exhibited enhanced stability at <0.2 mol·L^{-1} NaCl osmolarity and grew at higher temperatures [127]. In another experimental set-up different NaCl concentrations of 0.7 to 3.4 mol·L^{-1} were applied to a methanogen growth medium resulting in accumulation of K^+. Furthermore, β-glutamate was detected when methanogens were grown in a medium containing NaCl at concentrations <1.5 mol L^{-1} [128].

Another interesting characteristic of halotolerant methanogens was identified in *Methanogenium marinum* AK-1, a strain isolated from permanently cold marine sediments at Skan Bay (Alaska, USA). *M. marinum* AK-1 was found to grow in salinities of 0.25–1.25 mol L^{-1} Na^+. The authors concluded that *M. marinum* AK-1 and methanogens from similar saline habitats are capable of metabolizing at low pressures of H_2 (<1 Pa), but, however, this was found to be dependent on the partial pressure of CH_4 [95].

Recently, a novel methanogenic strain, *Methanocalculus natronophilus* Z-7105T was isolated from the bottom sediments of a collector next to a soda lake (Tanatar II, Altai, Russia) [121]. The pH spectrum of the strain was already discussed before, but interestingly *M. natronophilus* was found to be obligatory dependent on carbonates. An optimum carbonate concentration between 0.7–0.9 mol·L^{-1} enabled growth of *M. natronophilus* as well as Na^+ (but not Cl^- ions) were obligatory required at optimal concentrations of 1.4–1.9 mol·L^{-1}, too. The organism thus can be regarded as osmophil and halotolerant and it should be interesting to study osmo-adaptation mechanisms in *M. natronophilus* [121] and other methanogens.

Adaptation to high salt concentrations was achieved with the freshwater methanogen *Methanosarcina mazei* Gö1. It was able to tolerate 1 mol·L^{-1} salt by uptake of betaine from the growth medium through the osmoprotectant transporter A (OpuA), whose expression was confirmed to be salt inducible [129].

In *Methanohalophilus portucalensis* FDF1 also α-glutamate and the beta-amino acids β-glutamine as well as N-ε-acetyl-β-lysine have been described to act as osmoprotective substances in methanogens [128,130]. Again betaine is preferentially taken up from the growth medium instead of being synthesised *de novo* like other osmoprotective compounds such as β-glutamine and N-ε-acetyl-β-lysine [130]. Recently, however, an adenosine derivate has been proposed as a novel compatible solute of *Methanolobus psychrophilus* R15 [85]. Further studies suggest that some of the aforementioned compatible solutes might also be considered as cryoprotective compounds [85].

The role of other compatible solutes, including single species ions, towards higher growth temperature adaptation in methanogens would still require elucidation.

2.5. Ionizing and UV Radiation

Life on Earth is protected from cosmic and Solar radiation through the motion of Earth's liquid core inducing a protective shield referred to as magnetosphere. Furthermore, most of the UV irradiation is blocked from reaching Earth's surface through the ozone layer molecules. However,

the situation is completely different on, e.g., the Martian surface, because Mars is constantly exposed to UV radiation due to the lack of a significant ozone layer [131] and cosmic radiation will only be blocked in low quantity because of a weak and irregular magnetosphere [132].

Regarding the effect of UV damage on the ecophysiology and molecular biology of archaea only a limited number of studies have been published [133–137]. However, only two short and in some parts inconclusive conference reports are available focussing on the survival of methanogens upon exposure to UV light [138,139]. The knowledge generated from UV light experiments with methanogens is still too limited to describe general ecophysiological trends for methanogens confronted with ionizing and/or UV-radiation.

2.6. Desiccation

On the surface and possibly also in the subsurface of Mars as well as in different environments on Earth, e.g., deserts and salt formations, extremely dry conditions prevail [140]. Halophilic archaea were detected in salt rock by using culture independent and culture dependent methods [141]. Results from the cultivation of pure strains show cell survival rates between 0.1%–10% following freezing and embedding in salt crystals, indicating that low water activity and low temperature can be survived by halophilic archaea [140,142,143].

Not only halophilic archaea but also methanogens were investigated regarding their tolerance towards desiccation in order to determine their survival capacity. *Methanosarcina mazei* TM1, *Methanobacterium formicicum* and *Methanobrevibacter aboriphilicus* could recover from low water activity (a_w) when exposed to air or when kept under nitrogen atmosphere [144]. Moreover, soil had a protective effect on some methanogens when exposed to desiccation and air [144]. In another approach four methanogenic strains, *M. wolfeii*, *M. barkeri*, *M. formicicum* and *M. maripaludis* were applied in desiccation experiments in order to examine survival periods when incubated under different pressure conditions [58]. *M. barkeri*, *M. wolfeii* and *M. formicicum* survived 330, 180 and 120 days of desiccation at 10 kPa, respectively. *M. maripaludis* did not survive desiccation at 10 kPa. However, *M. wolfeii*, *M. barkeri* and *M. formicicum* survived desiccation for 120 days at 60 Pa, but *M. maripaludis* survived 60 days at 60 Pa [58].

M. soligelidi SMA-21 (formerly known as *Candidatus Ms. gelisolum*) was isolated from permafrost and exhibited astonishing survival capacity towards freeze-drying and desiccation as well as when being exposed to air. The strain grows optimally at 28 °C, pH = 7.8 and 0.02 mol·L^{-1} NaCl. To examine desiccation cell suspensions were put onto microscope cover slides, which were exposed to aerobic conditions or completely dried. *M. soligelidi* survived up to 25 days of desiccation as well as exposure to air for 72 h [34,81]. Recently, three methanogenic strains, *M. soligelidi*, *M. mazei* and *Methanobacterium movilense*, were shown to produce CH_4 when incubated in a regolith-like matrix lacking nutrients. Moreover, the survival of the three methanogens was analyzed after a 400 day desiccation period [145]. All the three tested methanogens could be reactivated, and CH_4 production could be observed, after the designated incubation period ended. However, especially *M. mazei* and *M. movilense* showed higher CH_4 production after reactivation from of 400 days of desiccation in different Mars regolith-like matrix analogues, as compared to *M. soligelidi*.

The aforementioned results indicate that especially methanogens of the genus *Methanosarcina*—*M. mazei*, *M. barkeri*, *M. soligelidi*—exhibit extraordinary physiological features making them promising organisms for astrobiological research endeavours.

3. Known and Potential Habitats for Methanogens in the Solar System

In this section we outline known (Earth) and potential habitats for methanogens in the Solar System. For the selection of these habitats we focused on those which may host liquid water and on which CH_4 has been detected. An overview of the selected Solar System bodies is given in Table 3 and Figure 3.

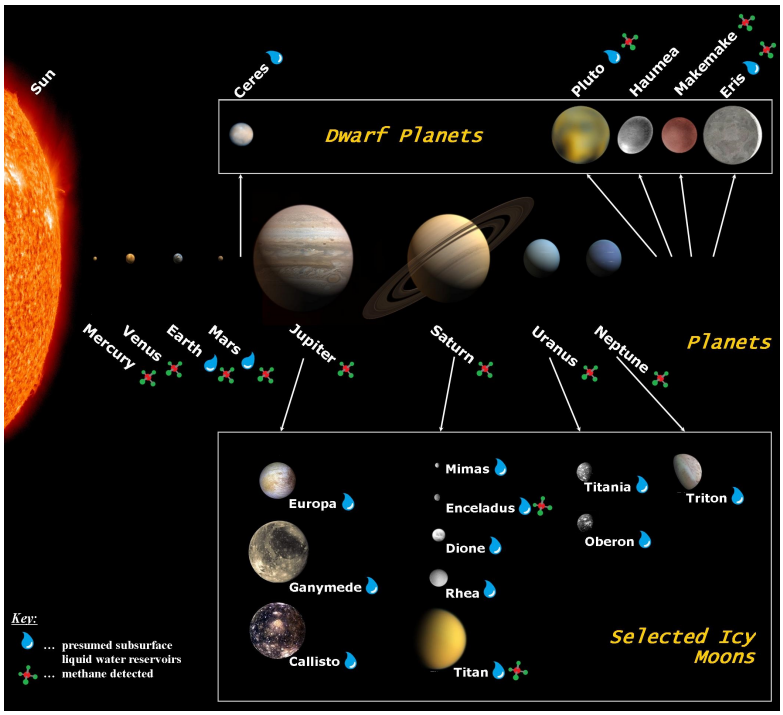

Figure 3. Artist's conception of the Solar System highlighting confirmed or modelled presence of CH_4 and liquid water on different Solar System bodies. The main focus of our study lies on Mars and the icy moons Enceladus, Europa, and Titan. The sizes within each of the three presented groups of Solar System bodies (planets, dwarf planets, and icy moons) are to scale. The distances between the bodies are not to scale; adapted from [146–149].

Table 3. Parameters of Mars, the Moon, and selected moons and icy bodies presented in this review-the last column shows if the potential subsurface aquifer is in direct contact with the underlying silicate core/mantle.

	Host Planet	R [km]	ρ [kg m^{-3}]	$T_{surface}$ [K]			Atmosphere	Water/Core
				T_{min}	T_{mean}	T_{max}		
Moon	Earth	1737.4 ± 1 [150]	3344 ± 5 [151]	26 [1] [152]	220 [153]	390 [2]	no	no
Mars	-	3389.50 ± 0.2 [150]	5.5134 ± 0.0006 [154]	150 [3] [155]	215 [155]	290 [4] [155]	yes [155]	-
Ceres	-	476.2 ± 1.7 [150]	2077 ± 36 [156]	n.a.	n.a.	n.a.	no	no (?)
Ganymede	Jupiter	2631.2 ± 1.7 [150]	1942 ± 5 [151]	70 [157]	109 [153]	152 [157]	no	no/yes [5]
Callisto	Jupiter	2410.3 ± 1.5 [150]	1834 ± 4 [151]	80±5 [158]	134 [153]	165 [158]	yes (thin)	no [6]
Europa	Jupiter	1560.8 ± 0.3 [150]	3013 ± 5 [151]	50 [153]	103 [153]	n.a.	yes (thin)	yes
Titan	Saturn	2574.73 ± 0.09 [150]	1882 ± 1 [151]	n.a.	94 [159]	n.a.	yes	no (?)
Enceladus	Saturn	252.1 ± 0.2 [160]	1609 ± 5 [160]	32.9 [161]	75 [161]	≥157 [162]	local [162]	yes (?) [163]
Dione	Saturn	561.4 ± 0.4 [150]	1476 ± 4 [151]	n.a.	n.a.	n.a.	no	n.a.
Mimas	Saturn	198.2 ± 0.4 [150]	1150 ± 4 [151]	n.a.	n.a.	n.a.	no	no
Triton	Neptune	1352.6 ± 2.4 [150]	2059 ± 5 [151]	n.a.	39 [155]	n.a.	yes (thin)	yes (?)
Pluto	-	1195 ± 5 [150]	2030±60 [164]	35 [165]	44	55 [165]	yes (thin)	yes (?)

[1] at Hermite crater, coldest temperature measured anywhere in the Solar System [152]; [2] at the equator; [3] at the poles in winter; [4] at latitudes ±60° in summer at midday; [5] Present studies indicate that Ganymede may host several alternate ice and liquid water layers with the lowest layer in contact to the rocky mantle [166] (see Figure 6b); [6] According to NASA's Galileo gravimetric data, Callisto is only partly differentiated which results in a mantle/core-structure being a mixture of ice and rocky material.

3.1. Earth

By now, Earth is the only known habitat for methanogens and generally life-as-we-know-it. Methanogens may have already appeared in the Archaean era (before 2.5 Gyr ago) [17,18], where the CH_4 in the fluid inclusions found in approximately 3.5-Gyr-old hydrothermal precipitates from Pilbara craton, Australia, is discussed to be of abiotic origin [167]. Methanogens are known to be widely distributed in nearly all habitats on Earth as already discussed in the previous section. Most of the CH_4 produced on Earth is of biotic origin, but there exist also abiotic processes that produce CH_4 like serpentinization or Fischer-Tropsch synthesis [168]. To distinguish between CH_4 of biogenic and thermogenic (*i.e.*, abiogenic) origin, the isotopic ratios have to be evaluated. Therefore, if we could measure the isotopic ratios of CH_4 on another celestial body, this would be a hint towards the presence of methanogens on this body. Furthermore, abiogenic CH_4 shows a near absence of C_2 and higher alkane [169].

3.2. Mars

Mars is the outermost terrestrial planet in our Solar System and lies just outside the classical habitable zone around the Sun. Its radius is about half and its mass about one-tenth of the Earth's. It has a thin atmosphere consisting of 96% CO_2, 1.93% argon (^{40}Ar) and 1.89% molecular nitrogen (N_2) along with traces of molecular oxygen (O_2) and CO [170]. The mean atmospheric pressure on the surface is about 0.6 kPa [155] and the scale height of the atmosphere is about 10.8 to 11.1 km [171,172] (compared to the Earth's scale height of 8.5 km [173]). The temperature varies between 310 K in summer (at noon at the equator) and 140 K in winter (at the poles), with an average temperature of 215–218 K [155].

Until the beginning of the last century, Mars was thought to be probably inhabited [174]. When Giovanni Schiaparelli observed Mars in 1882, he discovered a vast amount of linear features on the surface which were named *canali*. These *canali* had been interpreted as (artificial) waterways or even irrigation canals built by a supposed intelligent civilization on Mars. It took until the 1960s, when the first Mariner spacecraft visited Mars and refuted the idea of intelligent life on this planet. Up to now, dozens of Mars missions with orbiters, landers, and even rovers have not been able to detect definite signs for extant or extinct life.

Nevertheless, according to current knowledge, there was a wet period in Mars' history. According to a study of Villanueva *et al.*, in the Noachian period (about 4 billion years ago) almost half of Mars' northern hemisphere was covered by an ocean with depths of more than 1.6 km [175]. Due to this huge amount of liquid water, it is rather unlikely that the whole mass of water of the ancient oceans have been vaporized and been lost to space, but that there are subsurface water reservoirs or transient residues of near-surface melt water. However, today, we can find water just in the form of ice or, according to the latest findings of NASA's Mars Reconnaissance Orbiter, in brine flows [176]. So far, the majority of water ice has been found at the polar ice caps, but there are also buried ice deposits at nonpolar latitudes [177].

During the last decades there have been several reports about the detection of CH_4 on Mars. In 1969, George Pimentel announced in a press conference the detection of CH_4 for the first time. According to his presentation, NASA's Mariner 7 mission had detected CH_4 near Mars' south polar cap [178]. Just one month later the findings had to be retracted due to a misinterpretation of the data [179]. In the following years, announcements on detections of CH_4 on the one hand (e.g., ESA's Mars Express Orbiter in 2004 [3], NASA's Infrared Telescope Facility and the W.M. Keck telescope in 2009 [4], or NASA's Curiosity Rover in 2015 [5]) and proofs to the contrary (e.g., NASA's Curiosity Rover in 2013 [180]) on the other hand alternated periodically (for a critical review, see [181]). However, if there is CH_4 in the Martian atmosphere, its amount is very low (mean value of 0.69 ± 0.25 parts per billion by volume (ppbv) [5]). For comparison, the concentration of CH_4 in Earth's atmosphere amounts roughly to 1800 ppbv [181]. Another interesting aspect of the various reports on CH_4 detections is that there seems to be a seasonal variation in the CH_4 concentration [182].

The authors report that in the warmest season higher concentrations of CH_4 were found. This could imply that the amount of volatile release or/and the amount of potential biological activity is higher due to the higher available energy. However, it may indicate as well a systematic analysis error from ground based observations that are seasonally dependent.

In general, CH_4 on Mars can have three principal origins [183]: volcanism, biological activity like methanogenesis, or the condensation from the solar nebula. The latter would require a transport mechanism from Mars' interior to the outside, *i.e.*, a geological process which would be associated with volcanism (*i.e.*, the first mentioned potential source). Furthermore, CH_4 in the Martian atmosphere is extremely unstable. There are several potential sinks like its decay to CO_2 due to photochemical effects or undefined surface oxidation phenomena (see Figure 4). With lifetimes ranging from less than a year to up to 350 years for photochemical processes in the Martian atmosphere [182], CH_4 must be permanently produced. To sum up, if we detect a time-varying amount of CH_4 on Mars without any evidence for an ongoing geological activity, this could be an indirect sign for life on this planet.

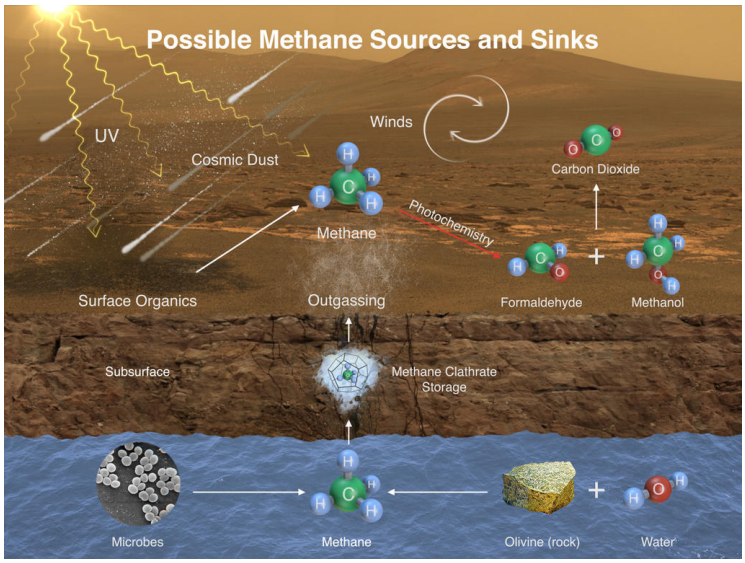

Figure 4. Possible sinks and sources of CH_4 on Mars (PIA19088), Image credit: NASA/JPL- Caltech/ SAM-GSFC/Univ. of Michigan.

Life on Mars would have to resist strong UV radiation due to the lack of an ozone layer [184]. However, life on early Earth was likely resistant to UV and therefore potential Martian microbes may possess resistance to this type of radiation as well [133]. Furthermore, the low surface temperature, low pressure, and desiccation on Mars' surface may act as an inhibitor for life forms, such that they could rather thrive in the subsurface water reservoirs which would be sheltered from radiation. Several studies have been performed to test the growth and survival of methanogens under Mars-like conditions (see Section 4.1).

3.3. Potential Habitable Moons and Small Icy Bodies

The findings of the last decades, that icy moons may harbour a large amount of liquid water under their ice shells have opened new horizons in the rising field of Astrobiology. Nevertheless, liquid water alone may be sufficient, but not necessary for icy moons to be habitable. Another necessary condition may be that the liquid water reservoir is in contact with the silicate core or seafloor to get heated by hydrothermal activity, radioactive decay, *etc.*, and to receive other compounds essential for life by various processes like, e.g., serpentinization. The processes between

the ocean and the underlying rocky layers may lead to the ocean being reducing or oxidizing. If it is more reducing than the Earth's ocean, then CH_4, rather than CO_2, would be the main carbon compound outgassed by potential hydrothermal vents which would inhibit methanogenesis [185]. On the other hand, the production of H_2 by serpentinization may tend to counter this trend and lead to feedstock for methanogens. However, due to the fact that the icy satellites likely accreted from a mixture of ice and rock, the subsurface water reservoirs should be rather oxidizing [186]. In addition, the salinity of the aquifers might vary. Estimates for subsurface oceans range from a few tens of grams of salt per kilogram water to scenarios of liquids saturated with $MgSO_4$ or NaCl. Methanogens are known to resist salinities of up to 1.71–2.57 mol L^{-1} NaCl [187]. Moreover, potential subsurface aquifers may consist of a non negligible amount of ammonia (NH_3). This could lower the freezing temperature of the aquifer but on the other hand it could act as an inhibitor for potential life, if concentrations are too high. Hussmann *et al.* stated that an NH_3-concentration of up to 33%, *i.e.*, 14.9 mol L^{-1} NH_4, seems geochemically plausible. For Europa's subsurface ocean a range of 2.1%–24.4% NH_3 was calculated depending on the assumptions about its interior structure [188]. Such a high ammonia concentration would definitely lead to a serious damage of amino acids [189]. A further important parameter is the time scale in which the aquifers have stayed liquid—at least 10^5 years, *i.e.*, geological timescales, are necessary in order for an aquifer to become a habitat for any life form [190].

In the following subsection we will describe several icy moons (for characteristic parameters see Table 3) and their potential to host methanogens.

3.3.1. Enceladus

Enceladus is a rather small icy moon that orbits Saturn at a mean distance of approximately 238 042 km [191]. It has a radius of about 252.1 km and a mass of $1.08 \cdot 10^{20}$ kg [151]. Enceladus has a mean density of about $1\,609 \pm 5\,\mathrm{kg\,m^{-3}}$ [160]. This is a rather high value for a small icy moon which strengthens the hypothesis that Enceladus contains a huge amount (about 50%) of rocky material [163]. If Enceladus is differentiated, which reflects the current state of knowledge, it might be separated into a rocky core and an icy shell. The icy shell likely contains "misty ice caverns" [192] and/or a (global) subsurface ocean in contact with the rocky core [163,193,194]. According to several models, the rocky core expands to a radius of about 160 to 190 km [193,195,196].

In 2004, the NASA spacecraft Cassini went into orbit around Saturn and since then it has been flown past Titan, Enceladus, and various other moons for numerous times. At least since the third close flyby around Enceladus in July 2005 there has been no doubt about the evidence of a plume of emerging water vapour and small icy grains from warm fractures near the south polar region (see, e.g., [162]). Since the detection of the plume, there has been a debate about its origin—two main points of view emerged: On the one hand, the idea that the plume's source is the decomposition of ice (sublimating ice) and on the other hand that the plume originates in a subsurface liquid source like caverns, a sea or even a global subsurface ocean. The latter theory was strengthened by new Cassini gravity data received in 2014 [163]. The authors estimate Enceladus' local subsurface sea to be situated under a 30 to 40 km thick ice shell and extending from the south pole to about 50° south latitude. Another indication for a subsurface aquifer was the detection of E-ring grains that are rich in sodium salts, which can only be formed in liquid water [194,197,198]. Just recently, Thomas *et al.* presented new findings about the physical libration of Enceladus, which point to a global ocean on Enceladus [199].

According to Cassini's INMS (Ion and Neutral Mass Spectrometer), the main components of Enceladus' plume are water (87 %, volume mixing ratio), H_2 (11 %), CO_2 (0.52 %), N_2 (less than 0.61 %), small amounts of organics (e.g., CH_4 and formaldehyde (H_2CO)), hydrogen sulfide (H_2S), and ^{40}Ar (for detailed composition, see [200,201]). In contrast to previous studies, Waite *et al.* were able to detect NH_3 for the first time [201]. Ammonia (coupled with the presence of CH_3OH and/or salts) acts as an antifreeze which can reduce the freezing point of the aquifer. The authors concluded

that the presence of NH_3 combined with the detection of Na^+- and K^+-salts in the E-ring (second outermost ring of the Saturnian ring system) ice particles is a strong indication for a liquid water reservoir in the interior of Enceladus.

There exist several problems in deducing the subsurface composition by plume observations. For example, the Cassini instrument can only detect neutral atoms and molecules and positive ions [197], which makes, e.g., chlorine ions (Cl^-) invisible for the detector. So anions can only be detected indirectly. Moreover, the closed ion source is used for most neutrals, but does not work for reactive neutrals such as salts, which must be detected by the open ion source at a much reduced sensitivity. Furthermore, it has to be considered that there may be far more types of complex molecules in the subsurface reservoir which do not find their way to the surface. Hence, Cassini's INMS was only able to detect relatively light organics due to the lack of proper instruments- just up to a molecular weight of 100 atomic mass units. This means, that if there are biologically relevant molecules like amino acids, nucleotides, or proteins in the plume material, Cassini has not been able to detect them.

Nevertheless, analysing the plume particles is the main starting point to estimate the chemical composition of the potential subsurface water aquifer. For example, Hsu *et al.* analysed the silicon-rich, nanometre-sized dust particles and reported an indirect proof for the existence of hydrothermal activities within Enceladus [202]. In the context of methanogenic life, it is interesting to note that CH_4 was part of the plume composition and its existence under conditions that would favour methane clathrate formation in the ocean has been argued as another indicator of hydrothermal activity [200]. If CH_4 is produced biologically, than this will likely take place in the subsurface aquifer. Further observations regarding the isotopic composition of this CH_4 would give an indication about the origin of the molecules (see Section 3.1).

However, the habitability of Enceladus is still strongly debated due to the high heat flux and loss rate from the plumes. However, recent reanalysis of Cassini's CIRS (Cassini Composite Infrared Spectrometer) data by Howett *et al.* suggest that the heat flux (4.64 ± 0.23 GW, [203]) is significantly lower than previously estimated (15.8 ± 3.1 GW, [204]). Nevertheless, the high loss rate from the plume indicates that the plumes and Enceladus' potential subsurface aquifer are temporary events. Hansen *et al.* reported the rate of water vapour injection to be 200 kg s^{-1} [205] (with a standard deviation of 30 kg s^{-1})—this would lead to a loss of 20% Enceladus mass if the current plume gas production rate had been constant over the age of the Solar System. It is assumed that Enceladus' plume is erupting and feeding Saturn's E-ring at an approximately constant rate at least for the last 300 years [206]. According to several numerical studies of the ring particle dynamics the lifetime of the ring particles is less than 200 years which implies that some kind of resupplying process, *i.e.*, permanent production of Enceladus' plume particles, must exist to keep the E-ring stable [207].

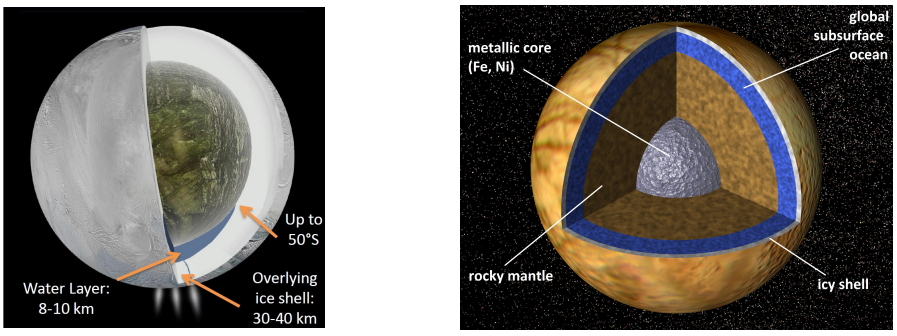

(a) **(b)**

Figure 5. Artist's concepts of the potential interior structure of Enceladus and Europa. (**a**) Potential interior of Enceladus according to [163], Image credit: NASA/JPL-Caltech (PIA18071), adapted; (**b**) Potential interior of Europa according to [208], Image credit: NASA/JPL (PIA01130), adapted.

3.3.2. Europa

Before Cassini detected Enceladus' plumes, Europa had been by far the most promising object in the outer Solar System concerning the possibility of being a habitat for putative extraterrestrial life. In a typical two-layer model of Europa assuming a moment of inertia factor (MoI) of 0.346 and the mean density of the outer shell to be about 1000 kg m^{-3}, the core radius is about 1400 km and has a density of about 3800 kg m^{-3} [209]. This results in a low density outer water shell with a thickness of about 80–170 km [186], depending on the assumed parameters and models. The hydrostatic pressure at the base of this water layer is about 84–180 MPa (according to typical three-layer models presented in [208,209]). Even if the pressure might be too high on the ocean's floor, methanogens could resist easily the pressure at a depth of approx. 30 km which would be comparable to the hydrostatic pressure at the average terrestrial seafloor depth of 4 km [190]. A main factor for the habitability of Europa's ocean will be active material cycles that transport reductants from the ocean floor and oxidants from the overlying ice shell to the habitable zone inside the aquifer [190].

NASA's Galileo mission launched in 1989 revealed Europa to have a subglacial liquid water layer beneath a solid icy crust [210]. The thickness of the ice shell and the liquid water layer is still highly debated due to the lack of accurate gravimetric and altimetric measurements. By now, there are two models proposed, that describe the dimensions of the liquid to the solid water shells in a contrasting way: the "thin" (e.g., [211,212]) and "thick" model. The first model implies, that the icy layer may be less than 10 km thick which means that there might be a link between the underlying ocean and the surface, e.g., through cracks. The "thick" model predicts an icy shell of about 20 km. It seems rather likely that the truth lies in a combination of these two models with a global variable ice shell thickness because none of these models can explain every single detection sufficiently. Notably, the amount of subsurface liquid water on Europa exceeds the water in Earth's oceans 2–3 times by volume [213].

Knowledge about the topography of Europa (*i.e.*, the existence of hydrothermal vents, volcanoes, and ridges) will remain hidden without future missions like the recently approved Europa multiple flyby missions of ESA (JUICE, launch planned for 2022) or NASA (Europa mission, launch in the 2020's) to this icy moon. Currently is is assumed that the subsurface ocean is most likely in direct contact with Europa's silicate core [190]. If so, these circumstances would have led to a geochemically rich environment with all necessary requirements for the existence of methanogens and life in general.

While there is some information about the potential composition of Enceladus' subsurface water reservoir due to the composition of the plume particles, the composition of Europa's ocean remains hidden. Though, there was an announcement of the discovery of plumes on Europa in 2012 [214], it was not possible to confirm these detections since then or even in older data. Further detections and subsequent analysis of the potential Europa plume particles would definitely help us to understand the interior ocean conditions at Europa. If we assume (chemical) exchange processes (e.g., serpentinization [215]) between the subsurface ocean and Europa's surface, one can draw inferences from the surface material about the composition of the aquifer. For example, the detection of CO_2 by NASA Galileo mission in the hydrate-rich terrains on Europa's surface gives a hint to the oxidizing state of the subsurface aquifer [186]. There might even be the chance that potential biomass would be transported to the surface, but the concentration would be extremely small which would make biosignatures hard to detect (about one cell per mL [190]). However, the conditions at the surface are extremely different from subsurface, *i.e.*, the particles undergo changes due to abrupt variation in temperature and the exposure to the high Jovian radiation. Nevertheless, there are several studies about its potential chemical composition (see, e.g., [215])

McCollom analysed the possibility of methanogenesis to occur for two different scenarios for a hydrothermally active Europa [216]. He considered a relatively reduced ocean (dominated by CH_4 and H_2S) and a relatively oxidized ocean (dominated by SO_4^{2-} and HCO_3^-) [216]. The author estimated a biomass productivity on Europa of 10^5 to 10^6 kg yr^{-1}, which is equal to 10 ppm of the hydrothermal biomass productivity on Earth [190].

3.3.3. Titan

Titan is unique among the Solar System satellites due to its dense atmosphere (1.5 bar) which just above the surface consists mainly of N_2 (approx. 94.5 % mole fraction), CH_4 (5.5 %), and various trace constituents like H_2, ethane (C_2H_6) and hydrogen cyanide (HCN) [217–219] and because it is the only other Solar System object besides the Earth with standing entities of some liquid at its surface. Its atmosphere extends to an altitude of 1 500 km [220]. Although much colder (mean surface temperature of 94 K, see Table 3), there are some similarities to the Earth like the qualitatively similar vertical structure of the atmosphere, the presence of a complex liquid solution cycle (on Titan CH_4 plays the role of water since the temperature and pressure conditions put methane at its triple point at the surface), or the active organic chemistry [218]. Titan is often quoted as a cold analogue for the prebiotic Earth [189,221–224]. There might be the possibility that liquid water (or at least liquid water-ammonia mixture) existed even at the surface caused by impacts of, e.g., comets that could melt surface water ice or due to cryovolcanism [225] for geological short periods of time (100 to 1 000 years assumed for a crater with 15 km diameter, 1000 to 10 000 years for the ones with 150 km [226]). Independent of these considerations, the average Titan surface is in fact too cold and not energetic enough to serve as a habitat for life-as-we-know-it [218].

However, Titan likely harbors a liquid water(-ammonia) ocean a few hundred kilometres thick under an ice shell of about 100 km [227,228]. In contrast to Europa or Enceladus, the ocean does not seem to be in contact with the rocky mantle/core but with an icy ocean floor (see Figure 6a) which makes life in this aquifer rather unlikely [228].

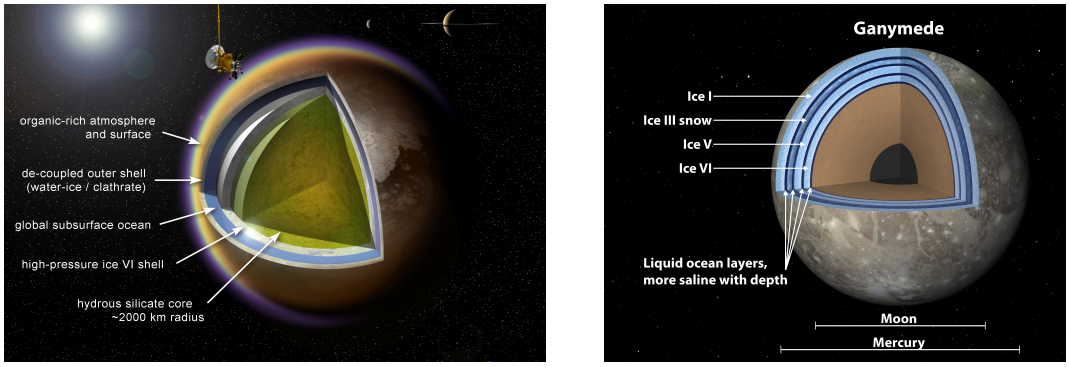

(a) **(b)**

Figure 6. Artist's concepts of the potential interior structure of Titan and Ganymede. (**a**) Potential interior of Titan according to [229], Image credit: A. D. Fortes/UCL/STFC (PIA14445); (**b**) Potential interior of Ganymede according to [166], Image credit: NASA/JPL-Caltech (PIA18005).

3.3.4. Other Icy Moons

In the following, we will present several other icy moons where a subsurface liquid water layer seems to be possible due to models and corresponding observations. However, these satellites are either unlikely to harbor life-as-we-know-it (Ganymede, Mimas, Dione, Callisto) or there are not enough data available to draw conclusions about their possible interior structure (Triton, Rhea, Oberon, Titania).

Ganymede

Ganymede is the largest satellite in the Solar System. Its interior seems to consist of several layers of different ice phases (due to the increasing pressure at increasing depth) separated by liquid water layers (see Figure 6b). The lowest liquid layer may be in contact with the rocky mantle of Ganymede. Due to the high pressure at this depth (about 800 km), the temperature is higher than in the upper

layers [166]. However, an estimated pressure of approx. 500 MPa at the ocean floor is possibly too high for life-as-we-know-it [209].

Mimas and Dione

Dione has the third highest density of the Saturnian satellites which suggests that it contains a large amount of dense material like silicates. Cassini's magnetometer detected hints of a faint plume of charged particles and bright, fresh fractures on its surface. On the other hand, Cassini's Visual Infrared Mapping Spectrometer (VIMS) was not able to detect any evidence for plumes [230]. According to the authors activity must be below our threshold of detection, or it could be occurring but was not yet captured on the observations at large solar phase angles [230]. However, current geologic activity or a subsurface water reservoir cannot absolutely be ruled out [231].

Mimas is another icy moon of the Saturnian system. A study published in 2014 shows that Mimas "has either a large nonhydrostatic interior, or a hydrostatic one with an internal ocean beneath a thick icy shell" [232].

There is currently too little information about these icy satellites available in order to make justifiable statements on the potential habitability of these bodies. Furthermore, the study of Hussmann *et al.* exclude Mimas and Dione (as well as Enceladus and Tethys) from possessing a subsurface water layer [188].

Callisto

It is rather likely that Callisto harbours a subsurface ocean, but due to the fact that its interior is most likely not fully differentiated, this aquifer should not be habitable for life-as-we-know-it.

Triton

The largest satellite of Neptune is special among the large moons in the outer Solar System due to its retrograde orbit. Triton is most likely a captured Kuiper belt object (KBO) [233] and its dimensions, density, temperature and chemical composition is similar to those of Pluto (see Table 3). Triton is most likely an active moon as Voyager 2 observed dark geyser-like eruptions in the summer of 1989 [234]. Although the surface of Triton is very harmful to life due to the fact that this moon lies within the magnetosphere of Neptune, there is still the possibility that the putative subsurface ocean may harbour life. On the other hand, the ocean may be ammonia-rich and there may be a limited abundance of carbon both of which would argue against life on Triton [233].

Rhea, Oberon, Titania

Saturn's second largest satellite Rhea and Uranus' largest moons Oberon and Titania may possess a liquid water layer [188]. According to a study by Hussmann *et al.*, Oberon may have a liquid layer of up to 40 km, Titania of 52 km, and Rhea of 17 km [188]. Rhea's layer may be relatively thin compared to its icy layer of about 400 km. However, these assumptions are just theoretical and have not been verified by observations yet (see [231]).

3.3.5. Dwarf Planets and Small Solar System Bodies

Currently, the International Astronomical Union (IAU) categorizes 5 bodies as dwarf planets: Ceres, Pluto, Haumea, Makemake, and Eris. A dwarf planet, as defined in the IAU Resolution B5, is "a celestial body that (a) is in orbit around the Sun; (b) has sufficient mass for its self-gravity to overcome rigid body forces so that it assumes a hydrostatic equilibrium (nearly round) shape; (c) has not cleared the neighbourhood around its orbit; and (d) is not a satellite. All other objects, except satellites, orbiting the Sun shall be referred to collectively as 'Small Solar System Bodies' " [235]. The latter includes small Trans-Neptunian Objects (TNOs), asteroids, comets, *etc.* According to the study

of Hussmann *et al.*, subsurface oceans are possible on the dwarf planets Pluto and Eris, as well as on the TNOs Sedna and 90482 Orcus [188].

Furthermore, Ceres, the largest object in the asteroid belt with an effective radius of 476.2 ± 1.7 km [150], may host a subsurface water reservoir, too. In January 2014, emissions of water vapour were detected by using ESA's Herschel space observatory [236]. Observations by NASA's Dawn spacecraft showed that the reason for the detected bright spots are more likely vaporization or sublimation of ice than cryovolcanism [237]. On the course of this mission new insights will be gained into the internal structure of this dwarf planet.

Another highlight in 2015 for solar system exploration was the NASA's New Horizons spacecraft flyby of Pluto (effective radius 1195 ± 5 km [150]) and its satellites. Based on measurements of Pluto's shape, we will receive better knowledge about the interior structure of Pluto and if this dwarf planet may harbour a subsurface aquifer [238]. Even Pluto's largest moon Charon (effective radius 605 ± 8 km [150]) might have possessed a subsurface aquifer in its past [239].

As can be seen from these examples, subsurface aquifers may be more frequent in small Solar System bodies than usually thought. Nevertheless, life on small bodies like TNOs is rather unlikely due to their huge distance to the Sun. The temperature is extremely low, the necessary supply of energy, e.g., tidal energy, is not clear in this context as it is for the Galilean satellites and at Enceladus. Furthermore, the availability of the necessary elements seems rather unlikely due to the history of these objects. TNOs are remnants of the early outer Solar System and therefore their average composition is mostly comet-like [240]. This means that they contain just a small amount of rocky material and hence may not host an adequate amount of chemical compounds essential for life.

4. Simulating Extraterrestrial Conditions

Over the last decades, a plethora of simulations under Mars-like conditions were performed with microorganisms. Due to the detection of CH_4 in the Martian atmosphere (see Section 3.2) or in Enceladus' plume particles [2] and due to the ability of methanogens to withstand extreme conditions (see Section 2), methanogens were emphasized as model organisms in Astrobiology. In the following, we will present a selection of various astrobiological experiments.

4.1. Mars-Like Conditions

Investigations regarding growth and survival of *Methanothermobacter wolfeii*, *Methanosarcina barkeri*, *Methanococcus maripaludis* and *Methanobacterium formicicum* under Martian-like conditions have been performed in the Pegasus planetary simulation chamber [58,59]. All methanogens tested survived 60 days at 600 Pa, a pressure found at the Martian surface/subsurface boundary [58]. Moreover, a mixed culture of methanogens has been tested under low-pressure conditions in the Pegasus planetary simulation chamber including desiccation and Martian regolith analogues. *M. wolfeii* and *M. formicicum* did only survive desiccation in a few experiments, whereas *M. barkeri* survived in most cases when incubated with different Martian soil analogues. *M. formicicium* survived only one of the desiccation experiments [59]. Another study by Mickol and Kral showed that the four tested strains were not affected by pressure values of 3.3 kPa and 6.7 kPa, respectively [60]. Furthermore, it was shown (e.g., in [61,62]) that the tested methanogens were able to propagate in the presence of the Martian-like soils *Mojave Mars Simulant* [63] and *JSC Mars-1* [241]. In addition, *M. maripaludis* was tested concerning its growth in the presence of montmorillonite (smectite clay mineral) [62] and (magnesium) perchlorate [64,65]. In both cases, significant amounts of CH_4 were still produced. It is important to note, that these experiments require liquid water and a protection from UV radiation present on Mars' surface, which would be possible in the potential subsurface water reservoirs. Chastain *et al.* published a study that determined "whether biological methanogenesis could occur in non-reduced, non-buffered environments containing only H_2, CO_2, montmorillonite, and the liquid fraction extracted from a montmorillonite/deionized water suspension" [66]. The authors concluded that montmorillonite can supply micronutrients

to the potential environmental system essential for methanogenesis. However, a mixture of montmorillonite and zero-valent iron would be even better [242]. On Mars, where ferrous minerals are abundant, zero-valent iron could be an alternative energy source for methanogens [67].

Other studies investigated the ability of methanogens to withstand freeze-thaw-cycles [243,244]. Djordjevic *et al.* tested the ability of *M. wolfeii*, *M. barkeri*, *M. maripaludis* and *M. formicicum* to survive short-term freeze/thaw cycles (approx. 20–50 days) between temperatures of −80 °C and +37 °C [243], whereas Mickol *et al.* tested *M. wolfeii* and *M. formicicum* in a longer period (about 281 days) in a temperature range of −80 °C and +55 °C [244]. In both studies, at least some of the strains were able to withstand prolonged low-temperature conditions. A further study tested the survivability of methanogens under Martian thermal conditions [68]. Here, six strains of methanogens [245] were tested for "diurnal temperature fluctuations in the range from −75 to +20 °C and humidity fluctuations between a_w-values of 0.1 and 0.9 in a Mars-like atmosphere dominated by CO_2 (95.3%)" [68]. This three weeks lasting study showed that methanogens found in the terrestrial permafrost have an unexpectedly high survivability rate under Mars-like thermal conditions. In the meantime, using laser spectroscopy Schirmack *et al.* were able to show the growth of *M. soligelidi* under Martian thermo-physical conditions continuously during the experiment and not just through comparison of the number of cells and CH_4 production rate at the beginning and at the end of the experiment [69].

The above mentioned experiments consolidated the role of methanogens to be a hot candidate for life on Mars.

The upcoming ExoMars mission, which consists of a Trace Gas Orbiter plus an entry, descent and landing demonstrator module as well as a rover and a surface platform (planned launches in 2016 and 2018, respectively) will focus on the search for biosignatures of Martian life. The rover will have a Raman spectrometer on board. Current studies describe how this instrument may be used to characterize potential methanogenic archaea, based on experiments with *M. soligelidi* on two different Martian-like soils [70,71].

4.2. Icy Moon-Like Conditions

If a subsurface ocean/water reservoir on an icy moon hosted life, the organisms would have to be chemolithoautotroph and anaerobic. In their paper, McKay *et al.* describe the fact that there are only three known microbial ecosystems on Earth which meet these requirements and, therefore, could exist on icy moons [246]. Two of these systems "are based on methanogens [247] that use H_2 derived from rock-water reactions [248,249] and a third on sulfur-reducing bacteria [250] that use redox couples produced ultimately by radioactive decay [251]" [246]. The latter process takes place at high temperature which might be a limiting factor for this metabolism on icy moons. Therefore, mainly psychrophilic methanogens are likely to be the only known terrestrial microorganisms that could thrive on an icy moon. For Enceladus, several of the compounds detected by Cassini can serve as substrates (e.g., H_2, N_2, or CH_3OH) for them or/and may even be products (e.g., CO_2, CO, or CH_4) of the methanogenic metabolism.

Several species of methanogens have already been tested in connection to icy moons (e.g., [252]), but none of these experiments were done under cold, general icy-moon like subsurface aquifer conditions, this means for example at temperatures of less than 20 °C (locally, the temperature can be higher, especially near hydrothermal vents [202]). Additionally, experiments aimed to determine the resistance of certain methanogens against a high amount of ammonia are also missing. Studies with ammonium chloride (NH_4Cl) with concentration up to 6%, *i.e.*, 0.272 mol L^{-1}, were performed [253]. The authors report that *M. wolfeii* show CH_4 production on concentrations of ammonium chloride as high as 4%, whereas *M. maripaludis* seems to be resistant against 3% NH_4Cl. These experiments are very important because there might be a certain amount of ammonia in the subsurface liquid that could act as an antifreezing agent (see Section 3.3). Furthermore, there are running studies that deal with the possibility to cultivate methanogens under Enceladus-like conditions [254]. These include

the composition of the medium, the gas phase, the temperature range, and the pressure conditions in the subsurface aquifer.

4.3. Terrestrial Analogues for Solar System Objects

There exist no perfect terrestrial analogues that would mimic an ecosystem on neither Mars nor any other Solar System object. However, several places on Earth seem to be at least similar to extraterrestrial locations. Preston and Dartnell present 33 analogous sites for Venus, Mars, Europa, Enceladus, and Titan, which reflect the mineralogical, geochemical, physical, and/or chemical conditions on these bodies [255]. From this list, we want to highlight the Bockfjord Volcanic Complex [256] (Svalbard, Norway) which serves as an analogue for Hesperian Mars [256], the Lidy Hot Springs [249] and the Columbia River Basalts [248] (both USA), which should both roughly represent the conditions on the sea floor of a potential subsurface water reservoir on icy moons. Another terrestrial Mars analogue is the permafrost in the Imuruk lake volcanic field area (Alaska, USA) [257]. In each of these ecosystem, methanogenic activity was detected.

For icy moons, important terrestrial analogues are the subglacial lakes in Antarctica, e.g., Lake Vostok. These ecosystems mirror the cold and dark environmental condition in subsurface aquifers in the best possible way. Ecosystems in such an environment may have been isolated from the outside for more than 15 million years [258]. So far, direct sampling of the liquid water of these systems proves to be rather difficult for similar reasons as for their extraterrestrial locations. For example, drilling through hundreds of meters to several kilometres thick ice shell is required whereby the formed drill hole has to be saved from freezing. On the other hand, the subglacial ecosystem has to be protected against contamination. On icy moons there are several further aggravating aspects that have to be kept in mind at the planning phase of such a drilling mission, e.g., the source of energy.

5. Conclusions

5.1. Discussion

Methanogens represent one of the most widespread group of microorganisms that span habitats from hot vents in the deep oceans to ice cold permafrost soils and a temperature range between below 0 and up to 122 °C. Their energy metabolism, which is independent of oxygen and often independent of the presence of any organic molecule, is unique and potentially developed early on Earth [19]. Moreover, many methanogens are known to be prototrophs (*i.e.*, microorganism that can synthesize its nutrients/growth factors from inorganic material [259,260]) and as such they are ideal candidates for inhabiting or surviving on planetary bodies other than Earth.

Only a limited number of inconclusive studies on the effect of UV light on methanogens is available in the literature. Few studies focussed on the response on the morphological, physiological and genetic level as a results of applying multiple stress factors in parallel. Analysing a multiple stress response would better enable deducing survival and ecophysiological characteristics of methanogens from laboratory experiments and inferences on a putative comparable situations on other celestial bodies.

Some of the physiological adaptations of methanogens, like "uncoupling", and their ability to regain a fully active metabolic potential after recovering from dormancy are intriguing features of these organisms. These demonstrate the versatility of methanogens in adapting to changing environmental conditions (e.g., temperature, pH). We hypothesize that uncoupling is a methanogenic ecophysiological adaptation feature not only to redirect the carbon flux from biomass formation, propagation and homoeostasis to energy generation just enabling cell survival, but also to be able to quickly reactivate to full metabolic potential from a state of dormancy. Under special environmental conditions, which can be found at the diffuse vent systems located next to hydrothermal vents on the sea-floor, methanogens are exposed to a narrow temperature gradient (e.g., from >20 °C to 190 °C within 12 cm) in which they might be physiologically active [19,79]. Hence, methanogens might be

able to rapidly respond to environmental changes through ecophysiological adaptations, as they are putatively also encountered on other bodies throughout the Solar System.

The strain and species-specific characteristics (specific growth rate, (cell) specific CH_4 productivity, $Y_{(x/CH4)}$) of methanogens (e.g., [13,78]) have not been considered much regarding their ecophysiological role in the context of astrobiology. However, the characteristics of methanogens to vary, e.g., $Y_{(x/CH4)}$) have been successfully employed in biotechnology when the organisms were utilized for the purpose of biological methanation [44,261]. These ecophysiological characteristics could eventually not only be varied during application of certain bioprocess technological conditions, but also be intriguing to study in the context of astrobiological research, when environmental constraints are forcing the methanogens into maintaining energy homoeostasis until the organisms are capable to propagate.

5.2. Outlook

The different adaptations and facets of methanogens make these organisms and their metabolism important study objects in the context of search for life on other planets and solar bodies as they help to define prerequisites and physical limits for life. Taken together recent data and missions to the moons of the outer Solar System have revealed a number of additional celestial bodies that could potentially have hosted an evolution of life independent (or parallel) to that of Earth.

In the future, research should focus on missions to other Solar System bodies that will not just identify potential habitats but signs for life with the aid of instruments adjusted to the respective environment. For example, the upcoming ExoMars rover will focus on the search for biosignatures of life on Mars. The rover will have a Raman spectrometer on board that can be used to characterize potential methanogenic archaea, based on experiments with *M. soligelidi* on two different Martian-like soils [70,71]. ESA's Jupiter Icy Moon Explorer (JUICE) is planned to start in 2022 and will arrive at the Jovian system most likely in 2030 [262]. The focus of this mission lies on Ganymede as a planetary body and potential habitat, but it will also do investigations of Callisto and Europa [263]. For the planned NASA Europa flyby mission, the focus will lie on the chemistry essential to life, including organic molecules, and it will search for characteristic surface features that could give a hint for future missions [264]. Both JUICE and the NASA Europa mission will have a spectrometer on board that will be able to detect molecules with a higher molecular mass than the compounds found with Cassini's INMS in Enceladus' plume. Hence, if there are plumes on Europa which are fed by the subsurface water reservoir, this spectrometer might be able to detect direct signs of life-as-we-know-it, like nucleotides, proteins, or even cells. *In situ* measurement with convenient instruments at the plumes of Europa (as already mentioned, the plumes on Europa are still not confirmed) or Enceladus will be a major step towards a better understanding of the potential of life in the Solar System. In the distant future, missions containing cryobots (*i.e.*, probes that will be able to penetrate water ice) might provide an opportunity to perform *in situ* measurements within the subsurface aquifer. In this context, e.g., NASA in cooperation with Stone Aerospace is already working on such robots. The next step for this project named VALKYRIE (Very-Deep Autonomous Laser-Powered Kilowatt-Class Yo-Yoing Robotic Ice Explorer) will be the testing of a small version of VALKYRIE during three field campaigns in Canada and Norway [265]. Nevertheless, to adapt this technical system to the prevailing conditions on Europa or Enceladus will be a major issue. At the moment, the exact thickness of the ice shell of these bodies is still not precisely known. It makes a great difference to drill through some hundreds of meters or 30 kilometres of ice. Furthermore, the energy source and the way of communication between the different instruments (at least between the cryobot, a landing probe, an orbiter, and instruments on Earth) remains still an unsolved problem.

The potential of methanogens for astrobiological studies is still a long way from being exhausted. Better understanding of the Solar System bodies will give us the chance to improve the experiments. Therefore, we would recommend a interdisciplinary collaboration among the various scientific fields of astrobiology to move closer to the ultimate goal: the detection of extraterrestrial life.

Acknowledgments: *J. Hunter Waite*, South West Research Institute, USA, is acknowledged for proof reading and critical comments on the manuscript. R.-S.T. acknowledges funding by the University of Vienna for her Ph.D. in the frame of the Research Platform: ExoLife (FPF-234).

Author Contributions: R.-S.T. and S.K.-M.R.R. reviewed the literature, designed and drafted the initial version of the manuscript. R.-S.T., C.S., M.G.F., and S.K.-M.R.R. wrote the final version of the manuscript.

Conflicts of Interest: All authors declare not to have any conflict of interest.

References and Notes

1. Niemann, H.B.; Atreya, S.K.; Bauer, S.J.; Carignan, G.R.; Demick, J.E.; Frost, R.L.; Gautier, D.; Haberman, J.A.; Harpold, D.N.; Hunten, D.M.; *et al.* The abundances of constituents of Titan's atmosphere from the GCMS instrument on the Huygens probe. *Nature* **2005**, *438*, 779–784.
2. Waite, J.H.; Brockwell, T.; Lewis, W.S.; Magee, B.; McKinnon, W.B.; Mousis, O.; Bouquet, A. Enceladus Plume Composition. *LPI Contrib.* **2014**, *1774*, 4013.
3. Formisano, V.; Atreya, S.; Encrenaz, T.; Ignatiev, N.; Giuranna, M. Detection of Methane in the Atmosphere of Mars. *Science* **2004**, *306*, 1758–1761.
4. Mumma, M.J.; Villanueva, G.L.; Novak, R.E.; Hewagama, T.; Bonev, B.P.; DiSanti, M.A.; Mandell, A.M.; Smith, M.D. Strong Release of Methane on Mars in Northern Summer 2003. *Science* **2009**, *323*, 1041–1045.
5. Webster, C.R.; Mahaffy, P.R.; Atreya, S.K.; Flesch, G.J.; Mischna, M.A.; Meslin, P.Y.; Farley, K.A.; Conrad, P.G.; Christensen, L.E.; Pavlov, A.A.; *et al.* Mars methane detection and variability at Gale crater. *Science* **2015**, *347*, 415–417.
6. Liu, Y.; Whitman, W.B. Metabolic, Phylogenetic, and Ecological Diversity of the Methanogenic Archaea. *Ann. N. Y. Acad. Sci.* **2008**, *1125*, 171–189.
7. There are also (aerobic) marine microorganisms known to produce CH_4 from methylphosphonic acid [266–268] .
8. Offre, P.; Spang, A.; Schleper, C. Archaea in Biogeochemical Cycles. *Annu. Rev. Microbiol.* **2013**, *67*, 437–457.
9. Evans, P.N.; Parks, D.H.; Chadwick, G.L.; Robbins, S.J.; Orphan, V.J.; Golding, S.D.; Tyson, G.W. Methane metabolism in the archaeal phylum Bathyarchaeota revealed by genome-centric metagenomics. *Science* **2015**, *350*, 434–438.
10. Thauer, R.K.; Kaster, A.K.; Seedorf, H.; Buckel, W.; Hedderich, R. Methanogenic archaea: Ecologically relevant differences in energy conservation. *Nat. Rev. Microbiol.* **2008**, *6*, 579–591.
11. Borrel, G.; O'Toole, P.W.; Harris, H.M.B.; Peyret, P.; Brugère, J.F.; Gribaldo, S. Phylogenomic Data Support a Seventh Order of Methylotrophic Methanogens and Provide Insights into the Evolution of Methanogenesis. *Genome Biol. Evol.* **2013**, *5*, 1769–1780.
12. Iino, T.; Tamaki, H.; Tamazawa, S.; Ueno, Y.; Ohkuma, M.; Suzuki, K.i.; Igarashi, Y.; Haruta, S. Candidatus Methanogranum caenicola: A Novel Methanogen from the Anaerobic Digested Sludge, and Proposal of Methanomassiliicoccaceae fam. nov. and Methanomassiliicoccales ord. nov., for a Methanogenic Lineage of the Class Thermoplasmata. *Microbes Environ.* **2013**, *28*, 244–250.
13. Rittmann, S.; Seifert, A.; Herwig, C. Essential prerequisites for successful bioprocess development of biological CH_4 production from CO_2 and H_2. *Crit. Rev. Biotechnol.* **2015**, *35*, 141–151.
14. Ferry, J.G. How to make a living by exhaling methane. *Annu. Rev. Microbiol.* **2010**, *64*, 453–473.
15. Oelgeschläger, E.; Rother, M. Influence of carbon monoxide on metabolite formation in Methanosarcina acetivorans. *FEMS Microbiol. Lett.* **2009**, *292*, 254–260.
16. Rother, M.; Metcalf, W.W. Anaerobic growth of Methanosarcina acetivorans C2A on carbon monoxide: An unusual way of life for a methanogenic archaeon. *Proc. Natl. Acad. Sci. USA* **2004**, *101*, 16929–16934.
17. Brocks, J.J.; Logan, G.A.; Buick, R.; Summons, R.E. Archean Molecular Fossils and the Early Rise of Eukaryotes. *Science* **1999**, *285*, 1033–1036.
18. Ueno, Y.; Yamada, K.; Yoshida, N.; Maruyama, S.; Isozak, Y. Evidence from fluid inclusions for microbial methanogenesis in the early Archaean era. *Nature* **2006**, *440*, 516–519.
19. Martin, W.; Baross, J.; Kelley, D.; Russell, M.J. Hydrothermal vents and the origin of life. *Nat. Rev. Microbiol.* **2008**, *6*, 805–814.
20. Brochier-Armanet, C.; Forterre, P.; Gribaldo, S. Phylogeny and evolution of the Archaea: One hundred genomes later. *Curr. Opin. Microbiol.* **2011**, *14*, 274–281.

21. Blank, C.E. Phylogenomic dating—The relative antiquity of archaeal metabolic and physiological traits. *Astrobiology* **2009**, *9*, 193–219.
22. Nakamura, K.; Takahashi, A.; Mori, C.; Tamaki, H.; Mochimaru, H.; Nakamura, K.; Takamizawa, K.; Kamagata, Y. Methanothermobacter tenebrarum sp. nov., a hydrogenotrophic, thermophilic methanogen isolated from gas-associated formation water of a natural gas field. *Int. J. Syst. Evol. Microbiol.* **2013**, *63*, 715–722.
23. Ma, K.; Liu, X.; Dong, X. Methanosaeta harundinacea sp. nov., a novel acetate-scavenging methanogen isolated from a UASB reactor. *Int. J. Syst. Evol. Microbiol.* **2006**, *56*, 127–131.
24. Lü, Z.; Lu, Y. *Methanocella conradii* sp. nov., a Thermophilic, Obligate Hydrogenotrophic Methanogen, Isolated from Chinese Rice Field Soil. *PLoS ONE* **2012**, *7*, e35279.
25. L'Haridon, S.; Reysenbach, A.L.; Banta, A.; Messner, P.; Schumann, P.; Stackebrandt, E.; Jeanthon, C. Methanocaldococcus indicus sp. nov., a novel hyperthermophilic methanogen isolated from the Central Indian Ridge. *Int. J. Syst. Evol. Microbiol.* **2003**, *53*, 1931–1935.
26. Jones, W.J.; Leigh, J.A.; Mayer, F.; Woese, C.R.; Wolfe, R.S. Methanococcus jannaschii sp. nov., an extremely thermophilic methanogen from a submarine hydrothermal vent. *Arch. Microbiol.* **1983**, *136*, 254–261.
27. Jiang, B.; Parshina, S.N.; Doesburg, W.V.; Lomans, B.P.; Stams, A.J.M. Methanomethylovorans thermophila sp. nov., a thermophilic, methylotrophic methanogen from an anaerobic reactor fed with methanol. *Int. J. Syst. Evol. Microbiol.* **2005**, *55*, 2465–2470.
28. Jeanthon, C.; L'Haridon, S.; Reysenbach, A.L.; Vernet, M.; Messner, P.; Sleytr, U.B.; Prieur, D. Methanococcus infernus sp. nov., a novel hyperthermophilic lithotrophic methanogen isolated from a deep-sea hydrothermal vent. *Int. J. Syst. Bacteriol.* **1998**, *48 Pt 3*, 913–919.
29. Jeanthon, C.; L'Haridon, S.; Reysenbach, A.L.; Corre, E.; Vernet, M.; Messner, P.; Sleytr, U.B.; Prieur, D. *Methanococcus vulcanius* sp. nov., a novel hyperthermophilic methanogen isolated from East Pacific Rise, and identification of *Methanococcus* sp. DSM 4213T as *Methanococcus fervens* sp. nov. *Int. J. Syst. Bacteriol.* **1999**, *49*, 583–589.
30. Cheng, L.; Qiu, T.L.; Yin, X.B.; Wu, X.L.; Hu, G.Q.; Deng, Y.; Zhang, H. Methermicoccus shengliensis gen. nov., sp. nov., a thermophilic, methylotrophic methanogen isolated from oil-production water, and proposal of Methermicoccaceae fam. nov. *Int. J. Syst. Evol. Microbiol.* **2007**, *57*, 2964–2969.
31. Parshina, S.N.; Ermakova, A.V.; Bomberg, M.; Detkova, E.N. Methanospirillum stamsii sp. nov., a psychrotolerant, hydrogenotrophic, methanogenic archaeon isolated from an anaerobic expanded granular sludge bed bioreactor operated at low temperature. *Int. J. Syst. Evol. Microbiol.* **2014**, *64*, 180–186.
32. Von Klein, D.v.; Arab, H.; Völker, H.; Thomm, M. Methanosarcina baltica, sp. nov., a novel methanogen isolated from the Gotland Deep of the Baltic Sea. *Extremophiles* **2002**, *6*, 103–110.
33. Franzmann, P.D.; Liu, Y.; Balkwill, D.L.; Aldrich, H.C.; Macario, E.C.D.; Boone, D.R. Methanogenium frigidum sp. nov., a Psychrophilic, H_2-Using Methanogen from Ace Lake, Antarctica. *Int. J. Syst. Bacteriol.* **1997**, *47*, 1068–1072.
34. Wagner, D.; Schirmack, J.; Ganzert, L.; Morozova, D.; Mangelsdorf, K. *Methanosarcina soligelidi* sp. nov., a desiccation- and freeze-thaw-resistant methanogenic archaeon from a Siberian permafrost-affected soil. *Int. J. Syst. Evol. Microbiol.* **2013**, *63*, 2986–2991.
35. Schirmack, J.; Mangelsdorf, K.; Ganzert, L.; Sand, W.; Hillebrand-Voiculescu, A.; Wagner, D. Methanobacterium movilense sp. nov., a hydrogenotrophic, secondary-alcohol-utilizing methanogen from the anoxic sediment of a subsurface lake. *Int. J. Syst. Evol. Microbiol.* **2014**, *64*, 522–527.
36. Mondav, R.; Woodcroft, B.J.; Kim, E.H.; McCalley, C.K.; Hodgkins, S.B.; Crill, P.M.; Chanton, J.; Hurst, G.B.; VerBerkmoes, N.C.; Saleska, S.R.; *et al.* Discovery of a novel methanogen prevalent in thawing permafrost. *Nat. Commun.* **2014**, *5*, doi:10.1038/ncomms4212.
37. Rittmann, S.; Holubar, P. Rapid extraction of total RNA from an anaerobic sludge biocoenosis. *Folia Microbiol.* **2014**, *59*, 127–132.
38. Cavicchioli, R. Cold-adapted archaea. *Nat. Rev. Microbiol.* **2006**, *4*, 331–343.
39. Huber, R.; Kurr, M.; Jannasch, H.W.; Stetter, K.O. A novel group of abyssal methanogenic archaebacteria (Methanopyrus) growing at 110 °C. *Nature* **1989**, *342*, 833–834.
40. Rittmann, S.K.-M.R.; Seifert, A.; Herwig, C. Quantitative analysis of media dilution rate effects on Methanothermobacter marburgensis grown in continuous culture on H_2 and CO_2. *Biomass Bioenergy* **2012**, *36*, 293–301.

41. Rittmann, S. K.-M. R. A critical assessment of microbiological biogas to biomethane upgrading systems. In *Biogas Science and Technology*; Guebitz, G.M., Ed.; Advances in Biochemical Engineering/Biotechnology; Springer International Publishing: New York, NY, USA, 2015.
42. Seifert, A.H.; Rittmann, S.; Bernacchi, S.; Herwig, C. Method for assessing the impact of emission gasses on physiology and productivity in biological methanogenesis. *Bioresour. Technol.* **2013**, *136*, 747–751.
43. Seifert, A.H.; Rittmann, S.; Herwig, C. Analysis of process related factors to increase volumetric productivity and quality of biomethane with Methanothermobacter marburgensis. *Appl. Energy* **2014**, *132*, 155–162.
44. Bernacchi, S.; Rittmann, S.; Seifert, A.H.; Krajete, A.; Herwig, C. Experimental methods for screening parameters influencing the growth to product yield ($Y_{(x/CH4)}$) of a biological methane production (BMP) process performed with Methanothermobacter marburgensis. *AIMS Bioeng.* **2014**, *1*, 72–86.
45. Albers, S.V.; Meyer, B.H. The archaeal cell envelope. *Nat. Rev. Microbiol.* **2011**, *9*, 414–426.
46. UWr Wydział Biotechnologii. Methanogens Database, 2013. Available online: http://metanogen.biotech.uni.wroc.pl/ (accessed on 13 November 2015).
47. Leibniz-Institut DSMZ. Catalogue of Microorganisms, 2015. Available online: http://www.dsmz.de/catalogues/catalogue-microorganisms.html (accessed on 13 November 2015).
48. Schönheit, P.; Moll, J.; Thauer, R.K. Nickel, cobalt, and molybdenum requirement for growth of Methanobacterium thermoautotrophicum. *Arch. Microbiol.* **1979**, *123*, 105–107.
49. Bonacker, L.G.; Baudner, S.; Mörschel, E.; Böcher, R.; Thauer, R.K. Properties of the two isoenzymes of methyl-coenzyme M reductase in Methanobacterium thermoautotrophicum. *Eur. J. Biochem./FEBS* **1993**, *217*, 587–595.
50. Wang, M.; Tomb, J.F.; Ferry, J.G. Electron transport in acetate-grown Methanosarcina acetivorans. *BMC Microbiol.* **2011**, *11*, 165.
51. Kaster, A.K.; Moll, J.; Parey, K.; Thauer, R.K. Coupling of ferredoxin and heterodisulfide reduction via electron bifurcation in hydrogenotrophic methanogenic archaea. *Proc. Natl. Acad. Sci. USA* **2011**, *108*, 2981–2986.
52. Huang, S.S. Occurrence of Life Outside the Solar System. *Am. Sci.* **1959**, *47*, 397–402.
53. Kasting, J.F.; Whitmire, D.P.; Reynolds, R.T. Habitable Zones around Main Sequence Stars. *Icarus* **1993**, *101*, 108–128.
54. Leitner, J.J.; Schwarz, R.; Firneis, M.G.; Hitzenberger, R.; Neubauer, D. Generalizing Habitable Zones in Exoplanetary Systems—The Concept of the Life Supporting Zone. *LPI Contrib.* **2010**, *1538*, 5255.
55. The water snow line describes the critical distance from a protostar in a protoplanetary disk where it is cold enough that water condenses into solid ice grains. In the Solar System, this line lies approx. at a distance of 2.7 AU from the Sun [269].
56. The Martian history is roughly divided into three main periods, namely Noachian, Hersperian, and the present period named Amazonian.
57. Martínez, G.M.; Renno, N.O. Water and Brines on Mars: Current Evidence and Implications for MSL. *Space Sci. Rev.* **2013**, *175*, 29–51.
58. Kral, T.A.; Altheide, T.S.; Lueders, A.E.; Schuerger, A.C. Low pressure and desiccation effects on methanogens: Implications for life on Mars. *Planet. Space Sci.* **2011**, *59*, 264–270.
59. Kral, T.A.; Altheide, S.T. Methanogen survival following exposure to desiccation, low pressure and martian regolith analogs. *Planet. Space Sci.* **2013**, *89*, 167–171.
60. Mickol, R.L.; Kral, T.A. Approaching Martian Conditions: Methanogen Survival at Low Pressure. In *Lunar and Planetary Institute Technical Report*, Proceedings of the 45th Lunar and Planetary Science Conference, Woodlands, TX, USA, 17–21 March 2014; Volume 45, p. 1602.
61. Kral, T.; Bekkum, C.; McKay, C. Growth of Methanogens on a Mars Soil Simulant. *Origin. Life Evol. Biosph.* **2004**, *34*, 615–626.
62. Mickol, R.L.; Waddell, W.H.; Kral, T.A. Methanogens as Models for Life on Mars. *LPI Contrib.* **2014**, *1791*, 1005.
63. Peters, G.H.; Abbey, W.; Bearman, G.H.; Mungas, G.S.; Smith, J.A.; Anderson, R.C.; Douglas, S.; Beegle, L.W. Mojave Mars simulant-Characterization of a new geologic Mars analog. *Icarus* **2008**, *197*, 470–479.
64. Kral, T.A.; Altheide, T.S.; Lueders, A.E.; Goodhart, T.H.; Virden, B.T.; Birch, W.; Howe, K.L.; Gavin, P. Methanogens: A Model for Life on Mars. *LPI Contrib.* **2010**, *1538*, 5084.

65. Goodhart, T.; Kral, T.A. The Effects of Perchlorate on Methane Production of Methanogens. *LPI Contrib.* **2010**, *1538*, 5524.
66. Chastain, B.K.; Kral, T.A. Approaching Mars-like Geochemical Conditions in the Laboratory: Omission of Artificial Buffers and Reductants in a Study of Biogenic Methane Production on a Smectite Clay. *Astrobiology* **2010**, *10*, 889–897.
67. Chastain, B.K.; Kral, T.A. Zero-valent iron on Mars: An alternative energy source for methanogens. *Icarus* **2010**, *208*, 198–201.
68. Morozova, D.; Möhlmann, D.; Wagner, D. Survival of Methanogenic Archaea from Siberian Permafrost under Simulated Martian Thermal Conditions. *Orig. Life Evol. Biosph.* **2007**, *37*, 189–200.
69. Schirmack, J.; Böhm, M.; Brauer, C.; Löhmannsröben, H.G.; de Vera, J.P.; Möhlmann, D.; Wagner, D. Laser spectroscopic real time measurements of methanogenic activity under simulated Martian subsurface analog conditions. *Planet. Space Sci.* **2014**, *98*, 198–204.
70. Serrano, P.; Wagner, D.; Böttger, U.; de Vera, J.P.; Lasch, P.; Hermelink, A. Single-cell analysis of the methanogenic archaeon Methanosarcina soligelidi from Siberian permafrost by means of confocal Raman microspectrocopy for astrobiological research. *Planet. Space Sci.* **2014**, *98*, 191–197.
71. De Vera, J.P.P.; Böttger, U.; Fritz, J.; Weber, I.; Malaszkiewicz, J.; Serrano, P.; Meessen, J.; Ott, S.; Wagner, D.; Hübers, H.W. Detection of cyanobacteria and methanogens embedded in Mars analogue minerals by the use of Raman spectroscopy. In Proceedings of the 2012 EGU General Assembly Conference, Vienna, Austria, 22–27 April 2012; Volume 14, p. 2334.
72. Archer, D.B. Uncoupling of Methanogenesis from Growth of Methanosarcina barkeri by Phosphate Limitation. *Appl. Environ. Microbiol.* **1985**, *50*, 1233–1237.
73. Liu, J.S.; Schill, N.; van Gulik, W.M.; Voisard, D.; Marison, I.W.; von Stockar, U. The coupling between catabolism and anabolism of Methanobacterium thermoautotrophicum in H_2- and iron-limited continuous cultures. *Enzym. Microb. Technol.* **1999**, *25*, 784–794.
74. Fardeau, M.L.; Belaich, J.P. Energetics of the growth of Methanococcus thermolithotrophicus. *Arch. Microbiol.* **1986**, *144*, 381–385.
75. Tsao, J.H.; Kaneshiro, S.M.; Yu, S.S.; Clark, D.S. Continuous culture of Methanococcus jannaschii, an extremely thermophilic methanogen. *Biotechnol. Bioeng.* **1994**, *43*, 258–261.
76. Mountfort, D.O.; Asher, R.A. Effect of inorganic sulfide on the growth and metabolism of Methanosarcina barkeri strain DM. *Appl. Environ. Microbiol.* **1979**, *37*, 670–675.
77. Pennings, J.L.A.; Vermeij, P.; Poorter, L.M.I.D.; Keltjens, J.T.; Vogels, G.D. Adaptation of methane formation and enzyme contents during growth of Methanobacterium thermoautotrophicum (strain ΔH) in a fed-batch fermentor. *Antonie Leeuwenhoek* **2000**, *77*, 281–291.
78. Ver Eecke, H.C.; Akerman, N.H.; Huber, J.A.; Butterfield, D.A.; Holden, J.F. Growth kinetics and energetics of a deep-sea hyperthermophilic methanogen under varying environmental conditions. *Environ. Microbiol. Rep.* **2013**, *5*, 665–671.
79. Ver Eecke, H.C.V.; Butterfield, D.A.; Huber, J.A.; Lilley, M.D.; Olson, E.J.; Roe, K.K.; Evans, L.J.; Merkel, A.Y.; Cantin, H.V.; Holden, J.F. Hydrogen-limited growth of hyperthermophilic methanogens at deep-sea hydrothermal vents. *Proc. Natl. Acad. Sci. USA* **2012**, *109*, 13674–13679.
80. Takai, K.; Nakamura, K.; Toki, T.; Tsunogai, U.; Miyazaki, M.; Miyazaki, J.; Hirayama, H.; Nakagawa, S.; Nunoura, T.; Horikoshi, K. Cell proliferation at 122 degrees C and isotopically heavy CH_4 production by a hyperthermophilic methanogen under high-pressure cultivation. *Proc. Natl. Acad. Sci. USA* **2008**, *105*, 10949–10954.
81. Morozova, D.; Wagner, D. Stress response of methanogenic archaea from Siberian permafrost compared with methanogens from nonpermafrost habitats. *FEMS Microbiol. Ecol.* **2007**, *61*, 16–25.
82. Schönheit, P.; Moll, J.; Thauer, R.K. Growth parameters (K_s, μ_{max}, Y_s) of Methanobacterium thermoautotrophicum. *Arch. Microbiol.* **1980**, *127*, 59–65.
83. Lai, M.C.; Chen, S.C.; Shu, C.M.; Chiou, M.S.; Wang, C.C.; Chuang, M.J.; Hong, T.Y.; Liu, C.C.; Lai, L.J.; Hua, J.J. Methanocalculus taiwanensis sp. nov., isolated from an estuarine environment. *Int. J. Syst. Evol. Microbiol.* **2002**, *52*, 1799–1806.
84. The latest findings show, that there is the possibility of hydrothermal vents on icy moons like Europa (e.g., [215]) or Enceladus [202], which would widen the potential temperature range for microbes in the outer Solar System.

85. Dong, X.; Chen, Z. Psychrotolerant methanogenic archaea: Diversity and cold adaptation mechanisms. *Sci. China Life Sci.* **2012**, *55*, 415–421.
86. Siddiqui, K.S.; Cavicchioli, R. Cold-Adapted Enzymes. *Annu. Rev. Biochem.* **2006**, *75*, 403–433.
87. Feller, G.; Gerday, C. Psychrophilic enzymes: Hot topics in cold adaptation. *Nat. Rev. Microbiol.* **2003**, *1*, 200–208.
88. Siddiqui, K.; Cavicchioli, R.; Thomas, T. Thermodynamic activation properties of elongation factor 2 (EF-2) proteins from psychrotolerant and thermophilic Archaea. *Extremophiles* **2002**, *6*, 143–150.
89. Thomas, T.; Cavicchioli, R. Effect of Temperature on Stability and Activity of Elongation Factor 2 Proteins from Antarctic and Thermophilic Methanogens. *J. Bacteriol.* **2000**, *182*, 1328–1332.
90. Thomas, T.; Kumar, N.; Cavicchioli, R. Effects of Ribosomes and Intracellular Solutes on Activities and Stabilities of Elongation Factor 2 Proteins from Psychrotolerant and Thermophilic Methanogens. *J. Bacteriol.* **2001**, *183*, 1974–1982.
91. Lim, J.; Thomas, T.; Cavicchioli, R. Low temperature regulated DEAD-box RNA helicase from the antarctic archaeon, Methanococcoides burtonii. *J. Mol. Biol.* **2000**, *297*, 553–567.
92. Zhou, L.; Liu, X.; Dong, X. Methanospirillum psychrodurum sp. nov., isolated from wetland soil. *Int. J. Syst. Evol. Microbiol.* **2014**, *64*, 638–641.
93. Simankova, M.V.; Parshina, S.N.; Tourova, T.P.; Kolganova, T.V.; Zehnder, A.J.; Nozhevnikova, A.N. Methanosarcina lacustris sp. nov., a new psychrotolerant methanogenic archaeon from anoxic lake sediments. *Syst. Appl. Microbiol.* **2001**, *24*, 362–367.
94. Zhang, G.; Jiang, N.; Liu, X.; Dong, X. Methanogenesis from Methanol at Low Temperatures by a Novel Psychrophilic Methanogen, "Methanolobus psychrophilus" sp. nov., Prevalent in Zoige Wetland of the Tibetan Plateau. *Appl. Environ. Microbiol.* **2008**, *74*, 6114–6120.
95. Chong, S.C.; Liu, Y.; Cummins, M.; Valentine, D.L.; Boone, D.R. Methanogenium marinum sp. nov., a H_2-using methanogen from Skan Bay, Alaska, and kinetics of H_2 utilization. *Antonie Van Leeuwenhoek* **2002**, *81*, 263–270.
96. Zhilina, T.N.; Zavarzin, G.A. Methanohalobium evestigatus, n. gen., n. sp. The extremely halophilic methanogenic Archaebacterium. *Dokl. Akad. Nauk SSSR* **1987**, *293*, 464–468.
97. Romesser, J.A.; Wolfe, R.S.; Mayer, F.; Spiess, E.; Walther-Mauruschat, A. Methanogenium, a new genus of marine methanogenic bacteria, and characterization of Methanogenium cariaci sp. nov. and Methanogenium marisnigri sp. nov. *Arch. Microbiol.* **1979**, *121*, 147–153.
98. Bräuer, S.L.; Cadillo-Quiroz, H.; Ward, R.J.; Yavitt, J.B.; Zinder, S.H. Methanoregula boonei gen. nov., sp. nov., an acidiphilic methanogen isolated from an acidic peat bog. *Int. J. Syst. Evol. Microbiol.* **2011**, *61*, 45–52.
99. Maestrojuán, G.M.; Boone, D.R.; Xun, L.; Mah, R.A.; Zhang, L. Transfer of Methanogenium bourgense, Methanogenium marisnigri, Methanogenium olentangyi, and Methanogenium thermophilicum to the Genus Methanoculleus gen. nov., Emendation of Methanoculleus marisnigri and Methanogenium, and Description of New Strains of Methanoculleus bourgense and Methanoculleus marisnigri. *Int. J. Syst. Bacteriol.* **1990**, *40*, 117–122.
100. Dianou, D.; Miyaki, T.; Asakawa, S.; Morii, H.; Nagaoka, K.; Oyaizu, H.; Matsumoto, S. Methanoculleus chikugoensis sp. nov., a novel methanogenic archaeon isolated from paddy field soil in Japan, and DNA-DNA hybridization among Methanoculleus species. *Int. J. Syst. Evol. Microbiol.* **2001**, *51*, 1663–1669.
101. Singh, N.; Kendall, M.M.; Liu, Y.; Boone, D.R. Isolation and characterization of methylotrophic methanogens from anoxic marine sediments in Skan Bay, Alaska: Description of Methanococcoides alaskense sp. nov., and emended description of Methanosarcina baltica. *Int. J. Syst. Evol. Microbiol.* **2005**, *55*, 2531–2538.
102. Franzmann, P.D.; Springer, N.; Ludwig, W.; De Macario, E.C.; Rohde, M. A Methanogenic Archaeon from Ace Lake, Antarctica: Methanococcoides burtonii sp. nov. *Syst. Appl. Microbiol.* **1992**, *15*, 573–581.
103. Shimada, Y.; Fukuda, W.; Akada, Y.; Ishida, M.; Nakayama, J.; Imanaka, T.; Fujiwara, S. Property of cold inducible DEAD-box RNA helicase in hyperthermophilic archaea. *Biochem. Biophys. Res. Commun.* **2009**, *389*, 622–627.
104. Saunders, N.F.W.; Thomas, T.; Curmi, P.M.G.; Mattick, J.S.; Kuczek, E.; Slade, R.; Davis, J.; Franzmann, P.D.; Boone, D.; Rusterholtz, K.; *et al.* Mechanisms of Thermal Adaptation Revealed From the Genomes of the Antarctic Archaea Methanogenium frigidum and Methanococcoides burtonii. *Genome Res.* **2003**, *13*, 1580–1588.

105. Gunnigle, E.; McCay, P.; Fuszard, M.; Botting, C.H.; Abram, F.; O'Flaherty, V. A Functional Approach to Uncover the Low-Temperature Adaptation Strategies of the Archaeon Methanosarcina barkeri. *Appl. Environ. Microbiol.* **2013**, *79*, 4210–4219.
106. Koga, Y. Thermal adaptation of the archaeal and bacterial lipid membranes. *Archaea (Vanc. B.C.)* **2012**, *2012*, 789652.
107. Nichols, D.S.; Miller, M.R.; Davies, N.W.; Goodchild, A.; Raftery, M.; Cavicchioli, R. Cold adaptation in the Antarctic Archaeon Methanococcoides burtonii involves membrane lipid unsaturation. *J. Bacteriol.* **2004**, *186*, 8508–8515.
108. Sprott, G.D.; Meloche, M.; Richards, J.C. Proportions of diether, macrocyclic diether, and tetraether lipids in Methanococcus jannaschii grown at different temperatures. *J. Bacteriol.* **1991**, *173*, 3907–3910.
109. Rittmann, S.; Herwig, C. A comprehensive and quantitative review of dark fermentative biohydrogen production. *Microb. Cell Fact.* **2012**, *11*, 115.
110. Nishimura, N.; Kitaura, S.; Mimura, A.; Takahara, Y. Cultivation of thermophilic methanogen KN-15 on H_2-CO_2 under pressurized conditions. *J. Ferment. Bioeng.* **1992**, *73*, 477–480.
111. Park, C.B.; Clark, D.S. Rupture of the Cell Envelope by Decompression of the Deep-Sea Methanogen Methanococcus jannaschii. *Appl. Environ. Microbiol.* **2002**, *68*, 1458–1463.
112. Miller, J.F.; Shah, N.N.; Nelson, C.M.; Ludlow, J.M.; Clark, D.S. Pressure and Temperature Effects on Growth and Methane Production of the Extreme Thermophile Methanococcus jannaschii. *Appl. Environ. Microbiol.* **1988**, *54*, 3039–3042.
113. Boonyaratanakornkit, B.; Córdova, J.; Park, C.B.; Clark, D.S. Pressure affects transcription profiles of Methanocaldococcus jannaschii despite the absence of barophilic growth under gas-transfer limitation. *Environ. Microbiol.* **2006**, *8*, 2031–2035.
114. Bernhardt, G.; Jaenicke, R.; Ludemann, H.D. High-Pressure Equipment for Growing Methanogenic Microorganisms on Gaseous Substrates at High Temperature. *Appl. Environ. Microbiol.* **1987**, *53*, 1876–1879.
115. Mayumi, D.; Dolfing, J.; Sakata, S.; Maeda, H.; Miyagawa, Y.; Ikarashi, M.; Tamaki, H.; Takeuchi, M.; Nakatsu, C.H.; Kamagata, Y. Carbon dioxide concentration dictates alternative methanogenic pathways in oil reservoirs. *Nat. Commun.* **2013**, *4*, doi:10.1038/ncomms2998.
116. Huber, G.; Stetter, K.O. Sulfolobus metallicus, sp. nov., a Novel Strictly Chemolithoautotrophic Thermophilic Archaeal Species of Metal-Mobilizers. *Syst. Appl. Microbiol.* **1991**, *14*, 372–378.
117. Suzuki, T.; Iwasaki, T.; Uzawa, T.; Hara, K.; Nemoto, N.; Kon, T.; Ueki, T.; Yamagishi, A.; Oshima, T. Sulfolobus tokodaii sp. nov. (f. Sulfolobus sp. strain 7), a new member of the genus Sulfolobus isolated from Beppu Hot Springs, Japan. *Extremophiles* **2002**, *6*, 39–44.
118. Xiang, X.; Dong, X.; Huang, L. Sulfolobus tengchongensis sp. nov., a novel thermoacidophilic archaeon isolated from a hot spring in Tengchong, China. *Extremophiles* **2003**, *7*, 493–498.
119. Schleper, C.; Piihler, G.; Kuhlmorgen, B.; Zillig, W. Life at extremely low pH. *Nature* **1995**, *375*, 741–742.
120. Cadillo-Quiroz, H.; Yavitt, J.B.; Zinder, S.H. Methanosphaerula palustris gen. nov., sp. nov., a hydrogenotrophic methanogen isolated from a minerotrophic fen peatland. *Int. J. Syst. Evol. Microbiol.* **2009**, *59*, 928–935.
121. Zhilina, T.N.; Zavarzina, D.G.; Kevbrin, V.V.; Kolganova, T.V. Methanocalculus natronophilus sp. nov., a new alkaliphilic hydrogenotrophic methanogenic archaeon from a soda lake, and proposal of the new family Methanocalculaceae. *Microbiology* **2013**, *82*, 698–706.
122. Rea, S.; Bowman, J.P.; Popovski, S.; Pimm, C.; Wright, A.D.G. Methanobrevibacter millerae sp. nov. and Methanobrevibacter olleyae sp. nov., methanogens from the ovine and bovine rumen that can utilize formate for growth. *Int. J. Syst. Evol. Microbiol.* **2007**, *57*, 450–456.
123. Burggraf, S.; Fricke, H.; Neuner, A.; Kristjansson, J.; Rouvier, P.; Mandelco, L.; Woese, C.R.; Stetter, K.O. Methanococcus igneus sp. nov., a Novel Hyperthermophilic Methanogen from a Shallow Submarine Hydrothermal System. *Syst. Appl. Microbiol.* **1990**, *13*, 263–269.
124. Jones, W.J.; Paynter, M.J.B.; Gupta, R. Characterization of Methanococcus maripaludis sp. nov., a new methanogen isolated from salt marsh sediment. *Arch. Microbiol.* **1983**, *135*, 91–97.
125. Robertson, D.E.; Noll, D.; Roberts, M.F.; Menaia, J.A.; Boone, D.R. Detection of the osmoregulator betaine in methanogens. *Appl. Environ. Microbiol.* **1990**, *56*, 563–565.

126. Proctor, L.M.; Lai, R.; Gunsalus, R.P. The methanogenic archaeon Methanosarcina thermophila TM-1 possesses a high-affinity glycine betaine transporter involved in osmotic adaptation. *Appl. Environ. Microbiol.* **1997**, *63*, 2252–2257.
127. Sowers, K.R.; Boone, J.E.; Gunsalus, R.P. Disaggregation of Methanosarcina spp. and Growth as Single Cells at Elevated Osmolarity. *Appl. Environ. Microbiol.* **1993**, *59*, 3832–3839.
128. Lai, M.C.; Sowers, K.R.; Robertson, D.E.; Roberts, M.F.; Gunsalus, R.P. Distribution of compatible solutes in the halophilic methanogenic archaebacteria. *J. Bacteriol.* **1991**, *173*, 5352–5358.
129. Roeßler, M.; Pflüger, K.; Flach, H.; Lienard, T.; Gottschalk, G.; Müller, V. Identification of a Salt-Induced Primary Transporter for Glycine Betaine in the Methanogen Methanosarcina mazei Gö1. *Appl. Environ. Microbiol.* **2002**, *68*, 2133–2139.
130. Lai, M.C.; Hong, T.Y.; Gunsalus, R.P. Glycine Betaine Transport in the Obligate Halophilic Archaeon Methanohalophilus portucalensis. *J. Bacteriol.* **2000**, *182*, 5020–5024.
131. Cockell, C.; Catling, D.; Wanda, L.; Snook, K.; Kepner, R.; Lee, P.; McKay, C. The Ultraviolet Environment of Mars: Biological Implications Past, Present, and Future. *Icarus* **2000**, *146*, 343–359.
132. Beatty, J.; Petersen, C.; Chaikin, A. (Eds.) *New Solar System*; Sky Pub.: Cambridge, MA, USA, 1999.
133. Fendrihan, S.; Bérces, A.; Lammer, H.; Musso, M.; Rontó, G.; Polacsek, T.K.; Holzinger, A.; Kolb, C.; Stan-Lotter, H. Investigating the Effects of Simulated Martian Ultraviolet Radiation on Halococcus dombrowskii and Other Extremely Halophilic Archaebacteria. *Astrobiology* **2009**, *9*, 104–112.
134. Ajon, M.; Fröls, S.; van Wolferen, M.; Stoecker, K.; Teichmann, D.; Driessen, A.J.M.; Grogan, D.W.; Albers, S.V.; Schleper, C. UV-inducible DNA exchange in hyperthermophilic archaea mediated by type IV pili. *Mol. Microbiol.* **2011**, *82*, 807–817.
135. Fröls, S.; Gordon, P.M.K.; Panlilio, M.A.; Duggin, I.G.; Bell, S.D.; Sensen, C.W.; Schleper, C. Response of the Hyperthermophilic Archaeon Sulfolobus solfataricus to UV Damage. *J. Bacteriol.* **2007**, *189*, 8708–8718.
136. Fröls, S.; Ajon, M.; Wagner, M.; Teichmann, D.; Zolghadr, B.; Folea, M.; Boekema, E.J.; Driessen, A.J.M.; Schleper, C.; Albers, S.V. UV-inducible cellular aggregation of the hyperthermophilic archaeon Sulfolobus solfataricus is mediated by pili formation. *Mol. Microbiol.* **2008**, *70*, 938–952.
137. Fröls, S.; White, M.F.; Schleper, C. Reactions to UV damage in the model archaeon Sulfolobus solfataricus. *Biochem. Soc. Trans.* **2009**, *37*, 36–41.
138. Kral, T.; Shina, N. Sensitivity of methanogens to ultraviolet radiation under aerobic and anaerobic conditions. In Proceedings of the 2012 Astrobiology Science Conference, Atlanta, GA, USA, 16–20 April 2012.
139. Sinha, N.; Kral, T.A. Methanogen Sensitivity to Ultraviolet Radiation: Implications for Life on Mars. *Meteorit. Planet. Sci. Suppl.* **2013**, *76*, 5071.
140. Stan-Lotter, H.; Legat, A.; Fendrihan, S.; Leuko, S.; Gruber, C.; Radax, C.; Pfaffenhuemer, M.; Weidler, G.; Rittmann, S. Haloarchaeal survival over geological times and the detection of extraterrestrial halite—Implications for the search for life on Mars. In Proceedings of the Third European Workshop on Exo-Astrobiology, Madrid, Spain, 18–20 November 2003; ESA Publications Division: Noordwijk, The Netherlands, 2004; Volume 545, pp. 63–66.
141. Radax, C.; Pfaffenhuemer, M.; Wieland, H.; Rittmann, S.; Leuko, S.; Weidler, G.; Gruber, C.; Stan-Lotter, H. Microbes in rock salt: How to find out what is in there. In Proceedings of the First European Workshop on Exo-Astrobiology, Graz, Austria, 16–19 September 2002; ESA Publications Division: Noordwijk, The Netherlands, 2002; Volume 518, pp. 485–486.
142. Rittmann, S.; Legat, A.; Fendrihan, S.; Stan-Lotter, H. Viability and morphology of Halobacterium species following desiccation—Implications for contaminants on Mars. In Proceedings of the Third European Workshop on Exo-Astrobiology, Madrid, Spain, 18–20 November 2003; ESA Publications Division: Noordwijk, The Netherlands, 2004; Volume 545, pp. 275–276.
143. Leuko, S.; Weidler, G.; Rittmann, S.; Stan-Lotter, H. LIVE/DEAD Kit: A powerful tool to detect haloarchaeal survival (and life?) in unknown environmental samples. In Proceedings of the Third European Workshop on Exo-Astrobiology, Madrid, Spain, 18–20 November 2003; ESA Publications Division: Noordwijk, The Netherlands, 2004; Volume 545, pp. 231–232.
144. Liu, C.T.; Miyaki, T.; Aono, T.; Oyaizu, H. Evaluation of methanogenic strains and their ability to endure aeration and water stress. *Curr. Microbiol.* **2008**, *56*, 214–218.

145. Schirmack, J.; Alawi, M.; Wagner, D. Influence of Martian regolith analogs on the activity and growth of methanogenic archaea, with special regard to long-term desiccation. *Extrem. Microbiol.* **2015**, 210, doi:10.3389/fmicb.2015.00210.
146. Solar Dynamics Observatory/Atmospheric Imaging Assembly. The Sun at 304 Angstroms, 2010. Available online: http://sdo.gsfc.nasa.gov/assets/img/browse/2010/08/ 19/20100819_003221_4096_0304.jpg (accessed on 13 November 2015).
147. International Astronomical Union. Eight Planets and New Solar System Designations, 2006. Available online: http://apod.nasa.gov/apod/ap060828.html (accessed on 13 November 2015).
148. Tate, K. Dwarf Planets in the Solar System, 2015. Available online: http://i.space.com/images/i/000/023/868/original/dwarf-planets-121120b-02.jpg?1353517196 (accessed on 13 November 2015).
149. National Aeronautics and Space Administration. Moons of the Solar System, 2004. Available online: http://solarsystem.nasa.gov/multimedia/ gallery/Many_Moons-browse.jpg (accessed on 13 November 2015)
150. Archinal, B.A.; A'Hearn, M.F.; Bowell, E.; Conrad, A.; Consolmagno, G.J.; Courtin, R.; Fukushima, T.; Hestroffer, D.; Hilton, J.L.; Krasinsky, G.A.; *et al.* Report of the IAU Working Group on Cartographic Coordinates and Rotational Elements: 2009. *Celest. Mech. Dyn. Astron.* **2011**, *109*, 101–135.
151. Chamberlin, A. Planetary Satellite Physical Parameters. Available online: http://ssd.jpl.nasa.gov/?sat_phys_par (accessed on 13 November 2015).
152. National Aeronautics and Space Administration. Ten Cool Things Seen in the First Year of LRO, 2010. Available online: http://www.nasa.gov/mission_pages/LRO/news/first-year.html (accessed on 13 November 2015).
153. Schenk, P. *Atlas of the Galilean Satellites*; Cambridge University Press: Cambridge, UK, 2010.
154. Chamberlin, A. Planets and Pluto: Physical Characteristics. Available online: http://ssd.jpl.nasa.gov/?planet_phys_par (accessed on 13 November 2015).
155. Spohn, T.; Breuer, D.; Johnson, T. (Eds.) *Encyclopedia of the Solar System*, 3rd ed.; Elsevier: Philadelphia, PA, USA, 2014.
156. Thomas, P.C.; Parker, J.W.; McFadden, L.A.; Russell, C.T.; Stern, S.A.; Sykes, M.V.; Young, E.F. Differentiation of the asteroid Ceres as revealed by its shape. *Nature* **2005**, *437*, 224–226.
157. Delitsky, M.L.; Lane, A.L. Ice chemistry on the Galilean satellites. *J. Geophys. Res.* **1998**, *103*, 31391–31404.
158. Moore, J.M.; Chapman, C.R.; Bierhaus, E.B.; Greeley, R.; Chuang, F.C.; Klemaszewski, J.; Clark, R.N.; Dalton, J.B.; Hibbitts, C.A.; Schenk, P.M.; *et al.* Callisto. In *Jupiter. The Planet, Satellites and Magnetosphere*; Bagenal, F., Dowling, T.E., McKinnon, W.B., Eds.; Cambridge University Press: Cambridge, UK, 2004; pp. 397–426.
159. Jaumann, R.; Kirk, R.L.; Lorenz, R.D.; Lopes, R.M.C.; Stofan, E.; Turtle, E.P.; Keller, H.U.; Wood, C.A.; Sotin, C.; Soderblom, L.A.; *et al.* Geology and Surface Processes on Titan. In *Titan from Cassini-Huygens*; Brown, R.H., Lebreton, J.P., Waite, J.H., Eds.; Springer: Berlin, Germany, 2010; p. 75.
160. Thomas, P.C. Sizes, shapes, and derived properties of the saturnian satellites after the Cassini nominal mission. *Icarus* **2010**, *208*, 395–401.
161. Spencer, J.R.; Pearl, J.C.; Segura, M.; Flasar, F.M.; Mamoutkine, A.; Romani, P.; Buratti, B.J.; Hendrix, A.R.; Spilker, L.J.; Lopes, R.M.C. Cassini Encounters Enceladus: Background and the Discovery of a South Polar Hot Spot. *Science* **2006**, *311*, 1401–1405.
162. Porco, C.C.; Helfenstein, P.; Thomas, P.C.; Ingersoll, A.P.; Wisdom, J.; West, R.; Neukum, G.; Denk, T.; Wagner, R.; Roatsch, T.; *et al.* Cassini Observes the Active South Pole of Enceladus. *Science* **2006**, *311*, 1393–1401.
163. Iess, L.; Stevenson, D.J.; Parisi, M.; Hemingway, D.; Jacobson, R.A.; Lunine, J.I.; Nimmo, F.; Armstrong, J.W.; Asmar, S.W.; Ducci, M.; *et al.* The Gravity Field and Interior Structure of Enceladus. *Science* **2014**, *344*, 78–80.
164. Buie, M.W.; Grundy, W.M.; Young, E.F.; Young, L.A.; Stern, S.A. Orbits and Photometry of Pluto's Satellites: Charon, S/2005 P1, and S/2005 P2. *AJ* **2006**, *132*, 290–298.
165. Stern, S.A.; Trafton, L.M. On the Atmospheres of Objects in the Kuiper Belt. In *The Solar System Beyond Neptune*; Barucci, M.A., Boehnhardt, H., Cruikshank, D.P., Morbidelli, A., Dotson, R., Eds.; University of Arizona Press: Tucson, AZ, USA, 2008; pp. 365–380.
166. Vance, S.; Bouffard, M.; Choukroun, M.; Sotin, C. Ganymede's internal structure including thermodynamics of magnesium sulfate oceans in contact with ice. *Planet. Space Sci.* **2014**, *96*, 62–70.

167. Lollar, B.S.; McCollom, T.M. Geochemistry: Biosignatures and abiotic constraints on early life. *Nature* **2006**, *444*, E18.
168. Guzmán-Marmolejo, A.; Segura, A.; Escobar-Briones, E. Abiotic Production of Methane in Terrestrial Planets. *Astrobiology* **2013**, *13*, 550–559.
169. White, W. *Isotope Geochemistry*; Wiley Works, Wiley: Hoboken, NJ, USA, 2015.
170. Mahaffy, P.R.; Webster, C.R.; Atreya, S.K.; Franz, H.; Wong, M.; Conrad, P.G.; Harpold, D.; Jones, J.J.; Leshin, L.A.; Manning, H.; *et al*. Abundance and Isotopic Composition of Gases in the Martian Atmosphere from the Curiosity Rover. *Science* **2013**, *341*, 263–266.
171. Hoekzema, N.; Gwinner, K.; Grieger, B.; Markiewicz, W.J.; Keller, H.; Hoffmann, H.; Meima, J.A.; Neukum, G. The Dust Scale Height of the Martian Atmosphere around Pavonis Mons from Hrsc Stereo Images; In *AAS/Division for Planetary Sciences Meeting Abstracts*; AAS/Division for Planetary Sciences Meeting Abstracts #38; American Astronomical Society: Washington, DC, USA, 2006; Volume 38, p. #60.30.
172. Williams, D.R. Mars Fact Sheet. Available online: http://nssdc.gsfc.nasa.gov/planetary/factsheet/marsfact.html (accessed on 19 November 2015).
173. Williams, D.R. Earth Fact Sheet. Available online: http://nssdc.gsfc.nasa.gov/planetary/factsheet/earthfact.html (accessed on 19 November 2015).
174. Lowell, P. *Mars and Its Canals*; Macmillan And Company Limited: London, UK, 1911.
175. Villanueva, G.L.; Mumma, M.J.; Novak, R.E.; Käufl, H.U.; Hartogh, P.; Encrenaz, T.; Tokunaga, A.; Khayat, A.; Smith, M.D. Strong water isotopic anomalies in the martian atmosphere: Probing current and ancient reservoirs. *Science* **2015**, *348*, 218–221.
176. Ojha, L.; Wilhelm, M.B.; Murchie, S.L.; McEwen, A.S.; Wray, J.J.; Hanley, J.; Massé, M.; Chojnacki, M. Spectral evidence for hydrated salts in recurring slope lineae on Mars. *Nature Geoscience* **2015**, *8*, 829–832.
177. Feldman, W.C.; Pathare, A.; Maurice, S.; Prettyman, T.H.; Lawrence, D.J.; Milliken, R.E.; Travis, B.J. Mars Odyssey neutron data: 2. Search for buried excess water ice deposits at nonpolar latitudes on Mars. *J. Geophys. Res. (Planets)* **2011**, *116*, 11009.
178. Hand, E. Curiosity set to weigh in on Mars methane puzzle. *Nature* **2012**, doi:10.1038/nature.2012.11721. Available online: http://www.nature.com/news/curiosity-set-to-weigh-in-on-mars-methane-puzzle-1.11721 (accessed on 19 November 2015).
179. The potential CH_4 signal was in fact coming from CO_2 ice.
180. Webster, C.R.; Mahaffy, P.R.; Atreya, S.K.; Flesch, G.J.; Farley, K.A.; Team, M.S. Low Upper Limit to Methane Abundance on Mars. *Science* **2013**, *342*, 355–357.
181. Zahnle, K.; Freedman, R.S.; Catling, D.C. Is there methane on Mars? *Icarus* **2011**, *212*, 493–503.
182. Fonti, S.; Marzo, G.A. Mapping the methane on Mars. *A & A* **2010**, *512*, A51.
183. Minor sources are, e.g., UV radiation induced generation of CH_4 from organic chemicals and released CH_4 from CH_4 hydrates (*i.e.*, clathrates), that may be a record of past biological activity.
184. Catling, D.C.; Cockell, C.S.; McKay, C.P. Ultraviolet Radiation on the Surface of Mars. In Proceedings of the Fifth International Conference on Mars, Pasadena, CA, USA, 18–23 July 1999; p. 6128.
185. Gaidos, E.J.; Nealson, K.H.; Kirschvink, J.L. Life in Ice-Covered Oceans. *Science* **1999**, *284*, 1631–1633.
186. McKinnon, W.B.; Pappalardo, R.T.; Khurana, K.K. Europa: Perspectives on an Ocean World. In *Europa*; Pappalardo, R.T., McKinnon, W.B., Khurana, K.K., Eds.; University of Arizona Space Science Series; University of Arizona Press: Tucson, AZ, USA, 2009; p. 697.
187. Oren, A. The bioenergetic basis for the decrease in metabolic diversity at increasing salt concentrations: Implications for the functioning of salt lake ecosystems. *Hydrobiologia* **2001**, *466*, 61–72.
188. Hussmann, H.; Sohl, F.; Spohn, T. Subsurface oceans and deep interiors of medium-sized outer planet satellites and large trans-neptunian objects. *Icarus* **2006**, *185*, 258–273.
189. Turse, C.; Leitner, J.J.; Firneis, M.G.; Schulze-Makuch, D. Simulations of Prebiotic Chemistry under Post-Impact Conditions on Titan. *Life* **2013**, *3*, 538–549.
190. Hand, K.P.; Chyba, C.F.; Priscu, J.C.; Carlson, R.W.; Nealson, K.H. Astrobiology and the Potential for Life on Europa. In *Europa*; Pappalardo, R.T., McKinnon, W.B., Khurana, K.K., Eds.; The University of Arizona Space Science Series; University of Arizona Press: Tucson, AZ, USA, 2009; p. 589.
191. Chamberlin, A. Planetary Satellite Mean Orbital Parameters. Available online: http://ssd.jpl.nasa.gov/?sat_elem (accessed on 19 November 2015).
192. Spencer, J. Planetary science: Enceladus with a grain of salt. *Nature* **2009**, *459*, 1067–1068.

193. McKinnon, W.B. Effect of Enceladus's rapid synchronous spin on interpretation of Cassini gravity. *Geophys. Res. Lett.* **2015**, *42*, 2137–2143.
194. Postberg, F.; Kempf, S.; Schmidt, J.; Brilliantov, N.; Beinsen, A.; Abel, B.; Buck, U.; Srama, R. Sodium salts in E-ring ice grains from an ocean below the surface of Enceladus. *Nature* **2009**, *459*, 1098–1101.
195. Taubner, R.S.; Leitner, J.; Firneis, M.; Hitzenberger, R. Modelling the Interior Structure of Enceladus Based on the 2014's Cassini Gravity Data. *J. Orig. Life Evol. Biosph.* **2015**, 1–6.
196. Schubert, G.; Anderson, J.D.; Travis, B.J.; Palguta, J. Enceladus: Present internal structure and differentiation by early and long-term radiogenic heating. *Icarus* **2007**, *188*, 345–355.
197. Postberg, F. Sodium salts in cryo-volcanic ice particles—Evidence for liquid water on Enceladus. In Proceedings of the CHARM Meeting, Leicester, UK, 29 May 2009; National Aeronautics and Space Administration: Washington, DC, USA.
198. Postberg, F.; Schmidt, J.; Hillier, J.; Kempf, S.; Srama, R. A salt-water reservoir as the source of a compositionally stratified plume on Enceladus. *Nature* **2011**, *474*, 620–622.
199. Thomas, P.; Tajeddine, R.; Tiscareno, M.; Burns, J.; Joseph, J.; Loredo, T.; Helfenstein, P.; Porco, C. Enceladus's measured physical libration requires a global subsurface ocean. *Icarus* **2016**, *264*, 37–47.
200. Bouquet, A.; Mousis, O.; Waite, J.H.; Picaud, S. Possible evidence for a methane source in Enceladus' ocean. *Geophys. Res. Lett.* **2015**, *42*, 1334–1339.
201. Waite, J.H., Jr.; Lewis, W.S.; Magee, B.A.; Lunine, J.I.; McKinnon, W.B.; Glein, C.R.; Mousis, O.; Young, D.T.; Brockwell, T.; Westlake, J.; *et al.* Liquid water on Enceladus from observations of ammonia and ^{40}Ar in the plume. *Nature* **2009**, *460*, 487–490.
202. Hsu, H.W.; Postberg, F.; Sekine, Y.; Shibuya, T.; Kempf, S.; Horányi, M.; Juhász, A.; Altobelli, N.; Suzuki, K.; Masaki, Y.; *et al.* Ongoing hydrothermal activities within Enceladus. *Nature* **2015**, *519*, 207–210.
203. Howett, C.; Spencer, J.; Verbiscer, A. Enceladus' enigmatic heat flow. In *AAS/Division for Planetary Sciences Meeting Abstracts*; American Astronomical Society: Washington, DC, USA, 2014; Volume 46, p. #405.02.
204. Howett, C.J.A.; Spencer, J.R.; Pearl, J.; Segura, M. High heat flow from Enceladus' south polar region measured using 10–600 cm^{-1} Cassini/CIRS data. *J. Geophys. Res. (Planets)* **2011**, *116*, 3003.
205. Hansen, C.J.; Shemansky, D.E.; Esposito, L.W.; Stewart, A.I.F.; Lewis, B.R.; Colwell, J.E.; Hendrix, A.R.; West, R.A.; Waite, J.H., Jr.; Teolis, B.; *et al.* The composition and structure of the Enceladus plume. *Geophys. Res. Lett.* **2011**, *38*, 11202.
206. Horányi, M.; Juhász, A.; Morfill, G.E. Large-scale structure of Saturn's E-ring. *Geophys. Res. Lett.* **2008**, *35*, 4203.
207. Kempf, S.; Srama, R.; Moragas-Klostermeyer, G.; Postberg, F.; Horányi, M.; Schmidt, J.; Spahn, F. The Structure of Saturn's E ring as seen by Cassini CDA. In Proceedings of the 2011 EPSC-DPS Joint Meeting, Nantes, France, 2–7 October 2011; p. 1643.
208. Schubert, G.; Sohl, F.; Hussmann, H. Interior of Europa. In *Europa*; Pappalardo, R.T., McKinnon, W.B., Khurana, K.K., Eds.; The University of Arizona Space Science Series; University of Arizona Press: Tucson, AZ, USA, 2009; p. 353.
209. Taubner, R.S.; Leitner, J.; Firneis, M.; Hitzenberger, R. Estimations on the Interior of Small Icy Bodies in the Solar System (EGU2014-7338). Presented at the European Geosciences Union General Assembly, Vienna, Austria, 27 April–2 May 2014.
210. Kivelson, M.G.; Khurana, K.K.; Russell, C.T.; Volwerk, M.; Walker, R.J.; Zimmer, C. Galileo Magnetometer Measurements: A Stronger Case for a Subsurface Ocean at Europa. *Science* **2000**, *289*, 1340–1343.
211. Carr, M.H.; Belton, M.J.S.; Chapman, C.R.; Davies, M.E.; Geissler, P.; Greenberg, R.; McEwen, A.S.; Tufts, B.R.; Greeley, R.; Sullivan, R.; *et al.* Evidence for a subsurface ocean on Europa. *Nature* **1998**, *391*, 363.
212. Greenberg, R.; Geissler, P.; Hoppa, G.; Tufts, B.R. Tidal-Tectonic Processes and Their Implications for the Character of Europa's Icy Crust. *Rev. Geophys.* **2002**, *40*, 1004.
213. Brown, M.E.; Hand, K.P. Salts and Radiation Products on the Surface of Europa. *AJ* **2013**, *145*, 110.
214. Roth, L.; Saur, J.; Retherford, K.D.; Strobel, D.F.; Feldman, P.D.; McGrath, M.A.; Nimmo, F. Transient Water Vapor at Europa's South Pole. *Science* **2014**, *343*, 171–174.
215. Zolotov, M.Y.; Kargel, J.S. On the Chemical Composition of Europa's Icy Shell, Ocean, and Underlying Rocks. In *Europa*; Pappalardo, R.T., McKinnon, W.B., Khurana, K.K., Eds.; The University of Arizona Space Science Series; University of Arizona Press: Tucson, AZ, USA, 2009; p. 431.

216. McCollom, T.M. Methanogenesis as a potential source of chemical energy for primary biomass production by autotrophic organisms in hydrothermal systems on Europa. *J. Geophys. Res. Planets* **1999**, *104*, 30729–30742.
217. Niemann, H.B.; Atreya, S.K.; Demick, J.E.; Gautier, D.; Haberman, J.A.; Harpold, D.N.; Kasprzak, W.T.; Lunine, J.I.; Owen, T.C.; Raulin, F. Composition of Titan's lower atmosphere and simple surface volatiles as measured by the Cassini-Huygens probe gas chromatograph mass spectrometer experiment. *J. Geophys. Res. (Planets)* **2010**, *115*, 12006.
218. Raulin, F. Astrobiology and habitability of Titan. *Space Sci. Rev.* **2008**, *135*, 37–48.
219. Raulin, F.; McKay, C.; Lunine, J.; Owen, T. Titan's Astrobiology. In *Titan from Cassini-Huygens*; Brown, R.H., Lebreton, J.P., Waite, J.H., Eds.; Springer Science & Business Media: Berlin, Germany, 2010; p. 215.
220. Fulchignoni, M.; Ferri, F.; Angrilli, F.; Ball, A.J.; Bar-Nun, A.; Barucci, M.A.; Bettanini, C.; Bianchini, G.; Borucki, W.; Colombatti, G.; *et al.* *In situ* measurements of the physical characteristics of Titan's environment. *Nature* **2005**, *438*, 785–791.
221. Clarke, D.W.; Ferris, J.P. Chemical Evolution on Titan: Comparisons to the Prebiotic Earth. In *Planetary and Interstellar Processes Relevant to the Origins of Life*; Whittet, D.C.B., Ed.; Springer Science & Business Media: Berlin, Germany, 1997; p. 225.
222. Balucani, N.; Cartechini, L.; Bergeat, A.; Casavecchia, P.; Volpi, G.G. Laboratory studies on the formation of CN containing molecules in the atmosphere of Titan and prebiotic Earth. In Proceedings of the First European Workshop on Exo-/Astro-Biology, Frascati, Italy, 21–23 May 2001; Ehrenfreund, P., Angerer, O., Battrick, B., Eds.; ESA Special Publication: Noordwijk, The Netherlands, 2001; Volume 496, pp. 159–162.
223. Neish, C.D.; Somogyi, Á.; Imanaka, H.; Lunine, J.I.; Smith, M.A. Rate Measurements of the Hydrolysis of Complex Organic Macromolecules in Cold Aqueous Solutions: Implications for Prebiotic Chemistry on the Early Earth and Titan. *Astrobiology* **2008**, *8*, 273–287.
224. He, C.; Smith, M.A. Identification of nitrogenous organic species in Titan aerosols analogs: Implication for prebiotic chemistry on Titan and early Earth. *Icarus* **2014**, *238*, 86–92.
225. Sotin, C.; Jaumann, R.; Buratti, B.J.; Brown, R.H.; Clark, R.N.; Soderblom, L.A.; Baines, K.H.; Bellucci, G.; Bibring, J.P.; Capaccioni, F.; *et al.* Release of volatiles from a possible cryovolcano from near-infrared imaging of Titan. *Nature* **2005**, *435*, 786–789.
226. O'Brien, D.P.; Lorenz, R.D.; Lunine, J.I. Numerical calculations of the longevity of impact oases on Titan. *Icarus* **2005**, *173*, 243–253.
227. Iess, L.; Jacobson, R.A.; Ducci, M.; Stevenson, D.J.; Lunine, J.I.; Armstrong, J.W.; Asmar, S.W.; Racioppa, P.; Rappaport, N.J.; Tortora, P. The Tides of Titan. *Science* **2012**, *337*, 457–459.
228. Kerr, R.A. Cassini Spies an Ocean Inside Saturn's Icy, Gassy Moon Titan. *Science* **2012**, *336*, 1629.
229. Sotin, C.; Mitri, G.; Rappaport, N.; Schubert, G.; Stevenson, D. Titan's Interior Structure. In *Titan from Cassini-Huygens*; Brown, R.H., Lebreton, J.P., Waite, J.H., Eds.; Springer Science & Business Media: Berlin, Germany, 2010; p. 61.
230. Buratti, B.; Faulk, S.; Mosher, J.; Baines, K.; Brown, R.; Clark, R.; Nicholson, P. Search for and limits on plume activity on Mimas, Tethys, and Dione with the Cassini Visual Infrared Mapping Spectrometer (VIMS). *Icarus* **2011**, *214*, 534–540.
231. There is an atmosphere indicating some material outflowing from the surface both at Dione and Rhea (J.H. Waite, personal communication, July, 2015).
232. Tajeddine, R.; Rambaux, N.; Lainey, V.; Charnoz, S.; Richard, A.; Rivoldini, A.; Noyelles, B. Constraints on Mimas' interior from Cassini ISS libration measurements. *Science* **2014**, *346*, 322–324.
233. Gaeman, J.; Hier-Majumder, S.; Roberts, J.H. Sustainability of a subsurface ocean within Triton's interior. *Icarus* **2012**, *220*, 339–347.
234. Soderblom, L.A.; Becker, T.L.; Kieffer, S.W.; Brown, R.H.; Hansen, C.J.; Johnson, T.V.; Kirk, R.L.; Shoemaker, E.M.; Cook, A.F. Triton's geyser-like plumes—Discovery and basic characterization. *Science* **1990**, *250*, 410–415.
235. International Astronomical Union (Ed.) *RESOLUTION B5—Definition of a Planet in the Solar System*; International Astronomical Union: Prague, Czech Republic, 2006.
236. Küppers, M.; O'Rourke, L.; Bockelée-Morvan, D.; Zakharov, V.; Lee, S.; von Allmen, P.; Carry, B.; Teyssier, D.; Marston, A.; Müller, T.; *et al.* Localized sources of water vapour on the dwarf planet (1)Ceres. *Nature* **2014**, *505*, 525–527.

237. Witze, A. Mystery haze appears above Ceres's bright spots. *Nat. NEWS* , 21 July 2015. Available online: http://www.nature.com/news/mystery-haze-appears-above-ceres-s-bright-spots-1.18032 (accessed on 19 November 2015).
238. Robuchon, G.; Nimmo, F. Thermal evolution of Pluto and implications for surface tectonics and a subsurface ocean. *Icarus* **2011**, *216*, 426–439.
239. Rhoden, A.R.; Henning, W.; Hurford, T.A.; Hamilton, D.P. The interior and orbital evolution of Charon as preserved in its geologic record. *Icarus* **2015**, *246*, 11–20.
240. Large TNOs show a higher amount of rocky material, especially Quaoar with a mean density of $4200 \pm 1300\ \mathrm{kg\,m^{-3}}$ [270].
241. Allen, C.C.; Morris, R.V.; Lindstrom, D.J.; Lindstrom, M.M.; Lockwood, J.P. JSC Mars-1—Martian regolith simulant. In *Lunar and Planetary Institute Technical Report*, Proceedings of the Lunar and Planetary Science Conference, Houston, TX, USA, 17–21 March 1997; Volume 28, p. 27.
242. According to the reaction $Fe^0 + 2H^+ \rightarrow Fe^{2+} + H_2$, zero-valent iron could serve as reactant to produce H_2 [67].
243. Djordjevic, S.; Mickol, R.L.; Kral, T.A. Simulating Martian Conditions: Methanogen Survivability during Freeze-Thaw Cycles. In Proceedings of the Lunar and Planetary Science Conference, Woodlands, TX, USA, 17–21 March 2014; Volume 45, p. 2539.
244. Mickol, R.L.; Kral, T.A.; Laird, S.K. Mesophile Methanogen Survival Under Freeze/Thaw Cycles. In *Lunar and Planetary Institute Technical Report*, Proceedings of the Lunar and Planetary Science Conference, Woodlands, TX, USA, 17–21 March 2014; Volume 45, p. 1603.
245. *Methanosarcina spec. SMA-16*, *SMA-23*, *M. soligelidi*, *Methanobacterium spec. MC-20*, *M. barkeri*, and *M. frigidum*.
246. McKay, C.P.; Porco, C.C.; Altheide, T.; Davis, W.L.; Kral, T.A. The Possible Origin and Persistence of Life on Enceladus and Detection of Biomarkers in the Plume. *Astrobiology* **2008**, *8*, 909–919.
247. Found in the Columbia River basalts and basalts in the Twin Falls area of Idaho, respectively [246].
248. Stevens, T.O.; McKinley, J.P. Lithoautotrophic Microbial Ecosystems in Deep Basalt Aquifers. *Science* **1995**, *270*, 450–455.
249. Chapelle, F.H.; O'Neill, K.; Bradley, P.M.; Methé, B.A.; Ciufo, S.A.; Knobel, L.L.; Lovley, D.R. A hydrogen-based subsurface microbial community dominated by methanogens. *Nature* **2002**, *415*, 312–315.
250. Found in the 3-to 4-km-deep fracture in the 2.7-billion-year-old Ventersdorp Supergroup metabasalt [251].
251. Lin, L.H.; Wang, P.L.; Rumble, D.; Lippmann-Pipke, J.; Boice, E.; Pratt, L.M.; Sherwood Lollar, B.; Brodie, E.L.; Hazen, T.C.; Andersen, G.L.; *et al.* Long-Term Sustainability of a High-Energy, Low-Diversity Crustal Biome. *Science* **2006**, *314*, 479–482.
252. McKay, C.P.; Khare, B.N.; Amin, R.; Klasson, M.; Kral, T.A. Possible sources for methane and C_2-C_5 organics in the plume of Enceladus. *Planet. Space Sci.* **2012**, *71*, 73–79.
253. Parashar, S.; Kral, T.A. Possibility of Methanogens on Enceladus. *LPI Contrib.* **2010**, *1538*, 5044.
254. Taubner, R.S.; Rittmann, S.; Leitner, J.; Schleper, C.; Firneis, M.; Hitzenberger, R. Assessing the feasibility to cultivate methanogens under Enceladus-like conditions reservoir. Presented at the 14th European Workshop on Astrobiology, Edinburgh, UK, 13–16 October 2014.
255. Preston, L.J.; Dartnell, L.R. Planetary habitability: Lessons learned from terrestrial analogues. *Int. J. Astrobiol.* **2014**, *13*, 81–98.
256. Morris, R.V.; Blake, D.F.; Bish, D.; Ming, D.W.; Agresti, D.G.; Treiman, A.H.; Steele, A.; Amundsen, H.E.F.; Amase Team. A Terrestrial Analogue from Spitsbergen (Svalbard, Norway) for the Comanche Carbonate at Gusev Crater, Mars. In *Lunar and Planetary Institute Technical Report*, Proceedings of the Lunar and Planetary Science Conference, Woodlands, TX, USA, 7–11 March 2011; Volume 42, p. 1699.
257. Gómez-Gómez, F.; Rodriguez-Manfredi, J.A.; Perez, L.; Prieto-Ballesteros, O.; Amils, R.; Gomez-Elvira, J. Martian Habitability Studies in Two Field Earth Analogues: The Permafrost in the Imuruk Lake Basaltic Field (Alaska) and the Atacama Desert. In Proceedings of the 38th COSPAR Scientific Assembly, Bremen, Germany, 15–18 July 2010; Volume 38, p. 3295.
258. Shtarkman, Y.M.; Koçer, Z.A.; Edgar, R.; Veerapaneni, R.S.; D'Elia, T.; Morris, P.F.; Rogers, S.O. Subglacial Lake Vostok (Antarctica) Accretion Ice Contains a Diverse Set of Sequences from Aquatic, Marine and Sediment-Inhabiting Bacteria and Eukarya. *PLoS ONE* **2013**, *8*, e67221.

259. Patil, U.; Muskan, K. *Essentials of Biotechnology*; I.K. International Publishing House Pvt. Limited: New Deli, India, 2009.
260. Fuchs, G.; Eitinger, T.; Schlegel, H. *Allgemeine Mikrobiologie*, 8th ed.; Thieme Georg Verlag: Stuttgart, Germany, 2007.
261. Krajete, A.; Herwig, C.; Rittmann, S.; Seifert, A.; Bernacchi, S. Method and System for Producing Methane Using Methanogenic Microorganisms and Applying Specific Nitrogen Concentrations in the Liquid Phase. Patent WO2014128300 A1, 28 August 2014.
262. Plaut, J.J.; Barabash, S.; Bruzzone, L.; Dougherty, M.; Erd, C.; Fletcher, L.; Gladstone, R.; Grasset, O.; Gurvits, L.; Hartogh, P.; *et al.* Jupiter Icy Moons Explorer (JUICE): Science Objectives, Mission and Instruments. In Proceedings of the Lunar and Planetary Science Conference, Woodlands, TX, USA, 17–21 March 2014; Volume 45, p. 2717.
263. Grasset, O.; Dougherty, M.K.; Coustenis, A.; Bunce, E.J.; Erd, C.; Titov, D.; Blanc, M.; Coates, A.; Drossart, P.; Fletcher, L.N.; *et al.* JUpiter ICy moons Explorer (JUICE): An ESA mission to orbit Ganymede and to characterise the Jupiter system. *Planet. Space Sci.* **2013**, *78*, 1–21.
264. European Space Agency/Science and Robotic Exploration. *JUICE Definition Study Report (Red Book)*; Technical Report 1.0; ESA: Paris, France, 2014.
265. National Aeronautics and Space Administration. VALKYRIE: Phase 2, 2015. Available online: https://astrobiology.nasa.gov/astep/projects/nra/ nnh11zda001n-astep/valkyrie-phase-2/ (accessed on 19 November 2015).
266. Karl, D.M.; Beversdorf, L.; Björkman, K.; Church, M.J.; Martinez, A.; Delong, E.F. Aerobic production of methane in the sea. *Nat. Geosci.* **2008**, *1*, 473–478.
267. Metcalf, W.W.; Griffin, B.M.; Cicchillo, R.M.; Gao, J.; Janga, S.C.; Cooke, H.A.; Circello, B.T.; Evans, B.S.; Martens-Habbena, W.; Stahl, D.A.; *et al.* Synthesis of Methylphosphonic Acid by Marine Microbes: A Source for Methane in the Aerobic Ocean. *Science* **2012**, *337*, 1104–1107.
268. Carini, P.; White, A.; Campbell, E.; Giovannoni, S. Methane production by phosphate-starved SAR11 chemoheterotrophic marine bacteria. *Nat. Commun.* **2014**, *5*, doi:10.1038/ncomms5346.
269. Lecar, M.; Podolak, M.; Sasselov, D.; Chiang, E. On the Location of the Snow Line in a Protoplanetary Disk. *ApJ* **2006**, *640*, 1115–1118.
270. Fraser, W.C.; Brown, M.E. Quaoar: A Rock in the Kuiper Belt. *ApJ* **2010**, *714*, 1547–1550.

4 New Method to Quantify CH_4 Production by Using Hydrogenotrophic Methanogens

4.1 Overview

A great variety in methods for quantifying the growth and CH_4 production of methanogens can be found in the literature. The most common way is to measure the change in optical density at a certain wavelength (*e.g.* 578 or 600 nm). Another favoured but time-consuming method is cell counting. Here, hemocytometer, *i.e.* counting chambers, are normally used which have a grid to manually count the number of cells in a certain area of known volume. However, these methods are not applicable for media with a high initial turbidity or for the monitoring of organisms that form aggregates. In anaerobic cultivation, CH_4 quantification by use of gas chromatography (GC) is also well established. This method requires a gas chromatograph (detector), specific carrier gas, and preferably an autosampler. This equipment is comparatively expensive and the samples often cannot be used for further studies after the GC measurements.

For the study presented in chapter 5, we had to screen our strain collection to find methanogens suitable for the Enceladus-like experiments. Therefore, we developed a novel method for indirect quantification of CH_4 evolution rate (MER) by measuring H_2O evolution rate (WER).

The method combines two rational concepts: Hydrogenotrophic methanogens use CO_2 as a source of carbon, and H_2 as an electron donor to produce CH_4 and H_2 according to the stochiometric equation $4\,H_2 + CO_2 \rightarrow CH_4 + 2\,H_2O$. In a closed batch setting, the molar ratio of the gaseous compounds of (4+1) to 1 leads to a decrease in pressure during incubation accompanied with an increase in the amount of water. The pressure drop can be measured by using a manometer and the gain in water can be easily measured by using an analytical balance after changing the gaseous phase to the initial conditions, *i.e.* before incubation. This method can easily be used for closed batch experiments by applying the Standard Operation Procedure (SOP) presented in this publication (see Fig. 4.1).

This method paper shows that this technique is extremely accurate, precise, fast and cheaper than GC measurements. Further, this method can be used within the cultivation process for continuous data collection without additional stress for the organisms.

4.2 Publication Details

Title: Method for Indirect Quantification of CH_4 Production via H_2O Production Using Hydrogenotrophic Methanogens
Authors: R.-S. Taubner, S. K.-M. R. Rittmann
Status: Published online in *Frontiers in Microbiology*, April 29^{th}, 2016
Bibliographic reference: Front Microbiol, Volume 7, Article 532
DOI: doi:10.3389/fmicb.2016.00532

Own contributions: Literature research, establishment of the Standard Operation Procedure, planing and performance of all experiments, software implementation, data analysis, preparation of figures and plots, writing of the first manuscript version, editing and approving manuscript, coordinating correction state and finalization.

frontiers in Microbiology

METHODS
published: 29 April 2016
doi: 10.3389/fmicb.2016.00532

Method for Indirect Quantification of CH_4 Production via H_2O Production Using Hydrogenotrophic Methanogens

Ruth-Sophie Taubner[1,2,3] *and Simon K.-M. R. Rittmann*[3]*

[1] Research Platform: ExoLife, University of Vienna, Vienna, Austria, [2] Institute of Astrophysics, University of Vienna, Vienna, Austria , [3] Archaea Biology and Ecogenomics Division, Department of Ecogenomics and Systems Biology, University of Vienna, Vienna, Austria

Hydrogenotrophic methanogens are an intriguing group of microorganisms from the domain Archaea. Methanogens exhibit extraordinary ecological, biochemical, and physiological characteristics and possess a huge biotechnological potential. Yet, the only possibility to assess the methane (CH_4) production potential of hydrogenotrophic methanogens is to apply gas chromatographic quantification of CH_4. In order to be able to effectively screen pure cultures of hydrogenotrophic methanogens regarding their CH_4 production potential we developed a novel method for indirect quantification of the volumetric CH_4 production rate by measuring the volumetric water production rate. This method was established in serum bottles for cultivation of methanogens in closed batch cultivation mode. Water production was estimated by determining the difference in mass increase in a quasi-isobaric setting. This novel CH_4 quantification method is an accurate and precise analytical technique, which can be used to rapidly screen pure cultures of methanogens regarding their volumetric CH_4 evolution rate. It is a cost effective alternative determining CH_4 production of methanogens over CH_4 quantification by using gas chromatography, especially if applied as a high throughput quantification method. Eventually, the method can be universally applied for quantification of CH_4 production from psychrophilic, thermophilic and hyperthermophilic hydrogenotrophic methanogens.

Keywords: Archaea, anaerobic cultivation, psychrophile, hyperthermophile, methanogenesis, water, methane, standard operation procedure (SOP)

OPEN ACCESS

Edited by:
Sabine Kleinsteuber, Helmholtz Centre for Environmental Research - UFZ, Germany

Reviewed by:
Caroline M. Plugge, Wageningen University, Netherlands
Heribert Insam, Universität Innsbruck, Austria

***Correspondence:**
Simon K.-M. R. Rittmann
simon.rittmann@univie.ac.at

Specialty section:
This article was submitted to Microbiotechnology, Ecotoxicology and Bioremediation, a section of the journal Frontiers in Microbiology

Received: *19 December 2015*
Accepted: *31 March 2016*
Published: *29 April 2016*

Citation:
Taubner R-S and Rittmann SK-MR (2016) Method for Indirect Quantification of CH_4 Production Via H_2O Production Using Hydrogenotrophic Methanogens. Front. Microbiol. 7:532. doi: 10.3389/fmicb.2016.00532

1. INTRODUCTION

Methanogens are an intriguing group of microorganisms with extraordinary ecological (Liu and Whitman, 2008), biochemical (Ferry, 2010; Thauer et al., 2010), physiological (Thauer et al., 2008; Taubner et al., 2015) characteristics, and promising biotechnological potential (Seifert et al., 2013, 2014; Rittmann et al., 2015; Rittmann, 2015). Currently all methanogens are phylogenetically classified into the phylum Euryarchaeota (Liu and Whitman, 2008; Borrel et al., 2013) but recently

Abbreviations: CH_4, methane; H_2O, water; H_2, molecular hydrogen; CO_2, carbon dioxide; x [g L^{-1}], biomass concentration; MER [mmol h^{-1} L^{-1}], methane evolution rate; WER [mmol h^{-1} L^{-1}], water evolution rate; HUR [mmol h^{-1} L^{-1}], hydrogen uptake rate; CUR [mmol h^{-1} L^{-1}], carbon dioxide uptake rate; DoR, Degree of Reduction; $C-mol$, moles of carbon; $Y_{(x/CH4)}$ [C-mol mol^{-1}], growth to product yield; r_x [C-mmol h^{-1} L^{-1}], biomass production rate.

the metabolism of a putative methane (CH_4) producing *Candidatus* lineage was reconstructed *in silico* and assigned to the phylum Bathyarchaeota (Evans et al., 2015).

Methanogens can be found in almost every anoxic environment, e.g., lakes (Franzmann et al., 1997), sediments (Schirmack et al., 2014), soils (Lü and Lu, 2012; Wagner et al., 2013), bog, fen and palsa of thawing permafrost (Mondav et al., 2014), sea floor (Jones et al., 1983; Jeanthon et al., 1999; von Klein et al., 2002; L'Haridon et al., 2003), and anaerobic digesters (Jiang et al., 2005; Ma et al., 2006; Parshina et al., 2014; Rittmann and Holubar, 2014). Methanogens are the only anaerobic organisms known to date that are capable of producing CH_4 as an end product of their energy conserving metabolism. Therefore, they play an important role in the terrestrial global carbon cycle (Liu and Whitman, 2008; Thauer et al., 2008; Mondav et al., 2014).

Methanogens are obligate chemolithoautotrophic or chemolithoheterotrophic organisms, which obtain cellular carbon and energy from C_1-, C_2-, and methylated compounds—either by reduction with molecular hydrogen (H_2) or by using a disproportionation reaction. Furthermore, some methanogens are known to metabolize carbon monoxide (Oelgeschläger and Rother, 2009; Ferry, 2010). A physiological characteristic of methanogens is that they may vary their growth to product yield ($Y_{(x/CH4)}$) upon experiencing a change in environmental conditions—a mechanism commonly referred to as uncoupling (Mountfort and Asher, 1979; Archer, 1985; Fardeau and Belaich, 1986; Tsao et al., 1994; Liu et al., 1999; Pennings et al., 2000; Ver Eecke et al., 2013; Bernacchi et al., 2014; Taubner et al., 2015).

In biotechnology, methanogens are integral members of the biocoenosis applied for biogas production in anaerobic digesters and they are commonly used in anaerobic waste water treatment plants. Furthermore, methanogens are utilized for biological CH_4 production in pure culture—a process also referred to as biomethanization. Especially hydrogenotrophic, autotrophic and thermophilic methanogens were found to exhibit extraordinary strain specific (e.g., specific growth rate (μ) and high specific CH_4 evolution rates Rittmann et al., 2012) and industrially relevant characteristics, such as high volumetric CH_4 production rates (MER) (Seifert et al., 2014).

Hydrogenotrophic methanogens utilize H_2 as the electron donor for the reduction of carbon dioxide (CO_2) to CH_4. These organisms produce CH_4 and water (H_2O) as metabolic products according to the following stoichiometric reaction (Liu and Whitman, 2008; Thauer et al., 2008; Rittmann et al., 2015):

$$4\,H_2 + CO_2 \rightarrow CH_4 + 2\,H_2O \quad \Delta G^\circ = -135\ \text{kJ/mol}\ CH_4. \quad (1)$$

The standard method to determine the CH_4 production potential of methanogens is to perform gas chromatographic measurements. The aim of this study was, however, to establish a cheaper, faster and at the same time a precise and accurate method to determine the CH_4 production potential of hydrogenotrophic methanogens grown in serum bottles via H_2O production.

The presented method is based on the following rationale: due to the conversion of four moles H_2 and one mole CO_2, one mole of CH_4 and two moles H_2O are produced, which leads to a decrease of serum bottle headspace pressure and a concomitant increase of liquid body mass due to H_2O formation. Based on this principle, we present a novel method for quantification of both the CH_4 production and the mass gain by determining the pressure reduction inside the serum bottle and the water accumulation, respectively—in one simple procedure.

2. MATERIALS AND METHODS

We examined four different strains of hydrogenotrophic and autotrophic methanogens (*Methanosarcina soligelidi* DSM 26065, *Methanothermococcus okinawensis* DSM 14208, *Methanocaldococcus villosus* DSM 22612, and *Methanothermobacter marburgensis* DSM 2133) (see **Table 1**). The strains were grown in 120 mL serum bottles (La-Pha-Pack, Langerwehe, Germany) in chemically defined media (see Section 2.1). The inoculation was performed inside an anaerobic chamber (Coy Laboratory Products, Grass Lake, USA). Residual CH_4 was replaced in regular intervals with a CO_2/H_2 test gas mixture (20 Vol.-% CO_2 in H_2) pressurizing each of the serum bottles to 1.4–2.0 barg.

2.1. Media

The medium for the cultivation of *M. marburgensis* contained 2.1 g NH_4Cl, 6.8 g KH_2PO_4, 3.6 g Na_2CO_3, 5 mL of 200× trace element solution, and was filled up to 1 L with ddH_2O. For the 200× trace element solution first 9.0 g Titriplex I was dissolved in 400 mL ddH_2O. A pH of 6.5 was adjusted by adding 5M NaOH. Then 4.0 g of $MgCl_2 \cdot 6H_2O$, 1.0 g $FeCl_2 \cdot 4H_2O$, 20 mg $CoCl_2 \cdot 6H_2O$, 120 mg $NiCl_2 \cdot 6H_2O$, and 20 mg $NaMoO_4 \cdot 2H_2O$ were added. A pH of 7.0 was adjusted by adding 1M NaOH and the volume of the trace element solution was filled up with ddH_2O to 500 mL. 50 mL of the medium were aliquoted into 120 mL serum bottles and sealed with blue rubber stoppers (pretreated by boiling ten times for 30 min in fresh ddH_2O; 20 mm, butyl rubber, CLS-3409-14, Chemglass Life Sciences) and crimp caps (20 mm aluminum, Ochs Laborbedarf, Bovenden, Germany). After anaerobization by five times gassing (0.8 barg) and four times drawing vacuum, the serum bottles were autoclaved. The last step of preparation was to anaerobically add 0.1 mL of sterile 0.5 M $Na_2S \cdot 9\,H_2O$ to the serum bottles in an anaerobic chamber.

For *M. villosus* and *M. okinawensis*, the DSMZ Medium 282 (2014) was used, with the following modifications: 0.14 g K_2HPO_4 was substituted with 0.183 g $K_2HPO_4 \cdot 3\,H_2O$ and 0.01 g $Fe(NH_4)_2(SO_4)_2 \cdot 6\,H_2O$ was replaced with 7 mg $FeSO_4 \cdot 7\,H_2O$ and we omitted the resazurin solution from the medium. The sterile filtered vitamin solution (modified from Balch et al., 1979) contained per L 20 mg biotin, 20 mg folic acid, 100 mg pyridoxamine dihydrochloride, 50 mg thiamine hydrochloride, 50 mg riboflavin, 50 mg niacin, 50 mg calcium-D(+)-pantothenat, 5 mg cyanocobalamin, 50 mg para-aminobenzoic acid, and 25 mg lipoic acid. Medium aliquots were prepared by adding 50 mL into 120 mL serum bottles. The bottles were sealed with blue rubber stoppers and crimp caps. After anaerobization by five times gassing (0.8 barg) and four times drawing vacuum, the serum bottles were autoclaved. Thereafter,

TABLE 1 | Overview of methanogens and cultivation settings used in this study.

Strain DSMZ number	*M. marburgensis* DSM 2133	*M. villosus* DSM 22612	*M. okinawensis* DSM 14208	*M. soligelidi* DSM 26065
Volume (medium) [mL]	50	50	50	50
Incubation temperature [°C]	45 55 65	80	65	28
Gas pressure [barg]	1.4–2.0	1.5–2.0	1.4–1.7	1.4–1.6
Gassing interval	daily	1–2 times a day	daily	Every fifth day
Number of incubation periods per experiment	8	8–9	8	7

0.5 mL of the two times sterile filtered aforementioned vitamin solution was added aseptically to the serum bottles. Eventually, 0.75 mL of sterile $NaHCO_3$ solution (of 3 g $NaHCO_3$ in 45 mL ddH_2O), 0.25 mL of sterile L-Cysteine-HCl · H_2O (solution 10 g L-Cysteine-HCl in 100 mL ddH_2O) and 0.2 mL of sterile 0.5 M Na_2S · 9 H_2O were added to the serum bottles in an anaerobic chamber.

For *M. soligelidi*, we used the medium described by Wagner et al. (2013) with the following modifications: 0.8 g KH_2PO_4 · 2 H_2O was substituted with 0.633 g KH_2PO_4 and we omitted the resazurin solution from the medium. For this medium we used the aforementioned vitamin solution and the trace element solution as reported by Balch et al. (1979). For the trace element solution we substituted 0.5 g $MnSO_4$ · 2 H_2O with 0.529 g $MnCl_2$ · 4 H_2O, 0.1 g $CoCl_2$ with 0.183 g $CoCl_2$ · 6 H_2O, 0.1 g $ZnSO_4$ with 0.178 g $ZnSO_4$ · 7 H_2O, 0.01 g $CuSO_4$ · 5 H_2O with 0.006 g $CuSO_4$, and 0.01 g $AlK(SO_4)_2$ with 0.018 g $AlK(SO_4)_2$ · 12 H_2O. After anaerobization by five times gassing (0.8 barg) and four times drawing vacuum, the serum bottles were autoclaved. The next step was to add 0.5 mL of the two times sterile filtered vitamin solution into each of the serum bottles. Finally, 0.2 mL of sterile 0.5 M Na_2S · 9 H_2O were anaerobically added to the serum bottles in an anaerobic chamber.

2.2. Culture setup

Before starting the experiments, the mass of the empty 120 mL serum bottles, the crimp caps, and the blue rubber stoppers has to be determined to quantify the exact amount of medium added afterwards. The balance should be capable to accurately weigh a difference in mass in the range of 0.1 mg (used balance here: AT261 Delta Range Analytical Balance, Mettler Toledo, USA). Based on these data we could calculate the respective gas volume in the serum bottles. All experiments were performed at least in triplicates plus two negative controls. The first negative control is treated like an inoculated flask (cultivation control) and the second is needed to determine the pressure in the serum bottles after the flush and purge process (gas control). For gassing, a gassing manifold was used (see **Figures 3B,C**). We used 3-way stopcocks (PSU, RED, 8501742, Fresenius Kabi AG, Germany), filters (sterile syringe filters, w/0.2c μm cellulose, 514-0061, VWR International, USA)), and cannulae (disposal hypodermic needle, Gr 14, 0.60 × 30 mm, 23 G × 1 1/4″, RX129.1, Braun, Germany) to add the H_2/CO_2 test gas to the serum bottles. To purge the gas phase, we opened the 3-way stopcocks one by one for 2–4 s so that the gas inside the bottle could be released. To measure the serum bottle headspace pressure we used digital manometer (LEO1-Ei, −1...3bar rel, Keller, Germany).

2.2.1. Inoculation

We inoculated the serum bottles with 1 mL (2 Vol.-%) of a respective pre-culture in exponential growth phase. The negative controls were inoculated with 1 mL of the respective fresh medium. The inoculation was performed in an anaerobic chamber. After inoculation the serum bottles were weighed again to determine the exact amount of inoculum. Subsequently, the serum bottles were pressurized with H_2/CO_2 (1.4–2.0 barg depending on the strain) as gaseous substrates and weighted again. Cultures were incubated either in a waterbath (*M. marburgensis* and *M. okinawensis*) or in an air bath (*M. soligelidi* and *M. villosus*) in the dark at their respective optimal temperatures (see **Table 1**, the temperature could vary ± 2°C).

2.3. Standard Operation Procedure (SOP)

The SOP outlined here describes the workflow for quantification of CH_4 production by using H_2O production. This routine has to be applied for each sampling and gassing round (further referred to as an experimental run). Each experiment consists of seven to ten experimental runs. The incubation period between these runs should be long enough so that sufficient methanogenesis can take place (e.g., for *M. marburgensis* about 15–20 h).

1. Preparation
   a. take the flasks out of the waterbath/airbath and dry the bottles with a tissue. Let them cool down to room temperature for approximately 1 h separated from one another by at least 15 cm distance (note the time)
2. Weight measurement
   a. note room temperature and time
   b. check if the balance is properly adjusted (check spirit level)

c. turn on the balance
d. tare the balance
e. measure the weight of each flask and note the values (**Figure 1**, step ①)
f. note room temperature and time

3. Pressure measurement and gassing

a. note room temperature and time
b. ensure that all globe valves are closed
c. clean the bench and the globe valves with *EtOH* (70 Vol.-%)
d. if not already in place, put a 3-way stopcock, a filter, and a cannula as can be seen in **Figure 3B** on to the H_2/CO_2-ports; ensure, that the 3-way stopcocks are half open:
e. measure the pressure of each flask with a digital manometer and note the values and time (**Figure 1**, step ②). For that purpose, put every time some *EtOH* (70 Vol.-%) on the rubber, wait until the *EtOH* (70 Vol.-%) is evaporated, and introduce the manometer-cannula and filter.
f. Remove the manometer-cannula and filter. Note if a droplet escapes while removing the manometer.
g. open the primary globe valve and adjust the pressure on the secondary valve (~1.4–2.0 bar)
h. Gassing the flasks:
   (1) put *EtOH* (70 Vol.-%) on all serum bottles and the reference flask
   (2) open the distribution valve
   (3) open the first H_2/CO_2-port valve and introduce the prepared H_2/CO_2-port cannula into the negative control flasks—repeat this step for the remaining flasks
   (4) wait ~1 min
   (5) flushing the headspace (see **Figure 1**, step ③): switch the position of the valve on the 3-way stopcock for 2–4 s: → → , repeat this step for the remaining serum bottles
   (6) repeat the previous step (5) another two times
   (7) wait ~3 min - in the meantime swirl the flasks slightly several times
   (8) close the distribution valve
   (9) close the H_2/CO_2-port valves as simultaneously as possible
   (10) pull out the H_2/CO_2-port cannula carefully and note if a droplet escaped while removing the cannula
   (11) put new cannulae on the H_2/CO_2-ports or close the cannulae carefully
   (12) measure the pressure in the reference flask as described in 3e and note the value
i. close the primary globe valve, open one of the unused H_2/CO_2-ports to release the pressure, close the secondary valve, close the H_2/CO_2-port valve
j. note room temperature and time

4. Weight measurement

a. repeat steps (2a to 2f) (**Figure 1**, step ④)

5. Finish

a. put the flasks in the corresponding waterbath or airbath for incubation (**Figure 1**, step ⑤)
b. note the time

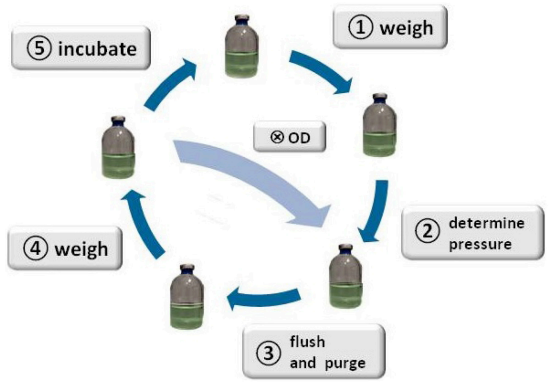

FIGURE 1 | Schematic illustration of the method. The figure illustrates the SOP: start with weighing the serum bottles ①, determine the head space pressure of the serum bottles ②, flush and purge to remove CH_4 from the headspace of the serum bottles ③, weigh the serum bottles ④, incubate the serum bottles ⑤, start again with step ①; taking a sample Ⓧ for OD measurement or cell counting is optional after step ④, whereas step ③ and ④ would have to be repeated after sampling for OD measurement.

Applying almost isothermal conditions during the determination of the headspace gas pressure in every step of the method is important in order to assure that the change in the headspace gas pressure is not caused by the varying temperature of the serum bottles or the medium, but due to the conversion of H_2/CO_2 to CH_4. Before gassing, the weight of the serum bottles should be the same as at the end of the previous run because in a closed system the mass stays constant. However, the pressure in the inoculated flasks should have dropped during incubation due to the ongoing process of methanogenesis (see **Figure 2**). To receive the same gas composition as on the day before, we flushed and purged the serum bottles with H_2/CO_2 (see **Figure 1**, step ③). This step is important in order to achieve a nearly isobaric setting in which it is possible to determine the increase in weight due to the production of H_2O. In other words, we removed the produced CH_4 and residual H_2/CO_2 and added new H_2/CO_2. The flush and purge routine was done in a parallel setting for all serum bottles of one experimental run at once (see **Figure 3B**). It is important to do this step carefully and attentively to avoid surrounding air entering or medium exiting the serum bottle. After the last purging (step 3.h(7)), the flasks were flushed for at least 3 min to establish roughly the same pressure in all of the flasks. After gassing, we measured the actual pressure of the gas control serum bottle to assess the amount of pressure in the serum bottles. Later, this value will be used to calculate the

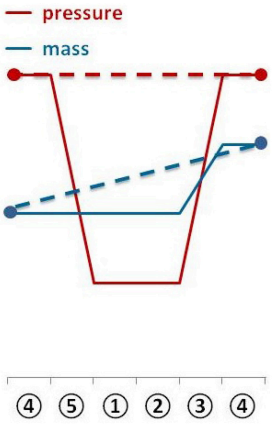

FIGURE 2 | The diagram shows the change of serum bottle mass and serum bottle headspace pressure during one experimental run.

respective conversion factor. The last step was to measure the mass of the serum bottles again. At this point, the increase in mass of the inoculated serum bottles should be observable (10–60 mg, depending on the strain). The routine was repeated seven to nine times (see **Table 1**). The whole experimental procedure is illustrated in **Figures 1** and **2**. The duration of each individual step of the SOP should be kept constant in each consecutive run to acquire reproducible results.

During some experiments, we additionally took samples to measure the optical density (OD, $\lambda = 578$ nm, blanked with ddH_2O) at each run. The sampling took place between step ④ and ⑤, whereas steps ③ and ④ were repeated after sampling.

2.4. Gas chromatography

Analysis of the headspace gas composition (CO_2, H_2, and CH_4) of selected serum bottles was determined at the end of the final incubation period by using a gas chromatograph (7890A GC System, Agilent Technologies, Santa Clara, USA) equipped with a TCD detector and a 19808 ShinCarbon ST Micropacked Column (Restek GmbH, Bad Homburg, Germany). Autosampling of serum bottle headspace and concomitant gas injection into the gas chromatograph was accomplished by using a gas injection and control unit (Joint Analytical Systems GmbH, Moers, Germany).

3. THEORY

To estimate the produced particle number of CH_4 in the gas phase after each incubation, the partial pressure of CH_4 has to be calculated. For that, Equation (1) has to be considered. Due to the stoichiometry presented in Equation (1), the partial pressure of CH_4 is equal to one fourth of the difference in pressure before and after incubation (see Equation (2)). Eventually, with the aid of the ideal gas law, the number of CH_4 in mol can be determined. This directly leads to the theoretical amount of produced H_2O, because, according to Equation (1), the production of one mole CH_4 is accompanied by the production of two moles of H_2O.

We included the varying gas pressure during the flushing process as well as the potential loss of liquid due to the leakage of the rubber stoppers into our calculations. For further information please refer to the Supplementary Material.

The MER, volumetric H_2 uptake rate (HUR), and volumetric CO_2 uptake rate (CUR) are the differences in the number of millimoles of CH_4, H_2, and CO_2, respectively, per time passed in hours and per medium volume in liters. The WER is the gain in mass in g per incubation time passed in hours and per volume in liters and divided by the molar mass of H_2O. The following equations show how the different variables were calculated. For those experiments where the OD was not measured, the contribution of the biomass (i.e., Δx, r_x, and $Y_{(x/CO2)}$) had to be neglected.

$$p_{CH4} = \frac{p_{\text{before}} - p_{\text{after}}}{4} \quad [\text{Pa}] \tag{2}$$

$$\text{MER} = \frac{\Delta n_{CH4}}{\Delta t \cdot V} \quad [\text{mmol h}^{-1}\,\text{L}^{-1}] \tag{3}$$

$$\text{HUR} = \frac{\Delta n_{H2}}{\Delta t \cdot V} \quad [\text{mmol h}^{-1}\,\text{L}^{-1}] \tag{4}$$

$$\text{CUR} = \frac{\Delta n_{CO2}}{\Delta t \cdot V} \quad [\text{mmol h}^{-1}\,\text{L}^{-1}] \tag{5}$$

$$\text{WER} = \frac{\Delta m_{H2O}}{\Delta t \cdot 18.01528 \cdot V} \quad [\text{mmol h}^{-1}\,\text{L}^{-1}] \tag{6}$$

$$x = OD \cdot 0.31 \quad [\text{g L}^{-1}] \tag{7}$$

$$r_x = \frac{\Delta x}{\Delta t \cdot 30.97} \quad [\text{C-mmol h}^{-1}\,\text{L}^{-1}] \tag{8}$$

$$Y_{(CH4/CO2)} = \frac{\text{MER}}{\text{CUR}} \tag{9}$$

$$Y_{(x/CO2)} = \frac{r_x}{\text{CUR}} \tag{10}$$

$$\text{C-balances} = Y_{(CH4/CO2)} + Y_{(x/CO2)} \tag{11}$$

$$\text{H-balances} = \frac{1.879 \cdot r_x + 2 \cdot \text{WER} + 4 \cdot \text{MER}}{2 \cdot \text{HUR}} \tag{12}$$

$$\text{DoR} = \frac{4.24 \cdot r_x + 8 \cdot \text{MER}}{2 \cdot \text{HUR}} \tag{13}$$

The values used in the Equations (8) and (13) were taken from Bernacchi et al. (2014). The values in Equations (7) and (12) were experimentally determined. These values were determined for *M. marburgensis* and therefore could vary for other methanogens (see Section 5.1 and 5.3).

4. RESULTS

4.1. Mass gain

The absolute mass gain of the different strains lies in average between 10 mg for *M. soligelidi* (please refer to Supplementary Material) and more than 25 mg for *M. villosus* (see **Figure 4**) per run. For about ten runs this sums up to a total mass gain of more than 80–250 mg of H_2O per serum bottle (see **Figure 5**). The cumulative mass gain is dependent on the gassing frequency and the mass of convertible substrates in the headspace of the serum bottle. The low mass gain of *M. soligelidi* can be attributed to the short incubation time of 5 days (Supplementary Material). Additional experiments with a longer incubation period would

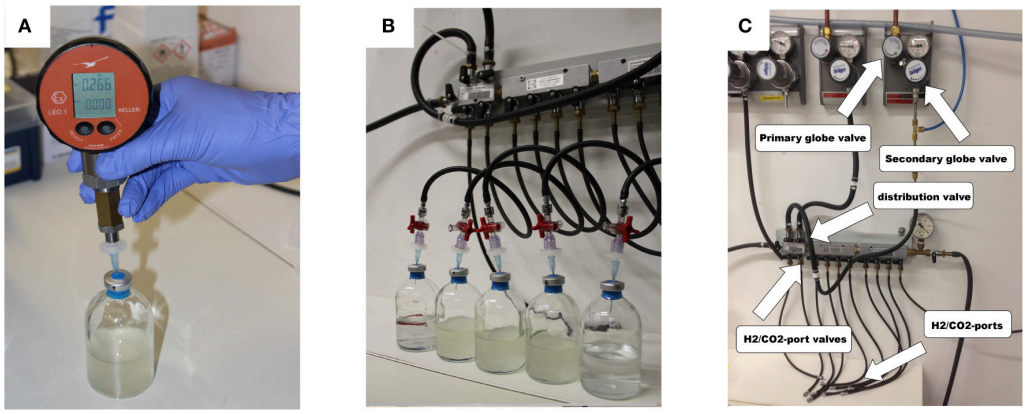

FIGURE 3 | (A) Measurement of the serum bottle headspace pressure with a digital manometer; **(B)** parallel gassing of the serum bottle headspace; **(C)** gassing manifold.

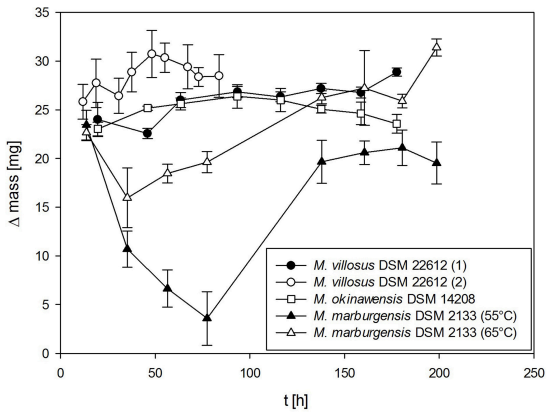

FIGURE 4 | Mass gain for *M. villosus*, *M. okinawensis* and *M. marburgensis*. For *M. villosus* an experiment with a daily gassing event [marked *M. villosus* (1)] and one experiment with two gassing events per day [marked as *M. villosus* (2)] were performed. For *M. marburgensis* cultivations at 55°C and at 65°C were performed. Negative controls are not shown.

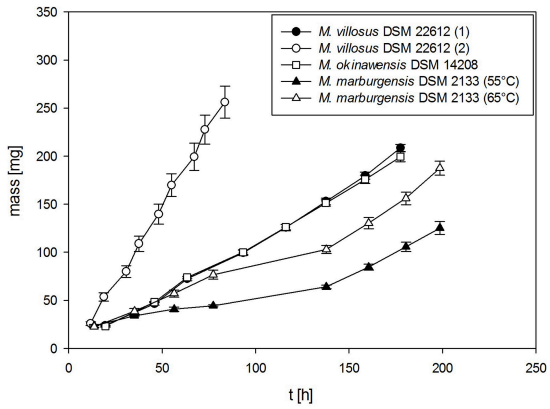

FIGURE 5 | Total cumulative mass gain for *M. villosus*, *M. okinawensis* and *M. marburgensis*. For *M. villosus* an experiment with a daily gassing event [marked *M. villosus* (1)] and one experiment with two gassing events per day [marked as *M. villosus* (2)] were performed. For *M. marburgensis* cultivations at 55°C and at 65°C were performed. Negative controls are not shown.

need to be performed. The results for *M. villosus* and *M. soligelidi* show that this method can be used to easily determine the minimum incubation period necessary until a strain has performed full H_2/CO_2 conversion to CH_4 by analysing the headspace gas pressure in parallel to the quantification of the H_2O production.

Additionally, we varied the temperature (45, 55, and 65°C) when analysing the WER for *M. marburgensis*. At 45°C no growth could be observed for *M. marburgensis*. Furthermore, we varied the incubation time for *M. villosus* [routine performed daily (marked with *M. villosus* (1)] and two times a day [marked with *M. villosus* (2), respectively].

4.2. Mass Balances

In **Tables 2**, **3** an overview of the results of the experiments is presented. The different values for $Y_{(H2O/CH4)}$ and the mass balances are listed for every specific run of each experiment at the respective time. The mass balances were calculated according to the equations shown in Section 3. In **Table 2** the mass balances for the experiments without OD sampling are shown, while in **Table 3** the balances for the experiments with OD sampling are presented. For the calculated mass balances presented in columns 3–5 of **Table 3** the biomass production rate was neglected, while for the mass balances given in column 6–8 the biomass production rate was taken into account. For detailed information

TABLE 2 | Mass balances of the different experiments without OD measurements.

Strain	t [h]	$Y_{(H2O/CH4)}$	C-balance (%)	H-balance (%)	DoR-balance (%)
M. marburgensis DSM 2133 (55°C)	13.68	11.95	92.39	92.38	92.38
M. marburgensis DSM 2133 (55°C)	35.23	12.33	187.45	187.25	187.25
M. marburgensis DSM 2133 (55°C)	56.45	3.00	119.90	119.93	119.93
M. marburgensis DSM 2133 (55°C)	77.35	0.62	96.20	96.20	96.20
M. marburgensis DSM 2133 (55°C)	137.90	2.76	95.27	95.25	95.25
M. marburgensis DSM 2133 (55°C)	160.57	1.25	98.35	98.35	98.35
M. marburgensis DSM 2133 (55°C)	180.47	2.29	97.40	97.41	97.41
M. marburgensis DSM 2133 (55°C)	198.55	1.86	99.86	99.86	99.86
M. marburgensis DSM 2133 (65°C)	13.68	11.66	94.10	94.09	94.09
M. marburgensis DSM 2133 (65°C)	35.23	1.83	105.08	105.08	105.08
M. marburgensis DSM 2133 (65°C)	56.45	1.11	102.26	102.26	102.26
M. marburgensis DSM 2133 (65°C)	77.35	1.22	99.52	99.52	99.52
M. marburgensis DSM 2133 (65°C)	137.90	1.70	98.98	98.98	98.98
M. marburgensis DSM 2133 (65°C)	160.57	1.63	99.52	99.52	99.52
M. marburgensis DSM 2133 (65°C)	180.47	1.59	99.27	99.26	99.26
M. marburgensis DSM 2133 (65°C)	198.55	1.84	99.94	99.94	99.94
M. villosus DSM 22612 (1)	19.68	1.39	97.07	97.06	97.06
M. villosus DSM 22612 (1)	45.93	1.28	100.38	100.37	100.37
M. villosus DSM 22612 (1)	63.45	1.50	98.06	98.05	98.05
M. villosus DSM 22612 (1)	93.35	1.51	100.23	100.22	100.22
M. villosus DSM 22612 (1)	116.15	1.43	102.28	102.27	102.27
M. villosus DSM 22612 (1)	137.67	1.52	100.02	100.02	100.02
M. villosus DSM 22612 (1)	158.65	1.50	100.28	100.28	100.28
M. villosus DSM 22612 (1)	177.53	1.61	100.44	100.44	100.44
M. villosus DSM 22612 (2)	11.83	1.50	93.02	93.03	93.03
M. villosus DSM 22612 (2)	18.82	1.52	99.65	99.65	99.65
M. villosus DSM 22612 (2)	30.82	1.41	102.05	102.05	102.05
M. villosus DSM 22612 (2)	37.62	1.56	100.40	100.39	100.39
M. villosus DSM 22612 (2)	48.20	1.65	100.63	100.63	100.63
M. villosus DSM 22612 (2)	55.07	1.75	100.97	100.97	100.97
M. villosus DSM 22612 (2)	67.20	1.60	100.60	100.60	100.60
M. villosus DSM 22612 (2)	72.93	1.87	99.87	99.87	99.87
M. villosus DSM 22612 (2)	83.63	1.45	100.16	100.16	100.16
M. okinawensis DSM 14208	19.68	1.36	95.88	95.89	95.89
M. okinawensis DSM 14208	45.93	1.48	97.47	97.46	97.46
M. okinawensis DSM 14208	63.45	1.53	97.54	97.54	97.54
M. okinawensis DSM 14208	93.35	1.48	100.22	100.22	100.22
M. okinawensis DSM 14208	116.15	1.58	98.33	98.32	98.32
M. okinawensis DSM 14208	137.67	1.62	98.06	98.06	98.06
M. okinawensis DSM 14208	158.65	1.57	98.59	98.58	98.58
M. okinawensis DSM 14208	177.53	1.55	100.00	100.01	100.01
M. soligelidi DSM 26065	120.00	2.67	81.70	81.64	81.64
M. soligelidi DSM 26065	236.83	2.83	81.35	81.35	81.35
M. soligelidi DSM 26065	351.92	2.21	86.45	86.48	86.48
M. soligelidi DSM 26065	478.25	1.33	95.18	95.23	95.23
M. soligelidi DSM 26065	589.80	2.01	100.39	100.34	100.34
M. soligelidi DSM 26065	715.77	1.69	94.25	94.20	94.20
M. soligelidi DSM 26065	831.03	0.94	100.00	99.94	99.94

TABLE 3 | Mass balances of the two experiments with OD measurements.

Strain	t [h]	C-balance (%)	H-balance (%)	DoR-balance (%)	C-balance incl. x (%)	H-balance incl. x (%)	DoR-balance incl. x (%)
M. marburgensis DSM 2133 (65°C)	13.68	100.00	201.92	99.99	98.76	201.62	99.33
M. marburgensis DSM 2133 (65°C)	35.23	100.00	96.32	100.01	105.51	97.62	102.93
M. marburgensis DSM 2133 (65°C)	56.45	100.00	92.44	100.00	105.80	93.80	103.08
M. marburgensis DSM 2133 (65°C)	77.35	100.00	93.12	100.00	105.34	94.37	102.83
M. marburgensis DSM 2133 (65°C)	137.90	100.00	105.73	100.00	113.43	108.88	107.12
M. marburgensis DSM 2133 (65°C)	160.57	100.00	103.90	100.00	101.21	104.19	100.64
M. marburgensis DSM 2133 (65°C)	180.47	100.00	102.40	100.00	103.46	103.22	101.83
M. marburgensis DSM 2133 (65°C)	198.55	100.00	108.25	100.00	101.87	108.69	100.99
M. villosus DSM 22612 (2)	11.83	100.00	97.00	100.00	107.93	98.87	89.69
M. villosus DSM 22612 (2)	18.82	100.00	97.34	100.00	106.87	98.96	95.97
M. villosus DSM 22612 (2)	30.82	100.00	98.03	100.00	102.47	98.60	97.37
M. villosus DSM 22612 (2)	37.62	100.00	103.46	100.00	100.46	103.57	95.72
M. villosus DSM 22612 (2)	48.20	100.00	102.52	100.00	102.98	103.22	98.74
M. villosus DSM 22612 (2)	55.07	100.00	99.47	100.00	101.79	99.89	99.91
M. villosus DSM 22612 (2)	67.20	100.00	99.40	100.00	100.84	99.60	101.70
M. villosus DSM 22612 (2)	72.93	100.00	104.63	100.00	100.89	104.84	103.88
M. villosus DSM 22612 (2)	83.63	100.00	96.81	100.00	102.01	97.28	101.70

about the calculation, please refer to the source code in the Supplementary Material.

In **Tables 4**, **5** the respective volumetric uptake and evolution rates and mass balances for each experimental run of the OD sampling experiments with *M. marburgensis* and *M. villosus* are shown. The first row (*pressure + weight*) represents the values of the method presented in this article. The values of the second row (*pressure + weight + OD*) include the biomass contribution calculated by the use of the OD data, and for the third row (*weight + OD + GC*) the GC measurements were taken into account.

5. DISCUSSION

5.1. Uncertainty Analysis

Several points have been included into the uncertainty analysis. First, when flushing the serum bottles, by inserting a needle, little droplets of the medium might stick to the bottom of the rubber stopper. These droplets could exit the serum bottles which would cause a decrease in mass. Therefore, we used a 3-way-stopcock to avoid this effect. Here, we purge and flush the bottles with the same needle which reduces losing medium/suspension during subsequent flush and purge cycles. If, however, a droplet still exits the flask for example when pulling out the needle this mass data point has to be neglected in the analysis and removed from data treatment procedure (see source code in the Supplementary Material). Another issue concerns the pressure difference during the gassing events and specifically the fact that there might be a small difference in mass when the pressure after gassing is slightly different than the day before (see Supplementary Material, source code).

As already mentioned before, the values in Equations (7) and (12) were experimentally determined. These values were determined for *M. marburgensis* and therefore could vary for other strains. Further experiments have to be done to determine the strain specific values, but the difference in the results should not change significantly due to the fact that the influence of the biomass to the mass balances is rather small.

As can be seen in **Tables 2** and **3** (as well as in Tables 1 and 2 of the Supplementary Material) the first two to three data points of each experiment do not match with the subsequent values. This could have several reasons, e.g. that there is some kind of growth lag phase in the beginning or that the yield is somehow shifted. In any case, we would advise to treat the first two data points of each experiment with caution.

5.2. Comparison of Gained Mass Values

To calculate the mass of the produced H_2O, several different data values can be used (see also **Figure 6**): change in pressure, mass increase, and (if available) GC data. As mentioned in Section 3, the change in pressure over the incubation period can be used to calculate the particle number of produced CH_4. If GC data are available, the percent by volume of CH_4 is equal to the conversion factor of CO_2 to CH_4. Therefore, the number of produced CH_4 can be calculated. As can be seen in Equation 1, the number of produced CH_4 is half of the number of the produced H_2O in mol. In Table 1 of the Supplementary Material the comparison of the results is presented and as can be seen, the discrepancy is very small.

5.3. Comparison of Mass Balances

As can be seen in **Tables 4** and **5**, the difference in the mass balances between the methods are very small. This leads to the conclusion that additional OD measurements are not necessary to determine the balances due to the fact that the contribution of

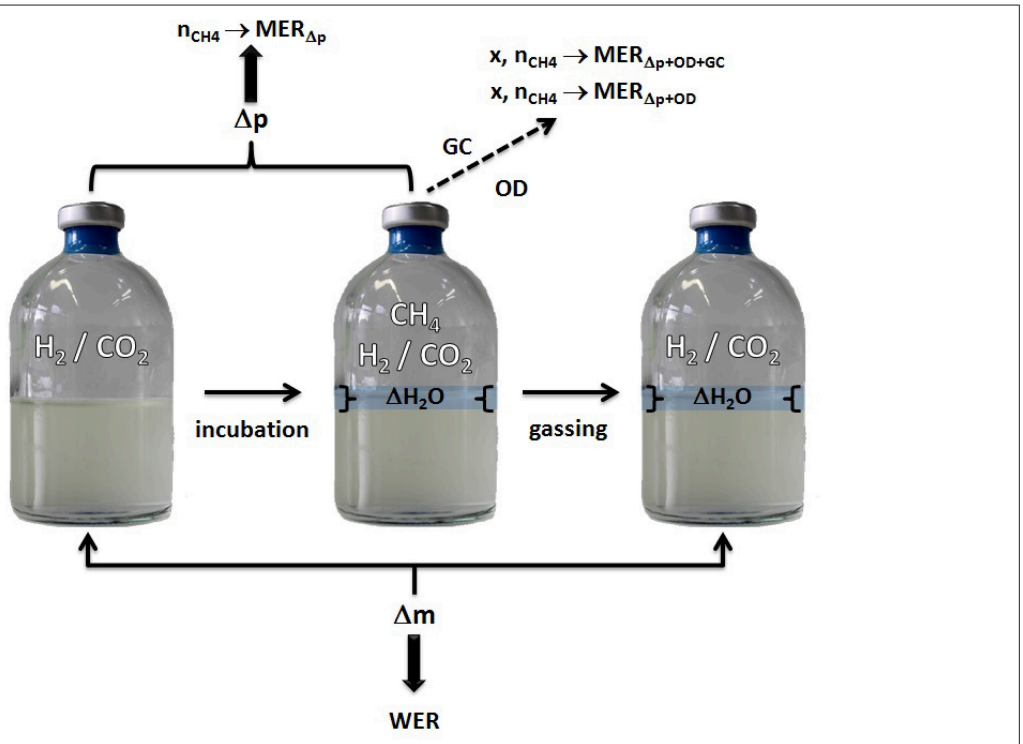

FIGURE 6 | Model for WER and MER determination using serum bottle headspace pressure and Δ water mass quantification.

TABLE 4 | Comparison of the volumetric uptake and production rates and mass balances for the three methods for *M. marburgensis* DSM 2133 (65°C, OD).

	WER	MER	CUR	HUR	C-balance (%)	H-balance (%)	DoR-balance (%)
Pressure + weight	3.62	1.15	−1.15	−6.21	100.00	108.25	100.00
Pressure + weight + OD	3.62	1.15	−1.15	−6.21	101.87	108.69	100.99
Weight + OD + GC	3.62	1.41	−1.36	−5.67	105.60	113.85	100.26

TABLE 5 | Comparison of the volumetric uptake and production rates and mass balances for the three methods for *M. villosus* DSM 22612 (OD).

	WER	MER	CUR	HUR	C-balance (%)	H-balance (%)	DoR-balance (%)
Pressure + weight	5.68	3.03	−3.03	−12.13	100.00	96.81	100.00
Pressure + weight + OD	5.68	3.03	−3.03	−12.13	102.01	97.28	101.70
Weight + OD + GC	5.68	2.86	−2.59	−11.73	113.10	97.72	98.74

biomass to these parameters is negligible. Therefore, even though we have not determined the exact elementary composition and degree of reduction of the strains other than *M. marburgensis*, these values do not have a significant influence on the balances. The discrepancy in the C-balances between the GC data and the others might lie in the fact that the used media contained hydrogen carbonates. This could lead to a shift in the CO_2 consumption and therefore in the composition of the gas phase because full conversion of the substrates could not be performed.

5.4. General Discussion

The utilization of an anaerobic chamber for the preparation of the media and for inoculation would be helpful but it is not a prerequisite. Alternatively, the aforementioned anaerobic working steps could be performed by either using

gas-filled/flushed syringes or by application of an argon bath. The application of resazurin to the medium would only indicate whether the system is above or below a certain oxidation-reduction potential but does not prevent the media from becoming aerobic.

The dependence of the serum bottle temperature on the gas phase headspace pressure and the cooling time was determined experimentally (data not shown). A cooling time of more than 45 min at room temperature is needed to receive proper values for a liquid volume of about 50 mL. However, a cooling time of 1 h would be recommended.

Gas chromatographic measurements in addition to OD measurements were performed at the end of some of the experiments. Therefore, only end point values are available for the mass balance calculations including the GC measurements. The lack of GC data values throughout the experiment demonstrates another advantage of the presented method, namely the possibility of regular screening of the CH_4 production. For the experiment with *M. soligelidi* the incubation time of 5 days might have been too short, as this time is equal to the doubling time of the strain (Wagner et al., 2013). Hence, it would be necessary to investigate the influence of the gassing pressure or gassing frequency. This method can also be used in the case of turbid media (e.g., *M. soligelidi*), for which spectrophotometric measurement of the optical density is not feasible. Furthermore, the method can also be applied if the determination of optical density is not feasible due to low cell density or in case aggregate forming organisms should be analyzed.

Eventually, this method could also be applied to quantify the production of metabolic end products from non-methanogenic pure cultures—e.g., acetate production by acetogens from CO_2 and H_2 in order to be able to quantify gas to liquid conversion rates.

6. CONCLUSIONS

In order to be able to effectively screen pure cultures of hydrogenotrophic methanogens regarding their CH_4 production potential we developed a novel method for indirect quantification of CH_4 production via H_2O production. This novel method was established in serum bottles for cultivation of hydrogenotrophic methanogens in closed batch cultivation mode. Water production was quantified by determining the difference in mass increase in a quasi-isobaric setting. We demonstrated that this method for the indirect CH_4 quantification is an extremely accurate and precise technique suited to rapidly screen pure culture of methanogens regarding their CH_4 production potential, especially if applied in high throughput screening experiments. We conclude that this novel method is a cost effective alternative to determine CH_4 production potential of methanogens over CH_4 quantification by using gas chromatography. We show that this method can be universally applied for quantification of CH_4 production from psychrophilic, thermophilic and hyperthermophilic hydrogenotrophic methanogens.

AUTHOR CONTRIBUTIONS

SR conceived the experiments. RT and SR designed the experiments. RT performed the experiments. RT and SR analyzed the data. RT wrote the source code. SR supervised research. RT and SR wrote the manuscript. RT and SR approved the final version of the manuscript.

FUNDING

RT acknowledges funding by the University of Vienna for her PhD in the frame of the Research Platform: ExoLife (FPF-234). This article was supported by the Open Access Publishing Fund of the University of Vienna.

ACKNOWLEDGMENTS

RT and SR gratefully acknowledge Univ.-Prof. Dr. Christa Schleper, head of the Archaea Biology and Ecogenomics Division, University of Vienna, for valuable and helpful discussions on experiments. RT and SR acknowledge Barbara Reischl, BSc and Philipp Kolar, BSc for assistance with gas chromatographic and spectrophotometric measurements. RT and SR acknowledge Annalisa Abdel Azim, MSc and Dr. Melina Kerou for proof reading and comments on the manuscript. SR acknowledges Krajete GmbH for helpful discussions.

SUPPLEMENTARY MATERIAL

The Supplementary Material for this article can be found online at: http://journal.frontiersin.org/article/10.3389/fmicb.2016.00532

REFERENCES

Archer, D. B. (1985). Uncoupling of Methanogenesis from Growth of Methanosarcina barkeri by Phosphate Limitation. *Appl. Environ. Microbiol.* 50, 1233–1237.

Balch, W. E., Fox, G. E., Magrum, L. J., Woese, C. R., and Wolfe, R. S. (1979). Methanogens: reevaluation of a unique biological group. *Microbiol. Rev.* 43, 260–296.

Bernacchi, S., Rittmann, S., Seifert, A., Krajete, A., and Herwig, C. (2014). Experimental methods for screening parameters influencing the growth to product yield ($Y_{(x/CH4)}$) of a biological methane production (BMP) process performed with Methanothermobacter marburgensis. *AIMS Bioeng.* 1, 72–86. doi: 10.3934/bioeng.2014.1.72

Borrel, G., O'Toole, P. W., Harris, H. M. B., Peyret, P., Brugère, J.-F., and Gribaldo, S. (2013). Phylogenomic data support a seventh order of methylotrophic methanogens and provide insights into the evolution of methanogenesis. *Genome Biol. Evol.* 5, 1769–1780. doi: 10.1093/gbe/evt128

Evans, P. N., Parks, D. H., Chadwick, G. L., Robbins, S. J., Orphan, V. J., Golding, S. D., et al. (2015). Methane metabolism in the archaeal phylum

Bathyarchaeota revealed by genome-centric metagenomics. *Science* 350, 434–438. doi: 10.1126/science.aac7745

Fardeau, M.-L., and Belaich, J.-P. (1986). Energetics of the growth of *Methanococcus* thermolithotrophicus. *Arch. Microbiol.* 144, 381–385. doi: 10.1007/BF00409888

Ferry, J. G. (2010). How to make a living by exhaling methane. *Ann. Rev. Microbiol.* 64, 453–473. doi: 10.1146/annurev.micro.112408.134051

Franzmann, P. D., Liu, Y., Balkwill, D. L., Aldrich, H. C., Macario, E. C. D., and Boone, D. R. (1997). Methanogenium frigidum sp. nov., a Psychrophilic, H_2-Using Methanogen from Ace Lake, Antarctica. *Int. J. Syst. Bacteriol.* 47, 1068–1072. doi: 10.1099/00207713-47-4-1068

Jeanthon, C., L'Haridon, S., Reysenbach, A.-L., Corre, E., Vernet, M., Messner, P., et al. (1999). Methanococcus vulcanius sp. nov., a novel hyperthermophilic methanogen isolated from East Pacific Rise, and identification of Methanococcus sp. DSM 4213T as Methanococcus fervens sp. nov. *Int. J. Syst. Bacteriol.* 49, 583–589.

Jiang, B., Parshina, S. N., Doesburg, W. V., Lomans, B. P., and Stams, A. J. M. (2005). Methanomethylovorans thermophila sp. nov., a thermophilic, methylotrophic methanogen from an anaerobic reactor fed with methanol. *Int. J. Syst. Evol. Microbiol.* 55, 2465–2470. doi: 10.1099/ijs.0.63818-0

Jones, W. J., Leigh, J. A., Mayer, F., Woese, C. R., and Wolfe, R. S. (1983). *Methanococcus jannaschii* sp. nov., an extremely thermophilic methanogen from a submarine hydrothermal vent. *Arch. Microbiol.* 136, 254–261. doi: 10.1007/BF00425213

L'Haridon, S., Reysenbach, A.-L., Banta, A., Messner, P., Schumann, P., Stackebrandt, E., et al. (2003). Methanocaldococcus indicus sp. nov., a novel hyperthermophilic methanogen isolated from the Central Indian Ridge. *Int. J. Syst. Evol. Microbiol.* 53, 1931–1935. doi: 10.1099/ijs.0.02700-0

Liu, J.-S., Schill, N., van Gulik, W. M., Voisard, D., Marison, I. W., and von Stockar, U. (1999). The coupling between catabolism and anabolism of Methanobacterium thermoautotrophicum in H_2- and iron-limited continuous cultures. *Enzyme Microb. Technol.* 25, 784–794. doi: 10.1016/S0141-0229(99)00109-X

Liu, Y., and Whitman, W. B. (2008). Metabolic, phylogenetic, and ecological diversity of the methanogenic archaea. *Ann. N. Y. Acad. Sci.* 1125, 171–189. doi: 10.1196/annals.1419.019

Lü, Z., and Lu, Y. (2012). Methanocella conradii sp. nov., a thermophilic, obligate hydrogenotrophic methanogen, isolated from Chinese rice field soil. *PLoS ONE* 7:e35279. doi: 10.1371/journal.pone.0035279

Ma, K., Liu, X., and Dong, X. (2006). Methanosaeta harundinacea sp. nov., a novel acetate-scavenging methanogen isolated from a UASB reactor. *Int. J. Syst. Evol. Microbiol.* 56, 127–131. doi: 10.1099/ijs.0.63887-0

Mondav, R., Woodcroft, B. J., Kim, E.-H., McCalley, C. K., Hodgkins, S. B., Crill, P. M., et al. (2014). Discovery of a novel methanogen prevalent in thawing permafrost. *Nat. Commun.* 5:3212. doi: 10.1038/ncomms4212

Mountfort, D. O., and Asher, R. A. (1979). Effect of inorganic sulfide on the growth and metabolism of Methanosarcina barkeri strain DM. *Appl. Environ. Microbiol.* 37, 670–675.

Oelgeschläger, E., and Rother, M. (2009). Influence of carbon monoxide on metabolite formation in Methanosarcina acetivorans. *FEMS Microbiol. Lett.* 292, 254–260. doi: 10.1111/j.1574-6968.2009.01492.x

Parshina, S. N., Ermakova, A. V., Bomberg, M., and Detkova, E. N. (2014). Methanospirillum stamsii sp. nov., a psychrotolerant, hydrogenotrophic, methanogenic archaeon isolated from an anaerobic expanded granular sludge bed bioreactor operated at low temperature. *Int. J. Syst. Evol. Microbiol.* 64(Pt 1), 180–186. doi: 10.1099/ijs.0.056218-0

Pennings, J. L. A., Vermeij, P., Poorter, L. M. I. D., Keltjens, J. T., and Vogels, G. D. (2000). Adaptation of methane formation and enzyme contents during growth of Methanobacterium thermoautotrophicum (strain ΔH) in a fed-batch fermentor. *Antonie van Leeuwenhoek* 77, 281–291. doi: 10.1023/A:1002443012525

Rittmann, S., and Holubar, P. (2014). Rapid extraction of total RNA from an anaerobic sludge biocoenosis. *Folia Microbiol.* 59, 127–132. doi: 10.1007/s12223-013-0274-2

Rittmann, S., Seifert, A., and Herwig, C. (2012). Quantitative analysis of media dilution rate effects on Methanothermobacter marburgensis grown in continuous culture on H2 and CO2. *Biomass Bioenergy* 36, 293–301. doi: 10.1016/j.biombioe.2011.10.038

Rittmann, S., Seifert, A., and Herwig, C. (2015). Essential prerequisites for successful bioprocess development of biological CH_4 production from CO_2 and H_2. *Crit. Rev. Biotechnol.* 35, 141–151. doi: 10.3109/07388551.2013.820685

Rittmann, S. K.-M. R. (2015). A critical assessment of microbiological biogas to biomethane upgrading systems. *Adv. Biochem. Eng. Biotechnol.* 151, 117–135. doi: 10.1007/978-3-319-21993-6_5

Schirmack, J., Mangelsdorf, K., Ganzert, L., Sand, W., Hillebrand-Voiculescu, A., and Wagner, D. (2014). Methanobacterium movilense sp. nov., a hydrogenotrophic, secondary-alcohol-utilizing methanogen from the anoxic sediment of a subsurface lake. *Int. J. Syst. Evol. Microbiol.* 64(Pt 2), 522–527. doi: 10.1099/ijs.0.057224-0

Seifert, A., Rittmann, S., Bernacchi, S., and Herwig, C. (2013). Method for assessing the impact of emission gasses on physiology and productivity in biological methanogenesis. *Bioresource Technol.* 136, 747–751. doi: 10.1016/j.biortech.2013.03.119

Seifert, A. H., Rittmann, S., and Herwig, C. (2014). Analysis of process related factors to increase volumetric productivity and quality of biomethane with *Methanothermobacter marburgensis*. *Appl. Energy* 132, 155–162. doi: 10.1016/j.apenergy.2014.07.002

Taubner, R.-S., Schleper, C., Firneis, M. G., and Rittmann, S. K.-M. R. (2015). Assessing the ecophysiology of methanogens in the context of recent astrobiological and planetological studies. *Life* 5, 1652–1686. doi: 10.3390/life5041652

Thauer, R. K., Kaster, A.-K., Goenrich, M., Schick, M., Hiromoto, T., and Shima, S. (2010). Hydrogenases from methanogenic archaea, nickel, a novel cofactor, and H2 storage. *Ann. Rev. Biochem.* 79, 507–536. doi: 10.1146/annurev.biochem.030508.152103

Thauer, R. K., Kaster, A.-K., Seedorf, H., Buckel, W., and Hedderich, R. (2008). Methanogenic archaea: ecologically relevant differences in energy conservation. *Nat. Rev. Microbiol.* 6, 579–591. doi: 10.1038/nrmicro1931

Tsao, J. H., Kaneshiro, S. M., Yu, S. S., and Clark, D. S. (1994). Continuous culture of *Methanococcus jannaschii*, an extremely thermophilic methanogen. *Biotechnol. Bioeng.* 43, 258–261. doi: 10.1002/bit.260430309

Ver Eecke, H. C., Akerman, N. H., Huber, J. A., Butterfield, D. A., and Holden, J. F. (2013). Growth kinetics and energetics of a deep-sea hyperthermophilic methanogen under varying environmental conditions. *Environ. Microbiol. Rep.* 5, 665–671. doi: 10.1111/1758-2229.12065

von Klein, D. V., Arab, H., Völker, H., and Thomm, M. (2002). Methanosarcina baltica, sp. nov., a novel methanogen isolated from the Gotland Deep of the Baltic Sea. *Extremophiles* 6, 103–110. doi: 10.1007/s007920100234

Wagner, D., Schirmack, J., Ganzert, L., Morozova, D., and Mangelsdorf, K. (2013). Methanosarcina soligelidi sp. nov., a desiccation- and freeze-thaw-resistant methanogenic archaeon from a Siberian permafrost-affected soil. *Int. J. Syst. Evol. Microbiol.* 63, 2986–2991. doi: 10.1099/ijs.0.046565-0

Conflict of Interest Statement: The authors declare that the research was conducted in the absence of any commercial or financial relationships that could be construed as a potential conflict of interest.

5 Biological methane production under putative Enceladus-like conditions

5.1 Overview

Enceladus is one of the most remarkable objects in the Solar System. Besides its spectacular plume located at the South Polar Terrain, it is the origin of the plume particles which makes Enceladus one of the hot spots in current Astrobiology: a subsurface liquid water ocean [Čadek et al., 2016, Thomas et al., 2016]. The molecules detected in the plume, *e.g.* H_2O, CO_2, or CH_4 [Waite et al., 2009], in combination with the possibility of hydrothermal vents at the ocean's floor [Hsu et al., 2015] lead to the assumption that this icy moon might be habitable for life as we know it. Serpentinization of olivine in the chondritic core may be the most prominent potential source of H_2 in Enceladus' interior. The presence of H_2 in Enceladus' plume was widely debated [Waite et al., 2009], but the last Cassini data confirmed that H_2 is native to Enceladus [Waite et al., 2017]. Along with that potential electron donor, many different organic and inorganic molecules like H_2O, CH_4, CO_2, and NH_3 were detected in the plume. Thus, Enceladus harbours many necessary ingredients for life. In this study the question is raised: Does some of the CH_4 detected in the plume might originate in methanogenic activity? The most promising area on Enceladus where life may exist is at the seafloor of the ice-covered ocean, where pressure was estimated to be 35 to 80 bar.

To explore if methanogenic microorganisms can in principle sustain their metabolism under Enceladus-like conditions, three methanogens (*Methanothermococcus okinawensis*, *Methanothermobacter marburgensis*, and *Methanococcus villosus*) were studied.

To prioritize one of the above mentioned strains, we tested these organisms for tolerance towards potential gaseous and liquid inhibitors detected in Enceladus' plume (high NH_3 levels, formaldehyde, ethene, and methanol). Only one strain, namely *M. okinawensis*, isolated from a deep marine trench [Takai et al., 2002], showed a continuous and stable growth rate. We therefore picked this strain for the final experiments, where the potential physical conditions of Enceladus' ocean were mimicked (65/80°C, 10-90 bar). These high pressure experiments were performed in

a 0.7 L bioreactor at the Johannes Kepler University Linz (JKU Linz). Here, a H_2/CO_2 to CH_4 gas conversion of >88% was demonstrated. The experiments showed that methanogenesis could in principle be feasible under Enceladus-like conditions.

Additionally, the computer code PHREEQC was used in this study to model serpentinization-based H_2 production rates to determine if serpentinization reactions on Enceladus support a rate of H_2 production that is high enough to sustain autotrophic, hydrogenotrophic methanogenic life. Depending on the applied mineral assemblage, an H_2 production rate of approximately 5 to 50 nmol $g^{-1}\,L^{-1}\,d^{-1}$ was estimated, which may be a sufficient H_2 gas production to serve as a substrate for biological CH_4 production on Enceladus.

This article combines studies of various scientific fields. It is the first systematic study on methanogenic physiology under high pressure and may enable a new assessment about potential habitats in the Solar System, especially icy moons.

5.2 Publication Details

Title: Biological methane production under putative Enceladus-like conditions
Authors: R.-S. Taubner, P. Pappenreiter, J. Zwicker, D. Smrzka, C. Pruckner, P. Kolar, S. Bernacchi, A. H. Seifert, A. Krajete, W. Bach, J. Peckmann, C. Paulik, M. G. Firneis, C. Schleper, S. K.-M. R. Rittmann
Status: Published online in *Nature Communications*, February 27th, 2018
Bibliographic reference: Nat Communications, Volume 9, Article 748
DOI: doi:10.1038/s41467-018-02876-y

Own contributions: Literature research, calculations regarding Enceladus' interior structure, estimations about physicochemical conditions in the subsurface ocean, planing and performance of all low pressure experiments, software implementation, data analysis, preparation of figures and plots, writing parts of the first manuscript version (focus on introduction, low pressure experiments, and corresponding parts of the discussion and methods section), editing and approving manuscript.

nature COMMUNICATIONS

ARTICLE

DOI: 10.1038/s41467-018-02876-y OPEN

Biological methane production under putative Enceladus-like conditions

Ruth-Sophie Taubner[1,2], Patricia Pappenreiter[3], Jennifer Zwicker[4], Daniel Smrzka[4], Christian Pruckner[1], Philipp Kolar[1], Sébastien Bernacchi[5], Arne H. Seifert[5], Alexander Krajete[5], Wolfgang Bach[6], Jörn Peckmann[4,7], Christian Paulik[3], Maria G. Firneis[2], Christa Schleper[1] & Simon K.-M.R. Rittmann[1]

The detection of silica-rich dust particles, as an indication for ongoing hydrothermal activity, and the presence of water and organic molecules in the plume of Enceladus, have made Saturn's icy moon a hot spot in the search for potential extraterrestrial life. Methanogenic archaea are among the organisms that could potentially thrive under the predicted conditions on Enceladus, considering that both molecular hydrogen (H_2) and methane (CH_4) have been detected in the plume. Here we show that a methanogenic archaeon, *Methanothermococcus okinawensis*, can produce CH_4 under physicochemical conditions extrapolated for Enceladus. Up to 72% carbon dioxide to CH_4 conversion is reached at 50 bar in the presence of potential inhibitors. Furthermore, kinetic and thermodynamic computations of low-temperature serpentinization indicate that there may be sufficient H_2 gas production to serve as a substrate for CH_4 production on Enceladus. We conclude that some of the CH_4 detected in the plume of Enceladus might, in principle, be produced by methanogens.

[1] Archaea Biology and Ecogenomics Division, Department of Ecogenomics and Systems Biology, Universität Wien, 1090 Vienna, Austria. [2] Department of Astrophysics, Universität Wien, 1180 Vienna, Austria. [3] Institute for Chemical Technology of Organic Materials, Johannes Kepler Universität Linz, 4040 Linz, Austria. [4] Department of Geodynamics and Sedimentology, Center for Earth Sciences, Universität Wien, 1090 Vienna, Austria. [5] Krajete GmbH, 4020 Linz, Austria. [6] Geoscience Department, Universität Bremen, 28359 Bremen, Germany. [7] Institute for Geology, Center for Earth System Research and Sustainability, Universität Hamburg, 20146 Hamburg, Germany. Correspondence and requests for materials should be addressed to S.K.-M.R.R. (email: simon.rittmann@univie.ac.at)

Saturn's icy moon Enceladus emits jets of mainly water (H_2O) from its south-polar region[1]. Besides H_2O, the ion and neutral mass spectrometer (INMS) onboard NASA's Cassini probe detected methane (CH_4), carbon dioxide (CO_2), ammonia (NH_3), molecular nitrogen (N_2), and molecular hydrogen (H_2) in the plume[2]. In addition, carbon monoxide (CO) and ethene (C_2H_4) were found among other substances with moderate ambiguity[3–6] (Table 1). At $1608.3 \pm 4.5\ kg\ m^{-3}$[1], Enceladus possesses a relatively high-bulk density for an icy moon, which leads to the assumption that a substantial part of its core consists of chondritic rocks[7]. At the boundary between the liquid water layer and the rocky core, geochemical interactions are assumed to occur at low to moderate temperatures (<100 °C)[2,7,8]. The most prominent potential source of H_2 in Enceladus' interior may be oxidation of native and ferrous iron in the course of serpentinization of olivine in the chondritic core. Olivine hydrolysis at low temperatures is a key process for sustaining chemolithoautotrophic life on Earth[9] and if H_2 is produced in significant amounts on Enceladus, then it could also serve as a substrate for biological CH_4 production. Considering that $139 \pm 28 \times 10^9$ to $160 \pm 43 \times 10^9$ kg carbon $year^{-1}$ of the CH_4 found in the atmosphere of Earth is emitted from natural sources[10], including biological methanogenesis, the question was raised if CH_4 detected in the plume of Enceladus could in principle also originate from biological activity[11].

To date, methanogenic archaea are the only known microorganisms that are capable of performing biological CH_4 production in the absence of oxygen[12,13]. On Earth, methanogens are found in a wide range of pH (4.5–10.2), temperatures (<0–122 °C), and pressures (0.005–759 bar)[13] that overlap with conditions predicted in Enceladus' subsurface ocean, i.e., temperatures between 0 and above 90 °C[8], pressures of 40–100 bar[8], a pH between 8.5–10.5[8] and 10.8–13.5[14], and a salinity in the range of our oceans. While autotrophic, hydrogenotrophic methanogens might metabolise some of the compounds found in Enceladus' plume, other compounds which were detected in the plume with different levels of ambiguity, such as formaldehyde (CH_2O), methanol (CH_3OH), NH_3, CO, and C_2H_4 are known to inhibit growth of methanogens on Earth at certain concentrations[15–17].

Here we show that methanogens can produce CH_4 under Enceladus-like conditions, and that the estimated H_2 production rates on this icy moon can potentially be high enough to support autotrophic, hydrogenotrophic methanogenic life.

Results

Effect of gaseous inhibitors on methanogens. To investigate growth of methanogens under Enceladus-like conditions, three thermophilic and methanogenic strains, *Methanothermococcus okinawensis* (65 °C)[18], *Methanothermobacter marburgensis* (65 °C)[19], and *Methanococcus villosus* (80 °C)[20], all able to fix carbon and gain energy through the reduction of CO_2 with H_2 to form CH_4, were investigated regarding growth and biological CH_4 production under different headspace gas compositions (Table 2) on H_2/CO_2, H_2/CO, H_2, Mix 1 (H_2, CO_2, CO, CH_4, and N_2) and Mix 2 (H_2, CO_2, CO, CH_4, N_2, and C_2H_4). These methanogens were prioritised due to their ability to grow (1) in a temperature range characteristic for the vicinity of hydrothermal vents[21], (2) in a chemically defined medium[22], and (3) at low partial pressures of H_2[23]. Also, in the case of *M. okinawensis*, the location of isolation was taken into consideration, since the organism was isolated from a deep-sea hydrothermal vent field at Iheya Ridge in the Okinawa Trough, Japan, at a depth of 972 m below sea level[18], suggesting a tolerance toward high pressure.

Table 1 Compilation of Cassini's INMS data on Enceladus' plume composition over the last decade

Species[a]	Volume mixing ratio					
	Waite et al. 2006[3]	Waite et al. 2009[4]	Waite et al. 2011[25]	Perry et al. 2015[26]	Bouquet et al. 2015[5]	Waite et al. 2017[b,2]
H_2O	90.7–91.5	90.0 ± 1.0	**92.0 ± 3.0**	>90	87	96–99
CO_2	3.14–3.26	5.3 ± 0.1	0.8 ± 0.3	**0.6 ± 0.2**	0.52	0.3–0.8
CO	(3.29–4.27)	(4.4)	<1.5		**≤0.64**	
H_2		(39)	$<3.4 \pm 1.0$	**1–5**	11	0.4–1.4
CH_2O		0.31 ± 0.01	**<0.032**			
CH_3OH		**0.015 ± 0.006**	0.003 ± 0.002			
C_2H_4		**<1.2**				
H_2S		0.0021 ± 0.0010	0.003 ± 0.001		**0.0021 ± 0.0010**	
NH_3		0.82 ± 0.02	0.8 ± 0.03	**0.9 ± 0.04**	0.61	0.4–1.3
N_2	(3.29–4.27)	<1.1			**≤0.61**	
HCN		<0.74	0.7 ± 0.3		**≤0.12**	
CH_4	1.63–1.68	0.91 ± 0.05	0.21 ± 0.09	**0.2 ± 0.1**	0.19	0.1–0.3

[a] Values used in this study are marked in bold
[b] These recent observations based on the data of flyby E21 lead to the assumption that H_2O is even more prominent, whereas the concentrations for the other major species (NH_3, CO_2, and CH_4) varied only slightly. The other components were categorised as minor species with moderate ambiguity (e.g., CO, N_2, C_2H_4, or CH_2O) or as potential species with high ambiguity (e.g., H_2S or CH_3OH)[6]

Table 2 Composition of the different test gases for the low-pressure experiments

	H_2 (Vol.-%)	CO_2 (Vol.-%)	CO (Vol.-%)	CH_4 (Vol.-%)	N_2 (Vol.-%)	C_2H_4 (Vol.-%)
H_2/CO_2	80.097	19.903	—	—	—	—
H_2/CO	80.290	—	19.710	—	—	—
H_2	99.999	—	—	—	—	—
Mix 1	22.900	19.490	27.790	14.430	15.390	—
Mix 2	22.430	19.210	28.151	14.510	12.410	3.289

While *M. okinawensis*, *M. marburgensis*, and *M. villosus* all showed growth on H_2/CO_2 to similar optical densities, no growth of *M. marburgensis* could be observed when C_2H_4 (Mix 2) was supplied in the headspace (Fig. 1). Growth of both *M. villosus* and *M. okinawensis* was observed even when CO and C_2H_4 were both present in the headspace gas. However, while *M. villosus* showed prolonged lag phases and irregular growth under certain conditions, *M. okinawensis* grew stably and reproducibly on the different gas mixtures without extended lag phases (Fig. 1). As expected, the final optical densities did not reach those of the experiments with H_2/CO_2, likely because in Mix 1 and Mix 2 lower absolute amounts of convertible gaseous substrate (H_2/CO_2) were available compared to the growth under pure H_2/CO_2. Consequently, growth kinetics showed a different, gas-limited linear inclination in the closed batch setup when using Mix 1 and Mix 2[22,24]. Due to its reproducible growth, *M. okinawensis* was chosen for more extensive studies on biological CH_4 production under putative Enceladus-like conditions.

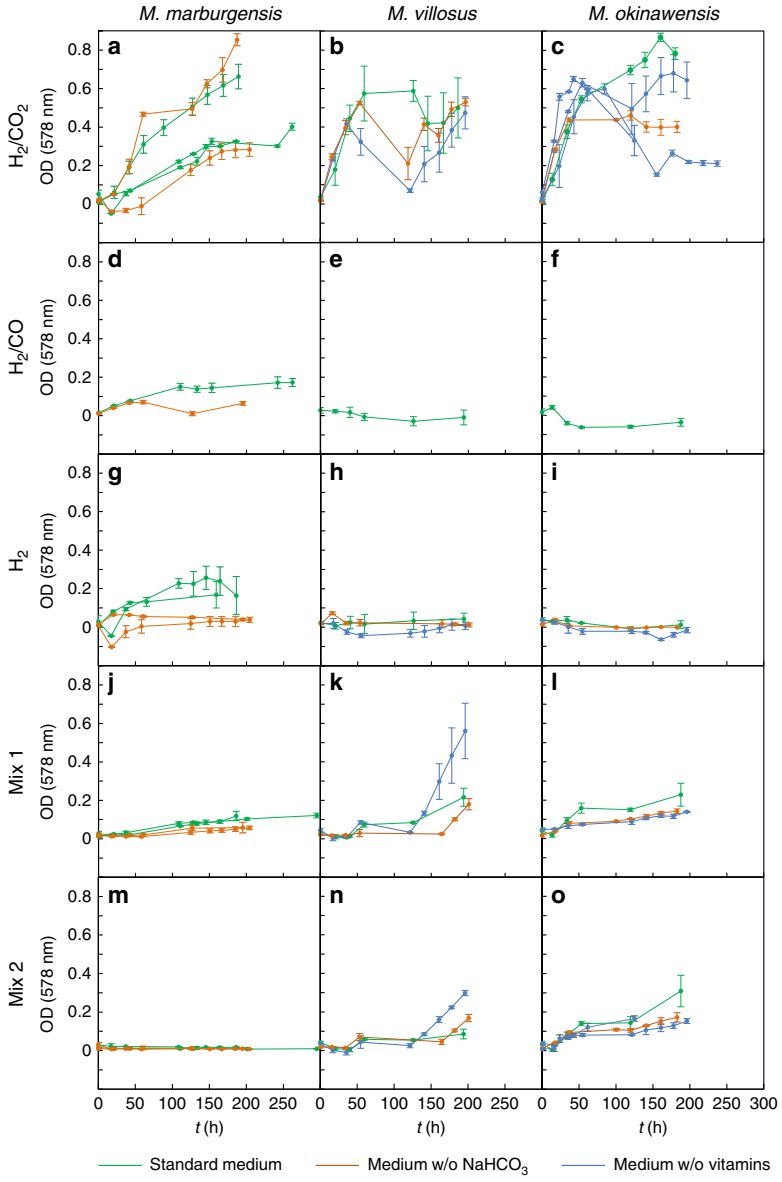

Fig. 1 Influence of the different headspace gas compositions on growth of *M. marburgensis*, *M. villosus*, and *M. okinawensis*. The error bars show standard deviations calculated from triplicates. OD curves of **a**, **d**, **g**, **j**, **m** *M. marburgensis*, **b**, **e**, **h**, **k**, **n** *M. villosus* and **c**, **f**, **i**, **l**, **o** *M. marburgensis* for **a**–**c** H_2/CO_2, **d**–**f** H_2/CO, **g**–**i** H_2, **j**–**l** Mix 1, and **m**–**o** Mix 2. Growth of *M. marburgensis* was inhibited by the presence of C_2H_4 (see Table 2 for detailed gas composition). Only *M. marburgensis* seemed to be able to use sodium hydrogen carbonate (supplied in the medium) as C-source in case of a lack of CO_2 (H_2 or H_2/CO as sole gas in the headspace). Both, *M. villosus* and *M. okinawensis* showed growth when Mix 1 and Mix 2 were applied to the serum bottle headspace; however, *M. villosus* exhibited extended lag phases. The dips in the graphs **b**, **c** were caused by substrate limitation due to depletion of serum bottle headspace of H_2/CO_2 at high-optical cell densities

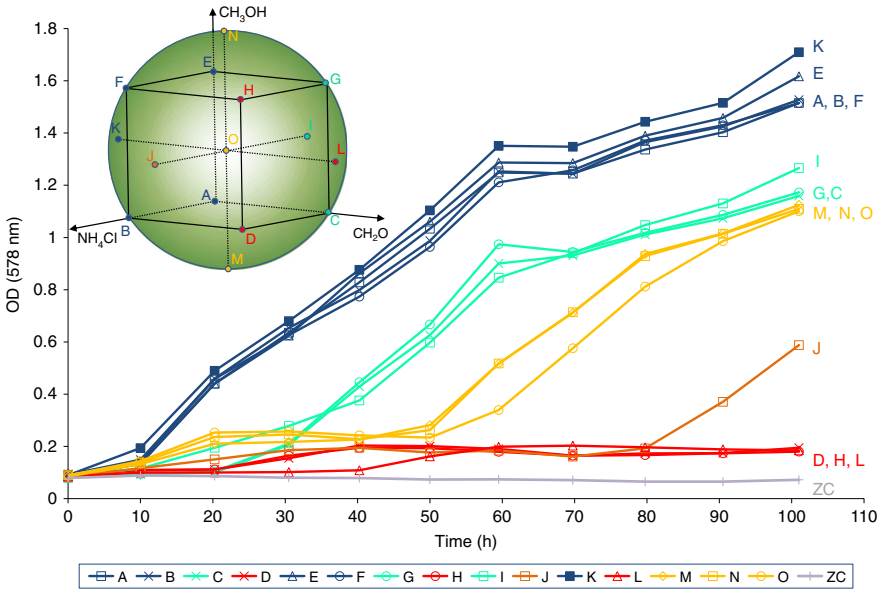

Fig. 2 Schematic of the experimental setting and DoE raw data growth curves showing OD measurements. The DoE is based on a central composite design (figure in the upper left corner). NH_4Cl, CH_2O, and CH_3OH were used as factors during the experiment and systematically varied in a multivariate design space (see Supplementary Table 1 for the concrete values). Each of the factors setting was examined in triplicates. The centre point (O) was examined in quintuplicates. The colours of the dots and the letters of the figure in the upper left corner correspond to the growth curves. The line labelled ZC represents the optical density of a corresponding zero control experiment, which was done with the same medium as the experiments labelled with O (central point), but without inoculum. The different colours represent different performances. For better readability, the error bars in this diagram were excluded, which were in a standard deviation range between 0.0009 and 0.1544. According to statistical selection criteria three experiments (one experiment F and two experiments O) were excluded from ANOVA analysis (Supplementary Table 2)

Table 3 Concentrations of gaseous species in growth medium

Gas phase	P_{H2} (bar)[a]	P_{CO2} (bar)[a]	Concentration (H_2, mol L^{-1})	Concentration (CO_2, mol L^{-1})
120 mL bottles (2 bar)				
H_2/CO_2[a]	2.40	0.60	1.52×10^{-3}	7.73×10^{-3}
H_2/CO[a]	2.41		1.52×10^{-3}	
H_2[a]	3.00		1.89×10^{-3}	
Mix 1[a]	0.69	0.58	4.34×10^{-4}	7.57×10^{-3}
Mix 2[a]	0.67	0.58	4.25×10^{-4}	7.46×10^{-3}
0.7 L reactor pressure tests				
H_2/CO_2[b] (~10 bar)	8.00	2.00	5.05×10^{-3}	2.59×10^{-2}
H_2/CO_2[b] (~20 bar)	16.00	4.00	1.01×10^{-2}	5.18×10^{-2}
H_2/CO_2[b] (~50 bar)	40.00	10.00	2.53×10^{-2}	1.29×10^{-1}
$H_2/CO_2/N_2$[c] (~20 bar)	8.00	2.00	5.05×10^{-3}	2.59×10^{-2}
$H_2/CO_2/N_2$[c] (~90 bar)	36.00	9.00	2.27×10^{-2}	1.17×10^{-1}
2.0 L reactor pressure and inhibitor tests I				
Mix[d] (~10 bar)	5.60	0.70	3.53×10^{-3}	9.07×10^{-3}
Mix[d] (~25 bar)	10.40	1.20	6.57×10^{-3}	1.55×10^{-2}
H_2/CO_2[b] (~20 bar)	16.30	4.00	1.03×10^{-2}	5.18×10^{-2}
Mix[d] (~50 bar)	27.50	3.10	1.74×10^{-2}	4.01×10^{-2}
2.0 L reactor pressure and inhibitor tests II				
Mix[d] (~10 bar)	5.90	0.70	3.72×10^{-3}	9.06×10^{-3}
Mix[d] (~25 bar)	11.00	1.20	6.94×10^{-3}	1.55×10^{-2}
H_2/CO_2[b] (~20 bar)	16.30	4.00	1.03×10^{-2}	5.18×10^{-2}
Mix[d] (~50 bar)	27.70	3.30	1.75×10^{-2}	4.27×10^{-2}
Cassini[e]				
1 bar	0.50	0.10	3.18×10^{-4}	1.31×10^{-3}
50 bar	25.21	5.04	1.59×10^{-2}	6.53×10^{-2}

[a] Detailed composition of the gases can be found in Table 2
[b] For the H_2/CO_2 experiments a ratio of 4:1 was applied
[c] For the $H_2/CO_2/N_2$ experiments a ratio of 4:1:5 was applied
[d] Detailed composition of the gases can be found in Table 4
[e] For the Cassini estimations, a hydrostatic pressure assumed to prevail in the Enceladus' ocean (50 bar) was applied. H_2 and CO_2 mixing ratio was taken from Table 1

Table 4 Gas composition of experiments performed in the 2.0 L bioreactor

	N_2 (Vol.-%)	H_2 (Vol.-%)	CO_2 (Vol.-%)	CO (Vol.-%)	C_2H_4 (Vol.-%)
2.0 L reactor pressure and inhibitor tests I					
20 bar (H_2/CO_2)		80.29	19.71		
10 bar	31.43	53.33	6.67	4.76	3.81
25 bar	42.91	42.11	4.86	4.45	5.67
50 bar	32.67	55.11	6.21	3.01	3.01
2.0 L reactor pressure and inhibitor tests II					
20 bar (H_2/CO_2)		80.30	19.70		
10 bar	29.25	55.66	6.60	4.72	3.77
25 bar	41.43	43.82	4.78	4.38	5.58
50 bar	32.41	55.07	6.56	2.98	2.98

***M. okinawensis* tolerates Enceladus-like conditions at 2 bar**. Growth and turnover rates (calculated via the decrease in headspace pressure) of *M. okinawensis* cultures were determined in the presence of selected putative liquid inhibitors detected in Enceladus' plume (NH_3, given as NH_4Cl, CH_2O, and CH_3OH). While growth of *M. okinawensis* could still be observed at the highest concentration of NH_4Cl added to the medium (16.25 g L^{-1} or 0.30 mol L^{-1}), the organism grew only in the presence of up to 0.28 mL L^{-1} (0.01 mol L^{-1}) CH_2O. This is less than, but importantly still in the same order of magnitude of, the observed maximum value of 0.343 mL L^{-1} CH_2O detected in the plume[25]. Growth and CH_4 production of *M. okinawensis* in closed batch cultivation was shown at CH_3OH and NH_4Cl concentrations exceeding those reported for Enceladus' plume[4,5,25,26].

To explore how the presence of these inhibitors might influence growth and turnover rates of *M. okinawensis*, we have applied these compounds at various concentrations in a multivariate design space setting (Design of Experiment (DoE)). At different concentrations of CH_2O, CH_3OH, and NH_4Cl, *M. okinawensis* cultures showed growth (Fig. 2) and turnover rates from 0.015 ± 0.012 to 0.084 ± 0.018 h^{-1} (Supplementary Fig. 1; experiments L and K in Fig. 2). CH_3OH amendments at concentrations between 9.09 and 210.91 µL L^{-1} (0.22–5.21 mmol L^{-1}) did not reduce or improve growth of *M. okinawensis* (Fig. 2 and Supplementary Tables 1 and 2). Compared to the highest applied CH_2O concentration, the turnover rate of *M. okinawensis* was ~5.6-fold higher at the lowest tested concentration. The results of this experiment indicated that *M. okinawensis* possessed a physiological tolerance towards a broad multivariate concentration range of CH_2O, CH_3OH, and NH_4Cl and was able to perform the autocatalytic conversion of H_2/CO_2 to CH_4 while gaining energy for growth.

We used the mean liquid inhibitor concentrations for CH_2O determined in the DoE experiment (DoE centre points) and Enceladus-like concentrations for CH_3OH and NH_4Cl (Supplementary Table 3) to test growth and turnover rates of *M. okinawensis*, using different gases in the headspace (H_2/CO_2, Mix 1, and Mix 2 (Fig. 3)). Under all tested headspace gas compositions, *M. okinawensis* showed gas-limited growth (max. OD values of 0.67 ± 0.02, 0.17 ± 0.03, and 0.13 ± 0.03 after ~237 h for H_2/CO_2, Mix 1 and Mix 2, respectively). The calculated turnover rates correlated with the different convertible amounts of H_2/CO_2 in Mix 1 and Mix 2. Hence, *M. okinawensis* was able to grow and to convert H_2/CO_2 to CH_4 when CH_2O, CH_3OH, NH_4Cl, CO and C_2H_4 were present in the growth medium at the concentrations calculated from Cassini's INMS data (assuming 1 bar, compare Tables 1 and 2). The mixing ratios of these putative inhibitors were based on INMS data[4,5,25,26] but higher than those calculated by using the most recent Cassini data[2,6] (Table 1). This demonstrates that growth and biological CH_4 production of *M. okinawensis* is possible even at higher inhibitor concentrations.

***M. okinawensis* tolerates Enceladus-like conditions up to 50 bar**. Due to the fact that methanogens on Enceladus would possibly need to grow at hydrostatic pressures up to 80 bar[8] and beyond, the effect of high pressure on the conversion of headspace gas for *M. okinawensis* was examined in a pressure-resistant closed batch bioreactor. Headspace H_2/CO_2 conversion and CH_4 production was examined at 10, 20, 50, and 90 bar, either using H_2/CO_2 in a 4:1 ratio or applying $H_2/CO_2/N_2$ in a 4:1:5 ratio. A gas conversion of >88% was shown for each of the experiments (Supplementary Fig. 2) except for the 90 bar experiment using $H_2/CO_2/N_2$, where the headspace gas conversion was found to be at 66.4%. However, no headspace gas conversion and CH_4 production could be detected when cultivating *M. okinawensis* at 90 bar using H_2/CO_2 only (data not shown).

Final experiments were designed to investigate headspace H_2/CO_2 conversion and CH_4 production of *M. okinawensis* according to INMS data (Table 3) and under conditions of high pressure (10.7 ± 0.1, 25.0 ± 0.7, and 50.4 ± 1.7 bar). Turnover rate, methane evolution rate (MER, calculated via pressure drop) and biological CH_4 production (calculated via gas chromatography measurements) for these experiments are shown in Fig. 4. When simultaneously applying putative gaseous (Table 4) and liquid inhibitors (Supplementary Table 3) under high-pressure conditions, we reproducibly demonstrated that *M. okinawensis* was able to perform H_2/CO_2 conversion and CH_4 production under Enceladus-like conditions.

Methanogenic life could be fuelled by H_2 from serpentinization. In light of these experimental findings and the presence of H_2 in Enceladus' plume[2], the question arose if serpentinization reactions can support a rate of H_2 production that is high enough to sustain autotrophic, hydrogenotrophic methanogenic life. To address this question, we used the PHREEQC[27] code to model serpentinization-based H_2 production rates under Enceladus-like conditions (Table 5) with the assumption that the rate-limiting step of the serpentinization reaction is the dissolution of olivine. H_2 production rates are poorly constrained, as they strongly depend on assumed grain size and temperature. These rates correspond to the low end of the range of H_2 production rates, which were based on a thermal cooling and cracking model[28]. Of the many reactions involved in serpentinization of peridotite, dissolution of the Fe(II)-bearing primary phases is a critical one[29], and the only one for which kinetic data are available. In the model, CO_2 reduction to CH_4 is predicted to take place once enough H_2 in the system was produced to generate thermodynamic drive for the reaction. While abiotic CH_4 production is kinetically more sluggish than olivine dissolution[30], biological CH_4 production is fast and may be controlled by the rate at which H_2 is supplied. The abiotic CH_4 production rates listed in Table 5 are hence also modelled such that olivine dissolution is the rate-limiting step. The results of these thermodynamic and kinetic computations show that H_2 and CH_4 production is predicted for a range of rock compositions (Table 5) and temperature conditions (Supplementary Table 4). The model system essentially represents a closed system with high-rock porosity, such as proposed for Enceladus[2]. The computational results predict how much H_2 and CH_4 should form within the intergranular space inside Enceladus' silicate core with water-to-rock-ratios between 0.09 and 0.12 (Table 5). The serpentinization reactions are predicted to produce solutions with circumneutral to high pH between 7.3 and 11.3, as well as amounts of H_2 that greatly exceed the amount of dissolved inorganic carbon (DIC) trapped in the

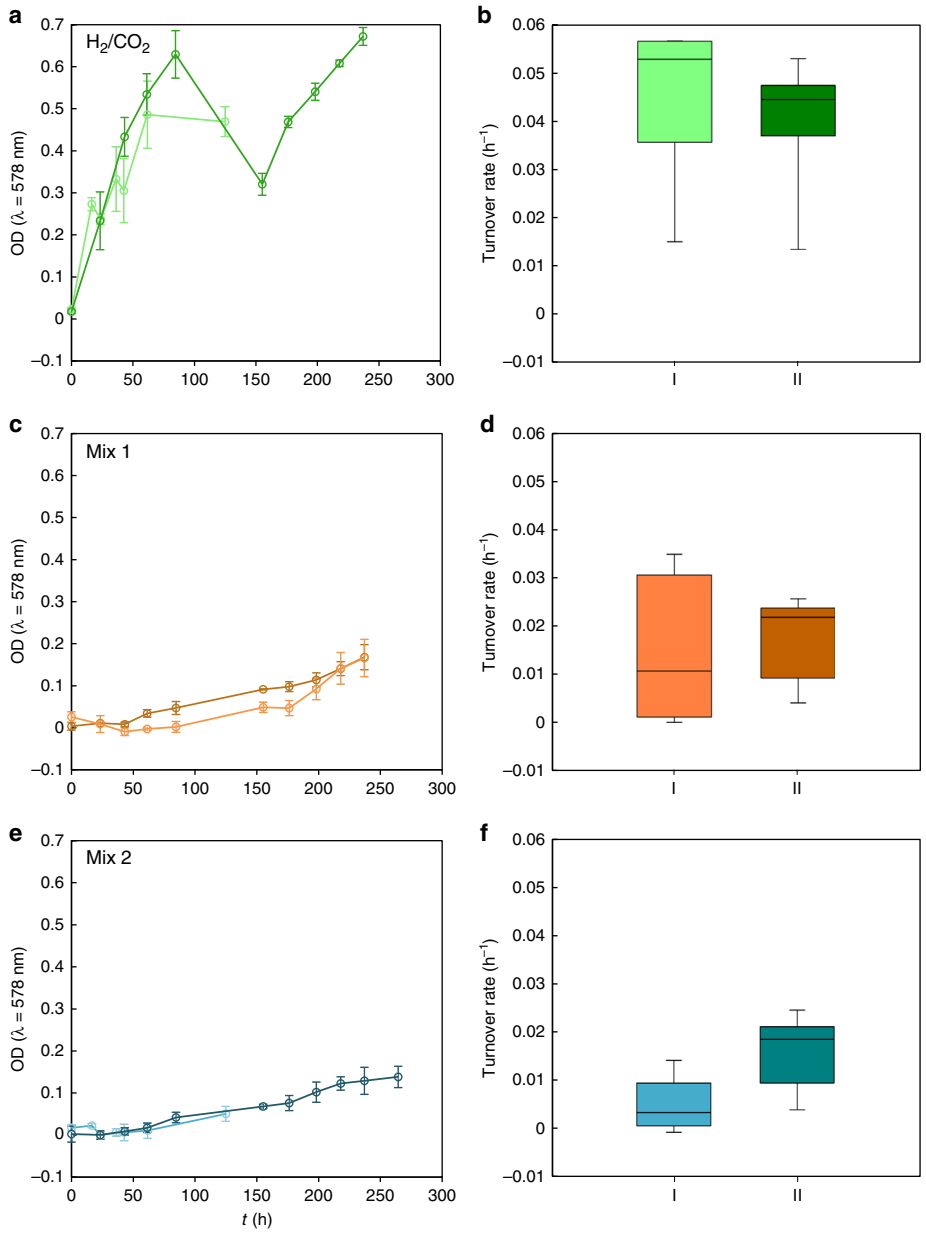

Fig. 3 Growth and turnover rate of *M. okinawensis* under Enceladus-like conditions at 2 bar. **a**, **c**, **e** Growth curves ($OD_{578\,nm}$) and **b**, **d**, **f** turnover rates (h^{-1}) as a measure of CH_4 production of *M. okinawensis* on **a**, **b** H_2/CO_2 (4:1), **c**, **d** Mix 1 and **e**, **f** Mix 2. For detailed composition of gases and media see Table 2 and Supplementary Table 3. I and II (light and dark colours, respectively) denote two independent experiments (each performed in triplicates, error bars = standard deviation). Enceladus-like concentrations were used for NH_4Cl and CH_3OH and mean liquid inhibitor concentrations determined in the DoE were used for CH_2O. The dip in **a** was caused by substrate limitation due to depletion of serum bottle headspace of H_2/CO_2 at high-optical cell densities

pore space. As the computations indicate that there is ample thermodynamic drive for reducing DIC to CH_4, these results corroborate the idea that serpentinization reactions on Enceladus might fuel autotrophic, hydrogenotrophic methanogenic life. However, we would like to point out that if methanogenic life were indeed active on Enceladus, biological CH_4 production would always compete with abiotic CH_4 generation processes resulting in a mixed CH_4 production.

Discussion

In this study, we show that the methanogenic strain *M. okinawensis* is able to propagate and/or to produce CH_4 under putative Enceladus-like conditions. *M. okinawensis* was cultivated under high-pressure (up to 50 bar) conditions in defined growth medium and gas phase, including several potential inhibitors that were detected in Enceladus' plume[2,4,6]. The only difference between the growth conditions of *M. okinawensis* and the

Table 5 H_2 and CH_4 production rates from serpentinization calculated for 50 °C and 50 bar

Mineral assemblage[a]	pH	H_2 production rate (nmol g^{-1} L^{-1} d^{-1})	CH_4 production rate[b] (nmol g^{-1} L^{-1} d^{-1})	Water: rock ratio	Mol H_2 produced per mol olivine
Fo_{90}:En:Diop = 8:1:1	11.3	4.58	2.05	0.126	0.002
Fo_{90}	8.60	4.03	1.07	0.124	0.004
Fo_{50}	7.50	34.7	1.35	0.104	0.033
Fo_{20}	7.29	50.7	1.32	0.094	0.053

[a] Fo_{90} = forsteritic olivine (forsterite:fayalaite = 9:1), En = enstatite, Diop = diopside, Fo_{50} = (Fo:Fa = 1:1), Fo_{20} = (Fo:Fa = 2:8)
[b] CH_4 production is predicted from allowing H_2 and dissolved inorganic carbon (DIC) to equilibrate readily, while H_2 production is kinetically controlled by dissolution of primary phases

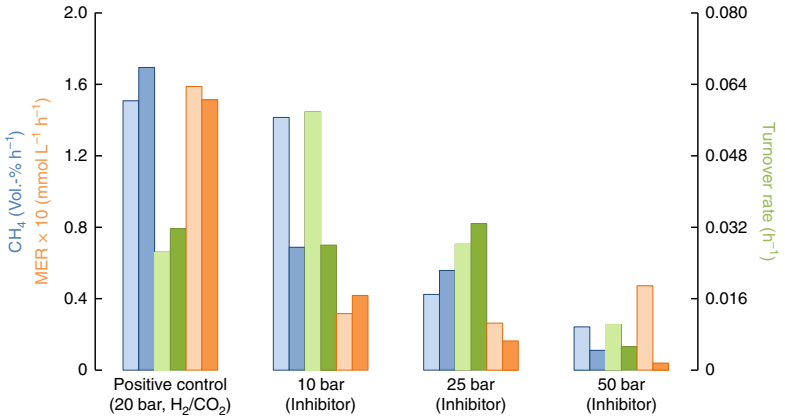

Fig. 4 CH_4 production, MER, and turnover rate of *M. okinawensis* under Enceladus-like conditions at high pressure. Biological CH_4 production determined by gas chromatography (blue) (Vol.-% h^{-1}) and turnover rates (h^{-1}) (green) and MER·10 (mmol L^{-1} h^{-1}) (red) measured from headspace gas conversion using *M. okinawensis* (experiment 1 in light colours, experiment 2 in dark colours) under putative Enceladus-like conditions in a 2.0 L bioreactor (for detailed medium composition, see Supplementary Table 3 and for detailed gas composition see Table 4, $n = 2$). The positive control experiment contained also the liquid inhibitors but only H_2/CO_2 (4:1) in the headspace. For high-pressure experiments without any inhibitors see Supplementary Fig. 2

putative Enceladus-like conditions was the lower pH value applied during the high-pressure experiments. Due to the supply of CO_2 at high-pressure in the experiments the pH decreased to ~5, while pH values between 7.3 and 13.5 were estimated for Enceladus' subsurface ocean (this study and refs. [8,14]).

Another point of debate might be the cultivation temperatures used for the thermophilic and hyperthermophilic methanogens in this study. The mean temperature in the subsurface ocean of Enceladus might be just above 0 °C except for the areas where hydrothermal activity is assumed to occur. In these hydrothermal settings temperatures higher than 90 °C are supposedly possible[8], and are therefore the most likely sites for higher biological activity on Enceladus. Although methanogens are found over a wide temperature range on Earth, including temperatures around 0 °C[31], growth of these organisms at low temperatures is observed to be slow[13].

We estimated H_2 production rates between 4.03 and 50.7 nmol g^{-1} L^{-1} d^{-1} in the course of serpentinization on Enceladus (Table 5). These estimates are rather conservative, as they are based on the assumption of small specific mineral surface areas. In a recent study, the rate of serpentinization has been estimated from a physical model that predicts how fast cracking fronts propagate down into Enceladus' core[28]. Combining this physically controlled advancement of serpentinization (8×10^{11} g y^{-1}[28]) with our estimates for kinetically limited rates of H_2 production leads to overall rates of 3–40 × 10^4 mol H_2 y^{-1} for Enceladus. Although still high enough to support biological methanogenesis, these rates are orders of magnitude lower than the previously suggested 10×10^8 mol H_2 y^{-1}[28] assuming that the speed of cracking front propagation controls the rate of H_2 production. We hence suggest that reaction kinetics may play an important role in determining the overall H_2 production rate on Enceladus. Our computed steady-state H_2 production rates are lower than the 1–5 × 10^9 mol H_2 y^{-1} estimated from Cassini data[2]. This apparent discrepancy in flux rates can be reconciled if the Enceladus plume was a transient (i.e., non-steady state) phenomenon. The predicted H_2/CH_4 ratio of 2.5 (Fo_{90}:En:Diop = 8:1:1) to 4 (Fo_{90}) for the magnesian compositions of Enceladus' core (Table 5) are consistent with the relative proportions of the two gases in the plume (0.4–1.4% H_2, 0.1–0.3% CH_4)[2].

Based on our estimated H_2 production rate, we can calculate how much of the available DIC on Enceladus could be fixed into biomass through autotrophic, hydrogenotrophic methanogenesis. If we assume a typical elementary composition of methanogen biomass[32], 7.13 g carbon could be fixed per g hydrogen fixed. Under optimal growth conditions, ~3%[22,23] of the available carbon can be assimilated into biomass, and assuming that methanogens possess a molecular weight of ~30.97 g C-mol[−1][22] and that the total amount of H_2 produced would be available for the carbon and energy metabolism of autotrophic, hydrogenotrophic methanogens, a biomass production rate between 20 and 257 C-nmol g^{-1} L^{-1} y^{-1} could be achieved. In another approach, we can use the actually predicted CH_4 production rates of 1.32–2.05 nmol g^{-1} L^{-1} d^{-1} (Table 5) and a Gibbs energy dissipation approach in which we assume that 10% of the energy of CH_4 production is fuelling biosynthesis[28]. This yields similar numbers of biomass production rate, i.e., 28 and 56 C-nmol g^{-1} L^{-1} y^{-1}.

Based on our findings, it might be interesting to search for methanogenic biosignatures on icy moons in future space

missions. Methanogens produce distinct and lasting biosignatures, in particular lipid biomarkers like ether lipids and isoprenoid hydrocarbons. Other potential biomarkers for methanogens are high-nickel (Ni) concentrations (and its stable isotopes[33]), as Ni is e.g., part of methyl-coenzyme M reductase, the key enzyme of biological methanogenesis[23]. However, both lipid biomarkers and Ni-based biosignatures are likely only to be identifiable at the site of biological methanogenesis, and the effect of dilution with increasing distance away from the methanogen habitat is likely to prevent their use as a general marker for biological methanogenesis in Enceladus' plume or in a subsurface ocean. If, however, bubble scrubbing would occur, a process by which organic compounds and cells adhere to bubble surfaces and are carried away as bubbles rise, which was suggested to occur on Enceladus[34], the amount of bioorganic molecules and cells would be much higher and future lander missions could easily collect physical evidence for the presence of autotrophic, hydrogenotrophic methanogenic life on Enceladus.

Additionally, one could consider using stable isotopes of CH_4 and CO_2 and ratios of low-molecular weight hydrocarbons to evaluate the possibility of biological methanogenesis on Enceladus[11]. But given the uncertainties on the geological and hydrogeological boundary conditions that influence the targeted isotope and molecular patterns in Enceladus' plume, such an approach is not trivial. In contrast to biological and thermogenic CH_4 production, the latter resulting from the decomposition of organic matter, abiogenic CH_4 is believed to be produced by metal-catalysed Fischer–Tropsch or Sabatier type reactions under hydrothermal conditions and particularly in the course of serpentinization of ultramafic rocks[35]. Although biologically produced CH_4 is usually characterised by its strong ^{13}C depletion, growth of methanogens at high-hydrostatic pressures and high temperatures, which is typical of deep-sea hydrothermal systems, may significantly reduce kinetic isotope fractionation and result in relatively high $\delta^{13}C$ values of CH_4, hampering discrimination from non-microbial CH_4[36]. Given such uncertainties, multiply substituted, so-called 'clumped' isotopologues of CH_4 emerge as new proxy to constrain its mode of formation and to recognise formation environments like serpentinization sites[37].

Another approach to identify the origin of CH_4 could be CH_4/(ethane + propane) ratios, as low ratios are typical of settings dominated by thermogenic CH_4[38]. However, this ratio may fall short to unequivocally discriminate abiogenic from biologically produced CH_4. For instance the ratio of CH_4 concentration to the sum of C_{2+} hydrocarbon concentration (C_1/C_{2+}) in the serpentinite-hosted Lost City Hydrothermal Field of 950 ± 76 was found to be most similar to ratios obtained in experiments with Fischer–Tropsch type reactions (<100–>3000). Thermogenic reactions produce C_1/C_{2+} ratios less than ~100, whereas biological methanogenesis results in ratios of 2000–13000[39]. More than 30 years of research on CH_4 production have revealed that its biologic, thermogenic or abiogenic origin on Earth is often difficult to trace[40]. However, the experimental and modelling results presented in this study together with the estimates of the physicochemical conditions on Enceladus from earlier contributions make it worthwhile to increase efforts in the search for signatures for autotrophic, hydrogenotrophic methanogenic life on Enceladus and beyond.

Methods

Estimations of Enceladus' interior structure. Due to its rather small radius, the uncompressed density of the satellite is almost equal to its bulk density, which makes a simplified model of Enceladus' interior reasonable. Enceladus was divided into a rocky core (core density of 2300–2550 kg m^{-3}), a liquid water layer (density of 960–1080 kg m^{-3}), and an icy shell (ice density of 850–960 kg m^{-3}) and hydrostatic equilibrium was assumed. Calculations of the hydrostatic pressure based on Enceladus mass of 1.0794×10^{20} kg[41] and its mean radius of 252.1 km[41] assuming a core radius of 190–200 km, an subsurface ocean depth of 60–10 km and a corresponding ice shell thickness of 2.1–52.1 km results in a pressure of ~44.3–25.2 bar or 80.1–56.2 bar (depending on the method, Supplementary Methods) at the water-core-boundary. For the high-pressure experiments in this study, including all inhibitors, three pressure values were chosen that lie in the range given by Hsu et al. (10–80 bar)[8] and are related to our calculations, i.e., 10, 25, and 50 bar.

Low-pressure experiments. Growth and tolerance towards putative inhibitors of the three methanogenic strains *Methanothermococcus okinawensis* DSM 14208, *Methanothermobacter marburgensis* DSM 2133, and *Methanococcus villosus* DSM 22612 were elucidated (Fig. 1). All strains were obtained from the Deutsche Stammsammlung von Mikroorganismen und Zellkulturen GmbH, Braunschweig, Germany. Growth was resolved by optical density (OD) measurements ($\lambda = 578$ nm). H_2/CO_2–CH_4 gas conversion [%], turnover rate [h^{-1}] (see Equation (2) below), and MER were calculated from the decrease of the bottle headspace pressure and/or from measuring CH_4 production in a closed batch setup[22,24]. The headspace pressures were measured using a digital manometer (LEO1-Ei, −1… 3barrel, Keller, Jestetten, Germany) with filters (sterile syringe filters, w/0.2c µm cellulose, 514-0061, VWR International, Vienna, Austria), and cannulas (Gr 14, 0.60 × 30 mm, 23 G × 1 1/4", RX129.1, Braun, Maria Enzersdorf, Austria). The detailed setting can be seen in Fig. 3(a) in Taubner and Rittmann[22]. All pressure values presented in this study are indicated as relative pressure in bar.

For the experiments at 2 bar regarding CO and C_2H_4 tolerance (see Figs. 1 and 3), the strains were incubated in the dark either in a water bath (*M. marburgensis* and *M. okinawensis*, 65 ± 1 °C) or in an air bath (*M. villosus*, 80 ± 1 °C). The methanogens were cultivated in 50 mL of their respective chemically defined growth medium. Compositions of the different growth media of the experiments shown in Figs. 1 and 3 can be found in Supplementary Tables 3 and 5–10. The final preparation of the medium in the anaerobic culture flasks was performed in an anaerobic chamber (Coy Laboratory Products, Grass Lake, USA). Experiments were performed over a time of 210–270 h. After each incubation period, serum bottle headspace pressure measurement (in order to be unbiased, flasks were previously cooled down to room temperature), OD-sampling, and gassing with designated gas or test gas was performed. OD measurement was performed at 578 nm in a spectrophotometer (DU800, Beckman Coulter, USA). A zero control was incubated together with each individual experiment and the OD of this control was subtracted from the measured OD from the inoculated flasks each time.

For hydrogenotrophic methanogens, which utilise H_2 as electron donor for the reduction of CO_2 to produce CH_4 and H_2O as their metabolic products, the following stoichiometric reaction equation was used[12,23,24]:

$$4H_{2(g)} + CO_{2(g)} \rightarrow CH_{4(g)} + 2H_2O_{(aq)} \quad \Delta G^0 = -135\,\mathrm{kJ\,mol^{-1}}. \qquad (1)$$

The turnover rate [h^{-1}] correlates with the catalytic efficiency per unit of time, i.e., it is a way to indirectly quantify CH_4 productivity. By assuming the above-mentioned chemical CO_2 methanation stoichiometry and neglecting biomass formation, the turnover rate is an equivalent method for indirect quantification of CH_4 production. It is defined as

$$\text{turnover rate}\,[\mathrm{h^{-1}}] = \frac{\Delta p}{\Delta p_{max} \cdot \Delta t}, \qquad (2)$$

where Δp [bar] is the difference in pressure before and after incubation, Δp_{max} [bar] is the maximal theoretical difference that would be feasible due to stoichiometric reasons[22], and Δt [h] is the time period of incubation.

For the initial pressure experiments at 2 bar, the three methanogenic strains were tested under five different gas phase compositions (Table 2). A significant change in OD and turnover rate was observed between these experiments (as can be seen in Fig. 1). When Mix 1 and Mix 2 were applied, only a maximum of 22.66 ± 0.23 Vol.-% H_2 (average, Table 2) could be converted to CH_4 and biomass.

To evaluate the influences of the potential inhibitors NH_3, CH_2O, and CH_3OH on the growth of *M. okinawensis*, several preliminary experiments were performed. For easier handling, NH_3 was substituted by NH_4Cl. Based on INMS data (Table 1) the amount of NH_4Cl was calculated according to Henry's law. For that, Henry's law constant was calculated to be 0.1084 mol m^{-3} Pa^{-1} at 64 °C. This results in 11.6 g L^{-1} (0.22 mol L^{-1}) NH_4Cl to have ~1% of NH_3 in the gaseous phase at equilibrium for the experiments under closed batch conditions. The influence of NH_4Cl between 0.25 and 16.25 g L^{-1} (4.67 and 303.79 mmol L^{-1}), CH_2O between 0 to 111 µL L^{-1} (0–4.03 mmol L^{-1}), and CH_3OH between 0 and 200 µL L^{-1} (0–4.94 mmol L^{-1}) was tested individually. CH_2O (37 Vol.-%) and CH_3OH (98 Vol.-%) were used as stock solutions.

To find an appropriate ratio for the final experiments, an experiment in a DoE setting was established. A central composite design with the parameters shown in Supplementary Table 1 and Fig. 2 was chosen. The design space is spherical with a normalised radius equal to one. Experiments A–N were done in triplicates; experiments O were performed in quintuplicate. The results of these experiments in terms of OD can be seen in Fig. 2 and in terms of turnover rate in

Supplementary Fig. 1. Each incubation time period was 10.0 ± 0.5 h. The ANOVA analysis of this study can be found in Supplementary Table 2.

The setting for the experiments under Enceladus-like conditions at 2 bar pressure included the medium described in Supplementary Table 3 and Mix 2 (Table 2) as gaseous phase. As can be seen in Fig. 3 there was a lag phase of two days, but after that continuous but slow growth was observed.

To calculate the molar concentration of H_2 and CO_2 in the medium (Table 3), Henry's law was used:

$$M = k_H \cdot p_X, \quad (3)$$

where p_X is the partial pressure of the respective gas and k_H is Henry's constant as a function of temperature:

$$k_H = k_H^{\ominus} \cdot e^{\left(\frac{-\Delta_{soln}H}{R}\left(\frac{1}{T}-\frac{1}{T^{\ominus}}\right)\right)}, \quad (4)$$

where $\Delta_{soln}H$ is the enthalpy change of the dissolution reaction. For $k_H^{\ominus}$ the values 7.9×10^{-4} mol L^{-1} bar^{-1} and 3.4×10^{-2} mol L^{-1} bar^{-1} and for $\frac{-\Delta_{soln}H}{R}$ the values 500 K and 2400 K for H_2 and CO_2, respectively, were used. This results in a Henry constant at 65 °C of 6.481×10^{-4} mol L^{-1} bar^{-1} and 1.329×10^{-2} mol L^{-1} bar^{-1} for H_2 and CO_2, respectively.

Another potential liquid inhibitor detected in Enceladus' plume was hydrogen cyanide (HCN)[3,4]. However, calculations on HCN stability under the assumed conditions on Enceladus show that HCN would hydrolyse into formic acid and ammonia[42]. Further investigations on the stability of HCN at different pH values and temperatures yielded similar results[43,44]. It was therefore assumed that HCN might originate either from a very young pool, a recent aqueous melt, or from the icy matrix on Enceladus[4,42]. Due to this reasoning and the low probability of HCN presence in the subsurface ocean of Enceladus, HCN was neglected in all growth media used to perform the experiments.

High-pressure experiments. *M. okinawensis* initial high-pressure experiments were performed at its optimal growth temperature of 65 ± 1 °C using a chemically defined medium (250 mL, see Supplementary Table 10 for exact composition) and a fixed stirrer speed of 100 r.p.m. in a 0.7 L stirred stainless steel Büchi reactor. Before each of the experiments, the reactor was filled with medium and the entire setting was autoclaved under CO_2 atmosphere to assure sterile conditions. Thereafter, the inoculum (1 Vol.-%), the $NaHCO_3$, L-cysteine, $Na_2S{\cdot}9\ H_2O$ (0.5 M) and trace element solution were transferred via a previously autoclaved transfer vessel into the reactor. Then the reactor was set under pressure with the selected gas mixture (added ~5 bar in discrete steps every 10 min). The initial high-pressure experiments were performed using both an H_2/CO_2 (4:1) gas phase and an $H_2/CO_2/N_2$ (4:1:5) mixture. The reactor was equipped with an online pressure (ASIC Performer pressure sensor 0–400 bar, Parker Hannifin Corporation, USA) and temperature probe (thermo element PT100, −75 °C − 350 °C, TC Mess- und Regeltechnik GmbH, Mönchengladbach, Germany). The conversion was always above 88% except for the 90 bar experiment, wherein also N_2 fixation into biomass could be assumed. Interestingly, the time until start of the conversion decreases for the H_2/CO_2 experiments upon an increase of headspace pressure in the initial setup. This could be an indication for a barophilic nature of this organism, but also due to the experimental closed batch setup.

Increasing p_{CO2} and associated pH change was determined using a pH probe (see Supplementary Fig. 3). This analysis showed that even a rather small p_{CO2} (2 bar) already decreases the pH from nearly neutral to >5 due to the medium composition, which is due to application of a medium with low-buffering capacity, also possibly occurring in Enceladus' subsurface ocean. However, it remains an open question if the medium on Enceladus is buffered. This would lead to higher possible p_{CO2}[45] without having a drastic influence on the reported pH. Furthermore, we calculated if $NaHCO_3$ could be used as source of dissolved inorganic carbon and what would be the effect on the pH of the medium. Postberg et al. suggested a concentration of 0.02–0.1 mol kg^{-1} $NaCO_3$ and 0.05–0.2 mol kg^{-1} NaCl in the medium to reach a pH level between 8.5 and 9[46]. Calculations on the concentrations of dissolved CO_2 in the high-pressure experiments were performed by using the mole fraction of dissolved CO_2 in H_2O depending on p_{CO2}. The mole fractions for p_{CO2} of 0.7, 1.2, and 3.1 bar (as used in the experiments) at 65 °C were generated by extrapolation of given values in the region of p_{CO2} = 0–1 bar. H_2/CO_2 conversion and CH_4 production could still be measured at 10 bar, 20 bar and 50 (i.e., p_{CO2} = 10) bar with H_2/CO_2 (4:1) gas phase, but no decrease in pressure was observed at 90 bar with H_2/CO_2 (4:1) gas phase (i.e., p_{CO2} = 18 bar) after >110 h (data not shown). It is assumed that no growth occurs under these conditions due to the high p_{CO2} (18 bar) and the associated decrease to a pH of <3, which is beyond the reported pH tolerance of *M. okinawensis*[18].

The high-pressure experiments under Enceladus-like conditions were carried out in the presence of both gaseous and liquid inhibitors applying the optimal growth temperature of 65 ± 1 °C at individual pressures of 10, 25, and 50 bar in a stirred 2.0 L Büchi reactor at 250 r.p.m. The gas ratios of the final gas mixtures are reported in Table 4. The final liquid medium was the same as the one used in the final 2 bar experiments (incl. the liquid inhibitors, Supplementary Table 3). Due to the results from the pH experiments (Supplementary Fig. 3), the low p_{CO2} (~3 bar) was chosen to avoid a pH shift to more acidic values, which is not representative of Enceladus-like conditions. For final high-pressure experiments, the medium volume was set to 1.1 L and *M. okinawensis* H_2/CO_2 grown pre cultures of an OD = 34.4 and OD = 34.5 were used as inoculums (11 mL each). Preparation of the high OD *M. okinawensis* suspension was performed by collecting 1 L of serum bottle grown fresh culture (OD ~0.7), centrifuging the cells at 5346×*g* anaerobically for 20 min (Heraeus Multifuge 4KR Centrifuge, Thermo Fisher Scientific, Osterode, Germany), and re-suspending the cells in 20 mL of freshly reduced appropriate growth medium. The gases were added into the bioreactor headspace in the following order: CO, N_2, CO_2, H_2, and C_2H_4 (5 bar every 10 min). During all high-pressure experiments OD measurements were not conducted because upon reactor depressurisation cell envelopes of *M. okinawensis* were found to be disrupted. To determine the amount of produced CH_4 in the high-pressure experiments, gas samples were taken after reducing the pressure in the reactor down to 1.36 ± 0.25 bar. The sample was stored in 120 mL serum bottles and sealed with black septa (3.0 mm, Butyl/PTFE, La Pha Pack, Langerwehe, Germany). The volumetric concentrations of CH_4 was determined using a gas chromatograph (7890 A GC System, Agilent Technologies, Santa Clara, USA) equipped with a TCD detector and a 19808 ShinCarbon ST Micropacked Column (Restek GmbH, Bad Homburg, Germany)[22].

To determine the CH_4 production [Vol.-% h^{-1}] shown in Fig. 4, the value of CH_4 Vol.-% was divided by the time of biological CH_4 production in h. To exclude a potential lag phase, the starting point of biological CH_4 production was set to the point in time when the decrease in pressure exceeded the initial pressure by 5% for 10 bar experiments or by 1% during the other experiments.

Serpentinization simulations. The PHREEQC[27] code was used to simulate serpentinization reactions from 25 to 100 °C and from 25 to 50 bar in order to assess H_2 production on Enceladus. The Amm.dat and llnl.dat databases were used for all simulations, which account for temperature and pressure dependent equilibrium constants for dissolved species and solid phases up to 100 °C and 1000 bar. Solution composition was taken from the chemical composition of erupting plume of Enceladus[4], as the true chemistry of its subsurface sea is unknown. Dissolved concentrations of Ca^{2+}, Fe^{2+}, Mg^{2+}, and SiO_2 were assumed to be seawater-like and values from McCollom and Bach[47] were used. At the very low water-to-rock ratios of our model, the compositions of the interacting fluids will be entirely rock buffered, so that the model results are insensitive to the choice of the starting fluid composition. DIC concentration was set to 0.04 mol L^{-1} taken from Glein et al.[14], who estimated a possible range of 0.005–1.2 molal DIC in Enceladus' subsurface ocean. The solid phase assemblage was composed of varying amounts of olivine, enstatite and diopside, as well as varying olivine compositions. Most planetary bodies exhibit olivine solid solutions $(Mg, Fe)_2SiO_4$ that are dominated by forsterite (Mg_2SiO_4). This has been shown for micrometeorites found on Earth, lunar meteorites, comets, and asteroids[48–51]. Stony iron meteorites, such as pallasites contain forsteritic olivine with up to 20% Fe^{2+} content[52]. Olivines in chondrites show a more varied compositions ranging between 7 and 70% ferrous iron[53,54], to almost pure fayalite (Fe_2SiO_4)[55]. A realistic assumption is that olivines on Enceladus have a more forsteritic composition that resembles those of stony iron and lunar meteorites.

A composition of Fo_{90} was adopted for olivine. Calculations were limited to Fo_{90}, fayalite, enstatite, and diopside, as experimental data on their dissolution kinetics at high pH and low temperature are available. Kinetic rate laws were applied for forsteritic olivine, fayalite, enstatite, and diopside from Wogelius and Walther[56,57], Daval et al.[58], Oelkers and Schott[59], and Knauss et al.[60], respectively. Dissolution rate laws for Fo_{90} and fayalite at 100 °C were extrapolated from rate data in Wogelius and Walther[57] using the Arrhenius equation. Enstatite and diopside rate laws at 100 °C were power-law fitted from experimental data provided by Oelkers and Schott[59] and Knauss et al.[60], respectively. All rate laws are valid over a pH range from 2 to 12 at all temperatures. Kinetic rate laws were multiplied by the total surface area of each mineral present in solution in order to calculate moles of minerals dissolved per time. Surface areas of 590 cm^2 g^{-1} for Fo_{90} and fayalite[61], 800 cm^2 g^{-1} for enstatite[59], and 550 cm^2 g^{-1} for diopside[60] were used. These specific surface areas have been suggested to be typical for fine-grained terrestrial rocks. We adopted these numbers in our computations, as we have no constraints on what specific surface areas in Enceladus may be. If the core of Enceladus was similar to carbonaceous chondrite, then the average mineral grain size is smaller and hence the specific surface areas greater than we assumed[62]. We choose to use fairly small specific surface areas to provide conservative estimates for H_2 production rates. Model 1 uses Fo_{90}, enstatite and diopside in a ratio of 8:1:1, model 2 uses a pure Fo_{90} composition. The effect of ferrous iron content in olivine on H_2 production rates was tested in computations where Fo_{50} (Fo:Fa 1:1, model 3) and Fo_{20} (Fo:Fa 2:8, model 4) were dissolved as the sole mineral. Fo_{50} and Fo_{20} were dissolved according to dissolution rates of Wogelius and Walther (their equation (6))[57], and for temperatures beyond 25 °C dissolution rates for fayalite were extrapolated to 50 and 100 °C after Daval et al.[58]. Model 1 contained 40 mol of Fo_{90} and 5 mol of enstatite and diopside. For models 2–4, 55 mol of Fo_{90}, Fo_{50}, and Fo_{20} were used. Applying these amounts yield water-to-rock-ratios between 0.09 and 0.12 (Table 5).

The most likely environmental conditions present within Enceladus are temperatures between 25 and higher than 90 °C at 25–80 bar[8], and temperatures of 50 °C and pressures of 50 bar were chosen for the four different models. In a separate set of computations, temperatures were altered to 25 and 100 °C, and pressures were set at 25 and 100 bar. These results are shown in Supplementary

Table 4. As pressure has a negligible effect on H_2 production, only the variations in temperature change are shown.

Data availability. The data sets analysed during the current study are available in this article and its Supplementary Information file, or from the corresponding author on request.

Received: 2 August 2017 Accepted: 4 January 2018
Published online: 27 February 2018

References

1. Porco, C. C. et al. Cassini observes the active south pole of Enceladus. *Science* **311**, 1393–1401 (2006).
2. Waite, J. H. et al. Cassini finds molecular hydrogen in the Enceladus plume: evidence for hydrothermal processes. *Science* **356**, 155–159 (2017).
3. Waite, J. H. et al. Cassini ion and neutral mass spectrometer: Enceladus plume composition and structure. *Science* **311**, 1419–1422 (2006).
4. Waite, J. H. et al. Liquid water on Enceladus from observations of ammonia and 40Ar in the plume. *Nature* **460**, 487–490 (2009).
5. Bouquet, A., Mousis, O., Waite, J. H. & Picaud, S. Possible evidence for a methane source in Enceladus' ocean. *Geophys. Res. Lett.* **42**, 1334–1339 (2015).
6. Magee, B. A. & Waite Jr, J. H. Neutral gas composition of Enceladus' plume – model parameter insights from Cassini-INMS. In *48th Lunar and Planetary Science Conference*, abstr. 2974 (2017).
7. Sekine, Y. et al. High-temperature water-rock interactions and hydrothermal environments in the chondrite-like core of Enceladus. *Nat. Commun.* **6**, 8604 (2015).
8. Hsu, H.-W. et al. Ongoing hydrothermal activities within Enceladus. *Nature* **519**, 207–210 (2015).
9. Mayhew, L. E., Ellison, E. T., McCollom, T. M., Trainor, T. P. & Templeton, A. S. Hydrogen generation from low-temperature water-rock reactions. *Nat. Geosci.* **6**, 478–484 (2013).
10. Tian, H. et al. The terrestrial biosphere as a net source of greenhouse gases to the atmosphere. *Nature* **531**, 225–228 (2016).
11. McKay, C. P., Porco, C. C., Altheide, T., Davis, W. L. & Kral, T. A. The possible origin and persistence of life on Enceladus and detection of biomarkers in the plume. *Astrobiology* **8**, 909–919 (2008).
12. Liu, Y. & Whitman, W. B. Metabolic, phylogenetic, and ecological diversity of the methanogenic archaea. in. *Ann. N. Y. Acad. Sci.* **1125**, 171–189 (2008).
13. Taubner, R.-S., Schleper, C., Firneis, M. G. & Rittmann, S. K.-M. R. Assessing the ecophysiology of methanogens in the context of recent astrobiological and planetological studies. *Life* **5**, 1652–1686 (2015).
14. Glein, C. R., Baross, J. A. & Waite, J. H. The pH of Enceladus' ocean. *Geochim. Cosmochim. Acta* **162**, 202–219 (2015).
15. Schink, B. Inhibition of methanogenesis by ethylene and other unsaturated hydrocarbons. *FEMS Microbiol. Lett.* **31**, 63–68 (1985).
16. Kato, S., Sasaki, K., Watanabe, K., Yumoto, I. & Kamagata, Y. Physiological and transcriptomic analyses of the thermophilic, aceticlastic methanogen methanosaeta thermophila responding to ammonia stress. *Microbes Environ.* **29**, 162–167 (2014).
17. Daniels, L., Fuchs, G., Thauer, R. K. & Zeikus, J. G. Carbon monoxide oxidation by methanogenic bacteria. *J. Bacteriol.* **132**, 118–126 (1977).
18. Takai, K., Inoue, A. & Horikoshi, K. Methanothermococcus okinawensis sp. nov., a thermophilic, methane-producing archaeon isolated from a western Pacific deep-sea hydrothermal vent system. *Int. J. Syst. Evol. Microbiol.* **52**, 1089–1095 (2002).
19. Schönheit, P., Moll, J. & Thauer, R. K. Growth parameters (Ks, μmax, Ys) of Methanobacterium thermoautotrophicum. *Arch. Microbiol.* **127**, 59–65 (1980).
20. Bellack, A., Huber, H., Rachel, R., Wanner, G. & Wirth, R. Methanocaldococcus villosus sp. nov., a heavily flagellated archaeon that adheres to surfaces and forms cell–cell contacts. *Int. J. Syst. Evol. Microbiol.* **61**, 1239–1245 (2011).
21. Martin, W., Baross, J., Kelley, D. & Russell, M. J. Hydrothermal vents and the origin of life. *Nat. Rev. Microbiol.* **6**, 805–814 (2008).
22. Taubner, R.-S. & Rittmann, S. K.-M. R. Method for indirect quantification of CH_4 production via H_2O production using hydrogenotrophic methanogens. *Front. Microbiol.* **7**, 532 (2016).
23. Thauer, R. K., Kaster, A.-K., Seedorf, H., Buckel, W. & Hedderich, R. Methanogenic archaea: ecologically relevant differences in energy conservation. *Nat. Rev. Microbiol.* **6**, 579–591 (2008).
24. Rittmann, S. K.-M. R., Seifert, A. & Herwig, C. Essential prerequisites for successful bioprocess development of biological CH_4 production from CO_2 and H_2. *Crit. Rev. Biotechnol.* **35**, 141–151 (2015).
25. Waite, J. H. et al. Enceladus plume composition. In *EPSC-DPS Joint Meeting 2011* (2011).
26. Perry, M. E. et al. Inside Enceladus' plumes: the view from Cassini's mass spectrometer. In *American Astronomical Society, DPS Meeting 47*, abstr. 410.04 (2015).
27. Parkhurst, D. L. & Appelo, C. A. J. *User's Guide to PHREEQC (Version 2): A Computer Program for Speciation, Batch-Reaction, One-Dimensional Transport, and Inverse Geochemical Calculations*. Water-Resources Investigations Report 99–4259 (USGS, 1999).
28. Steel, E. L., Davila, A. & McKay, C. P. Abiotic and biotic formation of amino acids in the Enceladus ocean. *Astrobiology* **17**, 862–875 (2017).
29. Bach, W. Some compositional and kinetic controls on the bioenergetic landscapes in oceanic basement. *Front. Microbiol.* **7**, 107 (2016).
30. McCollom, T. M. Abiotic methane formation during experimental serpentinization of olivine. *Proc. Natl Acad. Sci. USA* **113**, 13965–13970 (2016).
31. Cavicchioli, R. Cold-adapted archaea. *Nat. Rev. Microbiol.* **4**, 331–343 (2006).
32. Duboc, P., Schill, N., Menoud, L., Van Gulik, W. & Von Stockar, U. Measurements of sulfur, phosphorus and other ions in microbial biomass: influence on correct determination of elemental composition and degree of reduction. *J. Biotechnol.* **43**, 145–158 (1995).
33. Cameron, V., Vance, D., Archer, C. & House, C. H. A biomarker based on the stable isotopes of nickel. *Proc. Natl Acad. Sci. USA* **106**, 10944–10948 (2009).
34. Porco, C. C., Dones, L. & Mitchell, C. Could it be snowing microbes on Enceladus? Assessing conditions in its plume and implications for future missions. *Astrobiology* **17**, 876–901 (2017).
35. Horita, J. & Berndt, M. E. Abiogenic methane formation and isotopic fractionation under hydrothermal conditions. *Science* **285**, 1055–1057 (1999).
36. Takai, K. et al. Cell proliferation at 122 C and isotopically heavy CH4 production by a hyperthermophilic methanogen under high-pressure cultivation. *Proc. Natl Acad. Sci. USA* **105**, 10949–10954 (2008).
37. Wang, D. T. et al. Nonequilibrium clumped isotope signals in microbial methane. *Science* **348**, 428 LP–428431 (2015).
38. Whiticar, M. J. Carbon and hydrogen isotope systematics of bacterial formation and oxidation of methane. *Chem. Geol.* **161**, 291–314 (1999).
39. Proskurowski, G. et al. Abiogenic hydrocarbon production at lost city hydrothermal field. *Science* **319**, 604–607 (2008).
40. Etiope, G. & Sherwood Lollar, B. Abiotic methane on earth. *Rev. Geophys.* **51**, 276–299 (2013).
41. NASA. Enceladus: by the Numbers. https://solarsystem.nasa.gov/planets/enceladus/facts (2017).
42. Glein, C. R., Zolotov, M. Y. & Shock, E. L. Liquid water vs. hydrogen cyanide on Enceladus. In *American Geophysical Union, Fall Meeting,* abstract #P23B-1365 (2008).
43. Sanchez, R. A., Ferbis, J. P. & Orgel, L. E. Studies in prebiodc synthesis: II. Synthesis of purine precursors and amino acids from aqueous hydrogen cyanide. *J. Mol. Biol.* **30**, 223–253 (1967).
44. Miyakawa, S., James Cleaves, H. & Miller, S. L. The cold origin of life: A. Implications based on the hydrolytic stabilities of hydrogen cyanide and formamide. *Orig. Life. Evol. Biosphys.* **32**, 195–208 (2002).
45. Roosen, C., Ansorge-Schumacher, M., Mang, T., Leitner, W. & Greiner, L. Gaining pH-control in water/carbon dioxide biphasic systems. *Green Chem.* **9**, 455 (2007).
46. Postberg, F. et al. Sodium salts in E-ring ice grains from an ocean below the surface of Enceladus. *Nature* **459**, 1–4 (2009).
47. McCollom, T. M. & Bach, W. Thermodynamic constraints on hydrogen generation during serpentinization of ultramafic rocks. *Geochim. Cosmochim. Acta* **73**, 856–875 (2009).
48. Demidova, S. I., Nazarov, M. A., Ntaflos, T. & Brandstätter, F. Possible serpentine relicts in lunar meteorites. *Petrology* **23**, 116–126 (2015).
49. Kurat, G., Koeberl, C., Presper, T., Brandstätter, F. & Maurette, M. Petrology and geochemistry of Antarctic micrometeorites. *Geochim. Cosmochim. Acta* **58**, 3879–3904 (1994).
50. Lisse, C. M. et al. Comparison of the composition of the tempel 1 ejecta to the dust in Comet C/Hale–Bopp 1995 and YSO HD 100546. *ICARUS* **187**, 69–86 (2007).
51. Cruikshank, D. P. & Hartmann, W. K. The meteorite-asteroid connection: two olivine-rich asteroids. *Science* **223**, 281–283 (1984).
52. Buseck, P. R. & Goldstein, J. I. Olivine compositions and cooling rates of pallasitic meteorites. *Bull. Geol. Soc. Am.* **80**, 2141–2158 (1969).
53. Chizmadia, L. J., Rubin, A. E. & Wasson, J. T. Mineralogy and petrology of amoeboid olivine inclusions in CO_3 chondrites: relationship to parent-body aqueous alteration. *Meteorit. Planet. Sci.* **37**, 1781–1796 (2002).
54. Dodd, R. T. The petrology of chondrules in the sharps meteorite. *Contrib. Mineral. Petrol.* **31**, 201–227 (1971).

55. Hua, X. & Buseck, P. R. Fayalite in the Kaba and Mokoia carbonaceous chondrites. *Geochim. Cosmochim. Acta* **59**, 563–578 (1995).
56. Wogelius, R. A. & Walther, J. V. Olivine dissolution at 25 °C: effects of pH, CO_2, and organic acids. *Geochim. Cosmochim. Acta* **55**, 943–954 (1991).
57. Wogelius, R. A. & Walther, J. V. Olivine dissolution kinetics at near-surface conditions. *Chem. Geol.* **97**, 101–112 (1992).
58. Daval, D. et al. The effect of silica coatings on the weathering rates of wollastonite ($CaSiO_3$) and forsterite (Mg_2SiO_4): an apparent paradox? In *Water Rock Interaction -WRI-13 Proc. 13th International Conference on Water Rock Interaction* (eds Birkle, P. & Torres-Alvarado, I. S.) 713–717 (Taylor & Francis, 2010).
59. Oelkers, E. H. & Schott, J. An experimental study of enstatite dissolution rates as a function of pH, temperature, and aqueous Mg and Si concentration, and the mechanism of pyroxene/pyroxenoid dissolution. *Geochim. Cosmochim. Acta* **65**, 1219–1231 (2001).
60. Knauss, K. G., Nguyen, S. N. & Weed, H. C. Diopside dissolution kinetics as a function of pH, CO_2, temperature, and time. *Geochim. Cosmochim. Acta* **57**, 285–294 (1993).
61. Golubev, S. V., Pokrovsky, O. S. & Schott, J. Experimental determination of the effect of dissolved CO_2 on the dissolution kinetics of Mg and Ca silicates at 25 °C. *Chem. Geol.* **217**, 227–238 (2005).
62. Bland, P. A. et al. Why aqueous alteration in asteroids was isochemical: high porosity ≠ high permeability. *Earth Planet. Sci. Lett.* **287**, 559–568 (2009).

Acknowledgements

Barbara Reischl, MSc and Annalisa Abdel Azim, MSc are gratefully acknowledged for expert technical assistance during the closed batch experiments. We thank Dr. Jessica Koslowski for proofreading and comments on the manuscript. R.-S.T. would like to thank Mark Perry and Britney Schmidt for discussions. We also thank David Parkhust for helping with the PHREEQC code and Silas Boye Nissen for his support in the initial attempts of the serpentinization modelling. Financial support was obtained from the Österreichische Forschungsförderungsgesellschaft (FFG) with the Klimafonds Energieforschungprogramm in the frame of the BioHyMe project (grant 853615). R.-S.T. was financed by the University of Vienna (FPF-234) and a fellowship of L'Oréal Österreich.

Author contributions

R.-S.T., P.P., C.Pr., P.K., and S.K.-M.R.R. performed the experiments. R.-S.T., P.P., S.B., A.H.S., C.Pa., and S.K.-M.R.R. designed the experiments. D.S. and J.Z. designed and performed PHREEQC modelling. W.B. supervised the PHREEQC modelling. R.-S.T., P.P., J.Z., D.S., S.B., A.H.S., A.K., W.B., J.P., C.Pa, M.G.F., C.S., and S.K.-M.R.R. discussed the data. R.-S.T., J.Z., D.S., W.B., J.P., C.S., and S.K.-M.R.R. wrote the manuscript.

Additional information

Supplementary Information accompanies this paper at https://doi.org/10.1038/s41467-018-02876-y.

Competing interests: R.-S.T., P.P., D.S., J.Z., C.Pr., P.K., W.B., J.P., C.Pa., M.F., C.S., and S.K.-M.R.R. declare no competing financial interests. Due to an engagement in the Krajete GmbH, A.H.S., S.B., and A.K. declare competing financial interests.

Reprints and permission information is available online at http://npg.nature.com/reprintsandpermissions/

Publisher's note: Springer Nature remains neutral with regard to jurisdictional claims in published maps and institutional affiliations.

6 Conclusion

6.1 Summary of Results

The main topics of this thesis are the theoretical analysis of Enceladus' potential subsurface water reservoir and the evaluation of its habitability for terrestrial life under laboratory conditions. Methanogens were chosen as ideal test objects for cultivation experiments under Enceladus-like conditions. Methanogens are known for their ability to thrive under extreme conditions without having the need of complex or diverse substrates. In the extensive review presented in chapter 3, the diversity of this kind of microorganisms and their applications in astrobiological studies so far were shown. A screening of methanogens, regarding a high growth rate in closed batch fermentation, went hand in hand with literature research for this review. For the screening process, a new method was developed which is presented in chapter 4. This method enabled a faster, cheaper, and very effective way to screen the cultures regarding their growth rate, methane and water producing rate, H- and C-balances, and their degree of reduction (DoR). In the end, three hydrogenotrophic methanogens were prioritized for further experiments, namely *Methanothermococcus okinawensis*, *Methanothermobacter marburgensis*, and *Methanococcus villosus*. In various preliminary experiments regarding the tolerance of these strains towards various inhibitors detected in the Enceladian plume including settings based on multivariate statistics, *M. okinawensis* showed the highest and most stable growth rate. Therefore, this strain was chosen for the final experiments performed in a high pressure reactor at the JKU Linz. Here, *M. okinawensis* was exposed to high pressure of up to 90 bar and a combination of potential gaseous and liquid inhibitors in accordance to the components and their volume mixing ratio detected in the plume. *M. okinawensis* reached a CO_2 to CH_4 conversion rate of up to 72% at a pressure of 50 bar. This pressure value is in good agreement with the values estimated and presented in chapter 2 and in the methods part of the paper presented in chapter 5. Besides these planetological and microbiological analyses, this thesis also includes geochemical studies presented in chapter 5. In an international collaboration, the potential H_2 production rate of putative serpentinization processes on the seafloor of Enceladus' subsurface ocean was estimated to be between approximately 5 and 50 $\mathrm{nmol\,g^{-1}\,L^{-1}\,d^{-1}}$ (see Table 5.5). This concentration might be sufficient to power autotrophic, hydrogenotrophic methanogenic life on Enceladus over a longer time period.

To sum up, this study showed that the conditions on icy moons like Enceladus could be suitable for hydrogenotrophic methanogenic life and that, in principle, some of the CH_4 detected in Enceladus' plume could be produced by these extraordinary microorganisms.

6.2 The origin of life on Enceladus?

The indirect detection of hydrothermal vents on the seafloor of Enceladus raised the question if life could have had the chance to emerge and evolve on this icy moon. To examine this theory, one has to start with looking at Enceladus age and the age of the subsurface ocean. There are various studies about the age and origin of Enceladus, spanning from just 100 Myr or even younger [Ćuk et al., 2016] based on dynamical simulations, to approximately 4.5 Gyr [Castillo et al., 2005, Sekine et al., 2015] based on Iapetus' spin rate evolution. If the latter is true and Enceladus was formed from icy planetesimals embedded in the Saturnian subnebula initially produced in the solar nebula [McKinnon et al., 2016], the endogenic activity responsible for the hydrothermal activity generated by tidal friction inside the unconsolidated rocky core could have been sustained for the entire lifetime of Enceladus [Choblet et al., 2017]. However, if Enceladus was formed just less than 100 Myr ago, life may not have had enough time to emerge yet.

6.3 Impact of this study to future space missions

This study showed that life as we know it could, in principle, be able to thrive on icy moons like Enceladus. The next step would therefore be to send a mission back to Saturn to continue Cassini's work. The findings of this thesis can be used to select and calibrate instruments for future missions. Christopher Glein, a geochemist and planetary scientist at the Southwest Research Institute, Texas (USA), summarized it the following way when asked about the impact of the paper presented on chapter 5 to future space missions: "The next step is doing this hard work in the lab to figure out what life might look like from a spacecraft instrument's point of view. [...] It would be really useful in defining some future mission requirements for us." [Condé Nast, 2018].

As stated in chapter 5, methanogens produce specific lipids that could serve as distinct and lasting biosignatures. For detecting lipids in the Enceladian plume, the probe would have to take samples of the water-ice droplets and do on-board-analysis. Georgiou and Deamer [2014] are proposing to use a NCAR-CVI (National Center for Atmospheric Research counterflow virtual impactor). This instrument is normally used for studies of aerosol-cloud interactions and cloud physics. It

separates ice crystals or cloud droplets from the interstitial aerosol and water vapour by using a counterflow stream of gas [Twohy et al., 2003]. A hygrometer can be used as water sensor and a condensation nucleus counter to determine the particle number concentration. Further, a super-critical fluid system for lipid extraction in combination with a GC-MS lipid analysis instrument can be installed downstream of the CVI inlet tip [Georgiou and Deamer, 2014].

In addition to the studies presented in this thesis, we have started to analyse the lipid composition of *M. okinawensis* from the (pre-)experiments shown in the publications presented in the chapters 4 and 5. The preliminary data indicate that the lipid pattern strongly depends on the environmental conditions[1]. Therefore, if future space missions are able to detect lipids in the Enceladian plume, it will not "only" be an indirect sign for life on Enceladus, but the lipid pattern may also offer information about the type of organisms and the environmental conditions in the subsurface ocean. To draw the right conclusions from future data, further and maybe even more sophisticated experiments under Enceladus-like conditions have to be performed. However, this thesis can be seen as a starting point for applied simulations of the subsurface ocean's of icy moons.

Another possibility to determine, to some extent, if CH_4 is of biogenic or abiogenic origin is shown in several studies [Lollar et al., 2006, McKay et al., 2008] by analysing the carbon isotope ratio between CH_4, CO_2, and another low-molecular weight hydrocarbon like ethene (C_2H_4) or ethane (C_2H_6). There are two stable isotopes of carbon in nature, namely ^{12}C and ^{13}C, whereas ^{12}C is by far more common (ratio 99:1). In geochemistry, the difference in isotope content relative to a standard (*e.g.* Vienna Pee Dee Belemnite (VPDB) standard) is indicated as δ^{13}. While geophysical and chemical processes do not prefer any type, life tend to favour ^{12}C over ^{13}C which leads to a negative δ^{13} value. However, under high-pressure conditions in a deep-sea hydrothermal vent environment methanogens may produce CH_4 with a relatively high $\delta^{13}C$, which can lead to misinterpretations of the received data.

6.3.1 Planned Missions

Three potential lower-cost missions were proposed in 2015 for NASA's Discovery Mission 13 funding. The *Enceladus Life Finder* (ELF) was thought to search for biosignatures and biomolecules like amino acids and fatty acids. The mission *Journey to Enceladus and Titan* (JET) would have performed 16 flybys around Titan and Enceladus sampling Enceladus' plume. The main task of the third mission, *Life Investigation For Enceladus* (LIFE), was to capture icy particles from Enceladus and

[1]The final results of these analyses will most likely be published within the next months [Baumann et al., in prep., Taubner et al., in prep.].

return them to Earth. However, none of these missions was selected for Phase-A design study [Northon, 2015]. The reason for not selecting one of these missions was the too-high cost risk [Sherwood et al., 2017].

In the course of NASA's *New Frontiers program* competition for the fourth mission, two intermediate cost mission concepts dealing with a journey to Enceladus where submitted, but neither was selected: the *Enceladus Life Finder* (ELF) and *Enceladus Life Signatures and Habitability* (ELSAH). The later at least was chosen to receive funding for further development of cost-effective techniques which should help to limit spacecraft contamination [Northon, 2017].

In NASA's *Large Strategic Science Missions* program ("flagship missions"), which Cassini was part of, no mission to Enceladus is planned for the next years. One of the two finalists of this competition is the project *Dragonfly*, which includes a mobile robotic rotorcraft-lander to explore Titan's surface material [Lorenz et al., 2017].

In 2016, Brent Sherwood presented a strategy map for exploring the ocean-world of Enceladus [Sherwood, 2016]. Here, he pointed out the importance of a roadmap to systematically work on future missions to Enceladus. In 2015, the American politician John Abney Culberson presented a budget request to the US congress to create a (virtual) *Ocean Worlds Exploration Program* [Anderson, 2015]. This program would use a mix of flagship, New Frontiers, and Discovery class missions. As part of this program NASA is planning a flagship mission called *Europa Clipper* to Jupiter's Europa, the most promising icy moon in regard to the search for life besides Enceladus. For this mission, an orbiter was planed at the beginning but the US congress directed NASA to draft a lander in addition [Lunine, 2017]. However, this mission concept is heavily dependent on the yearly budget plan of the US government. Therefore, any predictions about the completion or launch of this mission are not possible at the moment.

The European Space Agency (ESA) is planning a Large-class mission (L-class) called *JUpiter ICy moons Explorer* (JUICE) to Jupiter's icy moons within the *Cosmic Vision Program 2015-2025*. The mission launch is scheduled for 2022 with a travel time to Jupiter of about 8 years. After arrival at the Jupiter system, JUICE will perform several flybys passing Callisto, Europa and Ganymede for a period of two years. After that, the probe will be put into an orbit around Ganymede being the first mission orbiting a moon other than the Earth's Moon. The primary mission is planned for a period of 3.5 years [Grasset et al., 2013, ESA, 2013].

In April 2016, ESA announced the fifth call for Medium-class (M-class) mission proposals within the Cosmic Vision Program and the outcome of the selection process should be announced soon [ESA, 2016]. One of the submitted space mission

concepts was the *Explorer of Enceladus and Titan* (E^2T), which is lead by Giuseppe Mitri from the Laboratoire de Planétologie et de Géodynamique of the University of Nantes (France) [Mitri et al., 2016, ESA, 2017]. The main goals of this mission regarding Enceladus would be to sample the plume, to determine the ice shell structure, and to map the thermal emission from the tiger stripes at meter scales. It's payload will consist among others of an improved versions of Cassini's INMS, the *Enceladus Icy Jet Analyzer* (ENIJA) time-of-flight mass spectrometers, and the *Radio Science Experiment* (RSE).

To have a direct proof for extraterrestrial lifeforms on icy moons seems not to be possible within the next few decades. For that, a probe would have to take samples directly from the subsurface oceans. To get access to the subsurface aquifer, the probe would have to drill through Enceladus' icy shell to reach regions where liquid water is already present. An interesting mission concept dealing with that issue is the Enceladus Explorer Initiative (EnEx), which is funded and directed by the German Aerospace Center (Deutsches Zentrum für Luft- und Raumfahrt; DLR) Space Administration [Konstantinidis et al., 2015]. Here, the idea is to have an orbiter and a lander. The latter would be equipped with a minimally invasive and manoeuvrable ice melting probe (EnEx-IceMole). The first IceMole was already tested in November 2014 at the Blood Falls, Taylor Glacier, Antarctica [DLR, 2015]. However, this project is just a testing concept without any immediate mission plan.

6.3.2 Planetary Protection

The main goal of planetary protection is to guide organisations that build probes going into space on how to prevent these probes from causing interplanetary biological and/or organic contamination. This applies both for not introducing terrestrial microbes on other celestial bodies (*forward contamination*) and for not contaminating Earth in case of sample-return missions (*back contamination*).

In 1958, the year after the first artificial Earth satellite named *Sputnik 1* successfully orbited our planet for several weeks, the UN General Assembly established the *Ad Hoc Committee on the Peaceful Uses of Outer Space* (COPUOS) [Perek, 2004, Tennen, 2004]. In the following years, many other international organisations or sub-groups of existing ones were established to deal with space politics including planetary protection. One of these organisations was the *Committee on Space Research* (COSPAR), to which the UN mandate was transferred to in the following year. In January 1967, the UN together with COSPAR formulated the *United Nations Outer Space Treaty* (Treaty on Principles Governing the Activities of States in the Exploration and Use of Outer Space, Including the Moon and Other Celestial Bodies; U.N. document 6347), in which Article IX is devoted to planetary protection [Raulin et al., 2010, Kminek et al., 2017]. More than 100 nations have signed but only 89

ratified this treaty since then [UNODA, 1967]. In parallel, the *International Council of Scientific Unions* (ICSU) established the *Ad Hoc Committee on Contamination by Extraterrestrial Exploration* (CETEX), which considered celestial bodies to be scientific preserves [Tennen, 2004].

The COSPAR has formulated a *Planetary Protection Policy* which has been updated regularly. Within this policy five categories for missions to celestial bodies are presented [Kminek et al., 2017]:

- *Category I*: missions to targets, that are not directly interesting for astrobiological observations (like the Sun or Io). For these targets, planetary protection is not required.

- *Category II*: mission to targets, that could be of interest regarding chemical evolution or the origin of life, but where the chance of contamination is negligible (like Moon, Venus, gas giants, comets).

- *Category III*: mostly flyby or orbiter missions to targets, that are of interest regarding chemical evolution or the origin of life and where contamination could have an effect on future investigations (like Mars, Europa, Enceladus).

- *Category IV*: mostly probe or lander missions to targets, that are of interest regarding chemical evolution or the origin of life and where contamination could have an effect on future investigations (like Mars, Europa, Enceladus).

- *Category V*: Earth-return missions, where the major concern is to protect the terrestrial system, including Earth and the Moon. Here, it is distinguished between *restricted Earth return* (for missions to *e.g.* Mars, Europa, Enceladus) and *unrestricted Earth return* (for missions to *e.g.* Venus or the Moon).

During the last few years, the categorization of icy moons has changed. Even in 2002, icy moons were not mentioned at all in the Planetary Protection Policy [Rummel et al., 2002]. That changed when the first indirect signs for subsurface water reservoirs on Europa, Ganymede, Callisto and later some Saturnian moons like Enceladus and Titan were found. Since then, neither the presence of indigenous life forms in the subsurface oceans of these moons nor the potential to contaminate these worlds can be ruled out. Both, NASA's *Galileo* and the Cassini-Huygens mission were classified as a Category II mission when launched in 1989 and 1997, respectively. This means, even if forward contamination is still unlikely, Cassini's companion, the probe *Huygens*, landed on Titan without being sterilized before sending it to the Saturnian system. At the end of the Galileo and Cassini missions, it was decided to crash Galileo into Jupiter and Cassini into Saturn to not accidentally contaminate the Galilean satellites or Titan and Enceladus, respectively.

Future missions to icy moons like Enceladus will be classified as Category III to V, depending on their mission strategy. The drafts of missions to Enceladus mentioned above include operations like *in situ* life detection, landers including an ice melting probe, and even sample return missions. These probes have to be as clean or even cleaner than the missions send to Mars. To compare, for Mars, there is an upper limit for the surface bioburden level of 30 spores for the entire lander systems either investigating extant Martian life or operating on a special Martian region like gullies or subsurface cavities [Kminek et al., 2017].

In the course of the *European Comission's Horizon 2020 Programme*, the *Planetary Protection of Outer Solar System* (PPOSS) project has received funding for the period from 2016 to 2018 [PPOSS, 2016]. This project provides an international platform for science, industry, and policy to find a common path through this important topic of global relevance. PPOSS will publish a handbook which should summarize the outcomes of the meetings and discussions. It will be targeted to the organizations and agencies that are involved in building the future space missions.

6.4 Concluding statement and Outlook

This thesis does not prove neither that there is life nor that there is an origin of life on Enceladus. There is still a huge debate on the origin of life on Earth (see section 1.1.6), and we are even further away of finding an answer to how an origin of life of potential Enceladian organisms might have looked like. If there is life on Enceladus (or somewhere else in the Solar System or beyond), it might be closely related to terrestrial life but could also be totally different. We will, most likely, not be able to give a proper statement on that issue before detecting extraterrestrial life at all- if we are able to detect it. Extraterrestrial life could metabolize and/or produce totally different biological material, which we might not be able to detect even with future space missions or which we might not interpret as such, respectively.

This thesis deals with the idea that the current environment in the Enceladian subsurface ocean could in principle be suitable for terrestrial methanogenic life. The simulations done for this study represent a first systematic study on methanogenic physiology under high pressure at putative Enceladus-like conditions. However, there are still many ways to improve the experimental setting. The first problem to deal with in future experiments will be the pH. Using computational geochemical models, the Enceladian ocean was predicted to be highly alkaline, which does not apply for the high pressure experiments performed in the present studies. So the first step would be to create a buffered medium (to keep the pH alkaline even at high partial pressure of CO_2) that contains all the (complex) organic compounds, salts, and siliceous materials found in the plume. Further, in future studies microbial

growth should be measured under different physical conditions, *e.g.* by varying the temperature and the pressure, to learn which regions of the subsurface oceans could, in principle, be inhabited. The temperatures might be really high next to the hydrothermal vents, but the average temperature of the Enceladian ocean is assumed to be around 0°C. If there is life on Enceladus that has similarities to methanogens, future space missions might be able to detect signs of this life from lipids or specific isotopic ratios. Therefore, another very interesting approach would be to test how the products of microbes (*e.g.* lipids) or even the organisms themselves change when being sampled at the same speed as they would be sampled by a probe performing a fly-by manoeuvre. Due to the high impact speed, changes in the structure of complex biogenic material will be hard to avoid. This implies that future missions to Enceladus have to be planned carefully and that they have to go hand in hand with studies like the ones presented in this thesis. Further, this thesis shows that future missions have to fulfil all requirements regarding planetary protection. Because, even if there is no life in Enceladus right now, the chance to contaminate this alien environment with terrestrial microbes is no longer negligible.

References

O. Čadek, G. Tobie, T. Van Hoolst, M. Massé, G. Choblet, A. Lefèvre, G. Mitri, R.-M. Baland, M. Běhounková, O. Bourgeois, and A. Trinh. Enceladus's internal ocean and ice shell constrained from Cassini gravity, shape, and libration data. *Geophysical Research Letters*, 43(11):5653–5660, 2016. doi:10.1002/2016GL068634.

P. S. Anderson. "Ocean Worlds Exploration Program": New Budget Proposal Calls for Missions to Europa, Enceladus, and Titan, 2015. URL `http://www.americaspace.com/2015/05/20/ocean-worlds-exploration-progra%m-new-budget-proposal-calls-for-missions-to-europa-enceladus-and-titan/`. Last access: 03.04.2018.

J. C. Angle, T. H. Morin, L. M. Solden, A. B. Narrowe, G. J. Smith, M. A. Borton, C. Rey-Sanchez, R. A. Daly, G. Mirfenderesgi, D. W. Hoyt, W. J. Riley, C. S. Miller, G. Bohrer, and K. C. Wrighton. Methanogenesis in oxygenated soils is a substantial fraction of wetland methane emissions. *Nature Communications*, 8:1567, 2017. doi:10.1038/s41467-017-01753-4.

A. C. Barr and W. B. McKinnon. Convection in Enceladus' ice shell: Conditions for initiation. *Geophysical Research Letters*, 34(9):L09202, 2007. doi:10.1029/2006GL028799.

L. Baumann, R. Taubner, T. Bauersachs, M. Steiner, C. Schleper, J. Peckmann, S. Rittmann, and D. Birgel. Intact polar lipid and core lipid inventory of the hydrothermal vent methanogens *Methanocaldococcus villosus* and *Methanothermobacter okinawensis (working title)*. in prep.

A. Caforio and A. J. Driessen. Archaeal phospholipids: Structural properties and biosynthesis. *Biochimica et Biophysica Acta*, 1862(11):1325 – 1339, 2017. doi:10.1016/j.bbalip.2016.12.006.

J. K. Campbell and J. D. Anderson. Gravity field of the Saturnian system from Pioneer and Voyager tracking data. *The Astronomical Journal*, 97:1485–1495,

1989. doi:10.1086/115088.

J. C. Castillo, D. L. Matson, T. V. Johnson, J. I. Lunine, T. B. McCord, C. Sotin, P. C. Thomas, and E. B. Turtle. ^{26}Al in the Saturnian System - New Interior Models for the Saturnian satellites. *AGU Fall Meeting Abstracts*, page A1, 2005.

G. Choblet, G. Tobie, C. Sotin, M. Běhounková, O. Čadek, F. Postberg, and O. Souček. Powering prolonged hydrothermal activity inside Enceladus. *Nature Astronomy*, 1: 841–847, 2017. doi:10.1038/s41550-017-0289-8.

S. C. Chong, Y. Liu, M. Cummins, D. L. Valentine, and D. R. Boone. *Methanogenium marinum* sp. nov., a H_2-using methanogen from Skan Bay, Alaska, and kinetics of H_2 utilization. *Antonie Van Leeuwenhoek*, 81(1-4):263–270, 2002.

G. C. Collins and J. C. Goodman. Enceladus' south polar sea. *Icarus*, 189:72–82, 2007. doi:10.1016/j.icarus.2007.01.010.

Condé Nast. If There's Life on Saturn's Moon Enceladus, It Might Look Like This. Christopher Glein interviewed by Emma Grey Ellis, published on URL: `https://www.wired.com/story/if-theres-life-on-saturns-moon-enceladus-it-might-look-like-this/`, 2018. Last access: 07.04.2018.

G. B. Dalrymple. The age of the Earth in the twentieth century: a problem (mostly) solved. *Geological Society of London Special Publications*, 190:205–221, 2001. doi:10.1144/GSL.SP.2001.190.01.14.

DLR. Blood Falls – EnEx probe collects first 'clean' water samples, 2015. URL `http://www.dlr.de/dlr/en/desktopdefault.aspx/tabid-10212/332_read-127%33/#/gallery/18546`. Last access: 03.04.2018.

M. S. Dodd, D. Papineau, T. Grenne, J. F. Slack, M. Rittner, F. Pirajno, and J. O'Neil. Evidence for early life in Earth's oldest hydrothermal vent precipitates. *Nature*, 543:60–64, 2017. doi:10.1038/nature21377.

S. Dole. *Habitable planets for man*. Blaisdell book in the pure and applied sciences. Blaisdell Pub. Co., 1964. ISBN 0833042270.

M. K. Dougherty, K. K. Khurana, F. M. Neubauer, C. T. Russell, J. Saur, J. S. Leisner, and M. E. Burton. Identification of a Dynamic Atmosphere at Enceladus with the Cassini Magnetometer. *Science*, 311(5766):1406–1409, 2006. doi:10.1126/science.1120985.

ESA. Juice, 2013. URL `http://sci.esa.int/juice/`. Last access: 07.04.2018.

ESA. Call for a Medium-size mission opportunity in ESA's Science Programme (M5), 2016. URL https://www.cosmos.esa.int/web/call-for-m5-missions. Last access: 07.04.2018.

ESA. E2T - Explorer of Enceladus and Titan: Investigating the habitability and evolution of ocean worlds in the Saturn system, 2017. URL https://e2tmission.wordpress.com/. Last access: 07.04.2018.

P. N. Evans, D. H. Parks, G. L. Chadwick, S. J. Robbins, V. J. Orphan, S. D. Golding, and G. W. Tyson. Methane metabolism in the archaeal phylum bathyarchaeota revealed by genome-centric metagenomics. *Science*, 350(6259):434–438, 2015. doi:10.1126/science.aac7745.

P. Forterre and S. Gribaldo. The origin of modern terrestrial life. *HFSP Journal*, 1 (3):156–168, 2007. doi:10.2976/1.2759103.

C. D. Georgiou and D. W. Deamer. Lipids as Universal Biomarkers of Extraterrestrial Life. *Astrobiology*, 14(6):541–549, 2014. doi:10.1089/ast.2013.1134.

J. D. Goguen, B. J. Buratti, R. H. Brown, R. N. Clark, P. D. Nicholson, M. M. Hedman, R. R. Howell, C. Sotin, D. P. Cruikshank, K. H. Baines, K. J. Lawrence, J. R. Spencer, and D. G. Blackburn. The temperature and width of an active fissure on Enceladus measured with Cassini VIMS during the 14 April 2012 South Pole flyover. *Icarus*, 226:1128–1137, Sept. 2013. doi:10.1016/j.icarus.2013.07.012.

O. Grasset, M. K. Dougherty, A. Coustenis, E. J. Bunce, C. Erd, D. Titov, M. Blanc, A. Coates, P. Drossart, L. N. Fletcher, H. Hussmann, R. Jaumann, N. Krupp, J.-P. Lebreton, O. Prieto-Ballesteros, P. Tortora, F. Tosi, and T. Van Hoolst. JUpiter ICy moons Explorer (JUICE): An ESA mission to orbit Ganymede and to characterise the Jupiter system. *Planetary and Space Science*, 78:1–21, 2013. doi:10.1016/j.pss.2012.12.002.

C. J. Hansen, D. E. Shemansky, L. W. Esposito, A. I. F. Stewart, B. R. Lewis, J. E. Colwell, A. R. Hendrix, R. A. West, J. H. Waite, Jr., B. Teolis, and B. A. Magee. The composition and structure of the Enceladus plume. *Geophysical Research Letters*, 38:L11202, 2011. doi:10.1029/2011GL047415.

M. M. Hedman, C. M. Gosmeyer, P. D. Nicholson, C. Sotin, R. H. Brown, R. N. Clark, K. H. Baines, B. J. Buratti, and M. R. Showalter. An observed correlation between plume activity and tidal stresses on Enceladus. *Nature*, 500:182–184, 2013. doi:10.1038/nature12371.

A. R. Hendrix, C. J. Hansen, and G. M. Holsclaw. The ultraviolet reflectance of Enceladus: Implications for surface composition. *Icarus*, 206(2):608 – 617, 2010. doi:10.1016/j.icarus.2009.11.007.

W. Herschel. I. Account of the discovery of a sixth and seventh satellite of the planet Saturn; with remarks on the construction of its ring, its atmosphere, its rotation on an axis, and its spheroidical figure. *Philosophical Transactions of the Royal Society of London*, 80:1–20, 1790. doi:10.1098/rstl.1790.0001.

N. G. Holm, C. Oze, O. Mousis, J. H. Waite, and A. Guilbert-Lepoutre. Serpentinization and the Formation of H_2 and CH_4 on Celestial Bodies (Planets, Moons, Comets). *Astrobiology*, 15(7):587–600, 2015. doi:10.1089/ast.2014.1188.

C. J. A. Howett, J. R. Spencer, J. Pearl, and M. Segura. High heat flow from Enceladus' south polar region measured using 10-600 cm^{-1} Cassini/CIRS data. *Journal of Geophysical Research: Planets*, 116(E3):E03003, 2011. doi:10.1029/2010JE003718.

H.-W. Hsu, F. Postberg, Y. Sekine, T. Shibuya, S. Kempf, M. Horányi, A. Juhász, N. Altobelli, K. Suzuki, Y. Masaki, T. Kuwatani, S. Tachibana, S.-I. Sirono, G. Moragas-Klostermeyer, and R. Srama. Ongoing hydrothermal activities within Enceladus. *Nature*, 519:207–210, 2015. doi:10.1038/nature14262.

S.-S. Huang. The Problem of Life in the Universe and the Mode of Star Formation. *Publications of the Astronomical Society of the Pacific*, 71(422):421, 1959. doi:10.1086/127417.

L. Iess, N. J. Rappaport, R. A. Jacobson, P. Racioppa, D. J. Stevenson, P. Tortora, J. W. Armstrong, and S. W. Asmar. Gravity Field, Shape, and Moment of Inertia of Titan. *Science*, 327(5971):1367–1369, 2010. doi:10.1126/science.1182583.

L. Iess, D. J. Stevenson, M. Parisi, D. Hemingway, R. A. Jacobson, J. I. Lunine, F. Nimmo, J. W. Armstrong, S. W. Asmar, M. Ducci, and P. Tortora. The Gravity Field and Interior Structure of Enceladus. *Science*, 344:78–80, 2014. doi:10.1126/science.1250551.

A. P. Ingersoll and S. P. Ewald. Total particulate mass in Enceladus plumes and mass of Saturn's E ring inferred from Cassini ISS images. *Icarus*, 216:492–506, 2011. doi:10.1016/j.icarus.2011.09.018.

S. Jain, A. Caforio, and A. J. M. Driessen. Biosynthesis of archaeal membrane ether lipids. *Frontiers in Microbiology*, 5:641, 2014. doi:10.3389/fmicb.2014.00641.

X. Jia, M. G. Kivelson, K. K. Khurana, and W. S. Kurth. Evidence of a plume on Europa from Galileo magnetic and plasma wave signatures. *Nature Astronomy*, 2: 459–464, June 2018. doi:10.1038/s41550-018-0450-z.

G. Joyce. Foreward. In D. W. Deamer and G. R. Fleischaker, editors, *Origins of Life: The Central Concepts*, pages xi–xii. Jones & Barlett, Boston, 1994. ISBN 9780867201819.

J. F. Kasting, D. P. Whitmire, and R. T. Reynolds. Habitable Zones around Main Sequence Stars. *Icarus*, 101:108–128, 1993. doi:10.1006/icar.1993.1010.

S. Kempf, R. Srama, G. Moragas-Klostermeyer, F. Postberg, M. Horányi, J. Schmidt, and F. Spahn. The Structure of Saturn's E ring as seen by Cassini CDA. In *EPSC-DPS Joint Meeting 2011*, page 1643, Oct. 2011.

S. W. Kieffer, X. Lu, C. M. Bethke, J. R. Spencer, S. Marshak, and A. Navrotsky. A Clathrate Reservoir Hypothesis for Enceladus' South Polar Plume. *Science*, 314: 1764, 2006. doi:10.1126/science.1133519.

G. Kminek, C. Conley, V. Hipkin, and H. Yano. COSPAR's Planetary Protection Policy. *Space Research Today*, 200:12 – 25, 2017. doi:10.1016/j.srt.2017.11.010.

K. Konstantinidis, C. L. F. Martinez, B. Dachwald, A. Ohndorf, P. Dykta, P. Bowitz, M. Rudolph, I. Digel, J. Kowalski, K. Voigt, and R. Förstner. A lander mission to probe subglacial water on Saturn's moon Enceladus for life. *Acta Astronautica*, 106:63 – 89, 2015. doi:10.1016/j.actaastro.2014.09.012.

T. A. Kral, K. M. Brink, S. L. Miller, and C. P. McKay. Hydrogen Consumption by Methanogens on the Early Earth. *Origins of life and evolution of the biosphere*, 28 (3):311–319, 1998. doi:10.1023/A:1006552412928.

A. Le Gall, C. Leyrat, M. A. Janssen, G. Choblet, G. Tobie, O. Bourgeois, A. Lucas, C. Sotin, C. Howett, R. Kirk, R. D. Lorenz, R. D. West, A. Stolzenbach, M. Massé, A. H. Hayes, L. Bonnefoy, G. Veyssière, and F. Paganelli. Thermally anomalous features in the subsurface of Enceladus's south polar terrain. *Nature Astronomy*, 1: 0063, 2017. doi:10.1038/s41550-017-0063.

J. Leitner. *Exotic Life and the Life Supporting Zone as a Basis for the Search for Extraterrestrial Life*. PhD thesis, University of Vienna, 2014.

J. J. Lissauer. Habitable Zone. Encyclopaedia Britannica, 2018. URL `https://www.britannica.com/science/habitable-zone`. Last access: 26.03.2018.

Y. Liu and W. B. Whitman. Metabolic, Phylogenetic, and Ecological Diversity of the Methanogenic Archaea. *Annals of the New York Academy of Sciences*, 1125(1): 171–189, 2008. doi:10.1196/annals.1419.019.

B. S. Lollar, G. Lacrampe-Couloume, G. Slater, J. Ward, D. Moser, T. Gihring, L.-H. Lin, and T. Onstott. Unravelling abiogenic and biogenic sources of methane in the earth's deep subsurface. *Chemical Geology*, 226(3):328 – 339, 2006. doi:10.1016/j.chemgeo.2005.09.027. Special Issue in Honour of R.K. O'Nions.

R. D. Lorenz, E. P. Turtle, J. W. Barnes, M. G. Trainer, D. S. Adams, K. E. Hibbard, C. Z. Sheldon, K. Zacny, P. N. Peplowski, D. J. Lawrence, M. A. Ravine, T. G. McGee, K. S. Sotzen, S. M. MacKenzie, J. W. Langelaan, S. Schmitz, L. S. Wolfarth, , and P. D. Bedini. Dragonfly: A Rotorcraft Lander Concept for Scientific Exploration at Titan. *Johns Hopkins APL Technical Digest*, 2017. (pre-publication draft).

J. I. Lunine. Ocean worlds exploration. *Acta Astronautica*, 131:123 – 130, 2017. doi:10.1016/j.actaastro.2016.11.017.

A. Maczulak. *Allies and Enemies: How the World Depends on Bacteria*. FT Press Science. Pearson Education, 2010. ISBN 9780132119306.

B. A. Magee and J. H. Waite. Neutral Gas Composition of Enceladus' Plume - Model Parameter Insights from Cassini-INMS. In *Lunar and Planetary Science Conference*, volume 48 of *Lunar and Planetary Inst. Technical Report*, page 2974, Mar. 2017.

W. Martin and M. J. Russell. On the origins of cells: a hypothesis for the evolutionary transitions from abiotic geochemistry to chemoautotrophic prokaryotes, and from prokaryotes to nucleated cells. *Philosophical Transactions of the Royal Society of London B: Biological Sciences*, 358(1429):59–85, 2003. doi:10.1098/rstb.2002.1183.

W. Martin and M. J. Russell. On the origin of biochemistry at an alkaline hydrothermal vent. *Philosophical Transactions of the Royal Society of London B: Biological Sciences*, 362(1486):1887–1926, 2007. doi:10.1098/rstb.2006.1881.

D. Mayumi, H. Mochimaru, H. Tamaki, K. Yamamoto, H. Yoshioka, Y. Suzuki, Y. Kamagata, and S. Sakata. Methane production from coal by a single methanogen. *Science*, 354(6309):222–225, 2016. doi:10.1126/science.aaf8821.

C. P. McKay. What Is Life—and How Do We Search for It in Other Worlds? *PLOS Biology*, 2(9), 2004. doi:10.1371/journal.pbio.0020302.

C. P. McKay, C. C. Porco, T. Altheide, W. L. Davis, and T. A. Kral. The Possible Origin and Persistence of Life on Enceladus and Detection of Biomarkers in the Plume.

Astrobiology, 8:909–919, 2008. doi:10.1089/ast.2008.0265.

C. P. McKay, B. N. Khare, R. Amin, M. Klasson, and T. A. Kral. Possible sources for methane and C_2-C_5 organics in the plume of Enceladus. *Planetary and Space Science*, 71:73–79, 2012. doi:10.1016/j.pss.2012.07.011.

W. B. McKinnon. Effect of Enceladus's rapid synchronous spin on interpretation of Cassini gravity. *Geophysical Research Letters*, 42(7):2137–2143, 2015. doi:10.1002/2015GL063384.

W. B. McKinnon, J. H. Waite, O. Mousis, J. I. Lunine, and M. Y. Zolotov. Composition of Enceladus: Origin and Evolution. In *Enceladus and the Icy Moons of Saturn Conference*, page 3011, 2016.

S. Miller. A Production of Amino Acids Under Possible Primitive Earth Conditions. *Science*, 117(3046):528–529, 1953.

S. Miller and H. Urey. Organic Compound Synthesis on the Primitive Earth. *Science*, 130(3370):245–251, 1959.

G. Mitri, F. Postberg, J. M. Soderblom, G. Tobie, P. Tortora, P. Wurz, J. W. Barnes, N. Carrasco, A. Coustenis, F. Ferri, A. Hayes, J. Hillier, S. Kempf, J. P. Lebreton, R. D. Lorenz, R. Orosei, A. E. E. Petropoulos, K. R. Reh, J. Schmidt, C. Sotin, R. Srama, V. Vuitton, and C. W. Yen. Explorer of Enceladus and Titan (E^2T): Investigating Ocean Worlds' Evolution and Habitability in the Saturn System. *AGU Fall Meeting Abstracts*, art. P33A-2129, 2016.

NASA Planetary Science Division. Enceladus – By the Numbers | Planets – NASA Solar System Exploration, January 2018. URL `https://solarsystem.nasa.gov/planets/enceladus/facts`. Last access: 8.1.2018.

NASA's Jet Propulsion Laboratory. Cassini Legacy: 1997-2017 : Enceladus Flyby - October 09, 2008, October 2008. URL `https://saturn.jpl.nasa.gov/news/68/enceladus-flyby-october-09-2008/`. Last access: 25.10.2016.

NASA's Jet Propulsion Laboratory. Cassini Legacy: 1997-2017 : Enceladus Flyby 22 (E-22): Final Visit to Enceladus, December 2015. URL `https://saturn.jpl.nasa.gov/news/2849/enceladus-flyby-22-e-22-final-vi%sit-to-enceladus/`. Last access: 25.10.2016.

F. Nimmo and R. T. Pappalardo. Diapir-induced reorientation of Saturn's moon Enceladus. *Nature*, 441:614–616, 2006. doi:10.1038/nature04821.

K. Northon. NASA Selects Investigations for Future Key Planetary Mission, September 2015. URL https://www.nasa.gov/press-release/nasa-selects-investigations-for-fut%ure-key-planetary-mission. Last access: 03.04.2018.

K. Northon. NASA Invests in Concept Development for Missions to Comet, Saturn Moon Titan, December 2017. URL https://www.nasa.gov/press-release/nasa-invests-in-concept-development%-for-missions-to-comet-saturn-moon-titan. Last access: 03.04.2018.

J. G. Olgin, B. R. Smith-Konter, and R. T. Pappalardo. Limits of Enceladus's ice shell thickness from tidally driven tiger stripe shear failure. *Geophysical Research Letters*, 38:L02201, Jan. 2011. doi:10.1029/2010GL044950.

C. D. Parkinson, M.-C. Liang, Y. L. Yung, and J. L. Kirschivnk. Habitability of Enceladus: Planetary Conditions for Life. *Origins of Life and Evolution of Biospheres*, 38(4):355–369, 2008. doi:10.1007/s11084-008-9135-4.

D. A. Patthoff and S. A. Kattenhorn. A fracture history on Enceladus provides evidence for a global ocean. *Geophysical Research Letters*, 38:L18201, 2011. doi:10.1029/2011GL048387.

L. Perek. Planetary protection: lessons learned. *Advances in Space Research*, 34(11): 2368 – 2370, 2004. doi:10.1016/j.asr.2003.02.066.

C. Porco, D. DiNino, and F. Nimmo. How the Geysers, Tidal Stresses, and Thermal Emission across the South Polar Terrain of Enceladus are Related. *The Astronomical Journal*, 148:45, 2014. doi:10.1088/0004-6256/148/3/45.

C. C. Porco, P. Helfenstein, P. C. Thomas, A. P. Ingersoll, J. Wisdom, R. West, G. Neukum, T. Denk, R. Wagner, T. Roatsch, S. Kieffer, E. Turtle, A. McEwen, T. V. Johnson, J. Rathbun, J. Veverka, D. Wilson, J. Perry, J. Spitale, A. Brahic, J. A. Burns, A. D. Del Genio, L. Dones, C. D. Murray, and S. Squyres. Cassini Observes the Active South Pole of Enceladus. *Science*, 311:1393–1401, 2006. doi:10.1126/science.1123013.

F. Postberg, S. Kempf, J. Schmidt, N. Brilliantov, A. Beinsen, B. Abel, U. Buck, and R. Srama. Sodium salts in E-ring ice grains from an ocean below the surface of Enceladus. *Nature*, 459:1098–1101, 2009. doi:10.1038/nature08046.

PPOSS. Planetary Protection of Outer Solar System, 2016. URL http://pposs.org/. Last access: 09.04.2018.

N. J. Rappaport, L. Iess, P. Tortora, A. Anabtawi, S. W. Asmar, L. Somenzi, and F. Zingoni. Mass and interior of Enceladus from Cassini data analysis. *Icarus*, 190: 175–178, 2007. doi:10.1016/j.icarus.2007.03.025.

F. Raulin, K. P. Hand, C. P. McKay, and M. Viso. Exobiology and Planetary Protection of icy moons. *Space Science Reviews*, 153:511–535, 2010. doi:10.1007/s11214-009-9610-x.

T. Rodrigues-Oliveira, A. Belmok, D. Vasconcellos, B. Schuster, and C. M. Kyaw. Archaeal S-Layers: Overview and Current State of the Art. *Frontiers in Microbiology*, 8:2597, 2017. doi:10.3389/fmicb.2017.02597.

L. Roth, J. Saur, K. D. Retherford, D. F. Strobel, P. D. Feldman, M. A. McGrath, and F. Nimmo. Transient Water Vapor at Europa's South Pole. *Science*, 343:171–174, 2014. doi:10.1126/science.1247051.

J. Rummel, P. Stabekis, D. Devincenzi, and J. Barengoltz. Cospar's planetary protection policy: A consolidated draft. *Advances in Space Research*, 30(6):1567 – 1571, 2002. doi:10.1016/S0273-1177(02)00479-9.

M. J. Russell, A. J. Hall, and W. Martin. Serpentinization as a source of energy at the origin of life. *Geobiology*, 8(5):355–371, 2010. doi:10.1111/j.1472-4669.2010.00249.x.

J. W. Schopf. Fossil evidence of Archaean life. *Philosophical Transactions of the Royal Society of London B: Biological Sciences*, 361(1470):869–885, 2006. doi:10.1098/rstb.2006.1834.

M. O. Schrenk, W. J. Brazelton, and S. Q. Lang. Serpentinization, Carbon, and Deep Life. *Reviews in Mineralogy and Geochemistry*, 75(1):575, 2013. doi:10.2138/rmg.2013.75.18.

G. Schubert, J. D. Anderson, B. J. Travis, and J. Palguta. Enceladus: Present internal structure and differentiation by early and long-term radiogenic heating. *Icarus*, 188:345–355, 2007. doi:10.1016/j.icarus.2006.12.012.

Y. Sekine, T. Shibuya, F. Postberg, H.-W. Hsu, K. Suzuki, Y. Masaki, T. Kuwatani, M. Mori, P. K. Hong, M. Yoshizaki, S. Tachibana, and S.-i. Sirono. High-temperature water-rock interactions and hydrothermal environments in the chondrite-like core of Enceladus. *Nature Communications*, 6(8604), 2015.

B. Sherwood. Strategic map for exploring the ocean-world enceladus. *Acta Astronautica*, 126:52 – 58, 2016. doi:10.1016/j.actaastro.2016.04.013.

B. Sherwood, J. Lunine, C. Sotin, T. Cwik, and F. Naderi. Follow the (Outer Solar System) Water: Program Options to Explore Ocean Worlds. In *Planetary Science Vision 2050 Workshop*, volume 1989 of *LPI Contributions*, page 8034, Feb. 2017.

N. H. Sleep, A. Meibom, T. Fridriksson, R. G. Coleman, and D. K. Bird. h_2-rich fluids from serpentinization: Geochemical and biotic implications. *Proceedings of the National Academy of Sciences*, 101(35):12818–12823, 2004. doi:10.1073/pnas.0405289101.

C. Sotin, G. Mitri, N. Rappaport, G. Schubert, and D. Stevenson. *Titan's Interior Structure*, page 61. Springer Netherlands, 2010. ISBN 978-1-4020-9214-5. doi:10.1007/978-1-4020-9215-2_4.

W. B. Sparks, K. P. Hand, M. A. McGrath, E. Bergeron, M. Cracraft, and S. E. Deustua. Probing for Evidence of Plumes on Europa with HST/STIS. *The Astrophysical Journal*, 829(2):121, 2016. doi:10.3847/0004-637X/829/2/121.

J. R. Spencer, J. C. Pearl, M. Segura, F. M. Flasar, A. Mamoutkine, P. Romani, B. J. Buratti, A. R. Hendrix, L. J. Spilker, and R. M. C. Lopes. Cassini Encounters Enceladus: Background and the Discovery of a South Polar Hot Spot. *Science*, 311: 1401–1405, Mar. 2006. doi:10.1126/science.1121661.

J. N. Spitale, T. A. Hurford, A. R. Rhoden, E. E. Berkson, and S. S. Platts. Curtain eruptions from Enceladus' south-polar terrain. *Nature*, 521:57–60, 2015. doi:10.1038/nature14368.

H. Strughold. *The Green and Red Planet: A Physiological Study of the Possibility of Life on Mars*. University of New Mexico Press, 1953.

K. Takai, A. Inoue, and K. Horikoshi. *Methanothermococcus okinawensis* sp. nov., a thermophilic, methane-producing archaeon isolated from a Western Pacific deep-sea hydrothermal vent system. *International Journal of Systematic and Evolutionary Microbiology*, 52(4):1089–1095, 2002. doi:10.1099/00207713-52-4-1089.

R.-S. Taubner, L. Baumann, D. Birgel, and S. Rittmann. Lipid pattern of *Methanothermococcus okinawensis* under Enceladus-like conditions *(working title)*. in prep.

L. Tennen. Evolution of the planetary protection policy: conflict of science and jurisprudence? *Advances in Space Research*, 34(11):2354 – 2362, 2004. doi:10.1016/j.asr.2004.01.018.

B. D. Teolis, M. E. Perry, C. J. Hansen, J. H. Waite, C. C. Porco, J. R. Spencer, and C. J. A. Howett. Enceladus Plume Structure and Time Variability: Comparison of Cassini Observations. *Astrobiology*, 17(9):926–940, 2017. doi:10.1089%2Fast.2017.1647.

P. C. Thomas, R. Tajeddine, M. S. Tiscareno, J. A. Burns, J. Joseph, T. J. Loredo, P. Helfenstein, and C. Porco. Enceladus's measured physical libration requires a global subsurface ocean. *Icarus*, 264:37–47, 2016. doi:10.1016/j.icarus.2015.08.037.

B. Travis and G. Schubert. Keeping enceladus warm. *Icarus*, 250:32 – 42, 2015. doi:10.1016/j.icarus.2014.11.017.

E. N. Trifonov. Vocabulary of Definitions of Life Suggests a Definition. *Journal of Biomolecular Structure and Dynamics*, 29(2):259–266, 2011. doi:10.1080/073911011010524992.

S. A. Tsokolov. Why Is the Definition of Life So Elusive? Epistemological Considerations. *Astrobiology*, 9(4):401–412, 2009. doi:10.1089/ast.2007.0201.

C. H. Twohy, J. W. Strapp, and M. Wendisch. Performance of a Counterflow Virtual Impactor in the NASA Icing Research Tunnel. *Journal of Atmospheric and Oceanic Technology*, 20(6):781–790, 2003. doi:10.1175/1520-0426(2003)020<0781:POACVI>2.0.CO;2.

M. Ćuk, L. Dones, and D. Nesvorný. Dynamical Evidence for a Late Formation of Saturn's Moons. *The Astrophysical Journal*, 820(2):97, 2016. doi:10.3847/0004-637X/820/2/97.

UNODA. Treaty on Principles Governing the Activities of States in the Exploration and Use of Outer Space, including the Moon and Other Celestial Bodies, 1967. URL `http://disarmament.un.org/treaties/t/outer_space`. Last access: 09.04.2018.

J. H. Waite, C. R. Glein, R. S. Perryman, B. D. Teolis, B. A. Magee, G. Miller, J. Grimes, M. E. Perry, K. E. Miller, A. Bouquet, J. I. Lunine, T. Brockwell, and S. J. Bolton. Cassini finds molecular hydrogen in the Enceladus plume: Evidence for hydrothermal processes. *Science*, 356:155–159, 2017. doi:10.1126/science.aai8703.

J. H. Waite, Jr., W. S. Lewis, B. A. Magee, J. I. Lunine, W. B. McKinnon, C. R. Glein, O. Mousis, D. T. Young, T. Brockwell, J. Westlake, M.-J. Nguyen, B. D. Teolis, H. B. Niemann, R. L. McNutt, M. Perry, and W.-H. Ip. Liquid water on Enceladus from

observations of ammonia and ^{40}Ar in the plume. *Nature*, 460:487–490, 2009. doi:10.1038/nature08153.

G. Wächtershäuser. Groundworks for an evolutionary biochemistry: The iron-sulphur world. *Progress in Biophysics and Molecular Biology*, 58(2):85 – 201, 1992. doi:10.1016/0079-6107(92)90022-X.

M. C. Weiss, F. L. Sousa, N. Mrnjavac, S. Neukirchen, M. Roettger, S. Nelson-Sathi, and W. F. Martin. The physiology and habitat of the last universal common ancestor. *Nature Microbiology*, 1(16116), 2016. doi:10.1038/nmicrobiol.2016.116.

S. A. Wilde, J. W. Valley, W. H. Peck, and C. M. Graham. Evidence from detrital zircons for the existence of continental crust and oceans on the Earth 4.4 Gyr ago. *Nature*, 409:175–178, 2001. doi:10.1038/35051550.

J. Wisdom. Spin-Orbit Secondary Resonance Dynamics of Enceladus. *Astrophysical Journal*, 128:484–491, 2004. doi:10.1086/421360.

C. R. Woese and G. E. Fox. Phylogenetic structure of the prokaryotic domain: The primary kingdoms. *Proceedings of the National Academy of Sciences*, 74(11): 5088–5090, 1977. doi:10.1073/pnas.74.11.5088.

C. R. Woese, O. Kandler, and M. L. Wheelis. Towards a natural system of organisms: proposal for the domains Archaea, Bacteria, and Eucarya. *Proceedings of the National Academy of Sciences*, 87(12):4576–4579, 1990. doi:10.1073/pnas.87.12.4576.

Appendix

This Appendix provides the abstracts in English and German, the licence for the article presented in chapter 2, and supplementary material for the articles presented in the chapters 4 and 5.

Abstract

When the space probe Cassini, a joint mission by NASA (National Aeronautics and Space Administration), ESA (European Space Agency) and ASI (Italian Space Agency), sent back the first images from Saturn's icy moon Enceladus, it quickly became clear that Cassini made a sensational discovery. Ever since Enceladus is famous for its magnificent plume, which has its origin at the south pole of Enceladus [Porco et al., 2006] and which injects approximately 200 kg water vapour per second into Saturn's magnetosphere [Hansen et al., 2011]. The source of the plume material is most likely a global subsurface ocean [Thomas et al., 2016]. Analyses of the data received from Cassini imply the existence of hydrothermal vents at the ocean floor [Hsu et al., 2015]. Ongoing geochemical activities inside the moon, such as the serpentinization of olivine in the chondritic core, i.e. the oxidation of native and ferrous iron, may be the most prominent source of molecular hydrogen (H_2) in Enceladus' interior. Along with that potential electron donor, many different organic and inorganic molecules like water (H_2O), methane (CH_4), carbon dioxide (CO_2), and ammonia (NH_3) were detected in the plume. Thus, Enceladus harbours many necessary ingredients for life.

This thesis takes an interdisciplinary approach to analyse the habitability of this icy moon. For that, estimations about possible physical and chemical conditions have been made. In the frame of these studies, calculations about Enceladus' interior structure were performed, both for a local and a global ocean case, respectively. The next step was to analyse, which kind of organisms would theoretically be able to survive under Enceladus-like conditions. Due to their ability to live in anoxygenic environments that are independent of photosynthesis, and due to Cassini's observations of several potential substrates and products, this study focus on methanogenic archaea (methanogens). A comprehensive review about the ecophysiology of methanogens in an astrobiological context was compiled. In parallel, a new method to indirectly quantify the CH_4 production of hydrogenotrophic methanogens was developed. This method was used to perform a rapid screening to find suitable methanogenic strains for subsequent experiments.

For the final study, the plume composition data received from NASA's Cassini mission was used to prepare an Enceladus-like medium for cultivation. To explore if methanogenic microorganisms can in principle sustain their metabolism under

Enceladus-like conditions, we studied three strains of archaea (*Methanothermococcus okinawensis*, *Methanothermobacter marburgensis*, and *Methanococcus villosus*) that metabolize H_2 and CO_2 to produce CH_4 and H_2O. While mimicking potential physical conditions of Enceladus' ocean (65/80°C, 10-90 bar), tests on the tolerance towards potential gaseous and liquid inhibitors detected in Enceladus' plume were performed (high NH_3 levels, formaldehyde, ethene, and methanol). In particular, *M. okinawensis*, the isolate from a deep marine trench [Takai et al., 2002], showed tolerance towards all of the added inhibitors and maintained methanogenesis even in the range of 10 to 50 bar.

This thesis represents an interdisciplinary study, which showed that methanogenesis could in principle be feasible under Enceladus-like conditions and that some of the CH_4 detected in Enceladus' plume could be, in principle, of biological origin.

Abstract (German)

Als die von den Raumfahrtbehörden NASA (National Aeronautics and Space Administration), ESA (European Space Agency) und ASI (Italian Space Agency) geplante Raumsonde Cassini das erste Mal Aufnahmen von Saturns Eismond Enceladus an die Erde zurückschickte, wurde schnell klar, was für eine sensationelle Entdeckung hier gemacht wurde. Enceladus besticht durch seine gewaltigen Geysire (Gesamtheit der Geysire oder "jets" wird als "plume" bezeichnet), die sich nahe dem Südpol befinden [Porco et al., 2006] und etwa 200 kg Wasserdampf pro Sekunde [Hansen et al., 2011] ins All befördern. Dieses Wasser hat seinen Ursprung höchstwahrscheinlich in einem unterirdischen Wasserozean, der sich vermutlich über den ganzen Mond erstreckt [Thomas et al., 2016]. Cassini lieferte außerdem Hinweise darauf, dass es hydrothermale Quellen am Boden dieses Ozeans geben könnte [Hsu et al., 2015]. Dort könnte es zu geochemischen Wechselwirkungen wie z.B. Serpentinisierung kommen. Bei diesem Prozess wird olivinhaltiges Gestein zu Serpentinen umgewandelt, wobei zusätzlich Wasserstoff (H_2) produziert wird. Der so gebildete Wasserstoff könnte in weiterer Folge als Elektronendonor für mögliches Leben auf Enceladus verwendet werden. Neben H_2 konnte Cassini auch viele weitere organische und inorganische Moleküle wie etwa Methan (CH_4), Kohlendioxid (CO_2) oder Ammoniak (NH_3) im plume nachweisen.

Die hier vorliegende Doktorarbeit beschäftigt sich auf interdisziplinäre Weise mit der Frage, ob Leben wie wir es kennen auf Enceladus lebensfähig wäre. Zunächst wurden Berechnungen zu den physikalischen Bedingungen, d.h. vor allem dem Druck, der auf dem Ozeanboden herrschen könnte, angestellt. Dafür wurde die innere Struktur von Enceladus modelliert, wobei sowohl auf die Möglichkeit eines lokalen als auch eines globalen Ozeans eingegangen wurde. Im nächsten Schritt ging es darum zu analysieren, welche Art von Leben überhaupt auf Enceladus eine Chance haben könnte, denn es müsste absolut unabhängig von Photosynthese (direkt und indirekt) und nicht auf Sauerstoff angewiesen sein. Eine Gruppe von Mikroorganismen, die diesen Kriterien gerecht werden, sind die sogenannten Methanbildner ("Methanogene") aus der Domäne der Archaeen. In einer ausführlichen Literaturrecherche wurde daher ein Review über die Ökophysiologie von Methanogenen im Kontext von astrobiologischen Studien verfasst. Um geeignete Stämme dieser Methanogenen zu finden, führten wir eine Vorauswahl ("screening") durch. Dabei konnten wir

eine neue Methode entwickeln, mit der man ressourcenschonend und schnell die Methanproduktion von hydrogenotrophen Methanogenen bestimmen kann.

Für die große, abschließende Studie wurden die Cassini-Daten zur Zusammensetzung des plumes analysiert um daraus Rückschlüsse auf die mögliche Beschaffenheit des unterirdischen Ozeans zu gewinnen. Dies wurde dann genützt um ein Medium und eine Gaszusammensetzung zu entwickeln, die die Bedingungen auf Enceladus so gut wie möglich nachstellen sollten. In dieser Studie wurden dabei sowohl die physikalischen (65/80°C, 3-90 bar) als auch die chemischen Einflüsse (Zugabe von möglichen Inhibitoren, die im plume gefunden wurden, wie etwa NH_3, Formaldehyd, Ethen, und Methanol) analysiert. Unter diesen Bedingungen wurden dann drei hydrogenotrophe methanogene Stämme kultiviert (*Methanothermococcus okinawensis*, *Methanothermobacter marburgensis* und *Methanococcus villosus*), wobei sich *M. okinawensis* als besonders geeignet herausgestellt hat. Dieser Stamm wurde ursprünglich aus einem Tiefseegraben isoliert [Takai et al., 2002] und war daher an hohe Drücke angepasst. Weiters tolerierte er die zugeführten Inhibitoren und konnte noch bei 50 bar Methanogenese durchführen.

Diese Doktorarbeit stellt eine interdisziplinäre Studie da, in der gezeigt werden konnte, dass Methanogene unter Enceladus-ähnlichen Bedingungen vermehrungsfähig sind und somit ein Teil des im plume detektierten Methans biologischen Ursprungs sein könnte.

SPRINGER NATURE LICENSE
TERMS AND CONDITIONS

Feb 22, 2018

This Agreement between Ms. Ruth ("You") and Springer Nature ("Springer Nature") consists of your license details and the terms and conditions provided by Springer Nature and Copyright Clearance Center.

License Number	4293590318309
License date	Feb 21, 2018
Licensed Content Publisher	Springer Nature
Licensed Content Publication	Origins of Life & Evolution of the Biospheres
Licensed Content Title	Modelling the Interior Structure of Enceladus Based on the 2014's Cassini Gravity Data
Licensed Content Author	R.-S. Taubner, J. J. Leitner, M. G. Firneis et al
Licensed Content Date	Jan 1, 2015
Licensed Content Volume	46
Licensed Content Issue	2
Type of Use	Thesis/Dissertation
Requestor type	academic/university or research institute
Format	print and electronic
Portion	full article/chapter
Will you be translating?	no
Circulation/distribution	<501
Author of this Springer Nature content	yes
Title	An interdisciplinary Approach: On the Habitability of Enceladus' Potential Subsurface Water Reservoir
Instructor name	Prof. Maria G. Firneis and Prof. Christa Schleper
Institution name	Institute of Astrophysics, University of Vienna
Expected presentation date	Jun 2018
Requestor Location	Ms. Ruth-Sophie Taubner Pötzleinsdorferstraße 12 Vienna, 1180 Austria Attn: Ms. Ruth-Sophie Taubner
Billing Type	Invoice
Billing Address	Ms. Ruth-Sophie Taubner Pötzleinsdorferstraße 12 Vienna, Austria 1180 Attn: Ms. Ruth-Sophie Taubner
Total	0.00 EUR

Terms and Conditions

Springer Nature Terms and Conditions for RightsLink Permissions

Springer Customer Service Centre GmbH (the Licensor) hereby grants you a non-exclusive, world-wide licence to reproduce the material and for the purpose and requirements specified in the attached copy of your order form, and for no other use, subject to the conditions below:

1. The Licensor warrants that it has, to the best of its knowledge, the rights to license reuse of this material. However, you should ensure that the material you are requesting is original to the Licensor and does not carry the copyright of another entity (as credited in the published version).

   If the credit line on any part of the material you have requested indicates that it was reprinted or adapted with permission from another source, then you should also seek permission from that source to reuse the material.

2. Where **print only** permission has been granted for a fee, separate permission must be obtained for any additional electronic re-use.

3. Permission granted **free of charge** for material in print is also usually granted for any electronic version of that work, provided that the material is incidental to your work as a whole and that the electronic version is essentially equivalent to, or substitutes for, the print version.

4. A licence for 'post on a website' is valid for 12 months from the licence date. This licence does not cover use of full text articles on websites.

5. Where **'reuse in a dissertation/thesis'** has been selected the following terms apply: Print rights for up to 100 copies, electronic rights for use only on a personal website or institutional repository as defined by the Sherpa guideline (www.sherpa.ac.uk/romeo/).

6. Permission granted for books and journals is granted for the lifetime of the first edition and does not apply to second and subsequent editions (except where the first edition permission was granted free of charge or for signatories to the STM Permissions Guidelines http://www.stm-assoc.org/copyright-legal-affairs/permissions/permissions-guidelines/), and does not apply for editions in other languages unless additional translation rights have been granted separately in the licence.

7. Rights for additional components such as custom editions and derivatives require additional permission and may be subject to an additional fee. Please apply to Journalpermissions@springernature.com/bookpermissions@springernature.com for these rights.

8. The Licensor's permission must be acknowledged next to the licensed material in print. In electronic form, this acknowledgement must be visible at the same time as the figures/tables/illustrations or abstract, and must be hyperlinked to the journal/book's homepage. Our required acknowledgement format is in the Appendix below.

9. Use of the material for incidental promotional use, minor editing privileges (this does not include cropping, adapting, omitting material or any other changes that affect the meaning, intention or moral rights of the author) and copies for the disabled are permitted under this licence.

10. Minor adaptations of single figures (changes of format, colour and style) do not require the Licensor's approval. However, the adaptation should be credited as shown in Appendix below.

Appendix — Acknowledgements:

For Journal Content:

Reprinted by permission from [**the Licensor**]: [**Journal Publisher** (e.g. Nature/Springer/Palgrave)] [**JOURNAL NAME**] [**REFERENCE CITATION** (Article name, Author(s) Name), [**COPYRIGHT**] (year of publication)

For **Advance Online Publication papers:**
Reprinted by permission from [**the Licensor**]: [**Journal Publisher** (e.g. Nature/Springer/Palgrave)] [**JOURNAL NAME**] [**REFERENCE CITATION** (Article name, Author(s) Name), [**COPYRIGHT**] (year of publication), advance online publication, day month year (doi: 10.1038/sj.[JOURNAL ACRONYM].)

For Adaptations/Translations:
Adapted/Translated by permission from [**the Licensor**]: [**Journal Publisher** (e.g. Nature/Springer/Palgrave)] [**JOURNAL NAME**] [**REFERENCE CITATION** (Article name, Author(s) Name), [**COPYRIGHT**] (year of publication)

Note: For any republication from the British Journal of Cancer, the following credit line style applies:

Reprinted/adapted/translated by permission from [**the Licensor**]: on behalf of Cancer Research UK: : [**Journal Publisher** (e.g. Nature/Springer/Palgrave)] [**JOURNAL NAME**] [**REFERENCE CITATION** (Article name, Author(s) Name), [**COPYRIGHT]** (year of publication)

For **Advance Online Publication** papers:
Reprinted by permission from The [**the Licensor**]: on behalf of Cancer Research UK: [**Journal Publisher** (e.g. Nature/Springer/Palgrave)] [**JOURNAL NAME**] [**REFERENCE CITATION** (Article name, Author(s) Name), [**COPYRIGHT**] (year of publication), advance online publication, day month year (doi: 10.1038/sj.[JOURNAL ACRONYM])

For Book content:
Reprinted/adapted by permission from [**the Licensor**]: [**Book Publisher** (e.g. Palgrave Macmillan, Springer etc) [**Book Title**] by [**Book author**(s)] [**COPYRIGHT**] (year of publication)

Other Conditions:

Version 1.0

Questions? customercare@copyright.com or +1-855-239-3415 (toll free in the US) or +1-978-646-2777.

frontiers

Supplementary Material: Method for indirect quantification of CH_4 production via H_2O production using hydrogenotrophic methanogens

Ruth-Sophie Taubner and Simon K.-M. R. Rittmann*

*Correspondence:
Simon K.-M. R. Rittmann
simon.rittmann@univie.ac.at

1 SOURCE CODE

In the following section, the source code of the data analysing program written in MATLAB is presented. This file is appropriate for analysing a triplicate experiment plus a zero control. All explanations are proceeded with "%".

```
function [MER,WER,DeltaMass_p]=H2O_Exp(T1)

w=dlmread('H2ODATA.txt');   %Reads data from data sheet

V_med=50;  %volume of the liquid media in ml

[m,n]=size(w);  %n-1: number of bottles

x=(m-3)/4;  % number of runs

V=w(1,2:n);   %Volume in cm^3

for i=1:x;
     mass1(i,1:n-1)= w(4+4*(i-1),2:n);  %mass before gassing
     mass2(i,1:n-1)= w(7+4*(i-1),2:n);  %mass after gassing
     t1(i,1)=w(4+4*(i-1),1);     % time at first mass determination in h
     t2(i,1)=w(7+4*(i-1),1);     % time at second mass determination in h
     p_1(i,1:n-1)= w(5+4*(i-1),2:n)+1;            % pressure before gassing
     p_2(i,1)= w(2+4*(i-1),2)+1;            % pressure after gassing
end
p_2=[p_2;w(2+4*x,2)+1];   %pressure after gassing

for i=1:x;
    for j=1:n-1;
if p_1(i,j) ≥ p_2(i,1)
   p_2(i,1)=max(p_1(i,:));
else
end
    end
end
```

```
31
32 DeltaMass=mass2-mass1;
33 for i=2:x;
34    MassSum(1,:)=DeltaMass(1,:);
35    MassSum(i,:)=MassSum(i-1,:)+DeltaMass(i,:);
36 end
37
38
39 for i=1:x;
40     for j=1:n-1;
41 p_CH4(i,j)=(p_2(i)-p_1(i,j))/4*10^5            % CH4-partial pressure in Pascal
42 p_CO2(i,j)=p_2(i)/5*10^5-p_CH4(i,j);           % CO2-partial pressure in Pascal
43 Konversion(i,j)=p_CH4(i,j)/p_CO2(1)/10^5*100;
44      end
45 end
46
47
48 %ideal Gas equation:
49 V=V*10^-6;     %in m^3
50
51 T=T1+273.15; %K
52 R=8.3144621; %J/(mol K)
53
54 for i=1:x
55     for j=1:n-1
56 n_ref_CO2(i,j)=((V(i,j)*p_2(i)/5*10^5)/(R*T));
57 n_CH4(i,j)=((V(i,j)*p_CH4(i,j))/(R*T)); %mol   theoretical particle number in mol (based on ...
       pressure drop)
58 n_H2(i,j)=((V(i,j).*4*p_CO2(i,j))/(R*T)); %mol   theoretical particle number in mol (based on ...
       pressure drop)
59 n_CO2(i,j)=((V(i,j).*p_CO2(i,j))/(R*T)); %mol   theoretical particle number in mol (based on ...
       pressure drop)
60 m_H2O(i,j)=2*n_CH4(i,j)*18.01528*1000; %mg    theoretical water production in mg (based on ...
       pressure drop)
61 V(i+1,j)=V(i,j)-m_H2O(i,j)*10^(-9); %m^3  theoretical decrease in volume in m^3 (based on ...
       pressure drop)
62     end
63 end
64
65 %%%%%%%%%%%%%%%%%%%%%%%%%%%%%%%%%%%%%%%%%%%%%%%%%%%%%%%%%%%%%%%%%%%%%%%%%%%%
66 %MER:
67 Delta_t=t1-[0;t1(1:end-1)];
68 Delta_n_CH4=n_CH4;
69 Delta_n_H2=n_H2-4*n_ref_CO2(i,j);
70 Delta_n_CO2=n_CO2-n_ref_CO2(i,j);
71
72 for i=1:x
73     for j=1:n-1
74  MER(i,j)=Delta_n_CH4(i,j)*1000/(Delta_t(i))/V(i,j)/10^3; %mmol/h/L
75  HUR(i,j)=Delta_n_H2(i,j)*1000/(Delta_t(i))/V(i,j)/10^3; %mmol/h/L
76  CUR(i,j)=Delta_n_CO2(i,j)*1000/(Delta_t(i))/V(i,j)/10^3; %mmol/h/L
77     end
78 end
79 %%%%%%%%%%%%%%%%%%%%%%%%%%%%%%%%%%%%%%%%%%%%%%%%%%%%%%%%%%%%%%%%%%%%%%%%%%%%
```

```
80
81  %WER:
82
83  for i=1:x
84      for j=1:n-1
85  p_neu(i,j)=1/(8.314472/(0.8*2.01588+0.2*16.0425)*10^3*T)*(p_2(i+1)*10^5.*V(i+1,j)-p_2(i)*10^5.*V(i,j))*10^3; ...
          % in g   m=pV/(R_s*T), where R_s==R/(0.8H2+0.2CO2)
86  DeltaMass_p(i,j)=DeltaMass(i,j)-p_neu(i,j)-n_CH4(i,j)*16.043;      %in g    including mass ...
      difference due to variations in pressure from one run to the other
87      end
88  end
89
90  faktor_Med=1000/V_med;    %factor to scale media volume to 1 liter
91
92  for i=1:x
93      for j=1:n-1
94  WER(i,j)=DeltaMass_p(i,j)*faktor_Med*1000/(18.01528*Delta_t(i));   %WER in mmol/h/l
95      end
96  end
97
98  for i=1:x
99  MER_mean(i)=mean(MER(i,2:4));
100 WER_mean(i)=mean(WER(i,2:4));
101 HUR_mean(i)=mean(HUR(i,2:4));
102 CUR_mean(i)=mean(CUR(i,2:4));
103 % HUR_mean(i)=4*MER_mean(i);
104 % CUR_mean(i)=MER_mean(i);
105 Y_CH4_CO2(i)=MER_mean(i)/CUR_mean(i);
106 Y_CH4_H2(i)=MER_mean(i)/HUR_mean(i);
107 Y_H2O_H2(i)=WER_mean(i)/HUR_mean(i);
108 end
109
110 MER_mean=MER_mean';
111 WER_mean=WER_mean';
112 HUR_mean=HUR_mean';
113 CUR_mean=CUR_mean';
114
115 %%%%%%%%%%%%%%%%%%%%%%%%%%%%%%%%%%%%%%%%%%%%%%%%%%%%%%%%%%%%%%%%%%%%%%%%%%%%
116 fh1=figure(1);
117 set(fh1, 'color', 'white');
118 set(gca,'fontweight','bold','fontsize',16);
119
120 plot(t1(1:end-1),DeltaMass_p(1:end-1,:),'o-');
121
122 title(['\Delta mass']);
123 xlabel('time [h]');
124 ylabel(['\Delta mass [g]']);
125
126 hleg1=legend(['NK'],['I'],['II'],['III']);
127 set(hleg1,'Location','eastoutside');
128
129 %%%%%%%%%%%%%%%%%%%%%%%%%%%%%%%%%%%%%%%%%%%%%%%%%%%%%%%%%%%%%%%%%%%%%%%%%%%%
130
131 end
```

2 SUPPLEMENTARY DATA

Table 1. Comparison of water quantification via pressure and mass gain for the experiments without OD measurements.

Strain	t [h]	$\Delta m_{\Delta p}$	Δm_{weight}	$\Delta m_{\Delta p}$ / Δm_{weight}
M. marburgensis DSM 2133 (55°C)	*13.68*	5.27	25.78	20.45%
M. marburgensis DSM 2133 (55°C)	*35.23*	2.34	11.77	19.87%
M. marburgensis DSM 2133 (55°C)	*56.45*	5.95	9.28	64.12%
M. marburgensis DSM 2133 (55°C)	*77.35*	15.61	10.53	148.30%
M. marburgensis DSM 2133 (55°C)	*137.90*	19.19	28.22	67.99%
M. marburgensis DSM 2133 (55°C)	*160.57*	44.21	40.24	109.84%
M. marburgensis DSM 2133 (55°C)	*180.47*	24.72	32.12	76.95%
M. marburgensis DSM 2133 (55°C)	*198.55*	28.19	32.09	87.84%
M. marburgensis DSM 2133 (65°C)	*13.68*	5.24	25.02	20.94%
M. marburgensis DSM 2133 (65°C)	*35.23*	23.56	26.47	89.02%
M. marburgensis DSM 2133 (65°C)	*56.45*	44.60	38.33	116.35%
M. marburgensis DSM 2133 (65°C)	*77.35*	43.25	38.88	111.24%
M. marburgensis DSM 2133 (65°C)	*137.90*	41.41	44.69	92.66%
M. marburgensis DSM 2133 (65°C)	*160.57*	44.79	47.17	94.94%
M. marburgensis DSM 2133 (65°C)	*180.47*	43.60	45.30	96.24%
M. marburgensis DSM 2133 (65°C)	*198.55*	45.84	51.79	88.52%
M. villosus DSM 22612 (1)	*19.68*	43.08	43.19	99.76%
M. villosus DSM 22612 (1)	*45.93*	43.83	42.05	104.24%
M. villosus DSM 22612 (1)	*63.45*	43.30	45.26	95.67%
M. villosus DSM 22612 (1)	*93.35*	44.43	46.62	95.30%
M. villosus DSM 22612 (1)	*116.15*	45.71	46.67	97.94%
M. villosus DSM 22612 (1)	*137.67*	44.65	47.09	94.80%
M. villosus DSM 22612 (1)	*158.65*	44.41	46.55	95.41%
M. villosus DSM 22612 (1)	*177.53*	44.67	48.76	91.62%
M. villosus DSM 22612 (2)	*11.83*	45.35	46.04	98.50%
M. villosus DSM 22612 (2)	*18.82*	48.12	49.16	97.89%
M. villosus DSM 22612 (2)	*30.82*	49.31	48.37	101.95%
M. villosus DSM 22612 (2)	*37.62*	48.59	50.52	96.17%
M. villosus DSM 22612 (2)	*48.20*	48.84	52.48	93.07%
M. villosus DSM 22612 (2)	*55.07*	45.44	50.57	89.86%
M. villosus DSM 22612 (2)	*67.20*	48.00	50.76	94.56%
M. villosus DSM 22612 (2)	*72.93*	39.75	46.07	86.28%
M. villosus DSM 22612 (2)	*83.63*	51.24	51.28	99.92%
M. okinawensis DSM 14208	*19.68*	42.54	41.99	101.30%
M. okinawensis DSM 14208	*45.93*	42.69	44.19	96.59%
M. okinawensis DSM 14208	*63.45*	41.86	44.23	94.63%
M. okinawensis DSM 14208	*93.35*	44.53	46.16	96.47%
M. okinawensis DSM 14208	*116.15*	41.24	44.35	93.00%
M. okinawensis DSM 14208	*137.67*	38.82	42.36	91.63%
M. okinawensis DSM 14208	*158.65*	39.13	42.05	93.04%
M. okinawensis DSM 14208	*177.53*	37.90	40.43	93.74%
M. soligelidi DSM 26065	*120.00*	15.12	22.84	66.21%
M. soligelidi DSM 26065	*236.83*	14.61	22.99	63.54%
M. soligelidi DSM 26065	*351.92*	15.24	20.22	75.38%
M. soligelidi DSM 26065	*478.25*	14.06	13.72	102.46%
M. soligelidi DSM 26065	*589.80*	13.10	16.37	80.06%
M. soligelidi DSM 26065	*715.77*	14.41	16.14	89.26%
M. soligelidi DSM 26065	*831.03*	11.44	9.42	121.49%

Table 2. Comparison of water quantification via pressure, mass gain and GC for the experiments with OD measurements.

Strain	t [h]	$\Delta m_{\Delta p}$	Δm_{weight}	Δm_{GC}	$\Delta m_{\Delta p}$ / Δm_{weight}	Δm_{GC} / Δm_{weight}
M. marburgensis DSM 2133 (65°C)	*13.68*	6.35	19.29		303.81%	
M. marburgensis DSM 2133 (65°C)	*35.23*	15.80	14.64		92.63%	
M. marburgensis DSM 2133 (65°C)	*56.45*	46.06	39.09		84.86%	
M. marburgensis DSM 2133 (65°C)	*77.35*	45.17	38.95		86.23%	
M. marburgensis DSM 2133 (65°C)	*137.90*	37.50	41.79		111.42%	
M. marburgensis DSM 2133 (65°C)	*160.57*	44.40	47.87		107.81%	
M. marburgensis DSM 2133 (65°C)	*180.47*	43.36	45.44		104.79%	
M. marburgensis DSM 2133 (65°C)	*198.55*	45.86	53.42	41.59	116.48%	77.85%
M. villosus DSM 22612 (2)	*11.83*	45.90	43.15		94.01%	
M. villosus DSM 22612 (2)	*18.82*	48.49	45.91		94.68%	
M. villosus DSM 22612 (2)	*30.82*	50.82	48.81		96.05%	
M. villosus DSM 22612 (2)	*37.62*	44.77	47.87		106.92%	
M. villosus DSM 22612 (2)	*48.20*	47.26	49.64		105.04%	
M. villosus DSM 22612 (2)	*55.07*	48.02	47.51		98.95%	
M. villosus DSM 22612 (2)	*67.20*	53.17	52.52		98.79%	
M. villosus DSM 22612 (2)	*72.93*	39.43	43.07		109.25%	
M. villosus DSM 22612 (2)	*83.63*	54.28	50.82	51.29	93.62%	100.94%

3 SUPPLEMENTARY TABLES AND FIGURES

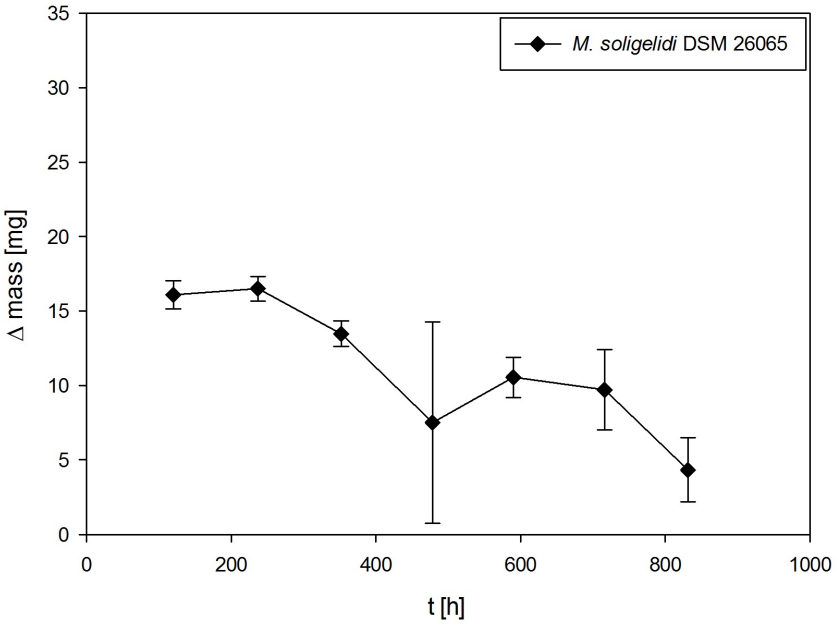

Figure 1. Mass gain of *M. soligelidi*. Negative control is not shown.

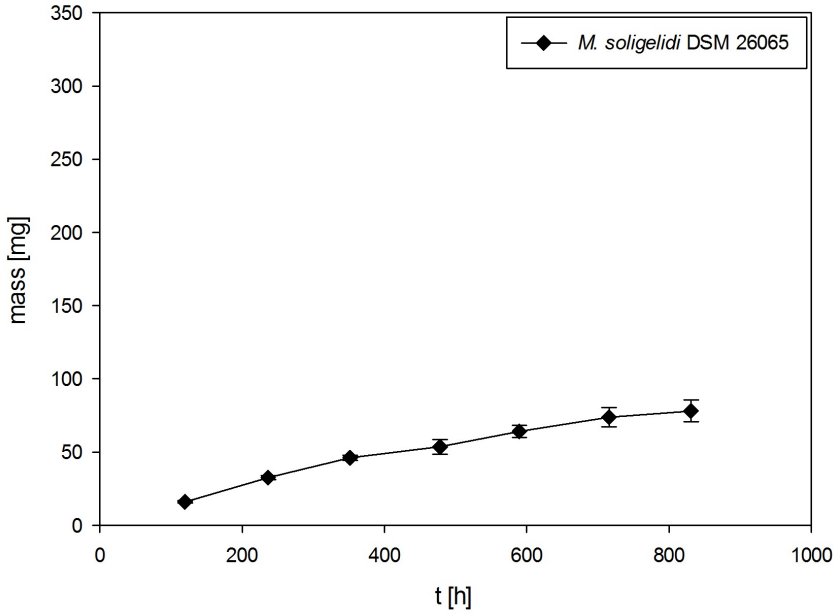

Figure 2. Total cumulative mass gain of *M. soligelidi*. Negative control is not shown.

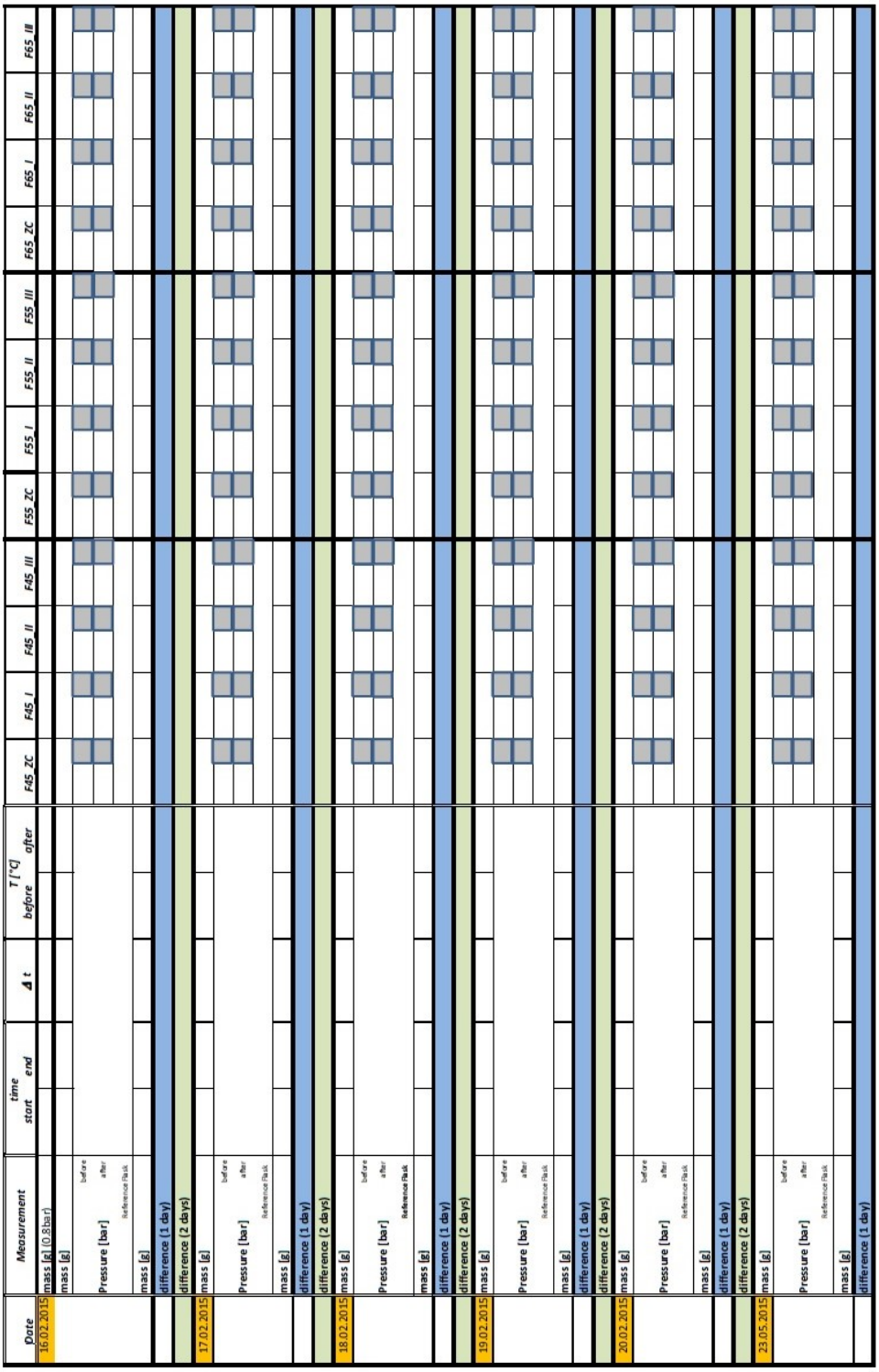

Date	Measurement	time start	time end	Δ t	T [°C] before	T [°C] after	F45_2C	F45_I	F45_II	F45_III	F55_2C	F55_I	F55_II	F55_III	F65_2C	F65_I	F65_II	F65_III
16.02.2015	mass [g] (0,8 bar)																	
	mass [g]																	
	Pressure [bar] before																	
	Pressure [bar] after																	
	Pressure [bar] Reference Rack																	
	mass [g]																	
	difference (1 day)																	
	difference (2 days)																	
17.02.2015	mass [g]																	
	Pressure [bar] before																	
	Pressure [bar] after																	
	Pressure [bar] Reference Rack																	
	mass [g]																	
	difference (1 day)																	
	difference (2 days)																	
18.02.2015	mass [g]																	
	Pressure [bar] before																	
	Pressure [bar] after																	
	Pressure [bar] Reference Rack																	
	mass [g]																	
	difference (1 day)																	
	difference (2 days)																	
19.02.2015	mass [g]																	
	Pressure [bar] before																	
	Pressure [bar] after																	
	Pressure [bar] Reference Rack																	
	mass [g]																	
	difference (1 day)																	
	difference (2 days)																	
20.02.2015	mass [g]																	
	Pressure [bar] before																	
	Pressure [bar] after																	
	Pressure [bar] Reference Rack																	
	mass [g]																	
	difference (1 day)																	
	difference (2 days)																	
23.05.2015	mass [g]																	
	Pressure [bar] before																	
	Pressure [bar] after																	
	Pressure [bar] Reference Rack																	
	mass [g]																	
	difference (1 day)																	

Supplementary Table 3. Blank data sheet for six experimental runs for a triplicate experiment for three different temperatures.

Supplementary Table 4. Example for input file for a triplicate experiment of the MATLAB file above – the first line and the first column (written text) should not be included into the file H2ODATA.txt

	time[h]	Zero Control	Bottle 1	Bottle 2	Bottle 3
mass [g]	0.00	68.0378	62.7352	62.7091	62.7126
pressure [barg]	0.00	1.5360			
mass [g]	0.00	147.0002	151.4489	152.3016	151.8365
mass [g]	18.88	146.9990	151.4493	152.3010	151.8367
pressure [barg]	18.88	1.5170	-0.3340	-0.3390	-0.3420
pressure [barg]	18.88	1.5690			
mass [g]	18.88	147.0082	151.4924	152.3427	151.8793
mass [g]	45.15	147.0089	151.4955	152.3447	151.8813
pressure [barg]	45.15	1.5770	-0.3070	-0.3100	-0.2990
pressure [barg]	45.15	1.5820			
mass [g]	45.15	147.0106	151.5396	152.3889	151.9257
mass [g]	62.53	147.0091	151.5390	152.3882	151.9240
pressure [barg]	62.53	1.5680	-0.2730	-0.2560	-0.2660
pressure [barg]	62.53	1.6350			
mass [g]	62.53	147.0132	151.5847	152.4325	151.9690
mass [g]	92.87	147.0125	151.5861	152.4323	151.9696
pressure [barg]	92.87	1.6470	-0.3240	-0.3200	-0.3140
pressure [barg]	92.87	1.5900			
mass [g]	92.87	147.0116	151.6329	152.4767	152.0153
mass [g]	115.62	147.0112	151.6334	152.4774	152.0165
pressure [barg]	115.62	1.6050	-0.2100	-0.2700	-0.1720
pressure [barg]	115.62	1.6030			
mass [g]	115.62	147.0113	151.6786	152.5225	152.0591
mass [g]	137.25	147.0103	151.6786	152.5221	152.0587
pressure [barg]	137.25	1.5900	-0.1200	-0.1380	-0.0820
pressure [barg]	137.25	1.6070			
mass [g]	137.25	147.0100	151.7216	152.5648	152.1005
mass [g]	157.53	147.0118	151.7239	152.5666	152.1027
pressure [barg]	157.53	1.6160	-0.1730	-0.0830	-0.0890
pressure [barg]	157.53	1.6490			
mass [g]	157.53	147.0122	151.7681	152.6076	152.1448
mass [g]	177.00	147.0109	151.7679	152.6071	152.1436
pressure [barg]	177.00	1.6490	-0.0600	-0.0210	-0.0050
pressure [barg]	177.00	1.5960			
mass [g]	177.00	147.0082	151.8090	152.6466	152.1823

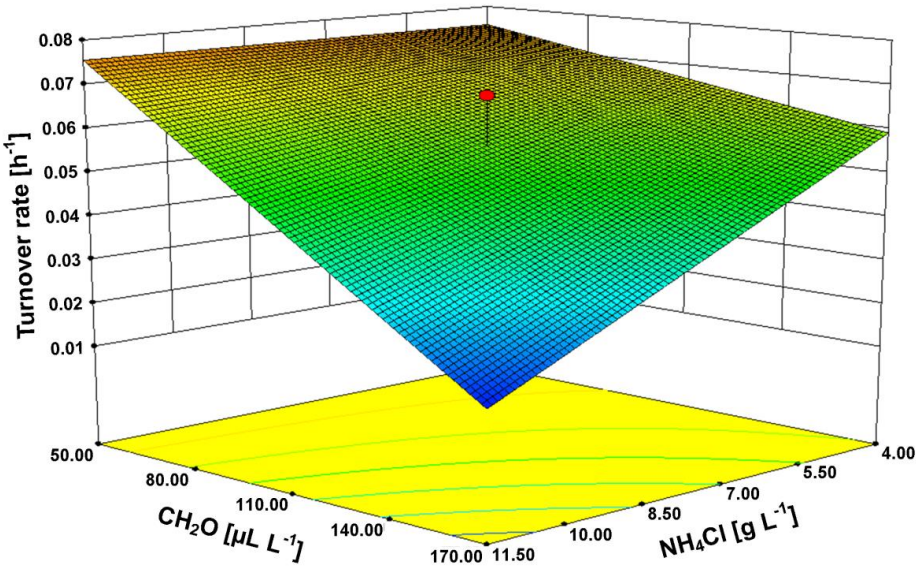

Supplementary Figure 1 | Turnover rate in [h^{-1}] as function of CH_2O and NH_4Cl concentrations. The turnover rate reached its maximum value at low CH_2O concentration. At high CH_2O concentration the turnover rate is higher for low NH_4Cl concentrations. This study was based on a DoE (see Methods and Fig. 2 and Supplementary Fig. 2 and Supplementary Tables 1 and 2). Supplementary Table 1 may be used for unit comparison.

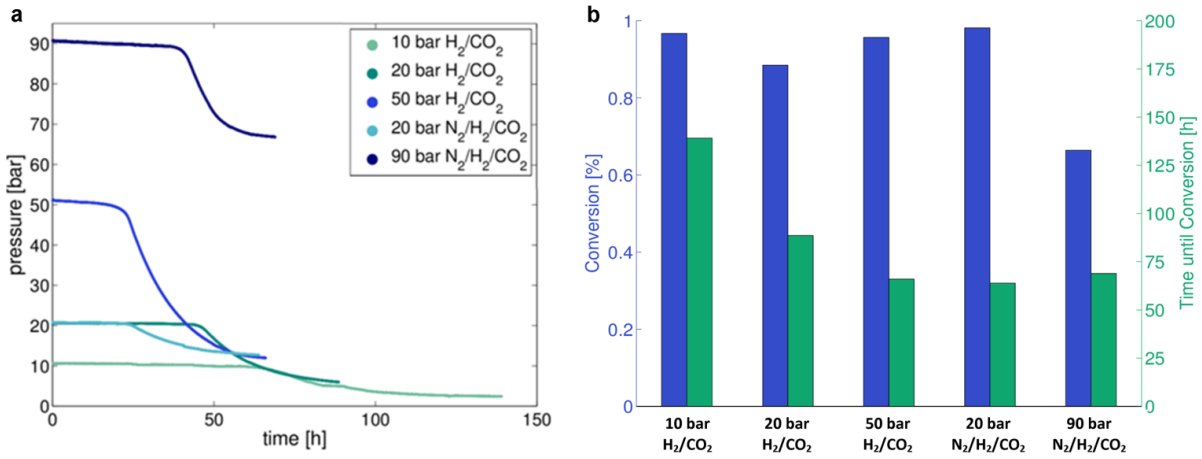

Supplementary Figure 2 | H_2/CO_2 conversion of *M. okinawensis* under high pressure conditions. a, decreasing pressure over time as indirect evidence for stoichiometric H_2/CO_2 to CH_4 conversion. If 50 Vol.-% N_2 is added to the gas phase, the time until conversion from CO_2 to CH_4 is even shorter (as seen for the experiments at 20 bar). **b,** the conversion (or turnover) was examined using the observed pressure drop according to equation (2) without the division by Δt.

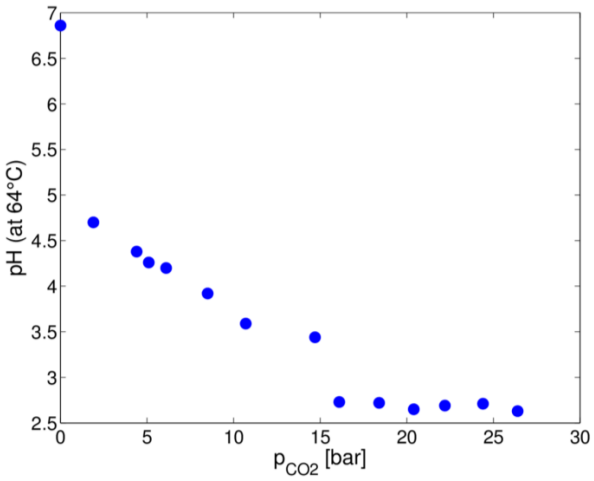

Supplementary Figure 3 | Analysis of p_{CO2} during high pressure experiments. The measurements were performed at 65 °C using the medium composition described in Supplementary Table 3. Already at a low p_{CO2} (1.9 bar), a pH < 5 is found.

Supplementary Table 1 | Concentrations of liquid inhibitors in the DoE study.

	NH_4Cl [g L^{-1}]	NH_4Cl [mol L^{-1}]	CH_2O (37%) [µL L^{-1}]	CH_2O (37%) [mmol L^{-1}]	CH_3OH [µL L^{-1}]	CH_3OH [mmol L^{-1}]
A	4.00	0.075	50.00	1.815	50.00	1.234
B	11.50	0.215	50.00	1.815	50.00	1.234
C	4.00	0.075	170.00	6.171	50.00	1.234
D	11.50	0.215	170.00	6.171	50.00	1.234
E	4.00	0.075	50.00	1.815	170.00	4.197
F	11.50	0.215	50.00	1.815	170.00	4.197
G	4.00	0.075	170.00	6.171	170.00	4.197
H	11.50	0.215	170.00	6.171	170.00	4.197
I	1.44	0.027	110.00	3.993	110.00	2.716
J	14.06	0.263	110.00	3.993	110.00	2.716
K	7.75	0.145	9.09	0.330	110.00	2.716
L	7.75	0.145	210.91	7.656	110.00	2.716
M	7.75	0.145	110.00	3.993	9.09	0.224
N	7.75	0.145	110.00	3.993	210.91	5.207
O	7.75	0.145	110.00	3.993	110.00	2.716

Supplementary Table 2 | ANOVA results of the statistical analysis for the turnover rate in the DoE study.

Source	Sum of Squares	df	Mean Square	F Value	p-value Prob > F	
Model	0.023165174	5	0.004633035	149.3953129	< 0.0001	significant
A-NH_4Cl	0.004846834	1	0.004846834	156.2894135	< 0.0001	
B-CH_2O	0.014655254	1	0.014655254	472.5684829	< 0.0001	
C-CH_3OH	$2.07293 \cdot 10^{-7}$	1	$2.07293 \cdot 10^{-7}$	0.006684316	0.9353	
AB	0.002798073	1	0.002798073	90.22573942	< 0.0001	
C^2	0.000566374	1	0.000566374	18.26312333	0.0001	
Residual	0.001178453	38	$3.10119 \cdot 10^{-5}$			
Pure Error	0.00023715	29	$8.1776 \cdot 10^{-6}$			
Cor Total	0.024343627	43				

Std. Dev.	0.005568834	**R-Squared**	0.951590911
Mean	0.059538329	**Adj R-Squared**	0.945221295
C.V. %	9.353359965	**Pred R-Squared**	0.935615849
PRESS	0.001567344	**Adeq Precision**	33.8204532

Factor	Coefficient Estimate	df	Standard Error	95% CI Low	95% CI High	VIF
Intercept	0.05630249	1	0.001201758	0.053869659	0.058735321	
A-NH_4Cl	-0.011029395	1	0.00088224	-0.012815397	-0.009243393	1.002624948
B-CH_2O	-0.019178706	1	0.00088224	-0.020964708	-0.017392704	1.002624948
C-C	$-7.21299 \cdot 10^{-5}$	1	0.00088224	-0.001858132	0.001713872	1.002624948
AB	-0.011055204	1	0.001163862	-0.01341132	-0.008699089	1.00362851
C^2	0.004040707	1	0.000945518	0.002126606	0.005954808	1.000031475

Supplementary Table 3 | Liquid medium composition (incl. inhibitors) used in the low and high pressure experiments for *M. okinawensis* (for final volume of 1 L).

Compound*	Amount
K_2HPO_4	0.14 g
$CaCl_2$ x 2 H_2O	0.14 g
NH_4Cl	11.50 g
$MgSO_4$ x 7 H_2O	3.40 g
$MgCl_2$ x 6 H_2O	4.10 g
KCl	0.33 g
$NiCl_2$ x 6 H_2O	0.50 mg
Na_2SeO_3 x 5 H_2O	0.50 mg
NaCl	30.00 g
$FeSO_4$ x 7 H_2O	7 mg
$NaHCO_3$	1.00 g
L-Cysteine-HCl x H_2O	0.50 g
Na_2S x 9 H_2O	0.50 g
H_2CO (37%)	0.11 mL
CH_3OH	0.16 mL
Trace Element Solution (DSMZ Medium 141)	10.00 mL
ddH_2O	ad 1000mL

*The medium composition is similar to DSMZ medium 282 (for **Methanococcus jannaschii**).

Supplementary Table 4 | Results of serpentinization models at 50 bar.

Model	pH	H_2 production rate [nmol g^{-1} L^{-1} d^{-1}]	CH_4 production rate [nmol g^{-1} L^{-1} d^{-1}]	water : rock ratio	Moles H_2 produced per mole olivine
Model 1:		**Fo_{90}* : En : Diop = 8 : 1 : 1**			
25 °C	12.2	0.138	0.064	0.126	0.002
50 °C	11.3	4.58	2.05	0.126	0.002
100 °C	9.82	49.2	19.2	0.126	0.003
Model 2:		**Fo_{90}***			
25 °C	9.33	0.250	0.056	0.124	0.004
50 °C	8.60	4.03	1.07	0.124	0.004
100 °C	7.45	80.4	16.9	0.124	0.004
Model 3:		**Fo_{50}†**			
25 °C	8.12	8.68	0.209	0.104	0.033
50 °C	7.50	34.7	1.35	0.104	0.033
100 °C	6.50	517	12.5	0.104	0.032
Model 4:		**Fo_{20}‡**			
25 °C	7.94	12.7	0.184	0.094	0.054
50 °C	7.29	50.7	1.32	0.094	0.053
100 °C	6.26	757	11.0	0.094	0.052

*Fo_{90} = Forsteritic olivine (Forsterite:Fayalaite = 9:1), En = Enstatite, Diop = Diopside
†Fo_{50} = Forsteritic olivine (Forsterite:Fayalaite = 1:1)
‡Fo_{20} = Fayalitic olivine (Forsterite:Fayalaite = 2:8)

Supplementary Table 5 | Liquid medium composition ("standard medium") used in the low pressure for *M. marburgensis* experiments (for final volume of 1 L).

Compound	Amount
KH_2PO_4	6.8 g
NH_4Cl	2.1 g
Na_2CO_3	3.6 g
Na_2S x 9 H_2O	0.25 g
Trace Element Solution (see Suppl. Tab.7)	10.00 mL
ddH_2O	ad 1000 mL

Supplementary Table 6 | Liquid medium composition ("Medium w/o $NaHCO_3$") used in the low pressure experiments for *M. marburgensis* (for final volume of 1 L).

Compound	Amount
KH_2PO_4	6.8 g
NH_4Cl	2.1 g
NaCl	1.0 g
Na_2S x 9 H_2O	0.25 g
with 10M NaOH adjust to pH=6.8	
Trace Element Solution (see Suppl. Tab.7)	10.00 mL
ddH_2O	ad 1000 mL

Supplementary Table 7 | Composition of the trace element solution used in the low pressure experiments for *M. marburgensis* (for final volume of 1 L).

Compound	Amount
Titriplex I	9.0 g
ddH_2O	800 mL
with 5M NaOH adjust to pH=6.5, then add following ingredients:	
$MgCl_2$ x $6H_2O$	4.0 g
$FeCl_2$ x $4H_2O$	1.0 g
$CoCl_2$ x $6H_2O$	20 mg
$NiCl_2$ x $6H_2O$	120 mg
$NaMoO_4$ x $2H_2O$	20 mg
with 1M NaOH adjust to pH=7.0	
ddH_2O	ad 1000 mL

Supplementary Table 8 | Liquid medium composition ("standard medium") used in the low pressure experiments for *M. villosus* (18 g NaCl) and *M. okinawensis* (30 g NaCl) (for final volume of 1 L).

Compound*	Amount
K_2HPO_4	0.14 g
$CaCl_2$ x 2 H_2O	0.14 g
NH_4Cl	0.25 g
$MgSO_4$ x 7 H_2O	3.40 g
$MgCl_2$ x 6 H_2O	4.10 g
KCl	0.33 g
$NiCl_2$ x 6 H_2O	0.50 mg
Na_2SeO_3 x 5 H_2O	0.50 mg
NaCl	18.00 g / 30.00 g
$FeSO_4$ x 7 H_2O	7 mg
$NaHCO_3$	1.00 g
L-Cysteine-HCl x H_2O	0.50 g
Na_2S x 9 H_2O	0.50 g
Vitamin Solution (DSMZ Medium 141)	10.00 mL
Trace Element Solution (DSMZ Medium 141)	10.00 mL
ddH_2O	ad 1000 mL

*The medium composition is similar to DSMZ medium 282 (for **Methanococcus jannaschii**).

Supplementary Table 9 | Liquid medium composition ("Medium w/o $NaHCO_3$") used in the low pressure experiments (for final volume of 1 L) for *M. villosus* (18.7 g NaCl) and *M. okinawensis* (30.7 g NaCl).

Compound*	Amount
K_2HPO_4	0.14 g
$CaCl_2$ x 2 H_2O	0.14 g
NH_4Cl	0.25 g
$MgSO_4$ x 7 H_2O	3.40 g
$MgCl_2$ x 6 H_2O	4.10 g
KCl	0.33 g
$NiCl_2$ x 6 H_2O	0.50 mg
Na_2SeO_3 x 5 H_2O	0.50 mg
NaCl	18.70 g / 30.70 g
$FeSO_4$ x 7 H_2O	7 mg
L-Cysteine-HCl x H_2O	0.50 g
Na_2S x 9 H_2O	0.50 g
Vitamin Solution (DSMZ Medium 141)	10.00 mL
Trace Element Solution (DSMZ Medium 141)	10.00 mL
ddH_2O	ad 1000 mL

*The medium composition is similar to DSMZ medium 282 (for **Methanococcus jannaschii**).

Supplementary Table 10 | Liquid medium composition ("Medium w/o Vitamins") used in the low pressure experiments for *M. villosus* (18 g NaCl) and *M. okinawensis* (30 g NaCl) and in the initial high pressure experiments for *M. okinawensis* (30 g NaCl) (for final volume of 1 L).

Compound*	Amount
K_2HPO_4	0.14 g
$CaCl_2$ x 2 H_2O	0.14 g
NH_4Cl	0.25 g
$MgSO_4$ x 7 H_2O	3.40 g
$MgCl_2$ x 6 H_2O	4.10 g
KCl	0.33 g
$NiCl_2$ x 6 H_2O	0.50 mg
Na_2SeO_3 x 5 H_2O	0.50 mg
NaCl	18.00 g / 30.00 g
$FeSO_4$ x 7 H_2O	7 mg
$NaHCO_3$	1.00 g
L-Cysteine-HCl x H_2O	0.50 g
Na_2S x 9 H_2O	0.50 g
Trace Element Solution (DSMZ Medium 141)	10.00 mL
ddH_2O	ad 1000 mL

*The medium composition is similar to DSMZ medium 282 (for **Methanococcus jannaschii**).

Supplementary Methods:

In the following section, the MATLAB© code used for the estimations of Enceladus' interior structure is given (2 methods).

```
function []=pressure(c,d,s) %c=core radius, d=thickness of the ocean,
s=steps

d=d*1000;
c=c*1000;

r1=1:s:c;
r2=c+1:s:c+1+d;
r3=c+2+d:s:252100;

M=107944591230692000000; %total mass in kg, source:
https://solarsystem.nasa.gov/planets/enceladus/facts
G=6.67408*10^(-11); %gravitational constant
rho1=2300:1:2550; %range for core density
rho2=960:1:1080; %range for ocean density
rho3=850:1:960; %range for ice crust density

for i=1:length(rho1)
    for j=1:length(r1)
M1(i,j)=4/3*pi.*r1(j)^3*rho1(i);     % < core mass
g1(i,j)=G*M1(i,j)/r1(j)^2;           % < core gravity acceleration
    end
end

M1max=M1(:,end);

for i=1:length(rho2)
    for j=1:length(r2)
        for k=1:length(M1max)
M2(i,j,k)=M1max(k)+4/3*pi*(r2(j)^3-r2(1)^3)*rho2(i); % < core + ocean mass
g2(i,j,k)=G*M2(i,j,k)/r2(j)^2;  % < core + ocean  gravity acceleration
        end
    end
end

M2max=M2(:,end,:);
x=size(M2max);
x1=x(1);
x2=x(end);

for i=1:length(rho3)
    for j=1:length(r3)
        for k=1:x1
            for l=1:x2
M3(i,j,k,l)=M2max(k,1,l)+4/3*pi*(r3(j)^3-r3(1)^3)*rho3(i);  % < total mass
g3(i,j,k,l)=G*M3(i,j,k)/r3(j)^2;  % < total gravity acceleration
            end
        end
    end
end

M_total1=M*0.999999;
M_total2=M*1.000001;
```

```
maxM3=M3(:,end,:,:);

[a,b,c,d] = ind2sub(size(maxM3),find(maxM3(:,end,:,:)>M_total1 &
maxM3(:,end,:,:)<M_total2));  %to find possible combination for the
densities

for i=1:length(a)
Mend(i)=maxM3(a(i),b(i),c(i),d(i));
rho1end(i)=rho1(d(i));
rho2end(i)=rho2(c(i));
rho3end(i)=rho3(a(i));
    for j=1:length(r1)
    g1end(i,j)=g1(d(i),j);
    end
    for j=1:length(r2)
    g2end(i,j)=g2(c(i),j,d(i));
    end
    for j=1:length(r3)
    g3end(i,j)=g3(a(i),j,c(i),d(i));
    end
end


%Method 1:

for i=1:length(a) %to determine the pressure at the water/ice boundary
    for j=1:length(r3)
        p3(i,j)=2/3*G*pi*rho3end(i)^2*(r3(end)^2-r3(end-j+1)^2);
    end
end

for i=1:length(a) to determine the pressure at the core/water boundary
    for j=1:length(r2)
        p2(i,j)=p3(i,end)+2/3*G*pi*rho2end(i)^2*(r2(end)^2-r2(end-j+1)^2);
    end
end

p_ocean_core1 = p2(:,end)   % pressure at the core/water boundary


%Method 2:

 for i=1:length(a)   %to determine the pressure at the water/ice boundary
     for j=1:length(r3)
p_ice(i,j)=rho3end(i)*g3end(i,j)*1000;
     end
p_ice_ocean(i)=sum(p_ice(i,:));
 end

  for i=1:length(a) %to determine the pressure at the core/water boundary
p_water(i,1)=p_ice_ocean(i);
     for j=2:length(r2)+1
p_water(i,j)=rho2end(i)*g2end(i,j-1)*1000;
     end
p_ocean_core2(i)=sum(p_water(i,:));
  end

p_ocean_core2 % pressure at the core/water boundary

end
```